GPR30 in breast cancer - from molecular mechanisms to clinical outcome

Tutzauer, Julia

2022

Document Version:
Förlagets slutgiltiga version

GPR30 in breast cancer

From molecular mechanisms to clinical outcome

JULIA TUTZAUER
DEPARTMENT OF EXPERIMENTAL MEDICAL SCIENCE | LUND UNIVERSITY

Julia Tutzauer was born in 1992 and grew up in Nynäshamn, Sweden. She started her PhD studies in molecular pharmacology in 2018 after studying biomedicine and biotechnology at Lund University. When Julia is not working, she enjoys working out, being in nature, making crumble pie, and hanging out with dogs.

Printed by Media-Tryck, Lund 2022 NORDIC SWAN ECOLABEL 3041 0903

LUND UNIVERSITY

FACULTY OF MEDICINE

Department of Experimental Medical Science

Lund University, Faculty of Medicine
Doctoral Dissertation Series 2022:113
ISBN 978-91-8021-274-8
ISSN 1652-8220

GPR30 in breast cancer

GPR30 in breast cancer

From molecular mechanisms to clinical outcome

Julia Tutzauer
Faculty of Medicine
Department of Experimental Medical Science, Lund University

LUND
UNIVERSITY

DOCTORAL DISSERTATION

Doctoral dissertation for the degree of Doctor of Philosophy (PhD) at the Faculty of Medicine at Lund University, Department of Experimental Medical Science.

To be publicly defended on 9 of September at 9.00 in Segerfalksalen, Biomedical Centre (BMC), Lund, Sweden.

Faculty opponent
Professor Helgi Schiöth
Department of Surgical Sciences, Functional Pharmacology and Neuroscience
Uppsala University

Organization LUND UNIVERSITY Faculty of Medicine Dept of Experimental Medical Science	**Document name** Doctoral dissertation **Date of issue** 2022-09-09
Author: Julia Tutzauer	Sponsoring organization

Title and subtitle GPR30 in breast cancer – from molecular mechanisms to clinical outcome

Abstract

With over 2 million new cases each year globally, breast cancer is the most common cancer diagnose worldwide, and with an aging population, the incidence is predicted to rise. Tumor cells are programmed to adapt and survive even during anti-cancer treatments, making drug resistance a concern in modern cancer care. Therefore, it is crucial to identify new drug targets and biomarkers to identify treatment resistant tumors.

To address this, the overall aim of this thesis was to explore molecular factors in breast cancer and how they impact the benefit of common modes of treatment. Special emphasis is placed on the G protein-coupled receptor 30 (GPR30), a putative membrane estrogen receptor, and hypoxia inducible factor 1α (HIF-1α), a transcription factor accumulates in response to low oxygen levels.

Four specific aims were set for the thesis. The first aim was to evaluate GPR30 as a prognostic and predictive marker, as well as a mediator of tamoxifen resistance in contralateral breast cancer. We found that plasma membrane expression of GPR30 was prognostic of poor outcome in contralateral breast cancer, but not predictive of tamoxifen treatment.

The second aim was to study the relationship between GPR30 and the proposed GPR30 ligands estrogen and G-1. Using a number of eukaryotic systems, we found no supporting that G-1 acts as a selective GPR30 agonist, or that GPR30 is an estrogen receptor. On the other hand, we found that GPR30 has considerable constitutive activity.

The third specific aim was to identify functional signaling complexes containing GPR30 in breast cancer cells. We found that GPR30 hetero-oligomerizes with the β_1-adrenergic receptor (β1AR), and that this influences β1AR-mediated signaling.

The fourth specific aim was to evaluate the relevance of tumor hypoxia in relation to breast cancer outcome in general and radiotherapy specifically. Our results showed that HIF-1α is prognostic of poor breast cancer outcome, but not predictive of radiotherapy response.

Key words Breast cancer, GPR30, GPCR, HIF1a, treatment, tamoxifen, radiotherapy

Classification system and/or index terms (if any)

Supplementary bibliographical information		**Language** English
ISSN 1652-8220		**ISBN** 978-91-8021-274-8
Recipient's notes	**Number of pages** 107	Price
	Security classification	

Signature  Date 2022-08-01

GPR30 in breast cancer

From molecular mechanisms to clinical outcome

Julia Tutzauer
Faculty of Medicine
Department of Experimental Medical Science

LUND
UNIVERSITY

Supervisors:
Professor Fredrik Leeb-Lundberg, Ph.D
Department of Experimental Medical Science
Lund University

Associate Professor Sara Alkner, M.D., Ph.D
Department of Clinical Sciences
Department of Hematology, Oncology, and Radiation Physics
Lund University, Skåne University Hospital

Martin Sjöström, MD, PhD, Assistant Researcher
Department of Radiation Oncology
University of California, San Francisco

Cover photo by Julia Tutzauer 2022.

The figures included in this thesis are, unless otherwise stated in the figure legend, constructed by the author.

Faculty of Medicine
Department of Experimental Medical Science

ISBN 978-91-8021-274-8
ISSN 1652-8220
Printed in Sweden by Media-Tryck, Lund University
Lund 2022

You're going to find that many of the truths we cling to depend greatly on our own point of view.

Obi-Wan Kenobi, Return of the Jedi

Table of Contents

Abstract

With over 2 million new cases each year globally, breast cancer is the most common cancer diagnose worldwide, and with an aging population, the incidence is predicted to rise. Tumor cells are programmed to adapt and survive even during anti-cancer treatments, making drug resistance a concern in modern cancer care. Therefore, it is crucial to identify new drug targets and biomarkers to identify treatment resistant tumors.

To address this, the overall aim of this thesis was to explore molecular factors in breast cancer and how they impact the benefit of common modes of treatment. Special emphasis is placed on the G protein-coupled receptor 30 (GPR30), a putative membrane estrogen receptor, and hypoxia inducible factor 1α (HIF-1α), a transcription factor accumulates in response to low oxygen levels.

Four specific aims were set for the thesis. The first aim was to evaluate GPR30 as a prognostic and predictive marker, as well as a mediator of tamoxifen resistance in contralateral breast cancer. We found that plasma membrane expression of GPR30 was prognostic of poor outcome in contralateral breast cancer, but not predictive of tamoxifen treatment.

The second aim was to study the relationship between GPR30 and the proposed GPR30 ligands estrogen and G-1. Using a number of eukaryotic systems, we found no supporting that G-1 acts as a selective GPR30 agonist, or that GPR30 is an estrogen receptor. On the other hand, we found that GPR30 has considerable constitutive activity.

The third specific aim was to identify functional signaling complexes containing GPR30 in breast cancer cells. We found that GPR30 hetero-oligomerizes with the β_1-adrenergic receptor (β1AR), and that this influences β1AR-mediated signaling.

The fourth specific aim was to evaluate the relevance of tumor hypoxia in relation to breast cancer outcome in general and radiotherapy specifically. Our results showed that HIF-1α is prognostic of poor breast cancer outcome, but not predictive of radiotherapy response.

Studies included in the thesis

1. Tutzauer J, Sjöström M, Bendahl PO, Rydén L, Fernö M, Leeb-Lundberg LMF, Alkner S. Plasma membrane expression of G protein-coupled estrogen receptor (GPER)/G protein-coupled receptor 30 (GPR30) is associated with worse outcome in metachronous contralateral breast cancer. PLoS One. 2020 Apr 17;15(4):e0231786. doi: 10.1371/journal.pone.0231786. PMID: 32302351; PMCID: PMC7164601.

2. Tutzauer J, Gonzalez de Valdivia E, Swärd K, Alexandrakis Eilard I, Broselid S, Kahn R, Olde B, Leeb-Lundberg LMF. Ligand-Independent G Protein-Coupled Estrogen Receptor/G Protein-Coupled Receptor 30 Activity: Lack of Receptor-Dependent Effects of G-1 and 17β-Estradiol. Mol Pharmacol. 2021 Sep;100(3):271-282. doi: 10.1124/molpharm.121.000259. Epub 2021 Jul 30. PMID: 34330822.

3. Tutzauer J, Sjöström M, Holmberg E, Karlsson P, Killander F, Leeb-Lundberg LMF, Malmström P, Niméus E, Fernö M, Jögi A. Breast cancer hypoxia in relation to prognosis and benefit from radiotherapy after breast-conserving surgery in a large, randomised trial with long-term follow-up. Br J Cancer. 2022 May;126(8):1145-1156. doi: 10.1038/s41416-021-01630-4. Epub 2022 Feb 9. PMID: 35140341; PMCID: PMC9023448.

4. Tutzauer J, Serafin S, Schmidt T, Caron K. M., Olde B, Leeb-Lundberg LMF. G protein-coupled estrogen receptor (GPER)/GPR30 forms a heteromeric complex with the β_1-adrenergic receptor, a membrane-associated guanylate kinase (MAGUK) scaffold protein, and protein kinase A anchoring protein (AKAP) 5 in MCF7 breast cancer cells. Manuscript under preparation.

Studies not included in the thesis

Berlin F, Mogren S, Tutzauer J, Andersson CK. Mast Cell Proteases Tryptase and Chymase Induce Migratory and Morphological Alterations in Bronchial Epithelial Cells. Int J Mol Sci. 2021 May 16;22(10):5250. doi: 10.3390/ijms22105250. PMID: 34065716; PMCID: PMC8156481.

Acronyms

A	
AC	Adenylyl cyclase
AI	Aromatase inhibitor
AKAP	A-kinase anchoring protein
AR	Adrenergic receptor
ATP	Adenosine 5'-triphosphate
B	
β1AR	β_1-adrenergic receptor
BC	Breast cancer
BC1	First primary breast cancer
BC2	Second primary breast cancer (contralateral breast cancer)
BCD	Breast cancer death
BRET	Bioluminescence resonance energy transfer
C	
cAMP	3'-5'-cyclic adenosine monophosphate
CBC	Contralateral breast cancer
CI	Confidence interval
CRLR	Calcitonin-receptor-like receptor
E	
E2	17β-estradiol
EGFP	Enhanced green fluorescent protein
ERK1/2	Extracellular signal-regulated protein kinase 1 and 2
ER	Endoplasmic reticulum
ERα	Estrogen receptor α
F	
FACS	Fluorescence-activated cell sorting

FIH	Factor inhibiting HIF-1
FSHR	Follicle-stimulating hormone receptor

G

GAP	GTPase-activating proteins
GEF	Guanine nucleotide exchange factors
GPCR	G protein-coupled receptor
GPER	G protein-coupled estrogen receptor
GPR30	G protein-coupled receptor 30
GRK	G protein-coupled receptor kinase
GTP	Guanosine triphosphate
G-1	(±)-1-[(3aR*,4S*,9bS*)-4-(6-bromo-1,3-benzodioxol-5-yl)-3a,4,5,9b-tetrahydro-3H-cyclopenta[c]quinolin-8-yl]-ethenone

H

HIF-1α	Hypoxia-inducible factor 1α
HR	Hazard ratio

I

IBTR	Ipsilateral breast tumor recurrence
IHC	Immunohistochemistry

L

LGL	Axillary lymph node metastasis

M

MAGUK	Membrane-associated guanylate kinase
MAPK	Mitogen-activated protein kinase

N

NFAT	Nuclear factor of activated T-cells

P

PHD-2	Proline-hydroxylase-2
PI3K	Phosphatidylinositol 3-kinase
PKA	Protein kinase A
PKC	Protein kinase C
PR	Progesterone receptor
PSD-95	Post-synaptic density-95

R

RAMP	Receptor-activity-modifying protein

S

SAP97	Synapse-associated protein 97
SDS-PAGE	Sodium dodecyl sulfate polyacrylamide gel electrophoresis
SERM	Selective ERα modulator
SERD	Selective ERα downregulator

T

TMA	Tissue microarray
TPA	12-O-Tetradecanoylphorbol 13-acetate
TRE	TPA responsive element

V

VHL	von-Hippel-Lindau

W

WT	Wild-type

Y

YFP	Yellow fluorescent protein

Populärvetenskaplig sammanfattning

År 2020 var bröstcancer den mest frekvent diagnosticerade cancertypen världen över, med över två miljoner nya fall. I Sverige drabbas mer än en av tio kvinnor av bröstcancer. Prognosen för dessa kvinnor har sett stadigt bättre ut under de senaste 50 åren, mycket på grund av nya och förbättrade behandlingar, men fortfarande kommer en del av de kvinnor som får en bröstcancerdiagnos att dö av sin sjukdom. Därför behövs bröstcancerforskning.

Bröstcancer är egentligen inte en sjukdom, utan flera. Detta beror på att cancerutvecklingens natur gör att varje tumör är mer eller mindre unik. Ändå har forskningen identifierat ett antal olika subtyper av bröstcancer som de flesta tumörer kan beskrivas genom. Kategoriseringen av tumörerna baseras på förekomst av ett antal olika proteiner, så kallade biomarkörer, som man har kunnat koppla till tumörens aggressivitet och respons på vanliga behandlingar. Med hjälp av denna klassificering kan man idag delvis individanpassa behandlingen av varje tumör, vilket minskar risken för att en patient måste genomgå en behandling som inte fungerar, och ökar chansen för att hon överlever sin sjukdom.

Östrogenreceptor alfa (ERα) är en biomarkör som uttrycks i ungefär åtta av tio brösttumörer. ERα aktiveras av könshormonet östrogen, och startar därefter processer i cancercellen som ofta leder till att den växer och bildar dotterceller. Tamoxifen är ett läkemedel som minskar aktiviteten hos ERα, och därmed hämmar tillväxten av ERα-positiva tumörer. Därför används ofta tamoxifen för att behandla ERα-positiva brösttumörer. Trots genomgången tamoxifenbehandling är det dock många brösttumörer som bildar återfall. En anledning kan vara att tumörcellerna kommit på en metod som gör att de inte längre skadas av tamoxifen. Denna typ av resistensutveckling är en klinisk utmaning. Inom bröstcancerforskning finns därför ett stort intresse för att förstå de bröstcancercellers resistensmekanismer, samt för att utveckla nya läkemedel att använda på tamoxifenresistenta tumörer.

I flera av delarbetena i denna avhandling undersöker vi en receptor som heter G-proteinkopplad receptor 30 (GPR30). GPR30 har länge klassats som en

östrogenreceptor, därmed har östrogen antagits vara den faktor som aktiverar receptorn. Viss data från tidigare studier har även pekat på att GPR30 kan vara inblandad i resistens mot tamoxifen. I delarbete I studerar vi GPR30 i förhållande till tamoxifenresistens och prognos i kontralateral bröstcancer, vilket är när en kvinna som tidigare haft bröstcancer i ena bröstet utvecklar en ny tumör i det andra bröstet. Genom att mäta mängden GPR30 i kontralateral bröstcancer som utvecklats under tamoxifenbehandling och jämföra det den med motsvarande som utvecklats utan tamoxifenbehandling, kunde vi visa att GPR30 inte följer ett mönster som hade förväntats av ett protein som bidrar till resistens. Vi såg även i studien att GPR30 är associerat till andra markörer för tumöraggressivitet, och att receptoruttryck specifikt i cancercellernas plasmamembran är kopplat till en sämre prognos.

Utöver östrogen finns en syntetisk substans som ofta används för att aktivera GPR30 inom forskning. Denna substans, som kallas G-1, har däremot blivit ifrågasatt genom åren då vissa data pekar på att G-1 inte verkar aktivera GPR30, eller att substansen aktiverar något annat protein i cellen. I delarbete II undersökte vi aktiveringen av GPR30 i förhållande till östrogen och G-1. Baserat på de data vi samlade in kunde vi inte finna något bevis för att varken östrogen eller G-1 aktiverar GPR30. Våra data tyder dessutom på att G-1 aktiverar signalering i celler som inte uttrycker GPR30. Slutligen såg vi att GPR30 tenderar att vara aktiv inom signalering även utan att något stimuli tillsatts. Baserat på detta föreslog vi att GPR30 har en hög grundaktivitet, att det inte finns data nog för att stärka att GPR30 är en östrogenreceptor, och att G-1 inte aktiverar GPR30.

Den grundläggande behandlingen vid bröstcancer är att tumören avlägsnas kirurgiskt. För att ta bort eventuella tumörceller som finns kvar i bröstet ges tilläggsbehandlingar. Strålbehandling är en av de vanligaste tilläggsbehandlingarna, och har god effekt mot återfall. Man vet dock att det finns patientgrupper där risken för återfall är så pass liten att strålbehandling inte är nödvändigt, och att det finns tumörer som är så aggressiva att det kan vara gynnsamt att ge extra strålbehandling. I delarbete III undersökte vi om proteinet HIF-1α, som finns i tumörer med låg syretillgång, kan verka som biomarkör för att prediktera behandlingssvar på strålbehandling. För att undersöka detta hade vi tillgång till kliniska och biologiska data från en studie där ca 1000 kvinnor med bröstcancer randomiserades att få eller inte få strålbehandling. Biologiska data inkluderade proteinuttryck av HIF-1α samt genuttryck. Vi fann att HIF-1α inte verkade predicera tumörens svar på strålbehandling, men kunde identifiera patienter

med sämre prognos. Vidare tittade vi på genuttryckssignaturer relaterade till en syrefattig tumörmikromiljö för att se om dessa kunde tjäna som alternativ för HIF-1α som prognostisk markör. Vi såg att medan genuttryckssignaturerna associerade med prognos, var ingen starkare kopplad till prognos än HIF-1α. Studiens slutsats var att HIF-1α är en prognostisk markör, men kan inte predicera strålbehandlingssvar.

I delarbete IV var vår hypotes att cellens respons på aktivering av GPR30 påverkas mycket av vilka proteiner som finns i receptorns omedelbara närhet. Vi fann att det i den omedelbara närheten kring GPR30 sitter en receptor som kallas β_1-adrenerg receptor (β1AR), som är involverad i kroppens svar på adrenalin. Dessutom kunde vi se att GPR30 hämmade aktiviteten hos β1AR, och därmed påverkade cellens svar på adrenalin. Detta kan ha en viktig funktion i bröstcancer, där β1AR kopplats till prognos och incidens.

Sammanfattningsvis har jag med denna avhandling arbetat för att bidra med ny kunskap om mekanismer viktiga för bröstcancerutveckling- och behandling, från proteininteraktioner och signalering, till patientens prognos och behandlingssvar (**Figure 1**).

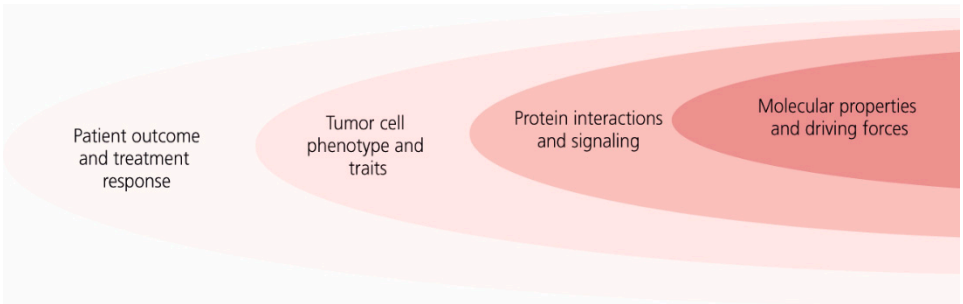

Figure 1. Hierarki inom bröstcancerforskning. Det slutgiltiga målet inom cancerforskning är att förstå, förutse och förbättra kliniska resultat, men detta kräver även kunskap på cellnivå, proteinnivå och på biofysisk nivå.

Introduction

Cell signaling and oncogenesis

With life on earth involving constant transformation, our bodies depend on their ability to resist change. We maintain our body temperature in warm and cold climates, readily clear out consumed toxins, and after exposure to harmful sunrays, our skin produces pigment to minimize future damage. Maintaining status quo at the chemical level is just as important, where factors essential for our survival often have harmful or even lethal effects when exceeding their stringent concentration intervals. Therefore, strict regulation of such factors is of utmost importance. In order to understand human physiology, it is central to recognize the fine-tuned balances of physiological, chemical, and biophysical conditions in our bodies.

The human body consists of trillions of cells with a high diversity in morphology and function. Cells communicate either physically, using sensor proteins that detect markers on the surface of neighboring cells, or chemically, by orchestrating release of messenger molecules that reach receptors on other cells by paracrine or endocrine communication. To maintain healthy tissues, cells are replaced continuously throughout life. This is governed by the processes of proliferation, where a healthy cell produces identical daughter cells, and apoptosis, where an old cell undergoes programmed cell death. These processes also play an important role in maintaining the genetic integrity of the tissue. Within each cell, sophisticated defense mechanisms are dedicated to detect DNA damage, foreign proteins, and pathogenic genetic material, and launch molecular programs to prevent the spreading of a detected abnormality. The latter is achieved by preventing a corrupt cell from proliferating, and either trigger defense and repair mechanisms, or initiate apoptosis. Evidently, proliferation and apoptosis are crucial pillars in maintaining healthy tissues. For this reason, cells express a plethora of proteins dedicated to these mechanisms exclusively, by sensing, regulating, and sending feedback information. However, occasionally these processes fail, and an

abnormal cell manages to divide and spread. This is the mechanism behind oncogenesis – the development of cancer.

Oncogenesis is a highly dynamic and complex process involving stepwise genetic and epigenetic alteration, generally assumed to be unique for each case. Yet, some general traits have been acknowledged as vital in the development of any tumor. In two articles in 2000 and 2011, Hanahan and Weinberg proposed ten universal biological attributes fundamental in tumor formation [3, 4] (**Figure 2**). These include adaptations in the behavior of the tumor cells – such as genome instability and capacity to grow and divide even in the absence of growth signals, and adaptations in the interaction between the tumor cells and their microenvironment – such as ability to promote growth of blood vessels to better provide nutrients and clear out toxic metabolites from the tumor. These attributes, called Hallmarks of Cancer, are to this day considered a useful model for rationalizing the intricate process of oncogenesis.

Figure 2. The ten Hallmarks of Cancer, as described by Hanahan and Weinberg 2000 and 2011 [1, 2].

The fundamentals of tumor genetics are often explained by categorizing mutated cancer-promoting genes into two groups; oncogenes and mutated tumor suppressor genes. An oncogene is a growth-promoting gene which through mutation has either been duplicated to an inordinate number, or acquired an activating mutation – resulting in an elevated growth-stimulatory effect. In their normal, healthy state, oncogenes are called proto-oncogenes. Tumor suppressor genes normally restrain cell growth and proliferation. When a tumor suppressor gene is mutated, resulting in either gene deletion or reduced function, the tumor suppressor fails to contribute to the control of cell division. If successive mutations of proto-oncogenes and tumor suppressor genes occur and the balance between the growth-stimulatory activity and growth suppression becomes skewed, a tumor may form [5].

Breast cancer

Epidemiology

As of 2020, breast cancer is the most commonly diagnosed cancer worldwide, with over 2 million new cases annually [6]. Breast cancer is among the most common causes of pre-term mortality in women globally [7, 8]. In Sweden, it represents almost 30% of all detected malignancies among women, and more than 1 in 10 Swedish women will receive a breast cancer diagnosis during her life [8].

The incidence of breast cancer has been rising in higher-income countries over the last 50 years, and recently also in lower-income countries. In Sweden, the number of breast cancer diagnoses per 100 000 women has increased by 70% since the early 70s [9], which to some degree may be explained by the implementation of breast cancer screening programs in recent years [6]. Changes in lifestyle patterns, including a growing prevalence of overweight, a trend of lower parity, higher age at first birth, earlier menarche, as well as use of hormone replacement during menopause are also believed to be reflected in the incidence [6]. However, the breast cancer survival rate has improved steadily the past 50 years. This improvement may partly, but not fully, be accredited to earlier detection [6]. The rising survival rate in combination with an increased incidence has made breast cancer the most prevalent cancer globally. In 2020, almost 8 million women were diagnosed with breast cancer within the preceding 5 years [7].

The strongest risk factors for breast cancer are gender and age; around 50% of all breast cancer patients have no other known risk factor than female sex and an age over 40 [7]. It is clear that family history and specific inherited genetic mutations are strong risk factors for breast cancer. More common breast cancer-related mutations often show marginal impact on the breast cancer risk, while mutations that increase the risk more severely are rare. Among the most notorious mutations in the latter group are those in tumor suppressor genes *BRCA1* and *BRCA2,* which are estimated to increase the lifetime breast cancer risk of up to 72% and 69%, respectively [10, 11].

Prognostic and predictive factors

While some data suggest that lifestyle factors including smoking, physical activity, and overweight may influence the outcome of breast cancer, most prognostic factors are purely tumor-related [12, 13]. For operable breast cancer, factors that strongly relate to outcome are tumor size, spread to regional lymph nodes, and histological grade. Histological grade is an estimate of tumor cell differentiation, i.e., how much they resemble normal cells in terms of nuclear pattern, mitotic activity, and ability to form ductal structures. Breast cancers are further classified based on a number of molecular markers and tumor traits that aid clinically in prediction of prognosis and treatment decisions. Molecular biomarkers currently used in the clinic are ERα, progesterone receptor (PR), human epidermal growth factor receptor 2 (HER2), and the proliferation marker Ki67. These markers are used in ensemble as surrogate markers for the four intrinsic subtypes Luminal A, Luminal B, HER2 positive, and triple-negative breast cancer (TNBC) based on definitions from the 13th St. Gallen International Breast Cancer Conference [14], a classification system initially based on gene expression data [15]. Both luminal A and luminal B are ERα-positive, which in Sweden means that more than 10% of tumor cells express ERα. Further, luminal A is HER2 negative, with low or intermediate Ki67 and histological grade 1 or 2. Luminal B is HER2 negative, with histological grade 2 or 3, and intermediate to high Ki67. The HER2 positive breast cancer subtypes may be luminal or non-luminal, and are defined by overexpression of the proliferative HER2 receptor [16]. Lastly, TNBC is defined by absence of both ERα, PR, and HER2 amplification [17]. TNBC is highly heterogeneous but often described as aggressive, with complex, prominently mutational genomes, younger age of presentation, and higher risk of early metastasis and mortality [18, 19].

ERα and HER2 are not only prognostic, but also predictive factors, meaning that they predict tumor sensitivity to breast cancer treatments. While ERα is a biomarker of the tumor being sensitive to hormonal agents, including tamoxifen and aromatase inhibitors, HER2 amplification predicts likeliness that a tumor responds well to anti-HER2 drugs, including trastuzumab (Herceptin) and trastuzumab emtansine (Kadzyla) [16].

Contralateral breast cancer

Contralateral breast cancer (CBC) is a second tumor developed in the contralateral breast after the first breast tumor (**Figure 3**). CBC is presumed to be a second primary tumor independent of the first tumor, but data suggest that some CBCs may be a metastatic spread from the first tumor [20]. A CBC may be synchronous, meaning that it is assumed to have existed concurrently with the first tumor. CBCs diagnosed later are referred to as metachronous.

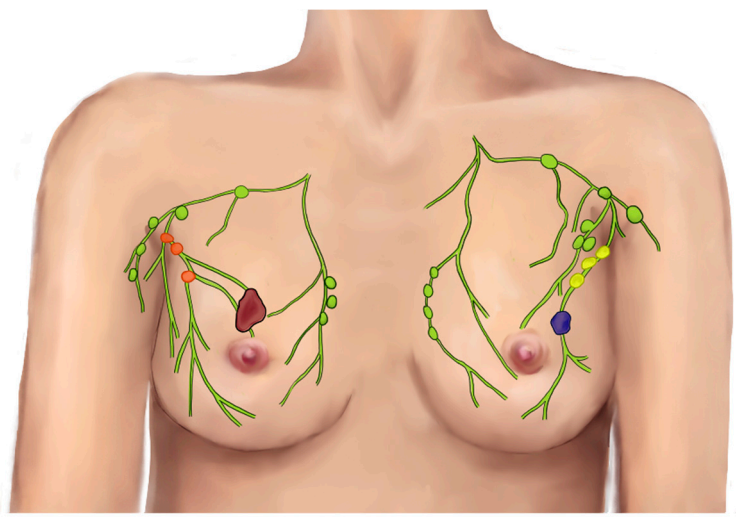

Figure 3. Contralateral breast cancer, here presented in a synchronous setting with both primary tumors present simultaneously. The primary tumors are colored blue and red, with lymph node metastases colored yellow and orange. Illustration by Madeleine Torén.

Current treatments

The standard treatments available for breast cancer management is surgery, postsurgical radiotherapy, and systemic therapy. Chemotherapy is most often given prior to RT, and sometimes in a neoadjuvant setting, meaning that the treatment is given before surgery to reduce tumor size [16].

Surgery

The most common surgical management of breast cancer is breast conserving surgery with axillary sentinel lymph node biopsy. The axillary sentinel node is the first site for lymph drainage from the tumor. This method has been proven as a safe alternative to the previous standard procedure of axillary clearance [21], where all identified axillary lymph nodes are removed, often causing side effects such as edema.

After surgery, further treatment may be given to target any microscopic tumor residues left after resection [22]. Mastectomy – surgical removal of one or both breasts – may be of benefit for women with a strong hereditary disposition of recurrence or contralateral breast cancer (for example, carriers of a mutation in *BRCA1/2* or other highly penetrant breast cancer genes), for large and/or multifocal cancers, or in cases where a patient wishes to avoid radiotherapy.

Radiotherapy

Radiotherapy is generally given after surgery. It decreases the risk of ipsilateral breast tumor recurrence (IBTR) substantially, and plays a central role in reducing the long-term risk of recurrence in breast cancer patients [23]. The benefit of radiotherapy varies between patients, and despite progresses in molecular profiling during the last decades, there is still a lack of knowledge regarding the molecular basis of breast cancer radiosensitivity. As of today, radiotherapy is normally prescribed based on tumor stage and type of surgery [24].

Systemic treatment – ERα and endocrine therapy

ERα is a steroid receptor expressed in around 80% of all breast cancers, where it mediates cell growth and proliferation stimulated by estrogen. Endocrine treatments designed to disrupt ERα signaling through suppression of receptor activity (e.g., selective ER modulators; SERMs, or downregulators; SERDs), or by inhibition of estrogen production (e.g., aromatase inhibitors) are central in management of these tumors. For young patients with a high risk of recurrence, ovarian suppression is also an option to decrease estrogen levels and reduce the risk of recurrence [16]. The SERM tamoxifen is one of the most widely prescribed endocrine agents for ER-positive breast cancer and has been a cornerstone treatment for over 30 years [25, 26]. Five years of adjuvant tamoxifen reduces the annual risk of breast cancer mortality by almost one-third, and the 10-year risk of recurrence by almost 50% [27, 28]. However, not all ER-positive tumors are susceptible to tamoxifen, and resistance may exist *de novo* or arise

during treatment. Surprisingly, resistance to ER targeting drugs often occurs without loss of ER expression, indicating the existence of growth signaling sidetracks allowing the cancer cells to keep proliferation independently of ER [29]. Mutations in the ER gene *ESR1* have been connected to, but cannot entirely explain, endocrine resistance mechanisms [30-32], and although widely studied, the machineries governing tamoxifen resistance remain relatively poorly understood.

Systemic treatment

The standard combination of chemotherapy agents is cyclophosphamide, epirubicin, and a taxane agent, which may be given in a neoadjuvant or an adjuvant setting.

Hypoxia and breast cancer

Oxygen is an essential element of cell homeostasis, acting as an electron acceptor in vital biochemical reactions including ATP production in normal cell metabolism. Hypoxia is a state where the oxygen saturation is beneath the requirements for normal cellular functions. This condition may occur systemically due to inadequate breathing, or locally through e.g. poor vessel support or obstructed blood flow. On a cellular level, adaptation to hypoxia is predominantly controlled by the hypoxia induced transcription factors HIF-1α and HIF-2α. In this thesis, emphasis will be on HIF-1α. In an oxygenated environment, HIF-1α is inhibited and targeted to proteasomal degradation by the Factor Inhibiting HIF-1 (FIH) and proline-hydroxylase-2 (PHD-2) proteins, together with von-Hippel-Lindau (VHL) ubiquitin ligase complexes. As cellular oxygen levels drop, these mechanisms are inhibited, as the VHL proteins, FIH and PHD-2 are oxygen-dependent. The HIF-1α subunits accumulate rapidly and translocate to the nucleus, where they dimerize with the constitutively expressed HIF-1β and activate transcription of genes that participate in hypoxic adaptation [33-37]. These genes are recognized by the HIF complex via a specific promoter sequence called a hypoxia response element (HRE) [38].

Solid tumors frequently exhibit fast and dense growth, often exceeding the support from local vascularization (**Figure 4**). Consequently, hypoxia is a common feature in solid tumors. Hypoxia represents a double-edged sword in cancer, as the limited oxygen supply may decrease metabolism and restrain proliferation, leading to apoptosis and necrosis. On the other hand, hypoxia may also select for more hostile traits, leading to a more aggressive phenotype among the enduring tumor cells.

The hypoxic response facilitated by HIF-related gene expression involves several of the Hallmarks of Cancer, including an increased proliferation, expression of growth factors and cytokines, and alters cellular metabolism [39]. Furthermore, HIF-1α-governed gene expression supports aggressive behavior and migration of cancer cells [40, 41]. In breast cancer, HIF-1α protein expression has been associated with development of distant metastases and poor prognosis [42-44].

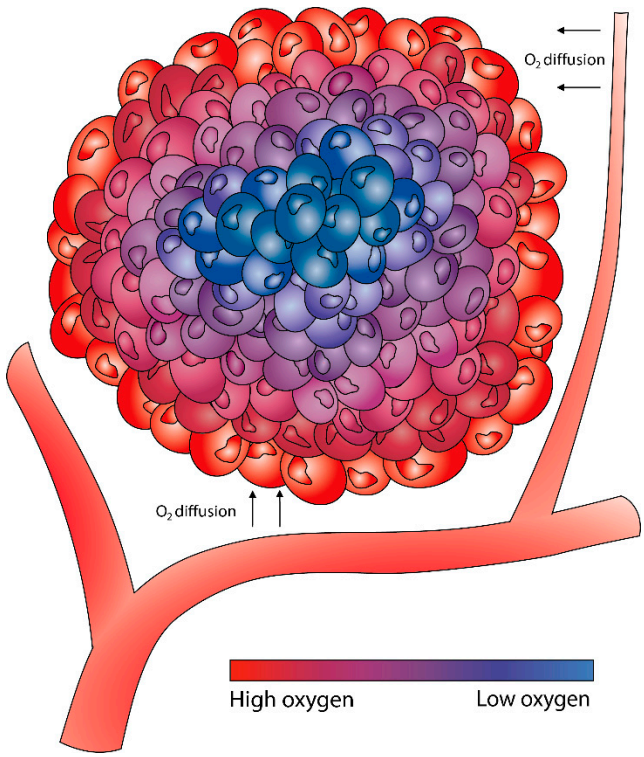

Figure 4. An illustration of tumor hypoxia. Solid tumors grow dense and fast, often leading to formation of areas of poor blood supply and hypoxia. The illusration was made for and first appeared on the blog post *How does intra-tumour low oxygen levels relate to the clinical outcome after radiotherapy in breast cancer?* by Jögi and Tutzauer published at Nature Portfolio Cancer Community. Re-used with permission from Nature Communities.

Hypoxia and tumor radiosensitivity

Studies have connected in-tumor hypoxia with disease progression and resistance to therapy, including radiotherapy [45]. Ever since the 50s, is has been known that a lack of oxygen reduces the biological effects of radiation. Clearly, effective radiation requires

oxygen to be present at the time of irradiation, or within microseconds after exposure. The theory behind this is debated, but a suggested explanation is the oxygen fixation hypothesis. This hypothesis describes the radical species that may form when ionizing particles interact with biological matter, of which the oxygen-based peroxyl radical $RO_2\bullet$ is anticipated to be most detrimental. In absence of $RO_2\bullet$, the radiation causes less irreparable DNA damage [46].

Protein conformation and activity

The central dogma of molecular biology states that DNA is transcribed into RNA, which in turn is translated into proteins. Synthesized as linear, disordered peptide chains, the newly translated proteins fold into the correct three-dimensional structure of their native state within microseconds to seconds. In 1969, Levinthal calculated that if protein folding would transpire through stochastic sampling of possible conformations, the folding process for one single protein would take longer than the age of the universe [47]. To this background, the rapidity by which these macromolecules enter correct folding states from almost infinite alternatives may appear astonishing.

The explanation lies in thermodynamics, the branch of physics that describes the transfer of energy in different forms. The laws of thermodynamics define that an event will occur spontaneously if it is accompanied by a decrease in the inner energy of the system. In the case of protein folding, a spontaneous event may be a reorganization that minimizes electrostatic repulsion, e.g. through arranging positive net charges close to negative net charges by formation of hydrogen bonds, ion-dipole forces, and Van der Waals forces, or by minimizing hydrophobic repulsion by assembling non-polar amino acids together to minimize hydrophobic-hydrophilic interfaces [48, 49]. Stepwise, the newly synthesized polypeptide selects new arrangements, and a near infinite number of folding variants funnel down to one or a few conformations of approximately equally low energy. If a multitude of conformations are of equally low energy, these will equilibrate with each other and the protein will fluctuate between them in its native state [50].

The propensity that a protein exists in a particular conformation at a given moment is called the conformational or basal equilibrium. Several different events may alter the conformational equilibrium of a protein. One example is post-translational covalent addition of side groups, e.g., disulphide bonds, glycosylation, acetylation, and

phosphorylation. This may alter the protein organization either sterically or by shifting the electrostatic properties of the protein. Another fundamental event that may influence the conformational equilibrium of a protein is the interaction with a ligand. A ligand is a substance that binds to a biomolecule, e.g., a protein, which also is reflected in the name origin "ligare", the Latin word for binding. Interaction of a protein with a ligand impacts the energy landscape of the protein, favoring one or several different conformations. Hence, ligand binding may increase the inclination of the protein taking active conformations and unlock functions, for example catalytic activity, dimerization, or the ability to interact and communicate with partner proteins.

For an enzyme, a protein with a catalytic function, the ligand is often the material for catalysis, i.e., the substrate. Some proteins lack catalytic function and instead respond to the ligand by prompting an effect on other proteins, often leading to chains of protein activities and the release of small signaling molecules (second messengers), resulting in a cascade-like activation. These proteins are called receptors and are critical for all functions in the human body and have become an important pillar in pharmacology and therapeutics.

G protein-coupled receptors (GPCRs)

G protein-coupled receptors (GPCR) are membrane-spanning proteins that reside in the plasma membrane and on intracellular membranes. GPCRs make up one of the largest and most versatile mammalian protein families, with more than 800 members in the human genome. The presence of GPCRs in nematode genomes demonstrates that these receptors evolved at least 600-1200 million years ago, at the time of our last common ancestor [51, 52]. Arguably, the notable conservation through millions of years of evolution emphasizes their extensive biological role. Certainly, GPCRs play a central part in a broad section of physiological processes studied in modern medicine – from metabolism and muscle function, vision, and cognition, perception of taste, smell, and pain, to the immune system. GPCRs are also among the most common drug targets in modern medicine, both for established drugs and for new compounds explored in clinical trials [53].

Basal structure

GPCRs exhibit a wide variation in amino acid sequence but share structural features. Arguably, the most distinctive attribute of a GPCR is the serpentine structure, with seven consecutive membrane-spanning alpha helices (**Figure 5**). The hydrophobic

profile of the helical structures allows them to pass through the lipid bilayers of cellular membranes, explaining why these receptors are also referred to as 7-transmembrane receptors. Flanking the ends, the GPCR has an extracellular amino (N)- terminal domain that often contains sites participating in binding extracellular signaling molecules, and an intracellular carboxyl (C)- terminal domain that houses interfaces for interaction with cytoplasmic and membrane-bound effector proteins that transfer signals further [54]. This structure enables the GPCR to detect extracellular signals, such as hormones or neurotransmitters, and promote a cellular response by activating a signaling cascade inside of the cell.

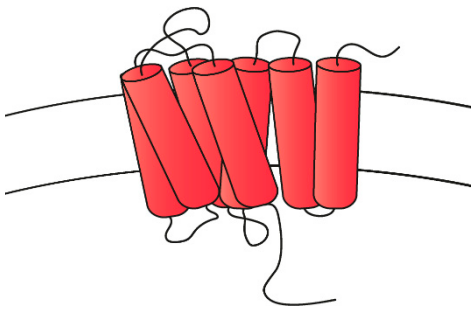

Figure 5. Structure of a GPCR.

Receptor conformations and the role of ligands

Biophysical studies show that GPCRs exist in a variety of conformations alternating in intervals of hundreds of microseconds, illustrating how GPCRs in their ground state equilibrate in a landscape of different low-energy conformations [55]. The propensity of a GPCR spontaneously entering an active state able to couple to intracellular effectors varies between different receptors. Based on this equilibrium, all GPCRs have some basal activity, also called constitutive activity. Basal activity is very low with most receptors, but some receptors do exhibit measurable basal activity.

Binding of a ligand shifts the conformational equilibrium towards one or more states (**Figure 6**) [55, 56]. Most GPCR ligands reach the receptor from the extracellular space and bind in a pocket created by the N-terminal and a helical bundle consisting of the transmembrane domains. This binding allosterically favors a structural reorganization

of the protein that promotes interaction with intracellular effector signaling proteins [54, 57]. A ligand that binds and stabilizes active receptor conformations, increasing the biological response, is called an agonist, whereas a ligand that reduces basal activity by stabilizing inactive receptor conformations is called an inverse agonist. A substance capable of blocking the action of an agonist by binding to the receptor is called an antagonist. The most common types of ligands are described in Table 1.

The effectiveness by which an agonist generates a cellular response through interacting with a receptor is described by the efficacy of the agonist, and the concentration at which a substance generates its maximal effect is designated to its potency. The strength of interaction between two species, in this case a receptor and a ligand, is described by their affinity to each other. In similarity to protein conformations, affinity is controlled by the strive to minimize inner energy, where interaction strength correlates with the decrease in free energy it permits.

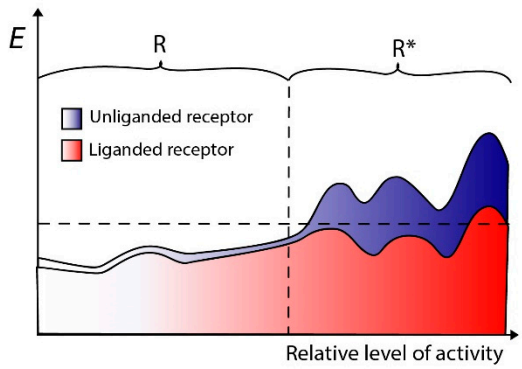

Figure 6. Activity associated to conformations of an arbitrary receptor in relation to inner energy. The blue graph illustrates the level of activity in relation to the inner energy of an unliganded receptor. The dotted line denotes the energy threshold above which the conformations will not be energetically favorable, thus not occur, in the normal repertoire of conformations. The red graph illustrates the activity in relation to the inner energy of a receptor that has bound an agonist, which reduces the energy required to go from relatively inactive conformations (R) to a relatively active conformations (R*). Note that even the unliganded receptor exhibits some degree of basal activity, as demonstrated by the area between the blue graph and dotted line in the R* space.

The members of the GPCR family show a high diversity in ligand recognition, ranging from endogenous compounds including peptides and adhesion molecules, to external stimuli such as odorants and even photons [58]. The significance of GPCRs in human physiology is vast, which may be illustrated by the fact that around 80% of known neurotransmitters and hormones act via GPCRs [59].

Table 1. A summary of different types of ligands [60-62].

Ligand	
Agonist	A ligand able to bind to and stabilize the receptor in one or several active conformations to increase activity.
Inverse agonist	A substance that binds to a receptor and stabilizes a less active state, to reduce basal activity and agonist-stimulated activity.
Partial agonist	Agonists that induce a submaximal response.
Biased agonist	An agonist with functional selectivity and stabilizes the receptor in a conformation that favors one or a few specific receptor activities, activating a distinct signaling profile.
Antagonist	A substance capable of blocking the action of an agonist.
Competitive antagonist	Competes with the agonist for the agonist binding site.
Non-competitive antagonist	Acts allosterically by binding at a different site than the agonist, stabilizing the receptor in a conformation to which the agonist has decreased affinity.
Allosteric regulator	A substance that binds to a receptor at a different site than the ligand, regulating ligand affinity by favoring specific conformations.

Regulation of GPCR activity

The archetypical model of G protein-dependent GPCR signaling starts with an agonist binding to the extracellular part of the receptor, stabilizing the receptor in an active state. This enables interaction with guanine nucleotide-binding (G) protein heterotrimers positioned near the plasma membrane, in proximity to the receptor C-terminus [63]. The active GPCR exchanges the guanosine diphosphate (GDP) on the alpha-subunit of the G protein trimer for guanosine triphosphate (GTP), activating the heterotrimer and leading to dissociation of the subunits Gα and Gβγ. These can in turn interact with other proteins nearby, which subsequently may influence a range of signaling pathways and cellular functions. One role of Gα is to regulate activity of the enzyme adenylate cyclase (AC). AC catalyzes the conversion of adenosine triphosphate (ATP) to cyclic adenosine monophosphate (cAMP), a second messenger that is crucial in many signaling pathways [64]. Four Gα classes have been described in humans. G_i and G_o inhibit AC, while G_s isoforms stimulate the enzyme [57]. G_{12}/G_{13} does not affect AC, but a variety of other signaling proteins [65]. Other proteins may influence the G protein-dependent signal transduction in terms of specificity, duration, efficiency, and strength. These include guanine nucleotide exchange modifying protein groups guanine nucleotide exchange factors (GEFs) and GTPase activating proteins (GAPs). GEFs stimulate the release of GDP, enabling GTP binding, and therefore boosting G protein activation. In contrast, GAPs enhance the rate of hydrolysis of G protein-bound GTP into GDP, terminating G protein activity.

In the last 30 years, it has become clear that GPCR signaling extends far beyond the G protein-dependent mechanisms. G protein-independent activity has been described for a range of GPCRs, including α- and β-adrenergic, dopamine, opioid, purinergic, bradykinin, rhodopsin, angiotensin, and muscarinic receptors [66], establishing that GPCRs may activate signal transduction systems without involvement of G-proteins. GPCRs show an extensive diversity in functional coupling, and the list of proteins identified to bind to GPCRs is rapidly expanding. GPCR-interacting proteins may act either by coupling the receptor to G protein-independent pathways, or even by altering ligand selectivity or specificity [67].

The cascade-like nature of GPCR signaling makes it possible to achieve a full cellular response with a comparatively sparse receptor pool. The expression of GPCRs is therefore often relatively low. Moreover, for some receptors, an agonist occupancy as low as <1% is enough to stimulate a maximum response in some cells [68], demonstrating a generous reserve capacity that enables tissues to respond to agonist stimulation even at very low concentrations.

GPCR desensitization

Active GPCR conformations initiate mechanisms of negative feedback, including regulation of G protein coupling and receptor desensitization. GPCR desensitization is a highly conserved process that involves inhibition of receptor sites critical for signaling, internalization of plasma membrane bound receptors, and general downscaling of the receptor pool through receptor degradation and reduction of receptor mRNA. The effect ranges from relative decreases to full termination of signaling [67]. Internalized receptors are retained for lysosomal or proteasomal degradation, or recycled back to the plasma membrane [69]. This regulatory loop averts physiologically harmful effects that may come from persistent receptor activity.

Specificity in space and time

A large fraction of the signaling proteins in human cells participate in a multitude of pathways, necessitating sophisticated molecular control systems to avoid signals from being over-processed or misdirected. A protein group with a key role in advocating signaling specificity are the scaffold proteins. Scaffold proteins are characterized by multiple binding modules for specific protein-protein interactions. This attribute allows them to gather and act as hubs in multi-molecular complexes which may include receptors, effectors, and positive or negative regulators of signaling (**Figure** 7). By recognizing distinct intracellular compartments such as the plasma membrane, or

interacting with spatially immobile proteins such as transmembrane receptors, the scaffold proteins may retain the complex at specific intracellular sites. Thereby, they control not only which effectors communicate, but also the efficiency of signal transduction in terms of both frequency and amplitude. Thus, scaffold proteins control signal transduction in both space and time, enabling specificity in the regulation of the cells' signaling profile [70]. The adaptor proteins are a group of proteins functionally related to the scaffold proteins. In resemblance to scaffold proteins, adaptor proteins act to bridge interactions between two or more proteins, but generally in a smaller scale and less commonly in a spatially defined manner [71].

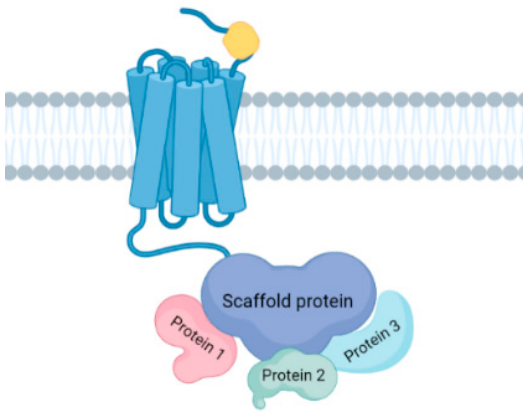

Figure 7. Illustration of a scaffold protein nucleating a complex where protein 1, 2, and 3 are aligned in proximity to a GPCR to promote their interactions and enhance signaling.

GPR30 – history, function, and controversies

For decades, cellular responses to the steroid hormone estrogen was assumed to mainly originate from the cell nucleus, where a larger fraction of estrogen receptor α (ERα) and β (ERβ) are found. These receptors act primarily as ligand-activated transcription factors, which upon activation translocate to the nucleus and activate transcription [72]. However, it had also been documented that estrogen triggers non-nuclear signaling within seconds to minutes after stimulation, including activation of phosphatidylinositol 3-kinase (PI3K), extracellular signal-regulated protein kinase 1/2 (ERK1/2), calcium flux, and production of the second messenger cyclic adenosine monophosphate (cAMP) [73]. Some data propose that classical ERs to some degree are also capable of localizing to the plasma membrane and initiate rapid signaling after

stimulation by estrogen [74], suggesting the existence of different ER pools with various roles in the estrogenic response [75]. However, the ER antagonist fulvestrant was found to be insufficient in blocking all rapid estrogenic mechanisms [76]. These observations led to the search for novel ERs eliciting rapid, non-genomic responses.

In the mid-90s, new molecular techniques led to the discovery of a surge of new GPCRs. During this era, G protein-coupled receptor 30 (GPR30) was cloned by several independent research groups [77-80]. Due to a high level of homology with peptide-binding chemoattractant receptors such as IL-8R-A and CCR5, GPR30 was initially believed to be a chemokine receptor. Yet, the receptor failed to respond to stimulation by a wide range of chemotactic peptides [81]. In 2005, two research groups reported that GPR30 binds 17β-estradiol (E2) with high affinity, mediating cAMP production and ERK½ phosphorylation [82, 83]. Following this, the receptor was officially named G protein-coupled estrogen receptor (GPER) by the International Union of Basic and Clinical Pharmacology [84]. However, many researchers refer to the receptor by the orphan name GPR30 due to persistent controversies regarding the identity of the native receptor ligand [85, 86].

GPR30-mediated signaling

GPR30 has been linked to a multitude of different pathways. Most consistently, the receptor has been described to influence intracellular cAMP levels, ERK1/2 phosphorylation, and Ca^{2+} releases [87-89]. The receptor was early described as a G_s coupled GPCR increasing intracellular levels of cAMP in response to E2 [82]. In contrast, later studies suggest the receptor to inhibit cAMP production, and several GPR30-dependent signaling event are $G_{i/o}$-dependent, as demonstrated by sensitivity to pertussis toxin [90].

The GPR30-mediated increase in ERK1/2 phosphorylation has been suggested to go via pertussis-toxin sensitive transactivation of epidermal growth factor receptor (EGFR) in MDA-MB-231 cells [88]. However, in HEK293 cells, inhibition of EGFR tyrosine kinase did not abolish the ERK1/2 activation, and neither did blockade of PLCβ activation. However, PI3K inhibitors wortmannin and LY-290002 did, suggesting that the GPR30-mediated ERK1/2 stimulation occurs via PI3K in HEK293 cells [90]. In summary, the GPR30-mediated signaling may be dependent on the system and experimental setting (**Figure 8**).

Subcellular localization

The subcellular localization of GPR30 is complex, with receptors both on intracellular membranes and in the plasma membrane. Through clear discrepancies between different studies on both native and recombinant systems have addressing the distribution of GPR30 *in vitro*, and image have emerged that the intracellular positioning of the GPR30 is highly dependent on cell line. An early study reported that an enhanced green fluorescent protein (EGFP)-GPR30 fusion protein transfected into COS7 cells localized to the endoplasmic reticulum, and that endogenous GPR30 in breast cancer cell lines MCF-7, MDA-MB231, and SkBr3 mainly stained intracellularly, leading to the idea that the receptor mainly signals from the endoplasmic reticulum [83]. In a study from 2008, Otto et al. stained for GPR30 in transfected HEK293 and COS-7 cells. They reported only cytoplasmic GPR30 staining co-localized with a marker for the endoplasmic reticulum, while also adding that none of their data can dismiss the probability that part of the receptor pool localizes to the plasma membrane, but that their signal was below the limit of detection [91].

Yet, several studies report expression and activity of GPR30 at the plasma membrane. Plasma membrane expressed GPR30 was reported in HEK293 cells stably expressing HA-tagged GPR30 [92]. Moreover, several studies show that GPR30 participates in protein-protein interactions with effectors positioned in the PM. For instance, GPR30 has been reported to interact with scaffold proteins of the membrane-associated guanylate kinase (MAGUK) family [89]. Interestingly, clinical data show that GPR30 staining specifically in the plasma membrane associates strongly to poor outcome in breast cancer, while total receptor expression did not, indicating that positioning of the receptor may have relevance in breast cancer pathophysiology [93].

Which factors contribute to determining the subcellular localization of GPR30 remains poorly understood. It was observed that estrogen treatment triggered GPR30 translocation to the plasma membrane [94]. Interestingly, the latter interaction appears to contribute to retaining GPR30 in a plasma membrane bound position, and depend on a four amino acids long [89].

Taken together, the existing data suggest the GPR30 subcellular distribution to be complex and highly dependent on the biological context. Importantly, the subcellular localization of the receptor may have important implications for receptor function on the cellular as well as physiological level (**Figure 8**).

Constitutive GPR30 activity and the C-terminal PDZ motif

In recent years, it has become clear that GPR30 harbors a considerable level of constitutive activity. It was shown early that knockdown and overexpression of GPR30 had opposing effects on baseline cell growth of breast cancer cell line MCF-7 in the absence of added ligands [95]. Similarly, GPR30 was found to constitutively suppress growth of MDA-MB-231, MDA-MB-468, and HEK293 cells [96, 97].

In later studies on recombinant mammalian systems, it has been demonstrated that the basal GPR30 activity also includes effects on cAMP and ERK1/2 phosphorylation [89, 90]. Interestingly, all constitutive GPR30 signaling studied in such systems has been found to rely on a canonical type I PDZ motif at the receptor C-terminal, -SSAV [89, 90, 98]. PDZ motifs are conserved interaction motifs found on the C-terminal of some GPCRs, where they govern interactions that are involved in regulation of receptor trafficking and signaling. Further, truncation of the GPR30 PDZ-motif led to an increased level of receptor endocytosis [89], indicating that this motif governs an interaction that retains the receptor in a plasma membrane position, and that this position is essential for constitutive GPR30 activity (**Figure 8**).

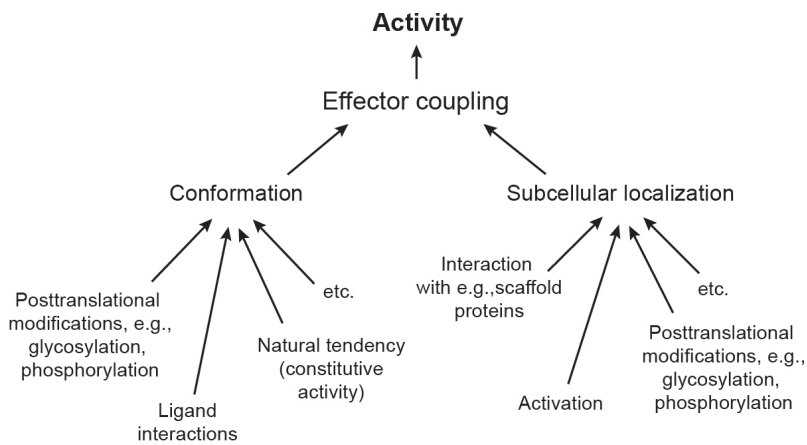

Figure 8. Factors that may influence GPCR activity. The activity of a GPCR balances on opposing mechanisms stimulating or preventing effector coupling. The main factors are the relative time in which the receptor exists in active conformations, and receptor presence at a localization where ligand and effector interactions are feasible. The third main factor is effector availability, which may depend on e.g. cell-specific expression of the effectors and other proteins competing for the same effector interactions, or presence of other receptor or effector-interacting molecules that may disturb essential interaction interfaces.

E2 and G-1 – the proposed natural ligand and synthetic agonist

Following the early reports that GPR30 mediates rapid signaling upon binding E2 (**Figure 9**) [82, 83], E2 has been assumed to be the native ligand of GPR30. As E2

could not offer selective pharmacological targeting of GPR30 due to potential background noise from ERα and ERβ, a screening project aiming on identifying selective GPR30 ligands was performed on a library of compounds pre-optimized for a GPCR-privileged substructure, and further narrowed down based on structural similarity to E2. This project led to the identification of G-1 (**Figure 9**), a proposed GPR30 agonist [1]. Since then, G-1 has been used extensively in research to implicate GPR30 activity, and the compound is commercially marketed as a selective GPR30 agonist [99].

Yet, a plethora of studies report findings questioning the identity of GPR30 as an estrogen receptor activated by G-1. In a study published only one year after the initial reports that GPR30 is an estrogen receptor, Levin and colleagues showed that membranes prepared from ER-positive MCF-7, but not ER-negative SkBr3, significantly binds isotope-labeled E2 [87]. Interestingly, both cell lines express GPR30. Additionally, treatment with E2 triggered rapid signaling in terms of ERK1/2, PI3K, calcium and cAMP in MCF-7 cells. In contrast, E2 triggered only a calcium flux in SkBr3 cells, a mechanism that was not sensitive to GPR30 knockdown [87]. Several other independent efforts have been made to confirm the initial observations through the years; some supporting the initial reports of E2 stimulating GPR30 activity [88, 100], while other report a lack of an E2-stimulated signal in systems expressing GPR30 [87, 89, 91, 101], or that the E2 signal was insensitive to GPR30 knockdown [87]. Similarly, GPR30-dependent G-1 effects have been presented in a number of studies, while other studies fail to observe any GPR30-dependent effects [91, 98, 101].

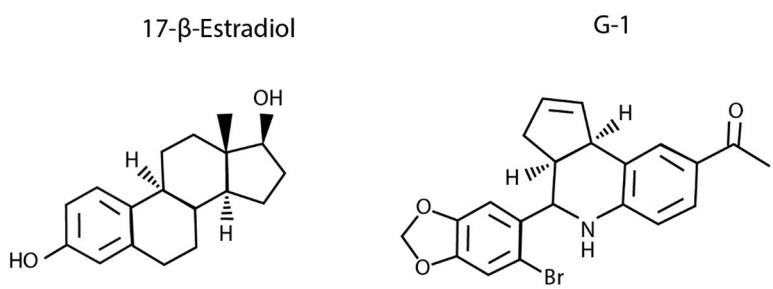

Figure 9. Structure of 17β-estradiol and G-1. Image adapted from [1, 2]

Interestingly, both E2 and G-1 have also been shown to elicit rapid, non-genomic signaling through the ERα splice variant ERα-36 [101], and E2 through a palmitoylated plasma membrane-anchored version of ERα [102].

In summary, the identity of GPR30 as an estrogen receptor, and G-1 as a selective GPR30 agonist, remain disputed. The conflicting findings through the years have led to discussions on the soundness of the initial reports [85, 86, 103], and some researchers still consider GPR30 an orphan receptor.

Potential interaction partners **of GPR30**

AKAP5

Protein kinase A (PKA) is a family of enzymes that respond to intracellular cAMP levels. When intracellular cAMP levels rise, cAMP binds to PKA and allosterically initiates a conformational change that enables the PKA holoenzyme to transfer a phosphate from cAMP to a target protein [104]. PKA has hundreds of substrates and participates in a plethora of pathways [105]. With this diverse signaling profile, and with numerous PKA-responsive events being simultaneously active at any given time, molecular systems dedicated to spatiotemporal regulation of PKA activity have evolved to prevent inadvertent crosstalk or over-stimulation of signaling pathways. Additionally, cAMP elevations often appear as gradients around the site of accumulation, making it crucial to position cAMP-dependent enzymes and ion channels correctly [106-108]. The idea that PKA specificity is governed by anchoring proteins that tether the holoenzyme to particular microdomains has been supported by a considerable body of data through the years [109, 110].

A-kinase anchoring proteins (AKAPs) are a growing group of scaffold proteins functionally related through their ability to link PKA to selected targets and specific subcellular locations. Due to distinct targeting repertoires of each specific AKAP, these proteins direct signaling transduction in different manners [111]. AKAP5, also named AKAP79/AKAP150, is an AKAP involved in e.g. directing β-adrenergic signaling [112].

Interestingly, a recent study found a prominent enrichment of somatic mutations and differential expression of AKAP genes in metastatic breast cancer lesions compared to primary tumors [113].

Membrane-associated guanylate kinases (MAGUKs)

The membrane-associated guanylate kinases (MAGUKs) constitute a well-conserved family of scaffold proteins that is widely expressed in human cells. MAGUKs reside by the plasma membrane, where they assemble protein complexes to streamline or direct

signaling. The defining trait of MAGUKs are their inclusion of three protein-protein interaction domains, including the PDZ domain. The PDZ domain recognizes PDZ motifs present on other proteins, including GPCRs [114]. A report that estrogen increases expression of a number of postsynaptic MAGUKs, especially synapse-associated protein 97 (SAP97), led to the finding that GPR30 interacts with SAP97 in the mouse hippocampus [115]. Since then, complexes between GPR30 and MAGUKs have been identified in a number of systems.

In HEK293 cells, ectopically expressed GPR30 interacts withSAP97 and post-synaptic density-95 (PSD-95). Truncation of the receptor PDZ motif to prevent this interaction leads to a reduced constitutive signaling, but also an increased receptor endocytosis, suggesting plasma membrane localization to be essential for this activity [89]. GPR30 has also been shown to interact with PSD-95 in the rat hippocampus, where the interaction supports receptor plasma membrane expression [116]. Lastly, members of the MAGUK family interacts with AKAP5 via a unique interaction domain [117, 118].

Other potential GPR30 interaction partners

Receptor-activity-modifying proteins (RAMP) proteins are a group of proteins previously known to influence the pharmacological profile and ligand recognition of the calcitonin-receptor-like receptor (CRLR) [119, 120]. Evidence show that GPR30 interacts with RAMP3 in some cell systems, and RAMP3 was increasingly located by the plasma membrane when co-expressed with GPR30 [121]. Additionally, RAMP3 is transcriptionally activated by estradiol, which is not the case for either RAMP1 or RAMP2 [122, 123]. However, RAMP3 did not promote plasma membrane positioning of GPR30 in MCF-7 breast cancer cells (unpublished data gathered for the projects of this thesis).

A study from 2020 studying the role of follicle-stimulating hormone receptor (FSHR) in cAMP-driven oocyte maturation reported that FSHR heteromerizes with GPR30. FSHR is generally assumed to be G_s-coupled, and therefore elevate intracellular cAMP, leading to a decrease in cell viability. Intriguingly, heteromerization with GPR30 shifted the signaling profile towards suppressing cAMP production, subsequently promoting oocyte viability. Interestingly, it was shown that this effect was dependent on AKAP5 expression [124].

ERα-36

Three major ERα isoforms have been reported in breast cancer cell line MCF-7, corresponding to three mRNA variants generated by different promoters and alternative splicing [125]. The full-length 66 kDa isotype (ERα-66) is the most explored and well-known of the ERs. However, in recent years, the splicing variant ERα-36 has caught attention in ER research. This variant is a 36 kDa isotype preserving the DNA-binding domain, dimerization faculty and a partial ligand-binding domain [126]. In contrast to the full-length variant, data suggest that a high fraction of ERα-36 resides in the plasma membrane. ERα-36 has been detected in both ER positive and ER negative breast cancer cells [127], and shown to mediate E2-effects in TNBC [128]. Studies report that ERα-36 activates ERK in response to estrogens, tamoxifen [127], and G-1 [101, 129]. Hence, there is an overlap in downstream events reported for GPR30 and ERα-36. Interestingly, GPR30 expression has been reported to induce endogenous expression of ERα-36 in HEK293 and COS7 cells [101].

Expression

GPR30 is ubiquitously expressed in normal human and rodent tissues [77, 79, 80, 130-132]. The receptor generally shows a sexually dimorphic pattern in rodents, but no clear data for humans currently exists [133]. Nonetheless, data suggest GPR30 expression to vary with periods of distinct hormonal changes, such as progression of puberty [134] and menopause in humans [135].

GPR30 in breast cancer

Being assumed to mediate rapid, non-genomic signaling events in response to estrogen, GPR30 has attracted attention in breast cancer research. Numerous studies have addressed GPR30 expression in relation to breast cancer outcome, with varying findings. High expression of the receptor has been associated with ER and PR positive status [93, 97]. However, while some reports show that high GPR30 expression associates to an improved prognosis [97, 136], other find either an association to a poor prognosis [93, 137] or no relationship to outcome [138].

Similarly, while the receptor has been shown to promote apoptosis in the ER-positive breast cancer cell line MCF-7 *in vitro*, receptor expression increased proliferation in the ER-negative breast cancer cell line SkBr3 [95, 97, 139], suggesting the biological context to influence the role of GPR30 in breast cancer. Interestingly, plasma

membrane expression of the receptor was found to be a strong prognostic factor for poor breast cancer outcome, while total receptor expression was not [93].

GPR30 as a mediator of tamoxifen resistance

Through the years, both *in vitro* and clinical data have suggested that there may be an association between GPR30 and the endocrine agent tamoxifen. An early study reported that tamoxifen resistant MCF-7 cells responded with an increased growth and ERK1/2 activity to low concentrations of tamoxifen, in contrast to the growth inhibition shown in native MCF-7. This effect was abrogated by GPR30 silencing, leading to the idea that tamoxifen acts as a GPR30 agonist [94]. Interestingly, a later study showed that ERα isotype ERα36 also inhibited growth and suppressed EGFR and ERK1/2 signaling. Additionally, it was shown that GPR30 induced ERα36 expression [140].

A clinical study reported that GPR30 was a favorable factor for risk-free survival (RFS) for breast cancers that was not treated with tamoxifen, with a non-significant indication that the prognostic function of the receptor was reversed in breast cancers receiving tamoxifen [141]. Similarly, a study from 2019 compared the outcome of breast cancer patients treated with tamoxifen or aromatase inhibitor in relation to their GPR30 status, declaring that patients with high GPR30 responded poorer to tamoxifen than aromatase inhibitor treatment. However, this conclusion was not supported graphically or by an interaction test [142]. A small study quantified GPR30 expression in 21 paired biopsies from breast cancer before and after adjuvant tamoxifen treatment. The observation that GPR30 expression generally was elevated in recurrences after treatment was interpreted that increased receptor expression may contribute to tamoxifen resistance [141].

Based on these findings, GPR30 has been proposed to facilitate a mechanism allowing breast cancer cells to resist tamoxifen. However, large-scale GPR30 expression data from tamoxifen resistant breast tumors is needed to further understand the role of GPR30 in tamoxifen resistance.

GPR30 in hypoxia

Several independent research groups have documented a link between GPR30 and hypoxia. GPR30 upregulation was reported after hypoxic exposure in mice muscle cells and human breast cancer cell line SkBr3, and it was shown that the promoter region of *GPER1* contains HRE [143, 144]. Knockdown of GPR30 was reported to abrogate

hypoxia-induced activation of the VEGF promoter in cancer associated fibroblasts, suggesting the receptor to play a part in hypoxic adaptation [145]. Interestingly, unpublished data from the contralateral breast cancer material presented in study I of this thesis revealed a linear relationship between HIF-1α and GPR30 protein levels in contralateral breast tumors. Additionally, HIF-1α-positive BC1 were more than twice as likely to express GPR30 at the plasma membrane, and HIF-1α-positive BC2 were four times as likely. These relationships were independent on ERα status (unpublished data).

The β_1-adrenergic receptor

The adrenergic receptors are a class of GPCRs activated by epinephrine and norepinephrine. Their functions are forged through evolution to optimize the mammalian fight-or-flight response, including mechanisms such as elevated heart rate and blood pressure. The adrenergic receptors comprise the two major types α and β, which despite sharing the same group of ligands wield different physiological functions due to tissue expression and ligand potency rank. Adrenergic targeting has been widely utilized in pharmaceutical management of cardiovascular diseases [146]. The β_1-adrenergic receptor (β1AR) is the predominant adrenergic receptor in the heart, where it regulates myocardial contractility and heart rate. Selective β1AR blockade is prescribed for several cardiovascular conditions, including hypertension, post-myocardial infarction, and heart failure, but also tremor and anxiety.

The activated β1AR increases cellular levels of cAMP via G_s-dependent activation of AC. In cardiomyocytes, the β1AR-induced rise in cAMP activate PKA, leading to phosphorylation of a number of Ca^{2+} regulatory proteins [147]. In summary, β1AR augments the reuptake of Ca^{2+} into the sarcoplasmic reticulum, which enables more frequent and stronger Ca^{2+} releases. This subsequently increases heart muscle contractility and amplifies the heart rate [148].

β1AR and GPR30

The interactomes of β1AR and GPR30 share several features. In similarity to GPR30, the C-terminal of β1AR contains a type 1 PDZ motif, through which the receptor interacts with the MAGUKs PSD-95 [149] and SAP97, regulating agonist-induced receptor trafficking. Additionally, β1AR interacts with AKAP5 and PKA through scaffolding by SAP97, which affects receptor phosphorylation by PKA [69, 150]. In

cardiomyocytes, β1AR forms a complex including AC, PKA, and AKAP5, and knockdown of AKAP5 impedes βAR-mediated signaling [151]. Interestingly, GPR30 impedes β1AR-mediated cAMP production through a PDZ-dependent, pertussis toxin-insensitive mechanism [89], indicating some level of intercommunion between the receptors.

β1AR and breast cancer

β1AR has been reported to be overexpressed in breast cancer [152]. A number of meta-analyses have been performed to approach the relationship between β-blockers and breast cancer, without a clear consensus. While some data suggest that β-blocker use is unrelated to breast cancer risk [153], some beneficial effect has been observed in relation to breast cancer specific survival [154], with trends of a favorable effect in relation to breast cancer incidence [153], progression and recurrences [154, 155]. As of today, most of the existing studies consider different types of β-antagonists grouped together, limiting the ability of drawing conclusions in a pharmacological and molecular sense. Indeed, some data suggests that different modes of selective β-targeting wields different biological effects. One study showing evidence of a protective effect of β-blocker reported the non-selective β-blocker propranolol to be of the greatest benefit [154]. Additionally, one study found that non-selective β-blockers reduced proliferation markers in early-stage breast tumors and breast cancer cell lines, while β1-selective atenolol did not associate to this beneficial effect [152]. Finally, a recent study on Swedish national registers found that hypertensive patients using β1-selective blockers metoprolol, atenolol, and bisoprolol faced a twofold risk of being diagnosed with breast cancer compared to propensity score matched non-users. Interestingly, the risk increased with dosage [156]. To summarize, current data is inconclusive – possibly due to differences in patient cohorts and pooling of different β-blockers – and the role of β-adrenergic signaling in breast cancer development and progression remains poorly understood.

Rationale

Breast cancer is the most commonly diagnosed cancer type worldwide as of today, and with an aging population, the prevalence is predicted to rise during the next decades. By nature, cancer is in constant evolution. Tumor cells are hardwired to strive to survive even during exposure to anti-cancer treatments, making drug resistance a substantial concern in modern cancer care. Thus, it is crucial to identify new, effective drug targets.

GPCRs are among the most common drug targets in modern medicine, accounting for up to 45% of all prescription pharmaceuticals [59, 157]. Yet, most GPCRs are not well enough understood to be medically useful. GPR30 was first cloned in the early 2000s, and soon reported to elicit rapid, non-genomic signaling in response to estrogen. Following these findings, the receptor was officially renamed G protein-coupled estrogen receptor (GPER) by the International Union of Pharmacology. However, the relationship between estrogen and GPR30 remains unclear, with several studies having failed to detect a GPR30-dependent response upon estrogen stimulation. As a result, some researchers still refer to the receptor by its orphan name, GPR30. GPR30 has been extensively studied in the context of numerous pathophysiological mechanisms both *in vitro* and *in vivo*, including breast cancer. However, the majority of these studies have used the synthetic agonist G-1 to implicate the receptor, and many lack proper negative controls for GPR30 expression. Thus, a large portion of the existing data on GPR30 relies profoundly on the selectivity of G-1. This is particularly concerning in light of earlier data questioning G-1 as a GPR30 agonist [103]. Understanding the pharmacological profile of GPR30 is essential in order to evaluate the receptor as a drug target. Nevertheless, the field of GPR30 research has been marbled with controversy due to inconsistent results and poorly validated methods, which most possibly decelerates the scientific progress. In order for the field to advance, there is a firm need to understand the relationship between G-1, E2, and GPR30 in terms of receptor activation.

A study from 2014 reported that plasma membrane expression of GPR30 associated to a poor prognosis in breast cancer [93], drawing attention to the question of which factors determine the subcellular localization of this GPCR. Interestingly, previous data from recombinant cell systems have shown that a plasma membrane position promotes constitutive activity of GPR30. The β1AR have also been associated with breast cancer incidence and outcome [153-155]. Interestingly, β1AR shares some interaction partners with GPR30, and GPR30 has been found to constitutively inhibit β1AR-mediated signaling [89]. The interaction between these GPCRs has never been characterized in a system with native receptors, and never in breast cancer. Characterization of the nature and causal effects from this interaction in breast cancer cells may increase our understanding regarding the pharmacology of GPR30, and the role of GPR30 and β1AR in breast cancer pathophysiology.

With treatment resistance being a central dilemma in modern breast cancer care, there is a need to discover new biomarkers that help identifying resistant tumors prior to treatment. In breast cancer, GPR30 has been associated to outcome and treatment response to the endocrine agent tamoxifen. Indeed, some data have indicated that tamoxifen is a GPR30 agonist. If GPR30 contributes to breast cancer pathology and is activated by the common breast cancer therapy tamoxifen, this could in the worst case mean that tamoxifen stimulates growth in tumors expressing GPR30. However, would this be the case, the receptor could also be utilized as a marker of tamoxifen resistance, which would be of considerable value in the quest of personalizing cancer treatment. Hence, it is motivated to address whether GPR30 helps tumors survive under tamoxifen exposure.

Post-surgical radiotherapy is standard of care for early-stage breast cancer, and reduces the risk of recurrences considerably. However, despite radiotherapy, many breast cancer patients suffer from recurrences [158]. An additional radiotherapy boost directed at the tumor bed has been shown to reduce the risk of recurrences [159], but also causes side effects and is possibly not necessary in a majority of the cases. New biomarkers are required to identify patients with an increased risk of recurrences, and who could possibly benefit from radiotherapy boost treatment. Tissue oxygen levels are known to influence the biological response to radiation [46]. Low oxygen levels, hypoxia, is frequently occurring in solid tumors, where it upregulates the transcription factor HIF-1α. HIF-1α regulates gene expression related to hypoxic adaptation, and has been linked to poor outcome in contralateral breast cancer [43]. However, it remains unclear

if HIF-1α could serve as a predictive marker of radiotherapy resistance. Additionally, while previous studies show promising data on the prognostic value of HIF-1α, using the protein as a biomarker would be technically difficult due to its minute-range half-life in an oxygenated environment. This motivates a search for surrogate markers of hypoxia, e.g., more stable proteins induced by hypoxia, or hypoxic gene expression signatures.

Aims of thesis

The overall aim of this thesis was to explore molecular factors in breast cancer and how they impact the benefit of common modes of treatment, in order to increase knowledge on how to design personalized treatment strategies.

The specific aims of this thesis were:

- To evaluate the G protein-coupled receptor GPR30, also known as G protein-coupled estrogen receptor 1 (GPER1) as a prognostic and predictive marker, as well as a mediator of tamoxifen resistance in contralateral breast cancer
- To address the relationship between GPR30 and the proposed ligands E2 and G-1
- To identify functional signaling complexes containing GPR30 in breast cancer cells and characterize their influence on receptor function
- To evaluate the relevance of tumor hypoxia in relation to breast cancer outcome in general and radiotherapy specifically

General methodology

Preclinical studies

Cell lines

Human cell lines

For pharmacological approaches, applied mainly in study II, we used cervical carcinoma cell line HeLa and human embryonic kidney cell line HEK293, cell systems that are well described for GPCR research.

In study IV, we addressed the function and interactions of GPR30 in breast cancer cells. Hypothesizing that GPR30 exists in a multi-protein complex containing β1AR, AKAP5, and a scaffold protein from the MAGUK family in breast cancer cells, we selected a breast cancer cell line natively expressing these proteins (**Figure 10**).

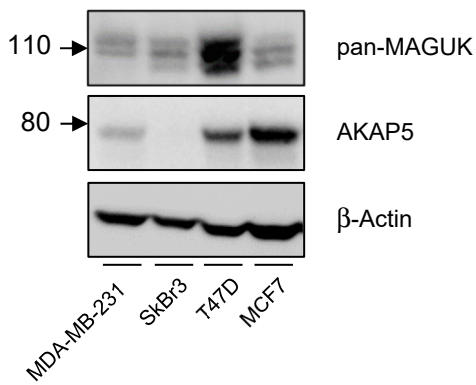

Figure 10. Expression of MAGUK proteins, AKAP5, and housekeeping reference β-Actin. Image from study IV.

Yeast

To reduce system complexity and risk of interference from medium- and cell-derived estrogen or other human GPCRs in pharmacological experiments in study II, we used the budding yeast *Saccharomyces cerevisiae* (*S. cerevisiae*). Endogenously, *S. cerevisiae* expresses one single GPCR (Ste2p/Ste3p) that couples to the MAPK pathway via the G_α protein Gpa1 in response to stimulation by pheromones. By coupling a heterologously expressed human GPCR to the pheromone pathway, the *S. cerevisiae* system has been utilized to characterize pharmacological profiles of several human GPCRs [160]. In Study II, we used the *S. cerevisiae* strain CY2797, in which the native *STE2* gene is disrupted. Furthermore, CY2797 is auxotrophic for histidine unless the pheromone pathway is activated, making a lack of activation reflect in growth rate.

Based on CY2797, we constructed the new strain EY-1, in which we expressed a chimeric G_α protein where the C-terminal Gpa1 residues were replaced with the sequence of the human G protein Gai2, the purpose being to promote coupling with heterologously expressed human GPR30.

Transfection

In study II and IV, the functions of particular proteins were studied by overexpressing the in cells that normally exhibit low or no expression of these proteins. This was performed by transfection, a method of artificially presenting DNA into cells *in vitro*. DNA is a negatively charged, relatively large macromolecule with poor plasma membrane permeability. To increase cellular uptake, the DNA is encapsulated into nano-sized phospholipid vesicles, liposomes, which are able to pass through the plasma membrane.

Fluorescence Microscopy – immunocytochemistry

In study I (supplemental material) and study IV, we applied immunocytochemistry with analysis using a fluorescence microscope; a common method to investigate protein expression. This can be performed on live cells or cells fixed using e.g. paraformaldehyde. The specimen is tagged with fluorophores that selectively bind to targets of interest, e.g. DNA, organelle markers, or a specific protein. Some fluorophores are designed to detect and bind directly to the target, but the most common approach for fluorescent tagging of proteins is a two-step procedure where the sample is incubated with a selective primary antibody that binds to the protein, and then with a fluorophore-conjugated secondary antibody that binds to the primary

antibody. The sample is then imaged while illuminated by lasers that excite the selected fluorophore markers.

Confocal microscopy

In this thesis, fluorescence microscopy is performed using a confocal microscope, also called a confocal laser scanning microscope. Using a spatial filter, or pinhole, the confocal microscope enables analysis of thin cross sections of the sample. This makes it possible to analyze markers spatially and in relation to other proteins or cell compartments.

Flow cytometry

In study II and IV, flow cytometry was applied to address protein expression and distribution. Flow cytometry is a quantitative laser-based technology used to analyze characteristics of individual cells in a population. Using specific antibodies, the proteins of interest are fluorescently tagged and detected by laser illumination. Once the lasers have excited the fluorescent markers, light signals are converted into data.

In this thesis, we analyze cells fixed in paraformaldehyde, either permeabilized with the detergent Triton-X100 for whole-cell analysis, or kept intact to quantify fluorescence from plasma membrane-bound proteins exclusively. Flow cytometry is often used to physically separate cells based on selected attributes, known as fluorescence-activated cell sorting (FACS).

Western blot and co-immunoprecipitation

Western blot is a method of detecting proteins in a sample using size-based separation and immunostaining. The idea is to run the proteins through a sieving matrix where they travel different lengths depending on size. After lysate collection, the proteins are heated with the detergent sodium dodecyl sulfate (SDS) or similar. This denatures the proteins, meaning that they lose their tertiary structure, and as SDS binds to the protein residues, the proteins gain negative charges corresponding to their molecular size. As the denatured sample is added to a polyacrylamide gel and subjected to an electric current, a process called polyacrylamide gel electrophoresis (PAGE), they begin traveling through the gel in the direction of the positively charged anode. The relative movement of each denatured protein is mainly decided by their charge and bulkiness. After separation, the proteins are transferred to a membrane, again by application of an electric current. Lastly, the protein of interest is visualized by incubating the membrane

with specific antibodies that react with a developing mixture and emit light detectable by a digital imager.

Co-immunoprecipitation is an extended version of immunoprecipitation, which is a method of purifying a specific protein from for example a cell lysate. A specific antibody is added to the sample, where it forms a complex with the protein of interest. The immune-complexes are then collected by incubation with sepharose beads to which an antibody-binding protein, often protein A or protein G, is bound. The protein-antibody complexes adhere to the beads, and remain in the sample as the rest of the protein slurry is rinsed off. Finally, the protein-antibody complex is eluted and may be analyzed by western blot. However, proteins in interaction with our protein of interest from native complexes formed before cell lysis may remain in the sample. This is utilized in co-immunoprecipitation, where an extra mild cell lysis and rinsing is applied to optimize the integrity of native complexes. After SDS-PAGE, the membrane may be stained for potential interaction partners of the isolated protein.

BRET

In study IV, we used Bioluminescence Resonance Energy Transfer (BRET) to characterize the interaction between GPR30 and β1AR. BRET has been extensively used to study the protein-protein interactions in the dynamics and activities of GPCRs, including effector coupling, trafficking, and multimerization [161]. The method is based on ectopic expression of two proteins of interest, where one has been fused with an energy donor molecule, normally the *Renilla* luciferase enzyme, while the other protein has been fused with an acceptor molecule, a fluorescent protein. When the proteins are in close proximity, normally within a distance 10 nm, an energy transfer between the donor and acceptor molecule activates the bioluminescence of the acceptor protein [161, 162]. Hence, the bioluminescence readout gives an idea on whether the proteins of interest interact physically.

Reporter systems used for assaying receptor activity

GloSensor cAMP assay

In study IV, we used the GloSensor cAMP assay from Promega to measure GPR30 activity in terms of cAMP production. The system enables real-time monitoring of intracellular cAMP levels of live cells, based on the bioluminescent reaction where the enzyme luciferase catalyzes a two-step reaction cleaving luciferin to oxyluciferin. After this catalysis, oxyluciferin is in an electronically excited state, and its decay to the

ground state emits light through the release of a photon [163]. To prepare for assaying, the cells are transfected to overexpress a circularly permuted firefly luciferase, and incubated with luciferin for 2 h. Upon binding cAMP, the overexpressed luciferase mutant undergoes a conformational change that increases the enzymatic activity. Hence, the luminescence detected in a cell sample is in proportion with the intracellular cAMP levels of the cells.

T-REx inducible protein expression system

In study II, we used a HFF11 based cell line with inducible expression of FLAG-tagged GPR30. This cell line stably expresses the Invitrogen T-REx expression system, a tetracycline based two-step inducible system [164]. The system includes three plasmids; the first containing a gene encoding the protein of interest (in our study FLAG-tagged GPR30), the second encoding a protein that represses the first plasmid, and the last plasmid is used as a control. In the absence of tetracycline, TetR, which is the protein product of the repression plasmid, forms a homodimer and binds with high affinity to the promoter of the GPR30 plasmid, blocking transcription. Upon introduction, tetracycline binds to TetR, triggering a conformational rearrangement that releases it from the operator, enabling transcription of GPR30.

pcFUS3

The HeLa-based reporter cell lines HFF11 and HFF11-2, both used in study II, stably express the vector pcFUS3 (**Figure 11**). This reporter vector has a pcDNA3 backbone and contains a synthetic promoter constituting 6 response elements for NFκB and STAT, which overlap, and 9 response elements for AP-1 (also known as TPA responsive element, TRE) upstream of a minimal c-FOS promoter [165]. This method funnels down the activity from a multitude of pathways into one single marker of transcriptional activity, enabling the reporter to respond to the activity of a wide range of receptor signals.

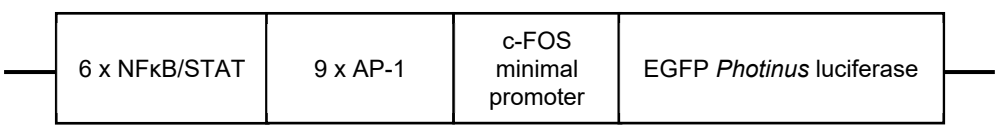

Figure 11. The pcFUS3 reporter construct, with response elements indicated.

Rac1Cluc

The Rac1 reporter construct used in study II was constructed using two previously described reporter plasmids; the ERK1/2 sensor called mitogen-activated protein kinase activity reporter ($MAPK_{AR}$) [166] and the RaichuEV-Rac1 [167]. The ERK1/2 sensor region of the $MAPK_{AR}$, which is positioned between the N-terminal and C-terminal regions of a click beetle luciferase, was replaced by the Rac1 sensor region of the RaichuEV-Rac1 plasmid. Upon phosphorylation of the click beetle luciferase-Rac1 fusion, a configurational reorganization results in the two parts of the luciferase being joined, which in turn makes the construct bioluminescent.

NFAT

The Nuclear factor of activated T-cells (NFAT) reporter construct is a transcriptional reporter responding to activity of NFAT. NFAT is a transcription factor responding to intracellular Ca^{2+} levels. When intracellular Ca^{2+} rises, the calcium-dependent phosphatase Calcineurin dephosphorylate NFAT, triggering nuclear translocation and transcriptional activation [168]. The reporter plasmid contains three NFAT binding sequences upstream of a luciferase reporter on the backbone of pGL3; a vector that lacks other promoters [169]. Therefore, increased bioluminescence of cells transfected with the reporter corresponds to elevated levels of intracellular Ca^{2+}.

Statistics – preclinical studies

Statistical analysis of preclinical data was performed in GraphPad Prism version 9.1.1 (GraphPad Software, Inc., San Diego, CA). Statistical tests used in the preclinical studies of this thesis are summarized in Table 2.

Table 2. Summary of statistical tests used in the preclinical studies in the thesis.

Analysis	Data type	No. of groups	Data distribution	Test
Data distribution				Shapiro-Wilk test, with alpha set to 0.05
Two-group comparison	Non-paired	2	Parametrical	Students t-test
Two-group comparison	Non-paired	2	Non-parametrical	Whitney-Mann U-test
Multiple groups comparison	Non-paired	2<	Parametrical	Ordinary one-way ANOVA with Tukey's multiple comparisons test
Multiple groups comparison	Non-paired	2<	Non-parametrical	Kruskal-Wallis test with Dunn's multiple comparisons test

Clinical studies

Patients and tumor material

Study I

Study I is based on a cohort of patients diagnosed with metachronous contralateral breast cancer (CBC) within the Southern Health Care Region of Sweden between 1977 and 2007. The cohort includes 688 patients with metachronous CBC as primary event. Among the patients analyzed in this particular article, the interval between the diagnosis of the first breast cancer (BC1) and the contralateral breast cancer (BC2) ranged between 6 months and 34.1 years. Median follow-up for event-free patients was 9.1 years from BC2 diagnosis.

We accessed a previously constructed, unique tissue microarray (TMA) containing tumor material from BC1, BC2, and, where available, paired lymph node metastases (LGL1 and LGL2) from this cohort. GPR30 was successfully stained using immunohistochemistry (IHC) in 559 BC1 and 595 BC2.

Study III

In study III, we accessed data from the SweBCG91-RT trial, a Swedish randomized controlled trial of radiotherapy after breast-conserving surgery. The SweBCG91-RT material encompasses 1178 women diagnosed with node-negative stage I and IIA breast cancer randomized between 1991 and 1997. While the control group was not subjected to radiotherapy, the patients in the radiotherapy treated group received whole-breast radiation in 24-27 fractions, 48-54 Gy with tangential opposed fields of 4-6 MV photons. According to regional guidelines at the time, systemic adjuvant treatment was sparsely administered. Ipsilateral breast tumor recurrence (IBTR) as first event within 5 years was used as primary endpoint, with any recurrence within 5 years and breast cancer-specific death (BCD) within 10 years as secondary endpoints. Median follow-up for event-free patients in the study was 15.2 years for IBTR, 15.2 years for any breast cancer recurrence, and 20.1 years for BCD. One thousand and four of the total 1178 primary tumors were available for tumor tissue analysis. RNA was successfully extracted from 766 primary tumors. For study III, 1004 of the total 1178 primary tumors were available for tumor tissue analysis.

Gene expression analysis

Gene expression analysis was performed in study III. RNA was successfully extracted from 766 primary tumors. Extraction of RNA, microarray hybridization, and quality control of RNA, cDNA, and microarray analysis were performed at Decipher Biosciences, a laboratory certified by Clinical Laboratory Improvement Amendments. Profiling of tumors were made using GeneChip Human Exon 1.0 ST microarray from Thermo Fisher, and normalization of gene expression data was made using Single Channel Array Normalization (SCAN) [170]. The SCAN method is developed to correct for batch effects, such as technological biases and variabilities from sample collection and processing. In personalized medicine workflows, non-biological variance may otherwise arise between samples not collected or processed at the same time.

Gene expression signature scoring

In study III, we hypothesized that a hypoxia-induced gene expression signature could serve as a surrogate marker for the hypoxia-induced transcription factor HIF-1α, and perform equally as a prognostic marker in a breast cancer cohort. We selected 11 previously described gene expression signatures condensed from both cancer tumor material or *in vitro* approaches. To evaluate concordance between these signatures and HIF-1α protein expression, we needed to translate gene expression from each tumor in the material into a continuous score. To this end, we used the R package *singscore*, which is developed to minimize the influence from the cohort by evaluating expression levels by intra-sample ranking [171], which is advantageous in a personalized medicine workflow.

Survival analyses

Time-to-event data in relation to selected biomarkers or transcriptomic signatures was analyzed using the cox proportional hazards model and graphically demonstrated using competing risk curves. The cox proportional hazards model is a regression model used to test for differences in outcome in relation to the variable of stratification, which may be dichotomous, nominal, or continuous. A hazard ratio (HR) is calculated for the full follow-up, therefore assumes a proportional hazard during this period. Proportionality in hazard can be assessed graphically or using Shoenfeld's test. In cases where the proportionality assumption is not met, the calculated HR should be interpreted cautiously as the mean hazard of the time studied. Non-proportional hazards may also be studied in intervals using truncated time variables, an approach used in study IV. To account for other established biomarkers, patient characteristics, or other suspected

confounders, multiple factors may be added to the model and computed simultaneously in a multivariable cox proportional hazards model. This is a way of testing whether the biomarker of interest is an independent predictor of the endpoint.

A common method of presenting stratified time-to-event data graphically is the Kaplan-Meier curve. In the Kaplan-Meier curve, groups are plotted separated by the studied exposure, starting at 1 or 100% to demonstrate that no participant has had an event at time=0, and successively dropping as events occur in the study groups. Differences between two or more groups may be tested using the log-rank test. The Kaplan-Meier method censors patients lost to follow-up, assuming the likelihood of censoring to be equal in the two groups. However, this may result in the graph being misleading, as events leading to censoring may associate to the studied exposure. For example, if we study a biomarker more common among elder patients in relation to cancer recurrences, the biomarker-positive group will possibly have a higher censoring rate due to death from other causes, and naturally fewer recurrences. Additionally, the censoring at competing events may lead to an overestimation of the risk. Competing risk curves is a different way of showing time-to-event data that takes this into consideration. Competing risk curves are based on the same idea as the Kaplan-Meier curves, but also stratifies the patients based on whether they experienced the event selected as the primary endpoint, or had a competing event. This way, we can more easily consider the events of interest in an isolated way.

In study I and IV, we addressed GPR30 and HIF-1α as predictive markers, meaning that the marker predicts the response to a particular mode of treatment. If a marker is predictive, the impact of the individual terms representing the biomarker and treatment status will not be additive, but instead either work in synergy (meaning that presence of the biomarker makes the treatment more efficient) or cancel each other (meaning that presence of the biomarker associates with treatment resistance). To assess this statistically, the biomarker variable and the variable describing treatment status are computed into a multivariable cox proportional hazards model along with an interaction term. This will indicate if there is a statistical interaction between the biomarker and the treatment in relation to outcome. A weakness of this method is that it requires high statistical power. Hence, a large cohort (or a highly pronounced interaction) is demanded to be able to reject the null hypothesis of no statistical interaction.

R Studio and statistical analyses

Statistical analyses for the clinical studies included in this thesis were all carried out in RStudio 1.1.442 (RStudio, Boston, MA, USA) using R 3.5.1 and up [172]. Statistical tests used in these studies are summarized in Table 3. Time-to-event analyses were graphically presented using functions from the *cmprsk* package [173]. Cox proportional hazards models with Wald test was used to calculate HR and test statistical strength globally and for each variable separately, using the *survminer* R package [174]. Proportional hazards were assessed using Schoenfeldt residuals. If the assumption of proportional hazard was not met, HR was interpreted cautiously as an average effect over the interval of follow-up. Descriptive statistics were attained using the R base packages and *DescTools* [175]. Forest plots were constructed using the package *forestplot*. The main package used for graphic presentation was *ggplot2*.

Table 3. Summary of the statistical tests used in the clinical studies of this thesis.

Analysis	Data type	No. of groups	Data	Test
Survival	Time-to-event	2≤	-	Cox proportional hazards model with Wald test and Log-rank test with Grays test
Hazard proportionality in relation to time				Schoenfeldt residuals
Association	Categorical	2	Large sample	Pearson's χ^2-test
Association	Categorical		Small sample	
Association	Categorical and ordinal	2≤		Mantel-Haenszel χ^2-test for trend and linear regression
Distribution	Ordinal data	2≤	Non-parametrical Paired samples	Wilcoxon matched pairs signed rank test

Major results, summary

	Main results, summary
Paper I	• GPR30 is a marker of poor prognosis for patients with contralateral breast cancer when expressed at a high level and/or in plasma membrane position in the contralateral tumor or its lymph node metastases. • GPR30 expression is downregulated in lymph node metastases compared to the primary breast cancers. • Contralateral tumors developed during tamoxifen treatment do not exhibit a change in total GPR30 expression, but are more likely to express GPR30 in the plasma membrane.
Paper II	• Among all systems tested, no evidence was provided that E2 or G-1 exerts GPR30-dependent activity. • Constitutive GPR30 activity was detected in several systems.
Paper III	• HIF-1α is an independent risk factor for ipsilateral breast tumor recurrence (IBTR) or any recurrence in early-stage breast cancer. HIF-1α also associated with breast cancer-specific death in univariate analysis. • HIF-1α was not predictive of radiotherapy response. • Ten hypoxia-related gene expression signatures identified in the literature were found to correlate with HIF-1α in early-stage breast cancer. • Several hypoxia-related gene expression signatures were prognostic of IBTR, any recurrence, and breast cancer-specific death. However, as a prognostic marker, HIF-1α outperformed all expression signatures in relation to all three endpoints. • HIF-1α protein expression correlated with detected HIF1A mRNA levels.
Paper IV	• GPR30 physically interacts with β1AR in a multi-protein complex by the plasma membrane of breast cancer cells. • The GPR30-β1AR complex also contains MAGUKs and AKAP5. • The GPR30-β1AR heteromer inhibits isoproterenol-stimulated β1AR signaling in a manner that depends on the GPR30 C-terminal PDZ-motif.

Results

Paper I

GPR30 as a prognostic and tamoxifen-predictive marker in contralateral breast cancer

Tamoxifen is an endocrine agent ordinarily prescribed to patients with ER-positive breast tumors. The compound exerts its action by binding to and decreasing the activity of ER. However, tamoxifen has also been reported to activate GPR30 signaling, and data suggests that GPR30 mediated tumor resistance to tamoxifen treatment. In study I, we addressed the role of GPR30 in contralateral breast cancer as a model of tamoxifen resistance. We also addressed GPR30 expression through tumor progression, from primary tumor to lymph node metastases. Lastly, we addressed GPR30 as a prognostic marker in contralateral breast cancer.

To this end, we used a unique tissue-microarray (TMA) from a cohort of 688 patients diagnosed with contralateral breast cancer in southern Sweden between 1977 and 2007. The TMA included tissue from the first primary tumor (BC1), the second primary tumor (BC2), and axillary lymph node metastases from the primary tumors (LGL1 and LGL2). GPR30 was immunohistochemically stained and evaluated in terms of total staining (**Figure 12**A-B) and plasma membrane-specific staining (**Figure 12**C-D).

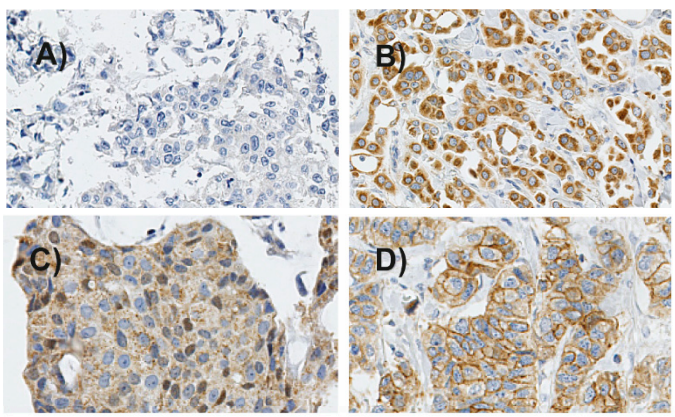

Figure 12. GPR30 staining on contralateral breast cancers; negative staining (A), high staining (B), plasma membrane negative staining (C) and plasma membrane positive (D). The figure is modified from Figure 2, Study I.

Patient survival was compared in relation to GPR30 expression using competing risk analyses and univariable and multivariable cox proportional hazards model in R. Primary endpoint was death from breast cancer (BCD). In both BC1 and BC2, plasma membrane-specific GPR30 expression associated with markers of breast cancer aggressiveness, including a lack of ER and PR expression, high staining of proliferation marker Ki67, and triple-negative subtype. As reported earlier, total GPR30 staining correlated with ER and PR in a biphasic manner, where tumors exhibiting no or very weak GPR30 staining as well as tumors with strong GPR30 staining were more likely to lack these hormone receptors. However, strong GPR30 staining associated with high levels of Ki67 and a triple-negative subtype in both BC1 and BC2.

Next, we related total and plasma membrane-specific GPR30 staining to patient outcome. We found that plasma membrane-specific GPR30 associated with an increased risk of BCD when expressed in BC2 (**Figure 13**A) as well as LGL2 (**Figure 13**B). Finally, there was a trend of increased risk of BCD among patients with strong total GPR30 expression in BC2.

To address the role of GPR30 through tumor progression, we compared total expression of GPR30 in BC1, LGL1, BC2, and LGL2 (**Figure 14**). We found that the GPR30 expression of BC2 was equally likely to be higher, lower, or the same as BC1.

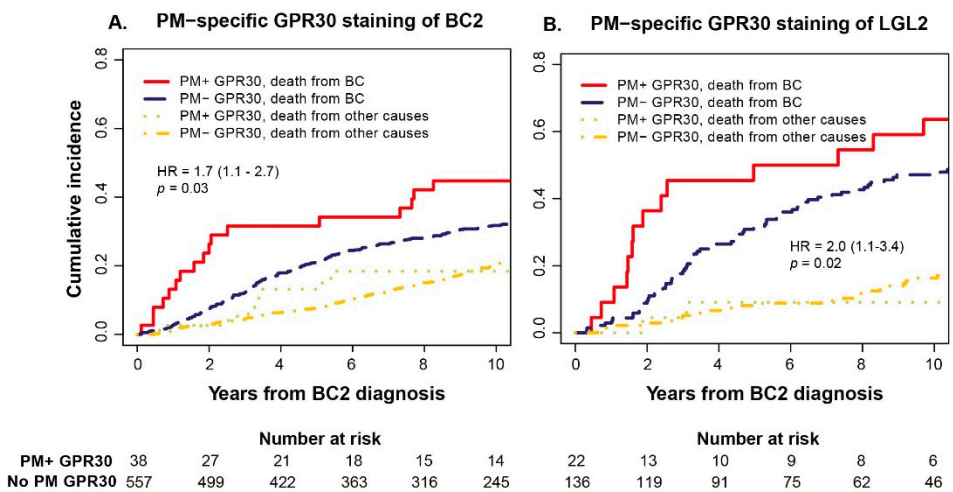

Figure 13. Competing risk curves presenting the outcome of patients with and without plasma membrane-specific (PM) GPR30 staining in their BC2 (A) and LGL2 (B). Dotted lines represent cumulative incidence of competing events in each group. The figure is modified from Figure 5, Study I.

To approach GPR30 as a mediator of tamoxifen resistance, we hypothesized that GPR30 expression would be elevated in tumors developed during treatment. However, the relationship between GPR30 expression in BC1 and BC2 was similar in tamoxifen treated and tamoxifen naïve groups, suggesting that high GPR30 levels do not provide a survival benefit under selection pressure from tamoxifen. This was in line with an analysis showing that the survival benefit from tamoxifen was equal irrespective of GPR30 expression level. Yet, a subgroup analysis showed that plasma membrane-specific GPR30 expression was significantly over-represented among BC2 diagnosed during ongoing tamoxifen treatment.

When comparing GPR30 expression of primary breast cancers BC1 and BC2 and their paired lymph node metastases LGL1 and LGL2, which were harvested at the same time as their primary tumor, we found a clear pattern of LGL expressing a lower amount of GPR30 than their primary tumor.

In summary, we found that plasma membrane-specific GPR30 associates with aggressive breast cancer markers and is prognostic of BCD in contralateral breast cancer. We found no evidence that the receptor mediates resistance to tamoxifen.

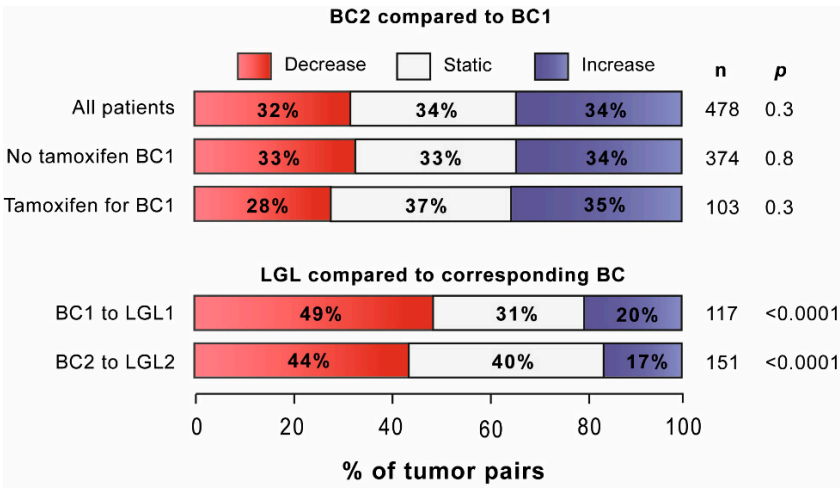

Figure 14. GPR30 expression in paired primary tumors (BC) and lymph node metastases (LGL). For every BC1/BC2, BC1/LGL1, and BC2/LGL2 tumor pair, the relative GPR30 intensity of the tumor assumed to have developed later was characterized as decreasing, stable, or increasing. Bar coloring represents the distribution among all tumor pairs available in the cohort. The change in GPR30 intensity was statistically evaluated using Wilcoxon matched pairs signed rank test. The figure is modified from Figure 4, Study I.

Paper II

Activation of GPR30 – constitutive activity and E2 and G-1 as agonists

GPR30 is classified as a membrane receptor that binds and responds to stimulation by estrogen (E2) [84, 176]. G-1 is a synthetic compound marketed as a selective GPR30 ligand, and extensively used to target GPR30 in research. However, multiple independent studies have failed to confirm the identity of E2 and G-1 as GPR30 agonists, which has made the proposed GPR30 ligands a matter of controversy [85, 86]. The aim of study II was to address the efficacy and selectivity of E2 and G-1 as GPR30 agonists.

To approach this, we used several eukaryotic systems both *in vitro* (**Figure 15**) and *ex vivo*. To indicate activity on several signaling pathways, we included real-time and transcriptional reporters for ERK1/2, RAC1, NFAT, and pcFUS3, a multifunctional promoter-reporter construct containing response elements for NFκB, STAT, and AP-1. We also addressed the proposed role of GPR30 in vascular relaxation in the mouse caudal artery by *ex vivo* myography. Finally, we coupled human GPR30 to the pheromone pathway in the *S. cerevisiae* strain CY2797, which is deficient of functional endogenous GPCRs. Furthermore, CY2797 depends on pheromone pathway activation in order to produce histidine, making GPCR activation reflected as increased yeast growth. Based on CY2797, we constructed EY-1, in which we inserted a gene for a chimeric G_{α} protein where the five C-terminal residues of the strains' native G protein Gpa1 were replaced by the five residues of human $G_{\alpha i2}$.

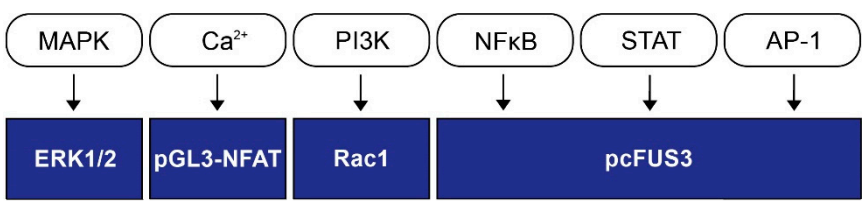

Figure 15. An overview of the reporter systems used in study II.

With all systems tested, we found neither E2 nor G-1 to initiate GPR30-dependent signaling (Table 4). The levels of vascular relaxation in caudal arteries from wild-type (WT) mice as compared to GPR30 knockout mice after treatment with 1, 3, and 10 μM of G-1 were essentially overlapping. Interestingly, G-1 instigated a

significant relaxation in caudal arteries even in the absence of GPR30 expression. To evaluate the effect of G-1 and E2 on GPR30-dependent activation of several signaling pathways including ERK1/2 phosphorylation, we used HeLa cells stably expressing the pcFUS3 multifunctional reporter construct (HFF11 cells) and transiently expressing GPR30 or stably expressing an inducible GPR30 construct (T-REx HFF11 cells). In the HFF11 cells, G-1 increased the reporter activity significantly independent on GPR30 expression (**Figure 16A**). The same pattern appeared when instead ectopically expressing a GPR30 construct lacking the C-terminal PDZ motif -SSAV (GPR30ΔSSAV). This truncation has earlier been shown to disrupt receptor interaction with membrane-associated guanylate kinases (MAGUKs), exhibit reduced constitutive activity, and increased level of receptor endocytosis [89, 90, 98, 116]. Using HEK293 cells transiently transfected with either WT-GPR30 or GPR30ΔSSAV, we observed no significant GPR30-dependent change in ERK1/2 phosphorylation in response to either 1 μM of G-1 or 0.1 μM E2 with either WT-GPRR30 or GPR30ΔSSAV. To address the effect of GPR30 on Ca^{2+} signaling, we used a reporter containing a luciferase gene downstream of an NFAT response element, which is sensitive to Ca^{2+} [169]. No GPR30-dependent reporter activity was observed after treatment with either G-1 (1 μM) or E2 (0.1 μM). Similarly, neither 0.1 μM E2 nor 1 μM G-1 had any effect on the Rac1 reporter, which responds to activation of phosphoinositide 3-kinase (PI3K), in mock transfected cells or cells expressing WT-GPR30 or GPR30ΔSSAV. Lastly, 1 μM of G-1 was unable to trigger a growth response of *S. cerevisiae* strains CY2797 and EY-1 expressing human WT-GPR30 (**Figure 16B**).

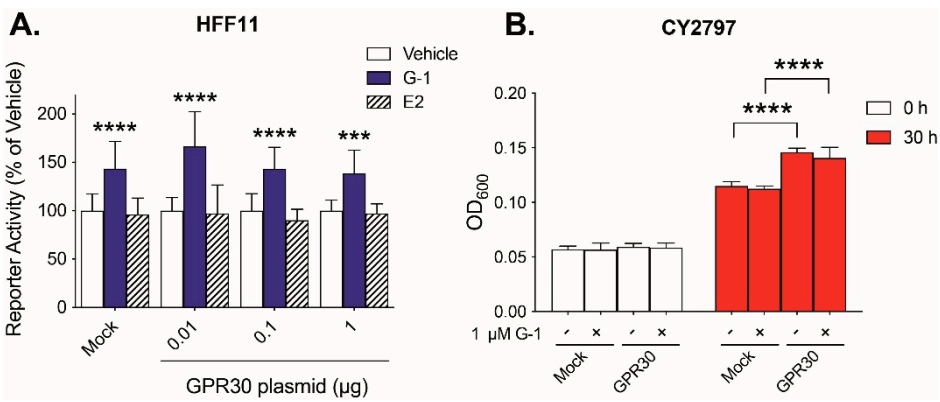

Figure 16. Reporter activity from two of the systems used in study II. Panel A demonstrates activity of the multifunctional pcFUS3 reporter stably expressed in HFF11. Panel B displays growth of the CY2797 yeast strain, measured as optical density (OD) with and without GPR30 and G-1.

Interestingly, GPR30 exhibited a measurable level of constitutive activity in several systems. In line with previous findings, GPR30 constitutively suppressed NFAT reporter activity and increased ERK1/2 activity [90]. Furthermore, the receptor constitutively inhibited Rac1 reporter activity and increased pcFUS3 activity. Finally, GPR30 expression led to an increase in the basal growth in both yeast strains.

To summarize, study II found no evidence of a GPR30-dependent effect of either G-1 or E2, suggesting that the classifications of GPR30 as an estrogen receptor and G-1 as a selective GPR30 ligand are unfounded, highlighting a need for novel GPR30 ligands. On the other hand, ample evidence was found that the receptor harbors constitutive activity.

Table 4. A summary of the results from the reporter systems used in study II; signals in response to G-1 and E2 with and without GPR30 expression, and constitutive GPR30 activity.

System	**G-1 response**		**E2 response**		**Constitutive GPR30 activity**
	GPR30 +	**GPR30 -**	**GPR30 +**	**GPR30-**	
Mouse caudal artery myography	Yes	Yes	-	-	-
ERK1/2 immunoblot	No	No	No	No	Yes [90]
pGL3-NFAT	No	No	No	No	Yes
RAC1	No	No	No	No	Yes
pcFUS3	Yes	Yes	No	No	-
T-REx pcFUS3	No	No	No	No	Yes
Pheromone response	No	No	-	-	Yes

Paper III

HIF-1α and hypoxic gene expression signatures as markers for prognosis and radiotherapy response in early breast cancer

The microenvironment of solid tumors is heterogeneous and often comprises areas where the oxygen demand exceeds the supply, leading to local hypoxia. When irradiated, oxygen atoms form highly reactive radicals, and therefore play a crucial role in the tissue response to ionizing radiation, including radiotherapy [46]. In study III, the primary aim was to address whether protein levels of HIF-1α, a transcription factor that participates in the cellular adaptation to hypoxia, associate with the benefit of radiotherapy.

To address this, we studied tumor expression of HIF-1α in terms of mRNA and protein in SweBCG91-RT, a large trial of early breast cancer where 1004 patients were randomized to either postsurgical radiotherapy or no radiotherapy. A secondary aim was to assess the relationship between HIF-1α and breast cancer outcome. Finally, we analyzed gene expression of hypoxia-related genes and performed scoring based on gene expression signatures found in the literatures, to address if hypoxia-related gene expression signatures could act as a complement or surrogate prognostic marker for HIF-1α protein expression.

In line with a previous study in contralateral breast cancer [43], our data confirmed that HIF-1α protein expression associates with poor outcome in breast cancer. The survival analyses used ipsilateral breast tumor recurrence (IBTR) as the primary endpoint (**Figure 17A**), and any breast cancer recurrence (**Figure 17B**) and BCD as secondary endpoints. After adjusting for patient age, tumor size, subtype and systemic adjuvant therapy, the 5-year risk of IBTR in HIF-1α positive tumors was 80% higher than for HIF-1α negative tumors, and the risk of developing any kind of recurrence was 70% higher. HIF-1α positivity associated with 10-year risk of breast cancer specific mortality in univariate but not multivariate analysis. Interestingly, the HIF-1α status of the IBTR was to a large extent inherited from the primary tumor (**Figure 17C**), and seemed to associate strongly to outcome.

Importantly; in contrast to our initial hypothesis, we found that postsurgical radiotherapy of early-stage breast cancer was equally beneficial regardless of HIF-1α expression, as demonstrated by similar HR values in HIF-1α positive and negative

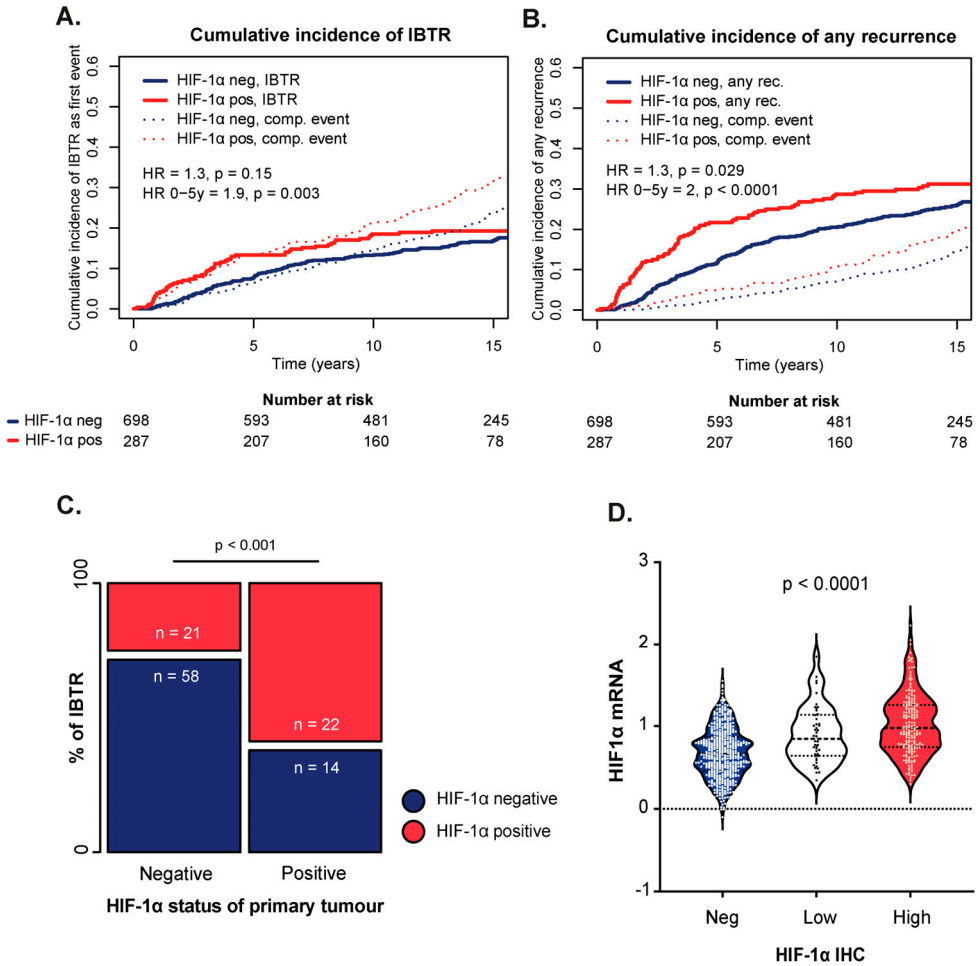

Figure 17. HIF-1α protein expression in relation to ipsilateral breast tumor recurrence (IBTR, A) and any recurrence (B). HIF-1α status of IBTR in relation to their primary tumor (C), and HIF-1α mRNA levels in relation to protein expression as measured by IHC (D). The figure is modified from Figure 2 and Figure 4 of Study III.

groups, as well as cox proportional hazards tests with a radiotherapy-HIF-1α interaction term.

Cellular HIF-1α levels are assumed to be mainly regulated at the post-transcriptional level, with involvement of the oxygen-sensitive VHL, FIH and PHD-2 degradation system. In this material, we found a correlation between HIF-1α mRNA and protein levels (**Figure 17D**). However, the HIF-1α mRNA lacked a significant prognostic value.

The short half-life of HIF-1α in an oxygenated environment may render the protein a technically difficult biomarker. We hypothesized that a hypoxia-induced gene expression signature could serve as a surrogate prognostic marker for HIF-1α. After performing a literature study, we selected 11 gene expression signatures derived from tumor material or *in vitro* experiments. Using the *singscore* package in R, we then scored each tumor in the cohort based on its concordance with each hypoxic gene expression signature individually. The score of 10 of the 11 signatures associated with HIF-1α protein expression. Furthermore, most signatures correlated strongly in terms of the calculated scores (**Figure 18**). Finally, for each endpoint considered in this study, at least three hypoxic gene expression signatures were found to correlate with outcome. Nevertheless, no gene expression signature was able to outperform HIF-1α as a prognostic marker in relation to any outcome.

The findings of this study highlight the relevance of understanding the role of factors in the tumor microenvironment, including the hypoxic response, in disease progression and treatment response.

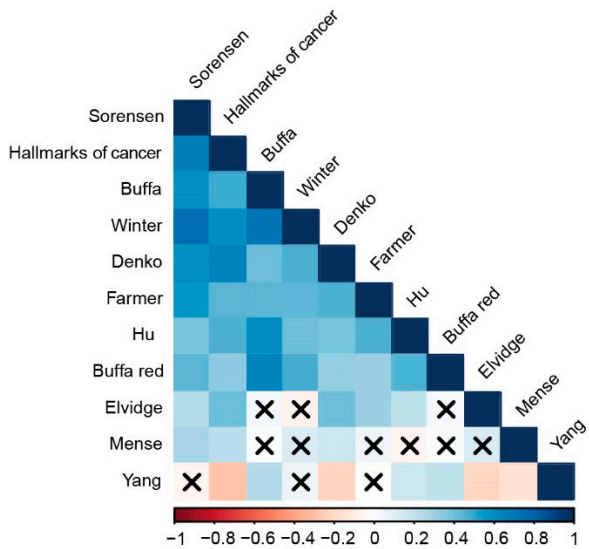

Figure 18. Correlation plot for the hypoxia signature scores calculated for the study. Positive correlations are shown in an increasing intensity of blue, while negative correlations are shown in read. Unless marked with a cross, correlation *p* values are <0.0001. Figure is modified from Figure 5 of study III.

Paper IV

A functional plasma membrane complex including GPR30 and β1AR

Previous data suggests that GPR30 is constitutively active, and that a plasma membrane localization is crucial for this activities. In turn, plasma membrane positioning of GPR30 depends partly on the C-terminal PDZ-motif, through which the receptor interacts with scaffold proteins from the MAGUK family and AKAP5 [89]. We have also shown that GPR30 expression concentrated at the plasma membrane associates with a more aggressive phenotype in breast cancer [93, 177]. The β–adrenergic receptor β1AR has been associated with breast cancer risk and progression. In similarity to GPR30, this receptor contains a C-terminal PDZ-motif through which the receptor interacts with MAGUKs and AKAP5. Additionally, GPR30 inhibits β1AR-mediated production of cAMP in a PDZ-dependent manner. In study IV, we hypothesized that GPR30 and β1AR exist in a multi-protein complex by the plasma membrane, and that this complex has functional effects on the function of both receptors in breast cancer and recombinant systems.

To address if GPR30 and β1AR form a complex, we first co-immunoprecipitated (co-IP) the two receptors in lysates of HEK293 cells ectopically expressing them. Co-IP revealed that both GPR30 and β1AR antibodies were able to precipitate the other receptor, suggesting that the two receptors exist in a complex. When replacing the wild-type (WT) GPR30 for the mutant receptor with a truncated PDZ motif (GPR30ΔSSAV), the co-IP appeared equally strong. This suggests that ectopic GPR30 and β1AR interacts in HEK293 cells independently on the GPR30 PDZ motif.

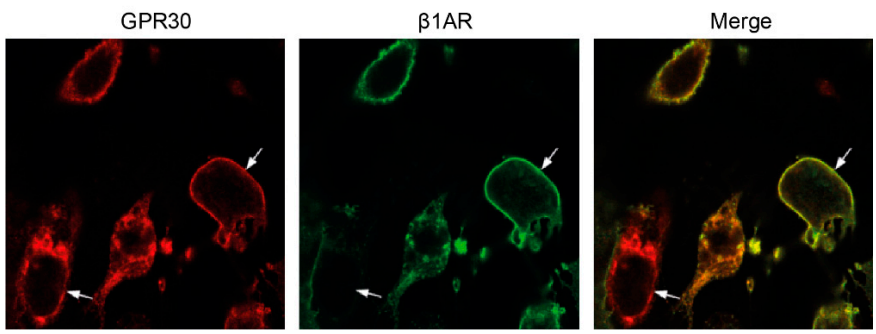

Figure 19. Confocal image of HEK293 cells ectopically expressing GPR30 (red) and β1AR (green).

Staining fixed HEK293 cells for GPR30 and β1AR revealed that the receptors co-localize in the plasma membrane in some cells (**Figure 19**). To further characterize the interaction between GPR30 and β1AR, we performed bioluminescence resonance energy transfer (BRET) on HEK293 cells transiently transfected with both receptors. This revealed that the GPR30-rLuc and β1AR-YFP are close enough for the YFP bioluminescence to be activated, indicating that the two receptors interact physically in HEK293 cells.

Having found that ectopic GPR30 and β1AR interact physically in HEK293 cells, we wanted to investigate if this interaction takes place between the native receptors in a breast cancer cell line. After confirming native expression of GPR30 and β1AR, MAGUKs, and AKAP5, we selected MCF-7 as a model system for breast cancer. To confirm data from the Human Protein Atlas mRNA database, showing that MCF-7 expresses mRNA encoding β1AR, but not β2AR or β3AR [130, 131], we performed a kinetic assay of cAMP production following beta-stimulation (**Figure 20**). We found that the non-specific β-agonist isoproterenol and the β1AR agonist dobutamine triggered rises in intracellular cAMP. The specific β1AR antagonist atenolol fully repressed the isoproterenol response, indicating that MCF7 cells express β1AR exclusively. Using FACS, we identified expression of both GPR30 and β1AR at the plasma membrane of this cell line. To address if the two GPCRs form a complex in

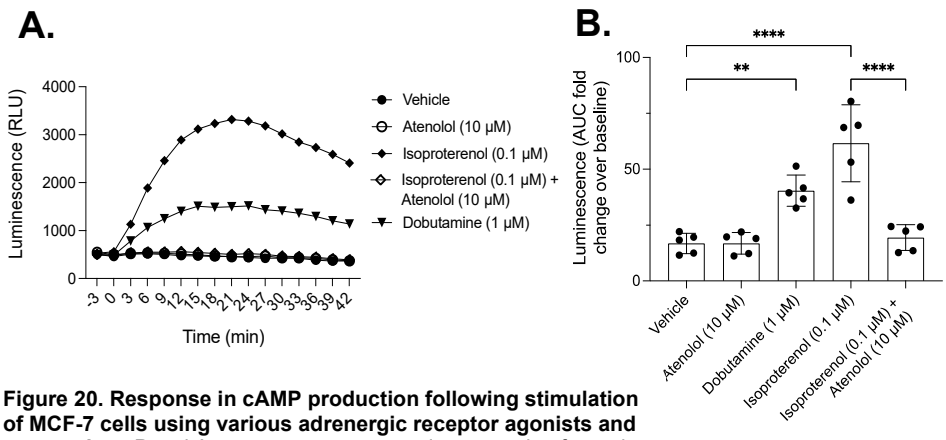

Figure 20. Response in cAMP production following stimulation of MCF-7 cells using various adrenergic receptor agonists and antagonists. Panel A presents a representative example of a real-time measurement, and panel B presents the area under curve (AUC) for three independent measurements.

MCF-7 cells, and if this complex also comprises MAGUKs and AKPA5, we performed a series of co-IP experiments (**Figure 21**). In short, the results indicated that GPR30 and β1AR exist in a complex (**Figure 21A**, panel 1-2) also containing a MAGUK (**Figure 21**Fel! Hittar inte referenskälla.**A**, panel 3). GPR30 also appeared to interact with AKAP5 (**Figure 21B**, panel 1), which in turn interacted with a MAGUK. These data indicate that native GPR30 and β1AR exist in a complex in MCF-7 cells, and this complex also contains MAGUKs and AKAP5.

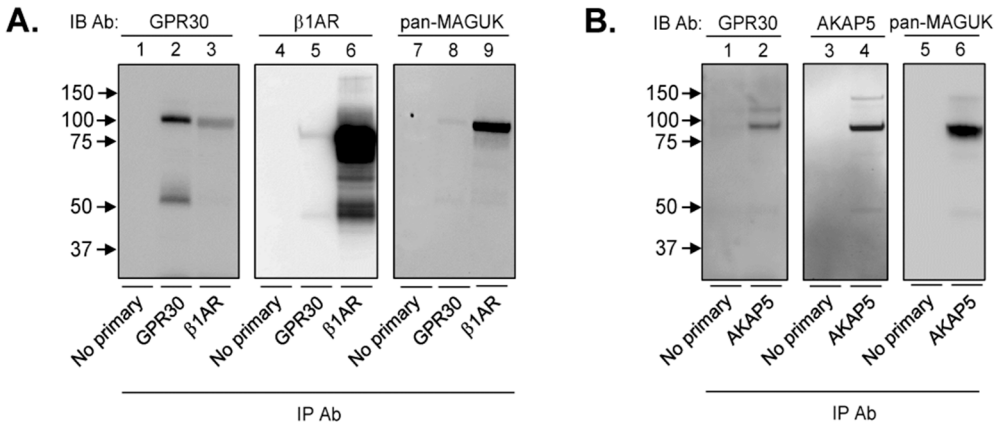

Figure 21. Co-IP of GPR30 and β1AR.

Finally, we wanted to determine if the complex including GPR30, β1AR, AKAP5, and MAGUK proteins has a functional role in regulating receptor-mediated signaling. Using isoproterenol to stimulate β1AR in MCF-7, we found that the triggered cAMP production was suppressed by GPR30 overexpression. Interestingly, overexpression of GPR30ΔSSAV did not affect β1AR-stimulated cAMP elevation. Overexpression of AKAP5 also exhibited a small inhibitory effect, while not additive to that exerted by GPR30.

In summary, study IV demonstrated that native GPR30 and β1AR exist in a multi-protein complex with scaffold proteins from the MAGUK family and adaptor protein AKAP5 in breast cancer cell line MCF-7. Further, we show that GPR30 has a functional effect on β1AR-mediated signaling in a manner that depends on the GPR30 C-terminal PDZ-motif.

Discussion and future perspectives

With over 2 million new cases annually, breast cancer is the most frequently diagnosed cancer worldwide. The survival rate has improved gradually during the past 50 years, in part due to earlier detection and more effective treatments [6]. However, tumors developing treatment resistance remain a main concern in the clinical management of breast cancer. Thus, there is a need for new predictive biomarkers to recognize treatment resistant tumors, and new drug targets for the breast cancer treatments of tomorrow. To address this need, the overarching aim of this thesis was to explore molecular factors in breast cancer and how they impact the benefit of common modes of treatment in order to increase knowledge on how to design personalized treatment strategies.

Due to their broad role in human physiology, GPCRs are common targets for pharmacological modulation. Today, 30-45% of all prescription pharmaceutical substances target GPCRs, and they account for a significant part of the top selling prescription drugs [59, 157]. However, only a small fraction of GPCRs are understood well enough to be useful in medicine. In this thesis, I aimed to improve our understanding of GPR30, GPCR currently assumed to bind and be activated by the female sex hormone estrogen, as well as the proposed synthetic agonist G-1. During the past 25 years, GPR30 has drawn considerable interest in breast cancer research. Yet, a clear consensus has not been reached regarding the role of the receptor in breast cancer pathophysiology. With GPR30 correlating with markers of breast cancer aggressiveness in a biphasic manner, inter-study inconsistencies in cutoff for GPR30 immunohistochemical staining may explain some variation. However, *in vitro* data has also suggested that the function of GPR30 may depend on the cellular context, as the receptor was reported to promote proliferation in some breast cancer cell lines, and apoptosis in others [95-97].

One factor that has emerged as an important determinant of GPR30 function is the subcellular localization of the receptor. In study I, we confirm that the subcellular

localization of GPR30 in contralateral breast cancer has a pronounced association with patient outcome. This agrees with previous findings in primary breast cancer [93]. Interestingly, while plasma membrane GPR30 expression associated with high expression of the receptor, high expression alone was not significantly associated with outcome. This indicate that positioning of the receptor may have relevance in breast cancer pathophysiology. Depending on the cell system, GPR30 is found in both the plasma membrane and intracellular membranes to different extents [83, 87, 91, 178]. As of today, the regulation behind the distribution of the receptor remains relatively poorly understood. However, one factor found to contribute to plasma membrane positioning of GPR30 is the receptor C-terminal PDZ-motif, through which the receptor interacts with scaffold proteins from the MAGUK family and AKAP5 [89]. This motif also promotes constitutive activity of the receptor [89, 90, 98]. It is an interesting thought that the cellular distribution and function of GPR30 partly may depend on the host cells' expression of PDZ-interacting scaffold proteins, and subsequently the expression of the effectors that these scaffold proteins may assemble. In study IV, we addressed the functional implications of a multi-protein complex involving GPR30 and the adrenergic G_s-coupled GPCR β1AR in breast cancer cells. Studies have associated β1AR to breast cancer incidence and outcome [153-155]. Like GPR30, this receptor has a C-terminal type I PDZ motif, through which the receptor interacts with the MAGUK SAP97 and AKAP5 [69, 179].

In study IV, we showed that GPR30 and β1AR form a functional multi-protein complex at the plasma membrane in native MCF-7 breast cancer cells. This complex was also found to contain AKAP5 and proteins from the MAGUK scaffold protein family, which contain PDZ domains and may interact with receptor PDZ-motifs. In agreement with what was earlier reported in recombinant HEK293 cells [89], we found that GPR30 suppressed β1AR-mediated cAMP production in a PDZ-dependent manner. Yet, the interaction between GPR30 and β1AR in HEK293 cells was independent on the GPR30 PDZ-motif. In line with this, BRET confirmed a close interaction between GPR30 and β1AR, suggesting that these receptors interact through hetero-oligomerization. Thus, while GPR30 and β1AR appears to form a complex independent on interaction with cytoplasmic PDZ-domain proteins, the PDZ-dependence of the inhibition of cAMP production indicates that a protein that contains a PDZ-domain – conceivably a MAGUK – is necessary to arrange the positions required to enable this mechanism. A recent study showed that GPR30 heteromerizes

with follicle-stimulating hormone receptor (FSHR), inhibiting cAMP production mediated by FSHR. Indeed, the formation of a heteromer between FSHR and GPR30 converted the cellular effect of FSHR-stimulation from proliferative to apoptotic [124]. It is an interesting thought that a similar mechanism may explain the differences in how GPR30 influences proliferation and apoptosis in breast cancer cell lines. Interestingly, unpublished data from our lab show that overexpression of the recombinant GPR30 mutant lacking a functional PDZ-motif increases proliferation of MCF-7 cells, whereas the wild-type receptor does not. The mechanisms behind such a functional switch are potentially highly complex, and need to be untangled in further studies. Nevertheless, the results of these studies put emphasis on the relevance of the interactome in determining the functional effect of a GPCR – to address the receptor as part of an orchestra instead of a solo instrument.

In study II, we aimed to characterize the relationship between GPR30 and the proposed ligands E2 and G-1. Although these compounds are routinely used experimentally in the purpose of activating GPR30, conflicting results have been published through the years, leading the matter to become controversial [85, 86, 103]. To address the relationship between GPR30 and these compounds, we utilized a range of reporter systems in several cellular contexts, ranging from *ex vivo* to human cell lines and yeast. For the *in vitro* experiments, we used HEK293 and HeLa cells, two human cell lines well described and extensively used in GPCR research. Studying the estrogenic response in several eukaryotic systems with or without the receptor, we found that overexpression of GPR30 is not enough to endorse an estrogenic response in any of the naturally non-responsive cell types tested. Similarly, our results from recombinant cell reporter systems with or without GPR30 failed to confirm G-1 as a selective GPR30 agonist, as GPR30 expression was neither sufficient, nor in some systems necessary, to invoke a G-1 response. However, one potential weakness of the reporter systems used in human cell lines is that they were all indicating signaling events assumed to occur several steps downstream of GPR30. Another potential weakness is that the overexpressed recombinant receptor could translate poorly to a human cell system naturally expressing the receptor in its habitual molecular context, as factors present in the cellular proteome may influence the receptor activity. Therefore, we wanted to address GPR30 activation in yeast, a less complex mammalian system extensively used in characterization of GPCRs and their pharmacological profiles. GPR30 was modified to recognize and communicate with native yeast G proteins, and was thereby coupled to an existing pathway; the growth-stimulatory pheromone pathway. Using this simple system, we

found that neither E2 nor G-1 stimulated GPR30. It is worth noting that factors that potentially could influence the activity and protein-protein interactions of GPR30 may require human-specific post-translational modifications. However, western blot of overexpressed human GPR30 from yeast lysates confirmed a molecular weight that agrees with previous reports, suggesting that this receptor corresponds to the GPR30 expressed in human cells.

To summarize, we found evidence that GPR30 is insufficient to make cells responsive to estrogen stimulation – adding to the body of data indicating that the identity of GPR30 as an estrogen receptor may be premature. Further, our conclusion that G-1 – the compound commercially marketed as a selective GPR30 agonist – lacks selectivity for GPR30 stresses the need of finding new approaches to study this receptor, such as a new agonist, or by monitoring constitutive activity. Yet, although the systems we used were selected to account for a broad range of signaling activities, we cannot rule out the risk that we missed a selective GPR30-effect triggered by G-1 or E2. Thus, further studies should be made to confirm our results. Interestingly, a study reported GPR30-independent effects of G-1 in glioblastoma shortly after the publication of study II [180].

Despite the fact that the results of study II questions GPR30 as an estrogen receptor, the existing literature offers a non-negligible body of data supporting that GPR30 either contributes, potentiates, or in some cases is indispensable in order to bring about an estrogenic response in various cell systems [181]. In light of these data and the results presented in study II, it is apparent that the mechanisms by which GPR30 participates in the rapid estrogenic response in human cells are still largely unknown. Certainly, whereas study II provides evidence that E2 and G-1 fails to activate GPR30, it does not address whether or not the receptor is involved in the cellular response of these substances. Here, it is interesting to note that GPR30 expression has been reported to induce expression of the ERα isotype ERα-36, which also has been reported to elicit rapid, non-genomic signaling in response to E2 and G-1 [101, 140]. Additionally, studies indicate that GPR30 interacts with the 66 kDa ERα isotype [182]. In order to understand GPR30 as a potential drug target, it is necessary to approach the relationship between GPR30, ERα-36, and estrogenic signaling.

Another compound suggested to act as a GPR30 agonist is the breast cancer drug tamoxifen, which acts as a selective ERα modulator (SERM). With data supporting GPR30 as a factor contributing to breast cancer pathology [93, 97], the idea of

tamoxifen acting as a GPR30 agonist appears concerning, as this could mean that tamoxifen may stimulate growth in tumors expressing GPR30. In study I, we aimed to address GPR30 as a potential mediator of tamoxifen resistance. To this end, we used a unique material of contralateral breast cancer where some tumors had developed during tamoxifen treatment as an *in vivo* model for tamoxifen resistance. We hypothesized that if GPR30 promotes tamoxifen resistance and offers a survival benefit under selection pressure from this drug, GPR30 expression would be enriched in contralateral breast cancer developed during tamoxifen treatment. Interestingly, we found the relationship between GPR30 expression in the primary breast cancer and the contralateral breast cancer to be similar in tamoxifen-treated and tamoxifen-naïve groups, suggesting that an increased expression of GPR30 does not provide an advantage under tamoxifen exposure. This is in contrast to an earlier study where the GPR30 expression was analyzed in 21 paired biopsies obtained before and after tamoxifen treatment, where the receptor staining was found to be upregulated [141]. While the data from study I of this paper is based on a considerably larger cohort, additional data is required to confirm our results.

GPR30 has previously been described both as a tumor promoting factor and a tumor suppressor in breast cancer [183, 184]. In study I, we found that plasma membrane expression of GPR30 associates with markers of tumor aggressiveness and poor outcome in contralateral breast cancer. This is in line with a previous study in primary breast cancer [93]. Interestingly, we found that plasma membrane GPR30 expression in lymph node metastases had an even more pronounced association with outcome. To address GPR30 through tumor progression, we compared receptor expression in primary breast tumors with that of their lymph node metastases in both the first primary breast cancer and the contralateral tumor. In this case, we observed a clear reduction in GPR30 expression in lymph node metastases from both primary tumors. With the observation that GPR30 expression in the plasma membrane associates with poor outcome in this material, it is tempting to assume that GPR30 expression would be beneficial as the tumor progresses and spreads. However, this data suggests the contrary. It is possible that the biological role of GPR30 in breast cancer is favorable in a growing tumor, but unfavorable in terms of migration. This is particularly interesting with the background that plasma membrane GPR30 staining in lymph node metastases showed a strong association with outcome in this material, suggesting that if GPR30 downregulation is favorable for breast cancer cell migration to the lymph node, upregulation while adhered to the new site seemingly provides a benefit in terms of

progressing. However, it is also necessary to consider that this may be due to technical factors rendering tumors raised in in the lymph tissue less susceptible to bind the GPR30 antibody.

Ever since GPR30 was discovered, the receptor has been considered a novel drug target in breast cancer. Certainly, GPR30 has been associated to both breast cancer outcome and breast cancer cell growth *in vitro* [93, 95, 97, 136, 137, 139], indicating the involvement of the receptor in processes relevant for tumor progression. Based on our understanding of GPR30 today – that the receptor has different functions in different systems, in different interactome constellations, and at distinct subcellular localizations – makes pharmacological exploitation of GPR30 a challenging, yet intriguing question. The observation that GPR30 expressed specifically in the plasma membrane appears to have a distinguished role in breast cancer [93, 177], along with data suggesting that interaction with a MAGUK scaffold protein contributes to plasma membrane GPR30 positioning [89], presents the idea that pharmacological interference with this interaction could offer a means to impede pathological GPR30 signaling in breast cancer. Additionally, in study IV, we showed that without the C-terminal PDZ-motif, GPR30 lost the ability to suppress β1AR-stimulated cAMP-production, while the receptor was still able to hetero-oligomerize. Thus, it is tempting to consider that a GPR30- β1AR heteromer may still be active in other PDZ-independent signaling events, and that a compound interrupting PDZ-dependent GPR30 interactions may act as a biased antagonist.

The final specific aim of this thesis was to evaluate the relevance of tumor hypoxia in relation to breast cancer outcome in general, and radiotherapy specifically. Low oxygen levels, hypoxia, is characteristic of the often poorly vascularized microenvironment of solid tumors. HIF-1α is a transcription factor that accumulates in human cells as a causal effect of low oxygen pressure. HIF-1α activates expression of a battery of genes that improves the cells fitness to survive in the challenging environment, including means of metabolic adaptation, angiogenesis, and other strategies that are also found among the Hallmarks of Cancer. Given this, it may not be surprising that HIF-1α expression has been associated with poor outcome in some cancer types. In study III of this thesis, we confirmed that HIF-1α predicts poor outcome in early-stage breast cancer, which was earlier reported in contralateral breast cancer [43]. Further, we addressed the HIF-1α and hypoxic gene expression signatures in relation to radiotherapy susceptibility. Although it is established that oxygen has a direct influence

on the biological response to radiation via the oxygen enhancement effect [46], this relationship had not yet been confirmed for radiation of breast cancer. In study III, we report that the benefit of radiotherapy in prevention of breast cancer death, local recurrences, and any recurrences, was equal for tumors with high and low levels of HIF-1α, as well as high and low scores of hypoxic gene expression. Although in contrast to our initial hypothesis, these results were not unexpected given the nature of the oxygen enhancement effect. This effect reflects immediate conditions. Thus, oxygen must be present at the time of, or within microseconds of, radiation [46]. In our material, radiotherapy was given in the post-surgical setting, aiming to damage any tumor cells remaining at the tumor site. With most of the tumor bulk supposedly removed, any residual tumor cells are likely to be in an oxygenated environment. Hence, when discussing the oxygen enhancement effect, a hypoxic status of the original tumor seems unlikely to be reflected in postsurgical radiotherapy.

HIF-1α serves to adapt cells and promote survival under conditions where the oxygen supply is sparse. This transcription factor is activated when reduced oxygen levels inhibit the machinery that normally coordinates its degradation. Hence, HIF-1α protein levels are often assumed to reflect the immediate oxygenation status of a tumor. Interestingly, in study III, we show that local recurrences of a HIF-1α positive primary breast tumor are more likely to be HIF-1α positive than recurrences of HIF-1α negative primary breast tumors. This seems curious based on the assumption that residual cancer cells remaining in the tumor bed after resection will not remain hypoxic. Still, our data show that if they originate from a hypoxic tumor, they are more likely to form a hypoxic recurrence. This may reflect an enhanced resistivity to the microenvironment often associated to hypoxic tumor centrum enabling some tumor genotypes to thrive even when under limited oxygenation.

In recent years, it has become increasingly clear that factors inherent of the tumor microenvironment, including hypoxia, may play a part in cancer cell evolution. As a tumor grow, clonal evolution and interaction with the local microenvironment may result in the formation of distinct intra-tumor niches with varying levels of hypoxia, extracellular accumulation of acidic rest products from tumor cell glycolysis, and cytokines [185, 186]. While such harsh environment would be toxic to normal cells, cancer cells manage to adapt and survive. In line with the results of study III of this thesis, others have reported that cells nursed in tumors containing harsh environments may exhibit an increased aggressiveness [187, 188]. However, it has been difficult to

draw any conclusions as to the causality between the challenging microenvironment and tumor cell aggressiveness. Do the microenvironment drill aggressive tumor traits, or were the aggressive cells found in the challenging tumor environment simply there because they were the only clones that resisted the toxicity? This cannot be addressed using tumor tissue from a single time-point, but requires serial biopsies to follow tumor evolution. Additionally, studies of the tumor microenvironment put high requirements on the spatial resolution of all analyses. Hence, it should be noted that one weakness of the HIF-1α study is that we address a factor in the tumor microenvironment using bulk tumor transcriptomics. However, modern spatial transcriptomics techniques may lead to a better understanding of tumor microenvironment.

Finally, study III demonstrated that mRNA levels of the *HIF1A* gene correlates with protein expression. This observation challenges the idea of HIF-1α expression being regulated on the protein level, and possibly reflects either a considerable transcriptional control of the HIF-1α expression, or existence of a loop for positive feedback regulation. The mechanisms behind this, and the regulation of HIF-1α in cancer, need to be further addressed.

While not directly addressed in this thesis, it is interesting to note that GPR30 has been linked to hypoxia in general, and HIF-1α specifically. The promoter of GPR30 contains a hypoxia response element (HRE) and the receptor is upregulated after hypoxic exposure, suggesting that GPR30 participates in hypoxic adaptation [143-145]. Yet, GPR30 was not represented in any of the hypoxic gene expression signatures studied in study III. However, this does not rule out that GPR30 has a function in hypoxic adaptation. Interestingly, unpublished data collected during our work with the contralateral breast cancer material in study I revealed a linear relationship between HIF-1α and GPR30 protein levels in contralateral breast tumors. Furthermore, plasma membrane GPR30 expression was overrepresented in a HIF-1α-positive BC1 and BC2. The relationship between subcellular localization and HIF-1α-regulated genes should be further addressed in the future.

Conclusions

- Plasma membrane expressed GPR30 associates with poor outcome in contralateral breast cancer.
- Contralateral breast cancers developed during tamoxifen treatment were not more likely to express high levels of GPR30, but more likely to express GPR30 in the plasma membrane. GPR30 was not predictive for adjuvant tamoxifen treatment.
- GPR30 expression in lymph node metastases is lower than in primary breast cancer tumors.
- The compound G-1, which is commercially marketed as a highly selective GPR30 agonist, activates signaling in several systems lacking GPR30, and is insufficient to stimulate GPR30 activity in several systems. Thus, G-1 is not selective to GPR30, and is not a GPR30 agonist. Discovery of a new, thoroughly validated synthetic ligand would be of high benefit for future GPR30 research.
- E2 did not stimulate GPR30 activity in any of the studied systems, suggesting that the classification of GPR30 as an estrogen receptor is unfounded. The relationship between E2 and GPR30 must be addressed in future studies, and the possibility that GPR30 acts as a co-factor in rapid estrogenic signaling should be considered.
- GPR30 harbors considerable constitutive activity. In future studies, monitoring constitutive GPR30 activity may be an alternative to using G-1 in hope of stimulating the receptor.
- High HIF-1α protein levels are prognostic of poor outcome in breast cancer, but not predictive of radiotherapy response.
- HIF-1α protein levels correlate with a number of hypoxic gene expression signatures from the literature. Several of these gene expression signatures associate to outcome, but none is superior to HIF-1α as a prognostic marker.

- The HIF-1α expression level of a local breast cancer recurrence is to a considerable degree inherited from the resected primary tumor. Whether this is because hypoxic adaptation via HIF-1α also makes a tumor more aggressive, or because an aggressive tumor grows denser and thus to a greater extent forms hypoxic areas, remains unclear. The causality of this relationship should be addressed in future studies.
- GPR30 forms a plasma membrane complex with β1AR, MAGUKs and AKAP5 in breast cancer cell line MCF-7, and inhibits β1AR-stimulated cAMP production.
- Hetero-oligomerization of GPR30 and β1AR is not dependent on the GPR30 C-terminal type I PDZ-motif. Hetero-oligomerization of GPR30 with other GPCRs could provide explanations for the different functions that GPR30 shows in different cell contexts. Interactions between GPR30 and other GPCRs should thus be addressed in future studies.

Acknowledgements

Through my years as a PhD student, I have been lucky to be surrounded by amazing people. On the following pages, I will take the opportunity to thank some of them.

First and foremost – this project would not have been possible without the support from my three supervisors. I would like to begin by thanking **Fredrik Leeb-Lundberg**, who was my main supervisor for the first three years of my PhD studies, and who gave me the opportunity to start this project in 2018. I am forever grateful to you for your support and guidance while I discovered science and molecular pharmacology. Thank you for always letting me follow my own interests and for always being open to my (sometimes far-fetched) theories and ideas. For countless hours discussing receptors, molecular interactions, and scientific methods. Remembering how you smiled and said that "science is never easy", while it is obvious for anyone that you love every day in science, will always be a source of inspiration for me.

My next thank you is to **Sara Alkner**, who was my main supervisor for my fourth and final year as a PhD student. Thank you for your optimism and all the support during the writing of my thesis (!), for always finding the time for a talk, and for sharing your knowledge from the clinical side of breast cancer research.

I also wish to thank my co-supervisor **Martin Sjöström**. You have been an important role model for me and I am grateful for having had your support in my research education, but also for all the postdoc and career discussions. Thank you for always having time for a Zoom call despite the time difference, for introducing me to the world of R programming and transcriptomics analysis, and for all the patience and encouragement.

To my lab group – to **Joanna Daszkiewicz-Nilsson** for all your thoughtful advice on everything important in life, for always sharing a laugh and a positive attitude, and for Thursday chocolate. To **Björn Olde**, my "extra supervisor". For hours of talks about methods, science, and life in academia. Also, a huge thank you for always being honest,

making fun of me when I deserved it, and for caring about my future. Also a big thank you to **Ernesto Gonzalez de Valdivia** for the lab supervision when I first started in the group. Lastly, a thank you to **Ioannis** and **Emil** for our time sharing the little office!

I wish to extend a very special thank you to **Mårten Fernö** for introducing me to breast cancer research, helping me attend clinical meetings, and for bringing me onboard the HIF-1α project. But most importantly, I will be forever grateful to you for taking the time to help me wrap my head around the question of what to do next. Next fika is on me.

Also, to all my co-authors - **Lisa Rydén**, **Ioannis Alexandrakis Eilard**, **Stefan Broselid**, **Tobias Schmidt**, **Karl Swärd, Robin Kahn**, **Stephen Serafin** and **Kathleen Caron**, **Erik Holmberg**, **Per Karlsson**, **Fredrika Killander**, **Per Malmström**, **Emma Niméus** and **Annika Jögi**. An extra thank you to **Pär-Ola Bendahl** for opening my eyes for the world of statistics.

Next, I want to thank everyone I met along the way when discovering science. To all the lecturers at the biotechnology and the biomedicine programs who made science sound like magic.

To everyone on D12, for creating a happy, open, and helpful atmosphere. Also, to everyone in **Lena Uller, Cecilia Andersson, and Anja Meissners' groups**, for being my extended lab group during my last two years as a PhD student.

To **Zacke Söderlund**, my LTH lab partner and BMC lab neighbor, with whom I took my first steps into science by spending far too much time on biochemistry reports. Thank you for always questioning me, always helping me, and always sharing a laugh.

Thanks to **Aftab Nadeem** for helping me get my first laboratory cancer biology project, and introducing me to cell biology.

For the valuable career advice and talks about life in science – **Lisa Rydén**, **Anja Meissner**, **Linda Lindström** – thank you for the support and inspiration.

Lastly, thanks to everyone outside of work who have supported me during these years. To **Sofia**. And to **Jeanette**. To all my friends from LTH, with a special thanks to my roommate **Alexander** for making me laugh even the day before my thesis deadline.

To **William**, **Anna**, **Madde**, **Rebecca**, and **Espen**, for everything.

To my parents **Bruno & Sylvia**, for encouraging me to follow the twists and turns of my path, even though it rarely was the path of least resistance. And for letting me discover the concept of experimenting using all of your hygiene products as a child (: And to my sister **Karin**, thank you for being my lifelong role model and support. I am grateful and proud to be related to the only person with whom I can discuss crumble pie and multiple imputation simultaneously.

Finally, I would like to thank **Cancerfonden** for financing my PhD studies and all of my laboratory projects.

References

1. Bologa, C.G., et al., *Virtual and biomolecular screening converge on a selective agonist for GPR30.* Nat Chem Biol, 2006. **2**(4): p. 207-12.
2. Lebesgue, D., et al., *Acute administration of non-classical estrogen receptor agonists attenuates ischemia-induced hippocampal neuron loss in middle-aged female rats.* PLoS One, 2010. **5**(1): p. e8642.
3. Hanahan, D. and R.A. Weinberg, *Hallmarks of cancer: the next generation.* Cell, 2011. **144**(5): p. 646-74.
4. Hanahan, D. and R.A. Weinberg, *The hallmarks of cancer.* Cell, 2000. **100**(1): p. 57-70.
5. Lee, E.Y. and W.J. Muller, *Oncogenes and tumor suppressor genes.* Cold Spring Harb Perspect Biol, 2010. **2**(10): p. a003236.
6. The International Agency for Research on Cancer, I., *World Cancer Report: Cancer Research for Cancer Prevention*, Christopher P. Wild and a.B.W.S. Elisabete Weiderpass, Editors. 2020.
7. *World Health Organization - Breast Cancer*. 2021 210927]; Available from: https://www.who.int/news-room/fact-sheets/detail/breast-cancer.
8. Socialstyrelsen, *Statistik om nyupptäckta cancerfall 2019*. 2019.
9. Socialstyrelsen. *Statistics on Cancer Incidence 2019 (official Swedish statistics in health and medicine)*. 2019.
10. Kuchenbaecker, K.B., et al., *Risks of Breast, Ovarian, and Contralateral Breast Cancer for BRCA1 and BRCA2 Mutation Carriers.* Jama, 2017. **317**(23): p. 2402-2416.
11. Chen, S. and G. Parmigiani, *Meta-analysis of BRCA1 and BRCA2 penetrance.* J Clin Oncol, 2007. **25**(11): p. 1329-33.
12. *Continuous Update Project: Diet, nutrition, physical activity and breast cancer survivors*, W.C.R.F.I.A.I.f.C. Research, Editor. 2014.
13. Braithwaite, D., et al., *Smoking and survival after breast cancer diagnosis: a prospective observational study and systematic review.* Breast Cancer Res Treat, 2012. **136**(2): p. 521-33.
14. Goldhirsch, A., et al., *Personalizing the treatment of women with early breast cancer: highlights of the St Gallen International Expert Consensus on the Primary Therapy of Early Breast Cancer 2013.* Ann Oncol, 2013. **24**(9): p. 2206-23.
15. Sørlie, T., et al., *Gene expression patterns of breast carcinomas distinguish tumor subclasses with clinical implications.* Proc Natl Acad Sci U S A, 2001. **98**(19): p. 10869-74.

16. *Nationellt Vårdprogram Bröstcancer* 2020 2020-10-22 2021-09-22]; 3.4:[Available from: https://kunskapsbanken.cancercentrum.se/globalassets/cancerdiagnoser/brost/vardprogram/nationellt-vardprogram-brostcancer.pdf.
17. Pareja, F., et al., *Triple-negative breast cancer: the importance of molecular and histologic subtyping, and recognition of low-grade variants.* NPJ Breast Cancer, 2016. **2**: p. 16036.
18. Foulkes, W.D., I.E. Smith, and J.S. Reis-Filho, *Triple-negative breast cancer.* N Engl J Med, 2010. **363**(20): p. 1938-48.
19. Rida, P., et al., *First international TNBC conference meeting report.* Breast Cancer Res Treat, 2018. **169**(3): p. 407-412.
20. Alkner, S., et al., *Contralateral breast cancer can represent a metastatic spread of the first primary tumor: determination of clonal relationship between contralateral breast cancers using next-generation whole genome sequencing.* Breast Cancer Research, 2015. **17**(1): p. 102.
21. Rovera, F., et al., *Axillary sentinel lymph node biopsy: An overview.* International Journal of Surgery, 2008. **6**: p. S109-S112.
22. Langlands, F.E., et al., *Breast cancer subtypes: response to radiotherapy and potential radiosensitisation.* The British journal of radiology, 2013. **86**(1023): p. 20120601-20120601.
23. *Favourable and unfavourable effects on long-term survival of radiotherapy for early breast cancer: an overview of the randomised trials. Early Breast Cancer Trialists' Collaborative Group.* Lancet, 2000. **355**(9217): p. 1757-70.
24. Choi, J., et al., *Predicting Radiation Resistance in Breast Cancer with Expression Status of Phosphorylated S6K1.* Scientific Reports, 2020. **10**(1): p. 641.
25. Ojo, D., et al., *Factors Promoting Tamoxifen Resistance in Breast Cancer via Stimulating Breast Cancer Stem Cell Expansion.* Curr Med Chem, 2015. **22**(19): p. 2360-74.
26. Carter, C.L., C. Allen, and D.E. Henson, *Relation of tumor size, lymph node status, and survival in 24,740 breast cancer cases.* Cancer, 1989. **63**(1): p. 181-7.
27. Davies, C., et al., *Relevance of breast cancer hormone receptors and other factors to the efficacy of adjuvant tamoxifen: patient-level meta-analysis of randomised trials.* Lancet, 2011. **378**(9793): p. 771-84.
28. *Effects of chemotherapy and hormonal therapy for early breast cancer on recurrence and 15-year survival: an overview of the randomised trials.* Lancet, 2005. **365**(9472): p. 1687-717.
29. Sledge, G.W., et al., *Past, present, and future challenges in breast cancer treatment.* J Clin Oncol, 2014. **32**(19): p. 1979-86.
30. Shiau, A.K., et al., *The structural basis of estrogen receptor/coactivator recognition and the antagonism of this interaction by tamoxifen.* Cell, 1998. **95**(7): p. 927-37.
31. Jordan, V.C., R. Curpan, and P.Y. Maximov, *Estrogen receptor mutations found in breast cancer metastases integrated with the molecular pharmacology of selective ER modulators.* J Natl Cancer Inst, 2015. **107**(6): p. djv075.
32. Gallo, D., et al., *Trophic effect in MCF-7 cells of ERalpha17p, a peptide corresponding to a platform regulatory motif of the estrogen receptor alpha--underlying mechanisms.* J Steroid Biochem Mol Biol, 2008. **109**(1-2): p. 138-49.

33. Wang, G.L., et al., *Hypoxia-inducible factor 1 is a basic-helix-loop-helix-PAS heterodimer regulated by cellular O2 tension.* Proc Natl Acad Sci U S A, 1995. **92**(12): p. 5510-5514.
34. Tian, H., et al., *The hypoxia-responsive transcription factor EPAS1 is essential for catecholamine homeostasis and protection against heart failure during embryonic development.* Genes Dev, 1998. **12**(21): p. 3320-3324.
35. Jaakkola, P., et al., *Targeting of HIF-a to the von Hippel-Lindau ubiquitylation complex by o2-regulated prolyl hydroxylation.* Science, 2001. **292**: p. 468-472.
36. Jiang, B.H., et al., *Dimerization, DNA binding, and transactivation properties of hypoxia-inducible factor 1.* J Biol Chem, 1996. **271**(30): p. 17771-17778.
37. Ziello, J.E., I.S. Jovin, and Y. Huang, *Hypoxia-Inducible Factor (HIF)-1 regulatory pathway and its potential for therapeutic intervention in malignancy and ischemia.* Yale J Biol Med, 2007. **80**(2): p. 51-60.
38. Miyazaki, K., et al., *Identification of functional hypoxia response elements in the promoter region of the DEC1 and DEC2 genes.* J Biol Chem, 2002. **277**(49): p. 47014-21.
39. Jögi, A., *Tumour hypoxia and the hypoxia-inducible transcription factors: Key players in cancer progression and metastasis*, in *Tumor Cell Metabolism*, S. Mazurek and M.C. Shoshan, Editors. 2014, Springer-Verlag: Wien.
40. Harris, A.L., *Hypoxia--a key regulatory factor in tumour growth.* Nature Rev Cancer, 2002. **2**(1): p. 38-47.
41. Rankin, E.B. and A.J. Giaccia, *Hypoxic control of metastasis.* Science, 2016. **352**(6282): p. 175-80.
42. Bos, R., et al., *Levels of hypoxia-inducible factor-1alpha independently predict prognosis in patients with lymph node negative breast carcinoma.* Cancer, 2003. **97**(6): p. 1573-81.
43. Jögi, A., et al., *Expression of HIF-1alpha is related to a poor prognosis and tamoxifen resistance in contralateral breast cancer.* PLoS One, 2019. **14**(12): p. e0226150.
44. Generali, D., et al., *Hypoxia-inducible factor-1alpha expression predicts a poor response to primary chemoendocrine therapy and disease-free survival in primary human breast cancer.* Clin Cancer Res, 2006. **12**(15): p. 4562-8.
45. Vaupel, P. and A. Mayer, *Hypoxia in cancer: significance and impact on clinical outcome.* Cancer Metastasis Rev, 2007. **26**(2): p. 225-39.
46. Grimes, D.R. and M. Partridge, *A mechanistic investigation of the oxygen fixation hypothesis and oxygen enhancement ratio.* Biomedical physics & engineering express, 2015. **1**(4): p. 045209-045209.
47. Levinthal, C., *How to Fold Graciously.* Mossbauer Spectroscopy in Biological Systems Proceedings, 1969. **67**(41): p. 22-26.
48. Ken A. Dill, S.B., *Molecular Driving Forces - Statistical Thermodynamics in Biology, Chemistry, Physics, and Nanoscience*. 2 ed. 2011: Garland Science, Taylor & Francis Group. 756.
49. Kenanin, T., *A Pharmacology Primer*. 2004: Elsevier Academic Press. 214.
50. Stryer, B., Tymoczko, *Biochemistry*. Seventh ed. 2012: W. H. Freeman and Company.
51. Gruber, J., et al., *Caenorhabditis elegans: What We Can and Cannot Learn from Aging Worms.* Antioxid Redox Signal, 2015. **23**(3): p. 256-79.

52. Bargmann, C.I., *Neurobiology of the Caenorhabditis elegans genome.* Science, 1998. **282**(5396): p. 2028-33.
53. Rask-Andersen, M., S. Masuram, and H.B. Schioth, *The druggable genome: Evaluation of drug targets in clinical trials suggests major shifts in molecular class and indication.* Annu Rev Pharmacol Toxicol, 2014. **54**: p. 9-26.
54. Fredriksson, R., et al., *The G-protein-coupled receptors in the human genome form five main families. Phylogenetic analysis, paralogon groups, and fingerprints.* Mol Pharmacol, 2003. **63**(6): p. 1256-72.
55. Gurevich, V.V. and E.V. Gurevich, *Molecular Mechanisms of GPCR Signaling: A Structural Perspective.* Int J Mol Sci, 2017. **18**(12).
56. Bockenhauer, S., et al., *Conformational dynamics of single G protein-coupled receptors in solution.* J Phys Chem B, 2011. **115**(45): p. 13328-38.
57. Wingler, L.M. and R.J. Lefkowitz, *Conformational Basis of G Protein-Coupled Receptor Signaling Versatility.* Trends in Cell Biology, 2020. **30**(9): p. 736-747.
58. Hilger, D., M. Masureel, and B.K. Kobilka, *Structure and dynamics of GPCR signaling complexes.* Nat Struct Mol Biol, 2018. **25**(1): p. 4-12.
59. Kristiansen, K., *Molecular mechanisms of ligand binding, signaling, and regulation within the superfamily of G-protein-coupled receptors: molecular modeling and mutagenesis approaches to receptor structure and function.* Pharmacol Ther, 2004. **103**(1): p. 21-80.
60. Neubig, R.R., et al., *International Union of Pharmacology Committee on Receptor Nomenclature and Drug Classification. XXXVIII. Update on terms and symbols in quantitative pharmacology.* Pharmacol Rev, 2003. **55**(4): p. 597-606.
61. Jarl E.S. Wikberg, M.E., Egon L. Willighagen, Ola Spjuth, Maris Lapins, Ola Engkvist, Jonathan Alvarsson, *Introduction to Pharmaceutical Bioinformatics*. Third ed. 2018.
62. Wootten, D., et al., *Mechanisms of signalling and biased agonism in G protein-coupled receptors.* Nature Reviews Molecular Cell Biology, 2018. **19**(10): p. 638-653.
63. Weis, W.I. and B.K. Kobilka, *The Molecular Basis of G Protein-Coupled Receptor Activation.* Annu Rev Biochem, 2018. **87**: p. 897-919.
64. Levitzki, A., *From epinephrine to cyclic AMP.* Science, 1988. **241**(4867): p. 800-6.
65. Dhanasekaran, N. and J.M. Dermott, *Signaling by the G12 class of G proteins.* Cellular Signalling, 1996. **8**(4): p. 235-245.
66. Heuss, C. and U. Gerber, *G-protein-independent signaling by G-protein-coupled receptors.* Trends in Neurosciences, 2000. **23**(10): p. 469-475.
67. Ferguson, S.S.G., *Evolving Concepts in G Protein-Coupled Receptor Endocytosis: The Role in Receptor Desensitization and Signaling.* Pharmacological Reviews, 2001. **53**(1): p. 1-24.
68. Timmerman, H. and H. van der Goot, *Histamine Receptors and their Ligands: Mechanisms and Applications*, in *Encyclopedia of Neuroscience*, L.R. Squire, Editor. 2009, Academic Press: Oxford. p. 1149-1166.
69. Gardner, L.A., A.P. Naren, and S.W. Bahouth, *Assembly of an SAP97-AKAP79-cAMP-dependent protein kinase scaffold at the type 1 PSD-95/DLG/ZO1 motif of the human beta(1)-adrenergic receptor generates a receptosome involved in receptor recycling and networking.* J Biol Chem, 2007. **282**(7): p. 5085-5099.

70. Good, M.C., J.G. Zalatan, and W.A. Lim, *Scaffold proteins: hubs for controlling the flow of cellular information.* Science, 2011. **332**(6030): p. 680-6.
71. Buday, L. and P. Tompa, *Functional classification of scaffold proteins and related molecules.* Febs j, 2010. **277**(21): p. 4348-55.
72. Paterni, I., et al., *Estrogen receptors alpha (ERα) and beta (ERβ): subtype-selective ligands and clinical potential.* Steroids, 2014. **90**: p. 13-29.
73. Losel, R.M., et al., *Nongenomic steroid action: controversies, questions, and answers.* Physiol Rev, 2003. **83**(3): p. 965-1016.
74. Razandi, M., et al., *Cell membrane and nuclear estrogen receptors (ERs) originate from a single transcript: studies of ERalpha and ERbeta expressed in Chinese hamster ovary cells.* Mol Endocrinol, 1999. **13**(2): p. 307-19.
75. Levin, E.R., *Integration of the Extranuclear and Nuclear Actions of Estrogen.* Molecular Endocrinology, 2005. **19**(8): p. 1951-1959.
76. Singh, M., et al., *Estrogen-induced activation of mitogen-activated protein kinase in cerebral cortical explants: convergence of estrogen and neurotrophin signaling pathways.* J Neurosci, 1999. **19**(4): p. 1179-88.
77. O'Dowd, B.F., et al., *Discovery of three novel G-protein-coupled receptor genes.* Genomics, 1998. **47**(2): p. 310-3.
78. Takada, Y., et al., *Cloning of cDNAs encoding G protein-coupled receptor expressed in human endothelial cells exposed to fluid shear stress.* Biochem Biophys Res Commun, 1997. **240**(3): p. 737-41.
79. Carmeci, C., et al., *Identification of a gene (GPR30) with homology to the G-protein-coupled receptor superfamily associated with estrogen receptor expression in breast cancer.* Genomics, 1997. **45**(3): p. 607-17.
80. Feng, Y. and P. Gregor, *Cloning of a novel member of the G protein-coupled receptor family related to peptide receptors.* Biochem Biophys Res Commun, 1997. **231**(3): p. 651-4.
81. Owman, C., et al., *Cloning of human cDNA encoding a novel heptahelix receptor expressed in Burkitt's lymphoma and widely distributed in brain and peripheral tissues.* Biochem Biophys Res Commun, 1996. **228**(2): p. 285-92.
82. Thomas, P., et al., *Identity of an estrogen membrane receptor coupled to a G protein in human breast cancer cells.* Endocrinology, 2005. **146**(2): p. 624-32.
83. Revankar, C.M., et al., *A transmembrane intracellular estrogen receptor mediates rapid cell signaling.* Science, 2005. **307**(5715): p. 1625-30.
84. Prossnitz, E.R. and J.B. Arterburn, *International Union of Basic and Clinical Pharmacology. XCVII. G Protein-Coupled Estrogen Receptor and Its Pharmacologic Modulators.* Pharmacol Rev, 2015. **67**(3): p. 505-40.
85. Olde, B. and L.M. Leeb-Lundberg, *GPR30/GPER1: searching for a role in estrogen physiology.* Trends Endocrinol Metab, 2009. **20**(8): p. 409-16.
86. Levin, E.R., *G protein-coupled receptor 30: estrogen receptor or collaborator?* Endocrinology, 2009. **150**(4): p. 1563-5.
87. Pedram, A., M. Razandi, and E.R. Levin, *Nature of Functional Estrogen Receptors at the Plasma Membrane.* Molecular Endocrinology, 2006. **20**(9): p. 1996-2009.

88. Filardo, E.J., et al., *Estrogen-induced activation of Erk-1 and Erk-2 requires the G protein-coupled receptor homolog, GPR30, and occurs via trans-activation of the epidermal growth factor receptor through release of HB-EGF.* Mol Endocrinol, 2000. **14**(10): p. 1649-60.
89. Broselid, S., et al., *G protein-coupled receptor 30 (GPR30) forms a plasma membrane complex with membrane-associated guanylate kinases (MAGUKs) and protein kinase A-anchoring protein 5 (AKAP5) that constitutively inhibits cAMP production.* J Biol Chem, 2014. **289**(32): p. 22117-27.
90. Gonzalez de Valdivia, E., et al., *G protein-coupled estrogen receptor 1 (GPER1)/GPR30 increases ERK1/2 activity through PDZ motif-dependent and -independent mechanisms.* J Biol Chem, 2017. **292**(24): p. 9932-9943.
91. Otto, C., et al., *G Protein-Coupled Receptor 30 Localizes to the Endoplasmic Reticulum and Is Not Activated by Estradiol.* Endocrinology, 2008. **149**(10): p. 4846-4856.
92. Filardo, E., et al., *Activation of the Novel Estrogen Receptor G Protein-Coupled Receptor 30 (GPR30) at the Plasma Membrane.* Endocrinology, 2007. **148**(7): p. 3236-3245.
93. Sjöström, M., et al., *Lack of G protein-coupled estrogen receptor (GPER) in the plasma membrane is associated with excellent long-term prognosis in breast cancer.* Breast Cancer Res Treat, 2014. **145**(1): p. 61-71.
94. Ignatov, A., et al., *Role of GPR30 in the mechanisms of tamoxifen resistance in breast cancer MCF-7 cells.* Breast Cancer Res Treat, 2010. **123**(1): p. 87-96.
95. Ahola, T.M., et al., *G Protein-Coupled Receptor 30 Is Critical for a Progestin-Induced Growth Inhibition in MCF-7 Breast Cancer Cells.* Endocrinology, 2002. **143**(9): p. 3376-3384.
96. Weißenborn, C., et al., *GPER functions as a tumor suppressor in triple-negative breast cancer cells.* Journal of Cancer Research and Clinical Oncology, 2014. **140**(5): p. 713-723.
97. Broselid, S., et al., *G protein-coupled estrogen receptor is apoptotic and correlates with increased distant disease-free survival of estrogen receptor-positive breast cancer patients.* Clin Cancer Res, 2013. **19**(7): p. 1681-92.
98. Tran, Q.K., et al., *Hetero-oligomeric Complex between the G Protein-coupled Estrogen Receptor 1 and the Plasma Membrane Ca2+-ATPase 4b.* J Biol Chem, 2015. **290**(21): p. 13293-307.
99. Prossnitz, E.R. and M. Barton, *Estrogen biology: New insights into GPER function and clinical opportunities.* Molecular and Cellular Endocrinology, 2014. **389**(1): p. 71-83.
100. Maggiolini, M., et al., *The G protein-coupled receptor GPR30 mediates c-fos up-regulation by 17beta-estradiol and phytoestrogens in breast cancer cells.* J Biol Chem, 2004. **279**(26): p. 27008-16.
101. Kang, L., et al., *Involvement of estrogen receptor variant ER-alpha36, not GPR30, in nongenomic estrogen signaling.* Mol Endocrinol, 2010. **24**(4): p. 709-21.
102. Acconcia, F., et al., *Palmitoylation-dependent estrogen receptor alpha membrane localization: regulation by 17beta-estradiol.* Mol Biol Cell, 2005. **16**(1): p. 231-7.
103. Langer, G., et al., *A critical review of fundamental controversies in the field of GPR30 research.* Steroids, 2010. **75**(8-9): p. 603-10.

104. Isensee, J., et al., *PKA-RII subunit phosphorylation precedes activation by cAMP and regulates activity termination.* J Cell Biol, 2018. **217**(6): p. 2167-2184.
105. Omar, M.H. and J.D. Scott, *AKAP Signaling Islands: Venues for Precision Pharmacology.* Trends Pharmacol Sci, 2020. **41**(12): p. 933-946.
106. Bacskai, B.J., et al., *Spatially resolved dynamics of cAMP and protein kinase A subunits in Aplysia sensory neurons.* Science, 1993. **260**(5105): p. 222-6.
107. Barsony, J. and S.J. Marx, *Immunocytology on microwave-fixed cells reveals rapid and agonist-specific changes in subcellular accumulation patterns for cAMP or cGMP.* Proc Natl Acad Sci U S A, 1990. **87**(3): p. 1188-92.
108. Zaccolo, M. and T. Pozzan, *Discrete microdomains with high concentration of cAMP in stimulated rat neonatal cardiac myocytes.* Science, 2002. **295**(5560): p. 1711-5.
109. Carr, D.W., et al., *Interaction of the regulatory subunit (RII) of cAMP-dependent protein kinase with RII-anchoring proteins occurs through an amphipathic helix binding motif.* Journal of Biological Chemistry, 1991. **266**(22): p. 14188-14192.
110. Omar, M.H. and J.D. Scott, *AKAP Signaling Islands: Venues for Precision Pharmacology.* Trends in Pharmacological Sciences, 2020. **41**(12): p. 933-946.
111. Wong, W. and J.D. Scott, *AKAP signalling complexes: focal points in space and time.* Nat Rev Mol Cell Biol, 2004. **5**(12): p. 959-70.
112. Zhang, M., et al., *Adenylyl cyclase anchoring by a kinase anchor protein AKAP5 (AKAP79/150) is important for postsynaptic beta-adrenergic signaling.* J Biol Chem, 2013. **288**(24): p. 17918-31.
113. Kjällquist, U., et al., *Exome sequencing of primary breast cancers with paired metastatic lesions reveals metastasis-enriched mutations in the A-kinase anchoring protein family (AKAPs).* BMC Cancer, 2018. **18**(1): p. 174.
114. Romero, G., M. von Zastrow, and P.A. Friedman, *9 - Role of PDZ Proteins in Regulating Trafficking, Signaling, and Function of GPCRs: Means, Motif, and Opportunity*, in *Advances in Pharmacology*, R.R. Neubig, Editor. 2011, Academic Press. p. 279-314.
115. Waters, E.M., et al., *G-protein-coupled estrogen receptor 1 is anatomically positioned to modulate synaptic plasticity in the mouse hippocampus.* J Neurosci, 2015. **35**(6): p. 2384-97.
116. Akama, K.T., et al., *Post-synaptic density-95 (PSD-95) binding capacity of G-protein-coupled receptor 30 (GPR30), an estrogen receptor that can be identified in hippocampal dendritic spines.* J Biol Chem, 2013. **288**(9): p. 6438-50.
117. Bhattacharyya, S., et al., *A critical role for PSD-95/AKAP interactions in endocytosis of synaptic AMPA receptors.* Nat Neurosci, 2009. **12**(2): p. 172-81.
118. Colledge, M., et al., *Targeting of PKA to glutamate receptors through a MAGUK-AKAP complex.* Neuron, 2000. **27**(1): p. 107-19.
119. Fluhmann, B., et al., *A human orphan calcitonin receptor-like structure.* Biochem Biophys Res Commun, 1995. **206**(1): p. 341-7.
120. Aiyar, N., et al., *A cDNA encoding the calcitonin gene-related peptide type 1 receptor.* J Biol Chem, 1996. **271**(19): p. 11325-9.

121. Lenhart, P.M., et al., *G-protein-coupled receptor 30 interacts with receptor activity-modifying protein 3 and confers sex-dependent cardioprotection.* J Mol Endocrinol, 2013. **51**(1): p. 191-202.
122. Watanabe, H., et al., *The estrogen-responsive adrenomedullin and receptor-modifying protein 3 gene identified by DNA microarray analysis are directly regulated by estrogen receptor.* J Mol Endocrinol, 2006. **36**(1): p. 81-9.
123. Hewitt, S.C., et al., *Global uterine genomics in vivo: microarray evaluation of the estrogen receptor alpha-growth factor cross-talk mechanism.* Mol Endocrinol, 2005. **19**(3): p. 657-68.
124. Casarini, L., et al., *Membrane Estrogen Receptor (GPER) and Follicle-Stimulating Hormone Receptor (FSHR) Heteromeric Complexes Promote Human Ovarian Follicle Survival.* iScience, 2020. **23**(12): p. 101812.
125. Wang, Z.Y. and L. Yin, *Estrogen receptor alpha-36 (ER-α36): A new player in human breast cancer.* Mol Cell Endocrinol, 2015. **418 Pt 3**: p. 193-206.
126. Omarjee, S., et al., *The molecular mechanisms underlying the ERalpha-36-mediated signaling in breast cancer.* Oncogene, 2017. **36**(18): p. 2503-2514.
127. Wang, Z., et al., *A variant of estrogen receptor-{alpha}, hER-{alpha}36: transduction of estrogen- and antiestrogen-dependent membrane-initiated mitogenic signaling.* Proc Natl Acad Sci U S A, 2006. **103**(24): p. 9063-8.
128. Chaudhri, R.A., et al., *Estrogen receptor-alpha 36 mediates the anti-apoptotic effect of estradiol in triple negative breast cancer cells via a membrane-associated mechanism.* Biochim Biophys Acta, 2014. **1843**(11): p. 2796-806.
129. Tong, J.S., et al., *ER-alpha36, a novel variant of ER-alpha, mediates estrogen-stimulated proliferation of endometrial carcinoma cells via the PKCdelta/ERK pathway.* PLoS One, 2010. **5**(11): p. e15408.
130. Uhlen, M., et al., *A pathology atlas of the human cancer transcriptome.* Science, 2017. **357**(6352).
131. *Human Protein Atlas*. 2021 210224 [cited 2021 210906]; #v20.1:[Available from: http://www.proteinatlas.org.
132. Kvingedal, A.M. and E.B. Smeland, *A novel putative G-protein-coupled receptor expressed in lung, heart and lymphoid tissue.* FEBS Lett, 1997. **407**(1): p. 59-62.
133. Baltgalvis, K.A., et al., *Estrogen regulates estrogen receptors and antioxidant gene expression in mouse skeletal muscle.* PLoS One, 2010. **5**(4): p. e10164.
134. Chagin, A.S. and L. Sävendahl, *GPR30 estrogen receptor expression in the growth plate declines as puberty progresses.* J Clin Endocrinol Metab, 2007. **92**(12): p. 4873-7.
135. Pöllänen, E., et al., *Differential influence of peripheral and systemic sex steroids on skeletal muscle quality in pre- and postmenopausal women.* Aging Cell, 2011. **10**(4): p. 650-60.
136. Martin, S.G., et al., *Low expression of G protein-coupled oestrogen receptor 1 (GPER) is associated with adverse survival of breast cancer patients.* Oncotarget, 2018. **9**(40): p. 25946-25956.
137. Filardo, E.J., et al., *Distribution of GPR30, a seven membrane-spanning estrogen receptor, in primary breast cancer and its association with clinicopathologic determinants of tumor progression.* Clin Cancer Res, 2006. **12**(21): p. 6359-66.

138. Kuo, W.-H., et al., *The Interactions Between GPR30 and the Major Biomarkers in Infiltrating Ductal Carcinoma of the Breast in an Asian Population.* Taiwanese Journal of Obstetrics and Gynecology, 2007. **46**(2): p. 135-145.
139. Ariazi, E.A., et al., *The G protein-coupled receptor GPR30 inhibits proliferation of estrogen receptor-positive breast cancer cells.* Cancer Res, 2010. **70**(3): p. 1184-94.
140. Li, G., et al., *ERα36 as a Potential Therapeutic Target for Tamoxifen-Resistant Breast Cancer Cell Line Through EGFR/ERK Signaling Pathway.* Cancer Manag Res, 2020. **12**: p. 265-275.
141. Ignatov, A., et al., *G-protein-coupled estrogen receptor GPR30 and tamoxifen resistance in breast cancer.* Breast Cancer Research and Treatment, 2011. **128**(2): p. 457-466.
142. Ignatov, T., et al., *G-protein-coupled estrogen receptor GPER-1 expression in hormone receptor-positive breast cancer is associated with poor benefit of tamoxifen.* Breast Cancer Research and Treatment, 2019. **174**(1): p. 121-127.
143. Recchia, A.G., et al., *The G protein-coupled receptor 30 is up-regulated by hypoxia-inducible factor-1alpha (HIF-1alpha) in breast cancer cells and cardiomyocytes.* J Biol Chem, 2011. **286**(12): p. 10773-82.
144. Kimura, M., et al., *Orphan G protein-coupled receptor, GPR41, induces apoptosis via a p53/Bax pathway during ischemic hypoxia and reoxygenation.* J Biol Chem, 2001. **276**(28): p. 26453-60.
145. De Francesco, E.M., et al., *HIF-1α/GPER signaling mediates the expression of VEGF induced by hypoxia in breast cancer associated fibroblasts (CAFs).* Breast Cancer Res, 2013. **15**(4): p. R64.
146. Bylund, D.B., *Beta Adrenoceptors**, in *xPharm: The Comprehensive Pharmacology Reference*, S.J. Enna and D.B. Bylund, Editors. 2007, Elsevier: New York. p. 1-7.
147. Bers, D.M., *Cardiac excitation-contraction coupling.* Nature, 2002. **415**(6868): p. 198-205.
148. Hagemann, D. and R.P. Xiao, *Dual site phospholamban phosphorylation and its physiological relevance in the heart.* Trends Cardiovasc Med, 2002. **12**(2): p. 51-6.
149. Hu, L.A., et al., *beta 1-adrenergic receptor association with PSD-95. Inhibition of receptor internalization and facilitation of beta 1-adrenergic receptor interaction with N-methyl-D-aspartate receptors.* J Biol Chem, 2000. **275**(49): p. 38659-66.
150. Gardner, L.A., et al., *AKAP79-mediated Targeting of the Cyclic AMP-dependent Protein Kinase to the β1-Adrenergic Receptor Promotes Recycling and Functional Resensitization of the Receptor*.* Journal of Biological Chemistry, 2006. **281**(44): p. 33537-33553.
151. Nichols, C.B., et al., *Sympathetic stimulation of adult cardiomyocytes requires association of AKAP5 with a subpopulation of L-type calcium channels.* Circ Res, 2010. **107**(6): p. 747-56.
152. Montoya, A., et al., *Use of non-selective β-blockers is associated with decreased tumor proliferative indices in early stage breast cancer.* Oncotarget, 2017. **8**(4): p. 6446-6460.
153. Devore, E.E., et al., *Antihypertensive medication use and incident breast cancer in women.* Breast Cancer Research and Treatment, 2015. **150**(1): p. 219-229.
154. Raimondi, S., et al., *Use of beta-blockers, angiotensin-converting enzyme inhibitors and angiotensin receptor blockers and breast cancer survival: Systematic review and meta-analysis.* Int J Cancer, 2016. **139**(1): p. 212-9.

155. Nagaraja, A.S., et al., *β-blockers: a new role in cancer chemotherapy?* Expert Opin Investig Drugs, 2013. **22**(11): p. 1359-63.
156. Zheng, G., et al., *Beta-Blockers Use and Risk of Breast Cancer in Women with Hypertension.* Cancer Epidemiol Biomarkers Prev, 2021. **30**(5): p. 965-973.
157. Robas, N., et al., *Maximizing serendipity: strategies for identifying ligands for orphan G-protein-coupled receptors.* Curr Opin Pharmacol, 2003. **3**(2): p. 121-6.
158. Darby, S., et al., *Effect of radiotherapy after breast-conserving surgery on 10-year recurrence and 15-year breast cancer death: meta-analysis of individual patient data for 10,801 women in 17 randomised trials.* Lancet, 2011. **378**(9804): p. 1707-16.
159. Bartelink, H., et al., *Impact of a higher radiation dose on local control and survival in breast-conserving therapy of early breast cancer: 10-year results of the randomized boost versus no boost EORTC 22881-10882 trial.* J Clin Oncol, 2007. **25**(22): p. 3259-65.
160. Liu, R., W. Wong, and A.P. Ijzerman, *Human G protein-coupled receptor studies in Saccharomyces cerevisiae.* Biochemical Pharmacology, 2016. **114**: p. 103-115.
161. Kobayashi, H., et al., *Bioluminescence resonance energy transfer–based imaging of protein–protein interactions in living cells.* Nature Protocols, 2019. **14**(4): p. 1084-1107.
162. Kocan, M., et al., *Enhanced BRET Technology for the Monitoring of Agonist-Induced and Agonist-Independent Interactions between GPCRs and β-Arrestins.* Front Endocrinol (Lausanne), 2010. **1**: p. 12.
163. Marques, S.M. and J.C. Esteves da Silva, *Firefly bioluminescence: a mechanistic approach of luciferase catalyzed reactions.* IUBMB Life, 2009. **61**(1): p. 6-17.
164. Yao, F., et al., *Tetracycline repressor, tetR, rather than the tetR-mammalian cell transcription factor fusion derivatives, regulates inducible gene expression in mammalian cells.* Hum Gene Ther, 1998. **9**(13): p. 1939-50.
165. Kotarsky, K., et al., *Optimized reporter gene assays based on a synthetic multifunctional promoter and a secreted luciferase.* Analytical Biochemistry, 2003. **316**(2): p. 208-215.
166. Gonzalez-Garcia, J.R., et al., *The dynamics of MAPK inactivation at fertilization in mouse eggs.* J Cell Sci, 2014. **127**(Pt 12): p. 2749-60.
167. Komatsu, N., et al., *Development of an optimized backbone of FRET biosensors for kinases and GTPases.* Mol Biol Cell, 2011. **22**(23): p. 4647-56.
168. Macian, F., *NFAT proteins: key regulators of T-cell development and function.* Nature Reviews Immunology, 2005. **5**(6): p. 472-484.
169. Clipstone, N.A. and G.R. Crabtree, *Identification of calcineurin as a key signalling enzyme in T-lymphocyte activation.* Nature, 1992. **357**(6380): p. 695-7.
170. Piccolo, S.R., et al., *A single-sample microarray normalization method to facilitate personalized-medicine workflows.* Genomics, 2012. **100**(6): p. 337-344.
171. Foroutan, M., et al., *Single sample scoring of molecular phenotypes.* BMC Bioinformatics, 2018. **19**(1): p. 404.
172. *R: A language and environment for statistical computing.* 2022; Available from: http://www.R-project.org/.
173. Gray, B., *cmprsk: Subdistribution Analysis of Competing Risks*. 2022.
174. Alboukadel Kassambara, M.K., Przemyslaw Biecek, *survminer: Drawing Survival Curves using 'ggplot2'*. 2021.

175. *DescTools: Tools for Descriptive Statistics*, A. Signorell, Editor. 2022, Andri Signorell.
176. Alexander, S.P., A. Mathie, and J.A. Peters, *Guide to Receptors and Channels (GRAC), 5th edition.* Br J Pharmacol, 2011. **164 Suppl 1**(Suppl 1): p. S1-324.
177. Tutzauer, J., et al., *Plasma membrane expression of G protein-coupled estrogen receptor (GPER)/G protein-coupled receptor 30 (GPR30) is associated with worse outcome in metachronous contralateral breast cancer.* PLoS One, 2020. **15**(4): p. e0231786.
178. Funakoshi, T., et al., *G protein-coupled receptor 30 is an estrogen receptor in the plasma membrane.* Biochemical and Biophysical Research Communications, 2006. **346**(3): p. 904-910.
179. Li, X., M.M. Nooh, and S.W. Bahouth, *Role of AKAP79/150 protein in β1-adrenergic receptor trafficking and signaling in mammalian cells.* J Biol Chem, 2013. **288**(47): p. 33797-33812.
180. Hirtz, A., et al., *GPER Agonist G-1 Disrupts Tubulin Dynamics and Potentiates Temozolomide to Impair Glioblastoma Cell Proliferation.* Cells, 2021. **10**(12): p. 3438.
181. Prossnitz, E.R. and J.B. Arterburn, *International Union of Basic and Clinical Pharmacology. XCVII. G Protein–Coupled Estrogen Receptor and Its Pharmacologic Modulators.* Pharmacological Reviews, 2015. **67**(3): p. 505.
182. Vivacqua, A., et al., *G Protein-Coupled Receptor 30 Expression Is Up-Regulated by EGF and TGFα in Estrogen Receptor α-Positive Cancer Cells.* Molecular Endocrinology, 2009. **23**(11): p. 1815-1826.
183. Weißenborn, C., et al., *GPER functions as a tumor suppressor in MCF-7 and SK-BR-3 breast cancer cells.* J Cancer Res Clin Oncol, 2014. **140**(4): p. 663-71.
184. Pandey, D.P., et al., *Estrogenic GPR30 signalling induces proliferation and migration of breast cancer cells through CTGF.* Embo j, 2009. **28**(5): p. 523-32.
185. Damaghi, M., et al., *The harsh microenvironment in early breast cancer selects for a Warburg phenotype.* Proceedings of the National Academy of Sciences, 2021. **118**(3): p. e2011342118.
186. Elingaard-Larsen, L.O., et al., *How Reciprocal Interactions Between the Tumor Microenvironment and Ion Transport Proteins Drive Cancer Progression.* Rev Physiol Biochem Pharmacol, 2022. **182**: p. 1-38.
187. van Kuijk, S.J., et al., *Prognostic Significance of Carbonic Anhydrase IX Expression in Cancer Patients: A Meta-Analysis.* Front Oncol, 2016. **6**: p. 69.
188. Ibrahim-Hashim, A. and V. Estrella, *Acidosis and cancer: from mechanism to neutralization.* Cancer Metastasis Rev, 2019. **38**(1-2): p. 149-155.

Paper I

PLOS ONE

RESEARCH ARTICLE

Plasma membrane expression of G protein-coupled estrogen receptor (GPER)/G protein-coupled receptor 30 (GPR30) is associated with worse outcome in metachronous contralateral breast cancer

Julia Tutzauer[1☯], Martin Sjöström[2☯¤], Pär-Ola Bendahl[2], Lisa Rydén[3,4], Mårten Fernö[2], L. M. Fredrik Leeb-Lundberg[1‡*], Sara Aïkner[2,5‡]

1 Department of Experimental Medical Science, Lund University, Lund, Sweden, **2** Department of Clinical Sciences Lund, Division of Oncology and Pathology, Lund University, Lund, Sweden, **3** Department of Clinical Sciences Lund, Division of Surgery, Lund University, Lund, Sweden, **4** Department of Surgery, Skåne University Hospital, Lund, Sweden, **5** Department of Oncology, Skåne University Hospital, Lund, Sweden

☯ These authors contributed equally to this work.
¤ Current address: Department of Radiation Oncology, University of California, San Francisco, California, United States of America
‡ These authors are joint senior authors on this work.
* Fredrik.Leeb-Lundberg@med.lu.se

OPEN ACCESS

Citation: Tutzauer J, Sjöström M, Bendahl P-O, Rydén L, Fernö M, Leeb-Lundberg LMF, et al. (2020) Plasma membrane expression of G protein-coupled estrogen receptor (GPER)/G protein-coupled receptor 30 (GPR30) is associated with worse outcome in metachronous contralateral breast cancer. PLoS ONE 15(4): e0231786. https://doi.org/10.1371/journal.pone.0231786

Editor: Pirkko L. Härkönen, Turun Yliopisto, FINLAND

Received: December 4, 2019

Accepted: March 31, 2020

Published: April 17, 2020

Data Availability Statement: All relevant data are within the manuscript and its Supporting Information files.

Funding: LMFLL: Swedish Cancer Foundation, CAN 2016/423, https://www.cancerfonden.se/; Swedish Research Council, 2016-02427, https://www.vr.se/ SA: Swedish Breast Cancer Association (BRO); Skåne University Hospital foundation; Percy Falks Stiftelse för Forskning Beträffande Prostata-

Abstract

Background

G protein-coupled estrogen receptor (GPER), or G protein-coupled receptor 30 (GPR30), is reported to mediate non-genomic estrogen signaling. GPR30 associates with breast cancer (BC) outcome and may contribute to tamoxifen resistance. We investigated the expression and prognostic significance of GPR30 in metachronous contralateral breast cancer (CBC) as a model of tamoxifen resistance.

Methods

Total GPR30 expression ($GPR30_{TOT}$) and plasma membrane-localized GPR30 expression ($GPR30_{PM}$) were analyzed by immunohistochemistry in primary (BC1; $n_{BC1} = 559$) and contralateral BC (BC2; $n_{BC2} = 595$), and in lymph node metastases (LGL; $n_{LGL1} = 213$; $n_{LGL2} = 196$). Death from BC (BCD), including BC death or death after documented distant metastasis, was used as primary end-point.

Results

$GPR30_{PM}$ in BC2 and LGL2 were associated with increased risk of BCD ($HR_{BC2} = 1.7$, $p = 0.03$; $HR_{LGL2} = 2.0$; $p = 0.02$). In BC1 and BC2, $GPR30_{PM}$ associated with estrogen receptor (ER)-negativity ($p_{BC1}<0.0001$; $p_{BC2}<0.0001$) and progesterone receptor (PR)-negativity ($p_{BC1} = 0.0007$; $p_{BC2}<0.0001$). The highest $GPR30_{TOT}$ and $GPR30_{PM}$ were observed in triple-negative BC. $GPR30_{PM}$ associated with high Ki67 staining in BC1 ($p<0.0001$) and BC2

och Bröstcancer; Skåne County Council's Research and Development Foundation; Swedish Governmental Funding of Clinical Research within the National Health Service The funders had no role in study design, data collection and analysis, decision to publish, or preparation of the manuscript.

Competing interests: The authors have declared that no competing interests exist.

($p<0.0001$). $GPR30_{TOT}$ in BC2 did not associate with tamoxifen treatment for BC1. However, BC2 that were diagnosed during tamoxifen treatment were more likely to express $GPR30_{PM}$ than BC2 diagnosed after treatment completion ($p = 0.01$). Furthermore, a trend was observed that patients with $GPR30_{PM}$ in an ER-positive BC2 had greater benefit from tamoxifen treatment.

Conclusion

PM-localized GPR30 staining is associated with increased risk of BC death when expressed in BC2 and LGL2. Additionally, PM-localized GPR30 correlates with prognostic markers of worse outcome, such as high Ki67 and a triple-negative subtype. Therefore, PM-localized GPR30 may be an interesting new target for therapeutic exploitation. We found no clear evidence that total GPR30 expression is affected by tamoxifen exposure during development of metachronous CBC, or that GPR30 contributes to tamoxifen resistance.

Introduction

Metachronous contralateral breast cancer (CBC) is a second, presumably independent primary tumor (BC2) developed in the contralateral breast after the first breast cancer (BC1). The lifetime risk of a breast cancer (BC) patient developing CBC has been estimated at 2–20%, depending on factors such as family history, prior endocrine treatment, and age at BC1 diagnosis [1–3]. Similar to BC in general, CBC is a heterogenous disease and both disease stage and the molecular characteristics of the tumor is used to assess prognosis and benefit of therapy, where axillary lymph node (LGL) involvement is one of the strongest prognostic factors [4]. At the molecular level, the tumor is generally characterized by the expression of estrogen receptor α (ER), progesterone receptor (PR), and human epidermal growth factor receptor 2 (HER2), as well as the proliferation rate [5]. About 80% of all BC exhibit overexpression of ER, through which the female steroid hormone estrogen acts to stimulate cell growth and proliferation. Therefore, endocrine therapies directed to disrupt ER signaling are central in current BC treatment, acting either by suppressing ER activity, e.g. selective ER modulators or down-regulators, or by inhibiting estrogen production, e.g. aromatase inhibitors. The selective ER modulator tamoxifen is one of the most widely prescribed endocrine agents for treatment of ER-positive BC [6]. In the adjuvant setting, 5 years of tamoxifen treatment reduces the 10-year risk of recurrence by almost 50%, and the annual risk of BC mortality by almost one-third [7, 8]. However, not all ER-positive tumors respond to tamoxifen therapy, and resistance may occur *de novo* or during treatment. Tamoxifen reduces the incidence of CBC, but CBC evolving during tamoxifen treatment is assumed to have intrinsic resistance. Efforts aimed to further understand resistance mechanisms have led to a number of important discoveries, including pathological epigenetic changes or mutations in the *ESR1* gene, and interference with other growth stimulatory signaling pathways. These mechanisms subsequently result in augmented receptor activity, ligand-independent growth and transcription, or reduced drug sensitivity [6, 9, 10]. Despite these discoveries, ER remains the only predictive marker for endocrine treatment.

G protein-coupled estrogen receptor (GPER), originally named G protein-coupled receptor 30 (GPR30), is a receptor involved in rapid, non-genomic responses to estrogen [11]. In contrast to the classical ER, which is a soluble receptor residing in the cytoplasm or cell nucleus,

GPR30 is a transmembrane receptor reported to be expressed both in the plasma membrane (PM) [12] and in the endoplasmatic reticulum [13]. As an estrogen receptor, GPR30 has caught significant attention in BC research, and the relationship between GPR30 and BC outcome has been addressed in multiple studies. However, results are inconsistent, with the receptor conveying either better [14, 15] or worse prognosis [16, 17], or lacking any prognostic value [18] for BC outcome. Additionally, *in vitro* studies have shown that GPR30 is pro-apoptotic in the ER-positive BC cell line MCF-7, but proliferative in the ER-negative cell line SkBr3 [19]. Thus, GPR30 may function differently depending on the environment in which it is expressed. Both clinical and pre-clinical studies have shown that subcellular localization is also a factor influencing GPR30 function. Indeed, GPR30 staining specifically located in the PM was found to be a strong prognostic factor for poor prognosis in BC, while the total level of GPR30 staining was not [17]. Consistent with this clinical observation, an *in vitro* study showed that PM localization of GPR30 is important for receptor stimulation of ERK1/2 activity [20], a cellular signal involved in proliferation and survival. Thus, the biological context of the tumor appears to be critical for GPR30 function in BC, with subcellular localization being a factor of potential importance.

Studies have reported that GPR30 may contribute to tamoxifen resistance [21–24]. Some *in vitro* data suggest that tamoxifen directly stimulates cell growth via GPR30 [22]. This situation would be of major clinical concern, as many ER-positive BC also express GPR30, and tamoxifen treatment of these BC partly could yield increased cell growth. On the other hand, these observations may also argue that GPR30 is a potential marker to identify BC with poor responsiveness to tamoxifen. GPR30 has been suggested to function as a resistance mechanism to escape tamoxifen responsiveness. However, whether GPR30 expression changes in tumors developing resistance to tamoxifen treatment, has not yet been addressed in a larger cohort of patients.

The aim of this study was to further understand how GPR30 expression relates to BC progression, patient outcome, and previous tamoxifen treatment. To this end, we used a unique retrospective cohort of patients with CBC, either naïve or exposed to tamoxifen following BC1, with paired expression data from primary tumors and lymph node metastases, as a stepwise model of tamoxifen resistance.

Materials and methods

Patient cohort and TMA preparation

A previously constructed tissue-microarray (TMA) from 728 patients diagnosed with CBC between 1977 and 2007 at 14 hospitals within the Southern Swedish Healthcare Region was used. Details of TMA construction have been previously described [25]. Patient inclusion and number of CBC successfully stained and scored for GPR30 are summarized in Fig 1. Follow-up information was retrieved from patient charts, and cause of death and overall survival data were accessed from the Swedish National Board of Health and Welfare in March 2014. Evaluation of ER, PR, Ki67 and HER2 have been previously described [26, 27].

Cell construction and culture

HFF11 cells, originally constructed from HeLa cells (American Type Culture Collection, ATCC), were kindly provided by K. Kotarsky [28]. HFF11 cells stably expressing the T-Rex system (HeLa TET-On/Off cells), in which the expression of human GPR30 is under the strict control by tetracycline, were constructed according to vendor instructions (ThermoFisher Scientific). MCF7 cells were obtained from ATCC. Cells were confirmed to be mycoplasma-free by the MycoSEQ™ Mycoplasma Detection System (ThermoFisher Scientific). HeLa TET-On/Off cells were grown in Dulbecco's modified Eagle's medium (DMEM; Invitrogen, Carlsbad,

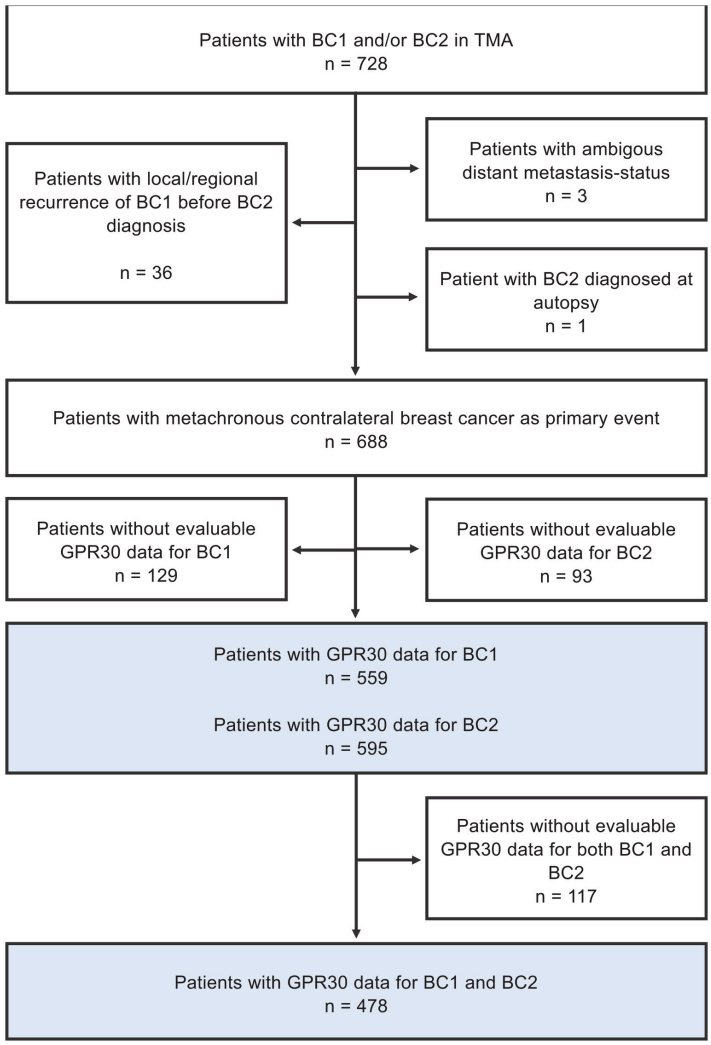

Fig 1. Flow-chart of inclusion and exclusion for the study cohort.

https://doi.org/10.1371/journal.pone.0231786.g001

CA), 10% fetal calf serum (FCS; HyClone Laboratories, Logan, UT), and 1% penicillin/streptomycin (Sigma-Aldrich), using blastidine and zeocin as clone selection markers. MCF7 cells were grown in DMEM supplemented with glucose and pyruvate, and with 10% FCS. Both cells were grown in 5% CO_2 at 37˚C.

GPR30 antibody validation

The specificity of the polyclonal goat GPR30 antibody (AF 5534; R&D Systems) was analyzed in MCF7 human breast cancer cells (American Type Culture Collection), a cell line used extensively to study native GPR30 [19]. Immunoblotting showed that the antibody recognized a receptor species with a molecular mass of 50–55 kDa in MCF7 cells (S1 Fig, panel A), consistent with that described by the vendor (R&D Systems). To ensure that the antibody reactivity was absolutely dependent on GPR30 expression, we immunoblotted HeLa TET-On/Off cells treated with and without 0.1 μM tetracycline. In these cells, the GPR30 antibody recognized three broad receptor species at about 50 kDa, 80 kDa, and 130 kDa following tetracycline treatment, whereas no significant immunoreactivity was observed in the absence of tetracycline treatment (S1 Fig, panel B). These results, and those published by us previously [15, 29], show that GPR30 antibody immunoreactivity is completely dependent on GPR30 expression. Slightly different molecular masses of the recognized receptor species were observed in native MCF7 cells and recombinant HeLa cells. This is common among G protein-coupled receptors (GPCR) and due to variations in posttranslational modifications (e.g. glycosylation, oligomerization, etc.). Confocal immunofluorescence microscopy of MCF7 cells stained live with the GPR30 antibody showed that the antibody detected receptors in the PM in these cells (S1 Fig, panel C). A similar subcellular localization was revealed using M1 FLAG antibodies (Sigma-Aldrich) to detect recombinant human GPR30 tagged at the N terminus with the FLAG epitope transiently expressed in MCF7 cells (S1 Fig, panel D). Thus, the GPR30 antibody is capable of recognizing GPR30 localized in the PM.

IHC staining and scoring of GPR30

GPR30 expression was monitored by immunohistochemical (IHC) staining with GPR30 antibody (1:50) on 1.0 mm TMA cores. Receptor expression was evaluated as total cellular staining intensity ($GPR30_{TOT;}$ Fig 2A) and PM-specific staining intensity ($GPR30_{PM}$; Fig 2B). PM-specific staining was defined as a clear increase of immunoreactivity on cell borders, as compared

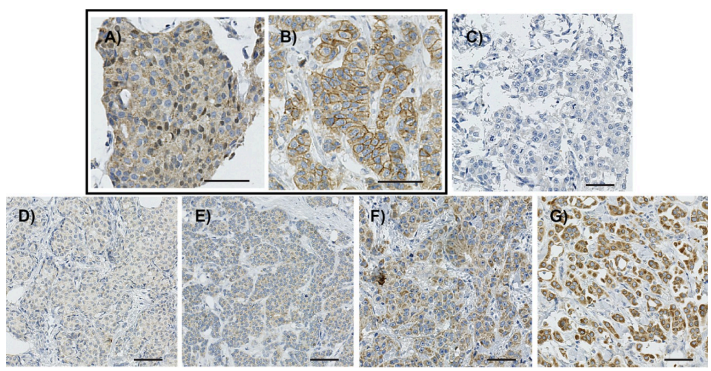

Fig 2. Representative images of GPR30 staining in BC samples. *A* and *B*, images of GPR30 staining intensity level 3 without plasma-membrane staining ($GPR30_{PM}$-) (*A*) and with plasma-membrane staining ($GPR30_{PM}$+) (*B*). *C-G*, images of GPR30 total staining ($GPR30_{TOT}$) as negative (*C*), very weak (level 1) (*D*), weak (level 2) (*E*), moderate (level 3) (*F*) and very strong (level 4) (*G*). *Bar*, 50 μm.

https://doi.org/10.1371/journal.pone.0231786.g002

to the cytoplasm. $GPR30_{TOT}$ was scored as overall intensity at 5 levels (Fig 2C–2G; 0 = negative; 1 = very weak; 2 = weak; 3 = moderate; 4 = strong), and $GPR30_{PM}$ at 3 levels (0 = no increase as compared to the cytoplasmic staining; 1 = weak PM-specific staining; and 2 = strong PM-specific staining). Percentage of stained tumor cells was scored, but as the vast majority of tumors had either 0% or >50% stained cells, the intensity was used for further analysis. The staining was visually evaluated by two independent investigators (M.S., K.L.), a well-established widely accepted method to evaluate IHC staining on TMA cores, and the mean score was used, rounding to nearest integer. Due to group sizes, $GPR30_{TOT}$ intensity was combined to two groups of weak (levels 0–2) *vs*. strong (levels 3–4). $GPR30_{PM}$+ scores were combined to create a binary variable (levels 0 *vs*. 1–2).

Statistical analysis

Death from BC (BCD), including BC death or death after documented distant metastasis, was used as primary end-point. Median follow-up time for patients alive at last follow-up was 9.1 years from BC2 diagnosis. Statistical analyses were carried out in RStudio 1.1.442 (RStudio, Boston, MA, USA) using R 3.5.1 [30]. Associations between GPR30 and factors such as patient attributes and clinicopathological markers were evaluated using Pearson's χ^2-test or Mantel-Haenszel χ^2-test for trend. GPR30 staining in paired tumors was compared using Wilcoxon matched pairs signed rank test. Cumulative incidence of BCD was calculated with death from other causes as competing risk event using the cmprsk R package [31]. Cox proportional hazards models with Wald test was used to calculate hazard ratios (HR), using the survival R package [32]. Proportional hazards were assessed using Schoenfeldt residuals. As the assumption was not reasonably well met in all the analyses, HRs should be cautiously interpreted as average effects over the follow-up interval, which was restricted to maximum 10 years to reduce the problem of non-proportional hazards.

Ethical approval

All procedures performed in studies involving human participants were approved by the Regional Ethical Review Board of Lund University (LU240-01) and in accordance with the 1964 Helsinki declaration and its later amendments or comparable ethical standards.

Informed consent

Since the study handled saved paraffin material, often several decades old, informed consent was not possible to retrieve from all patients. Nevertheless, all data was analyzed and presented anonymously, and a note was published in the local paper, informing previous BC patients to contact the research group if they did not want their tumor tissue to be used in scientific studies. This procedure was accepted by the Regional Ethical Review Board of Lund University (LU240-01).

Results

GPR30 expression in relation to patient and tumor characteristics

GPR30 expression was assessed in 688 women with metachronous CBC, where BC2 was diagnosed between 6 months and 34.1 years after BC1 diagnosis (Fig 3, median = 6.6 years). Receptor expression was monitored by immunohistochemistry in two variables; receptor staining at the PM ($GPR30_{PM}$+; Fig 2A and 2B) and total receptor staining intensity ($GPR30_{TOT}$; Fig 2C–2G). Increasing $GPR30_{TOT}$ was associated with a higher fraction of $GPR30_{PM}$+ tumors in both BC1 and BC2 (Table 1). As previously observed in three other cohorts [17], $GPR30_{TOT}$

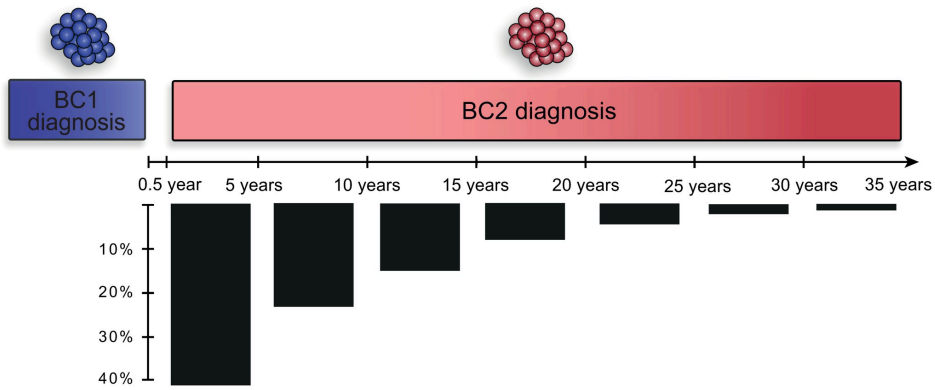

Fig 3. Timeline of CBC in the study cohort. Timeline showing the distribution of the interval between BC1 and BC2 in the study cohort.

https://doi.org/10.1371/journal.pone.0231786.g003

associated with ER and PR expression in a biphasic manner in both BC1 and BC2, where tumors with no or very weak $GPR30_{TOT}$ and tumors with strong $GPR30_{TOT}$ were more likely to be ER-negative and PR-negative, whereas tumors with weak or moderate $GPR30_{TOT}$ were more likely to be ER-positive and PR-positive (Table 1). Interestingly, $GPR30_{PM}$+ staining associated strongly with ER-negative and PR-negative status in both BC1 and BC2. $GPR30_{PM}$+ status also strongly associated with high Ki67 staining in both BC1 and BC2 in this cohort. Lastly, both $GPR30_{TOT}$ and $GPR30_{PM}$ correlated with tumor subtype, with strong $GPR30_{TOT}$ and $GPR30_{PM}$+ status being significantly more prevalent among triple-negative cancers in both BC1 and BC2 (Table 1).

To assess GPR30 expression through tumor progression, $GPR30_{TOT}$ staining was compared between BC1 and BC2, and with their corresponding LGL (Fig 4). A majority of the LGLs had a weaker $GPR30_{TOT}$ compared to the primary BC in both the BC1/LGL1 pair (Fig 4; $p<0.0001$) and the BC2/LGL2 pairs ($p<0.0001$).

GPR30 expression and risk of BCD in CBC patients

Previous studies by our group showed that characteristics of BC2 have the highest influence on prognosis after development of CBC, although the characteristics of BC1 continue to have some prognostic impact [33]. $GPR30_{PM}$+ staining in both BC2 and LGL2 was associated with increased risk of BCD (Table 2; Fig 5A and 5B; $HR_{BC2} = 1.7$; 95% CI = 1.1–2.7; $p = 0.03$, and $HR_{LGL2} = 2.0$; 95% CI = 1.1–3.4; $p = 0.02$). A trend was also observed that higher $GPR30_{TOT}$ associated with increased BCD in BC2 and LGL2 (Fig 6A–6C; $HR_{BC2} = 1.3$; 95% CI = 0.99–1.8; $p = 0.06$, and $HR_{LGL2} = 1.5$; 95% CI = 0.82–2.7; $p = 0.2$, respectively). Similar trends were seen when looking at GPR30 expression in BC1.

The trend that GPR30 is a negative prognostic marker for BCD remained in multivariate analysis (Table 2), although effect sizes generally decreased. When estimating the prognostic impact of GPR30 in multivariate analyses adjusted for each variable individually, the prognostic effect of GPR30 was found to mainly be affected when adjusting for ER-status (S1 Table). Interestingly, stratified survival analyses based on ER-status showed that both strong $GPR30_{TOT}$ and $GPR30_{PM}$+ staining in BC2 were graphically associated with increased BCD

Table 1. Association between total GPR30 intensity score ($GPR30_{TOT}$), plasma membrane GPR30 ($GPR30_{PM}$) status, and various clinicopathological variables.

BC1 n = 559	$GPR30_{TOT}$ intensity of BC1; n (%)						$GPR30_{PM}$+ BC1; n (%)			
	0	1	2	3	4	*p*	No PM GPR30 505 (90)	PM+ GPR30 54 (10)	*p*	Missing GPR30 data
	46 (8)	141 (25)	263 (47)	103 (18)	6 (1)					
BC1 diagnosis										
<1977 (n = 122)	11 (13)	24 (28)	36 (42)	14 (17)	0 (0)	0.703	74 (87)	11 (13)	0.52	37
1977–1986 (n = 210)	14 (8)	45 (27)	79 (47)	26 (16)	3 (2)		149 (89)	18 (11)		43
1987–1996 (n = 265)	15 (7)	55 (25)	108 (48)	43 (19)	2 (<1)	0.020[a]	204 (92)	19 (8)		42
1997–2007 (n = 91)	6 (7)	17 (20)	40 (48)	20 (24)	1 (1)		78 (93)	6 (7)		7
Age at BC1 diagnosis										
<50 years (n = 189)	18 (12)	43 (30)	63 (43)	19 (13)	3 (2)	0.027	127 (87)	19 (13)	0.15	43
≥50 years (n = 499)	28 (7)	98 (24)	200 (48)	84 (20)	3 (<1)	0.011[a]	378 (92)	35 (8)		86
Interval between tumors										
<5 years (n = 293)	21 (8)	61 (24)	115 (46)	51 (20)	4 (2)	0.67	222 (88)	30 (12)	0.14	41
≥5 years (n = 395)	25 (8)	80 (26)	148 (48)	52 (17)	2 (<1)	0.37[a]	283 (92)	24 (8)		88
Histological type BC1										
Ductal (n = 391)	21 (6)	83 (25)	167 (50)	58 (17)	4 (1)	0.26	298 (90)	35 (10)	0.01	58
Lobular (n = 95)	11 (14)	20 (25)	31 (38)	19 (24)	0 (0)	0.22[a]	79 (98)	2 (2)		14
Other (n = 125)	9 (9)	25 (26)	46 (48)	16 (17)	0 (0)		93 (97)	3 (3)		29
Missing (n = 77)	5	13	19	10	2		35	14		28
Tumor subclass										
Luminal A like (n = 401)	25 (7)	95 (25)	193 (51)	63 (17)	0 (0)	<0.0001	354 (94)	22 (6)	<0.0001	25
Luminal B like (n = 69)	2 (3)	15 (22)	36 (52)	16 (23)	0 (0)	0.93[a]	63 (91)	6 (9)		0
HER2+ luminal (n = 17)	1 (6)	2 (12)	10 (59)	4 (24)	0 (0)		13 (77)	4 (24)		0
HER2+ non-luminal (n = 13)	1 (8)	3 (23)	8 (62)	1 (8)	0 (0)		11 (85)	2 (15)		0
Triple-negative (n = 63)	12 (20)	19 (31)	11 (18)	13 (21)	6 (10)		43 (71)	18 (29)		2
Missing (n = 125)	5	7	5	6	0		21	2		102
Node status										
N0 (n = 416)	23 (7)	88 (26)	157 (46)	69 (20)	4 (1)	0.28	305 (89)	36 (11)	0.35	75
N+ (n = 213)	17 (9)	47 (26)	94 (51)	25 (14)	1 (<1)	0.11[a]	170 (92)	14 (8)		29
Missing (n = 59)	6	6	12	9	1		30	4		25
Size										
≤20 mm (n = 404)	19 (6)	79 (24)	160 (48)	68 (21)	5 (1)	0.047	298 (90)	33 (10)	0.76	73
>20 mm (n = 215)	23 (12)	54 (28)	86 (44)	30 (16)	1 (<1)	0.0033[a]	177 (91)	17 (9)		21
Missing (n = 69)	4	8	17	5	0		29	5		35
ER status										
<10% stained (n = 99)	17 (18)	29 (31)	23 (25)	19 (20)	6 (6)	<0.0001	73 (78)	21 (22)	<0.0001	5

(*Continued*)

Table 1. (Continued)

≥10% stained (n = 494)	28 (6)	112 (24)	240 (52)	83 (18)	0 (0)	0.11[a]	431 (93)	32 (7)		31
Missing (n = 95)	1	0	0	1	0		1	1		93
PR status										
<10% stained (n = 165)	22 (14)	41 (26)	56 (36)	32 (20)	6 (4)	<0.0001	131 (83)	26 (17)	0.00070	8
≥10% stained (n = 428)	23 (6)	100 (25)	207 (52)	70 (18)	0 (0)	0.38[a]	373 (93)	27 (7)		28
Missing (n = 95)	1	0	0	1	0		1	1		93
HER2 staining										
Negative (n = 544)	42 (8)	133 (26)	241 (47)	93 (18)	6 (1)	0.86	469 (91)	46 (9)	0.13	29
Positive (n = 40)	3 (7)	8 (20)	21 (53)	8 (20)	0 (0)	0.63[a]	33 (83)	7 (17)		0
Missing (n = 104)	1	0	1	2	0		3	1		100
Ki67 staining										
<20% stained (n = 356)	30 (9)	85 (26)	160 (48)	57 (17)	1 (<1)	0.19	315 (95)	18 (5)	<0.0001	23
≥20% stained (n = 227)	15 (7)	56 (25)	102 (46)	44 (20)	5 (2)	0.013[a]	187 (84)	35 (16)		5
Missing (n = 105)	1	0	1	2	0		3	1		101
PM GPR30 status										
Negative (n = 505)	46 (9)	137 (27)	235 (47)	87 (17)	0 (0)	<0.0001	-	-	-	0
Positive (n = 54)	0 (0)	4 (7)	28 (52)	16 (30)	6 (11)	<0.0001[a]	-	-		0
BC2 n = 595	**$GPR30_{TOT}$ intensity of BC2; n (%)**						**$GPR30_{PM}$+ BC2; n (%)**			
	0	1	2	3	4	*p*	No PM GPR30 557 (94)	PM+ GPR30 38 (6)	*p*	Missing GPR30data
	31 (5)	151 (25)	285 (48)	117 (20)	11 (2)					
CBC diagnosis										
1977–1986 (n = 136)	6 (6)	27 (25)	45 (42)	28 (26)	1 (<1)	0.072	96 (90)	11 (10)	0.18	29
1987–1996 (n = 243)	11 (5)	66 (32)	89 (44)	33 (16)	5 (3)	0.48[a]	192 (94)	12 (6)	0.10[1]	39
1997–2007 (n = 309)	14 (5)	58 (20)	151 (53)	56 (20)	5 (2)		269 (95)	15 (5)		25
Age at CBC diagnosis										
<50 years (n = 67)	1 (2)	18 (31)	26 (45)	12 (21)	1 (2)	0.65	53 (91)	5 (9)	0.65	9
≥50 years (n = 621)	30 (6)	133 (25)	259 (48)	105 (20)	10 (2)	0.84[a]	504 (94)	33 (6)		84
Interval between tumors										
<5 years (n = 293)	11 (5)	64 (26)	118 (48)	50 (20)	4 (2)	0.95	230 (93)	17 (7)	0.81	46
≥5 years (n = 395)	20 (6)	87 (25)	167 (48)	67 (19)	7 (2)	0.79[a]	327 (94)	21 (6)		47
Histology BC2										
Ductal (n = 450)	24 (6)	108 (27)	189 (46)	82 (20)	5 (1)	0.022	377 (92)	31 (8)	0.031	42
Lobular (n = 130)	2 (2)	32 (29)	59 (53)	17 (15)	2 (2)	0.032[a]	111 (99)	1 (1)		130
Other (n = 77)	2 (4)	8 (15)	28 (52)	12 (22)	4 (7)		51 (94)	3 (6)		77
Missing (n = 31)	3	3	9	6	0		18	3		10
Tumor subclass										
Luminal A like (n = 403)	16 (4)	88 (23)	193 (51)	75 (20)	4 (1)	<0.0001	367 (98)	9 (2)	<0.0001	27

(*Continued*)

Table 1. (Continued)

Luminal B like (n = 88)	4 (5)	25 (28)	48 (55)	11 (13)	0 (0)	0.76[a]	83 (94)	5 (6)		0
HER2+ luminal (n = 19)	0 (0)	5 (26)	10 (53)	4 (21)	0 (0)		17 (90)	2 (10)		0
HER2+ non-luminal (n = 10)	0 (0)	3 (30)	3 (30)	4 (40)	0 (0)		9 (90)	1 (10)		0
Triple-negative (n = 74)	7 (10)	19 (27)	19 (27)	18 (26)	7 (10)		50 (71)	20 (29)		4
Missing (n = 94)	4	11	12	5	0		31	1		94
Node status										
N0 (n = 371)	15 (5)	80 (26)	155 (50)	58 (19)	5 (2)	0.39	290 (93)	23 (7)	0.54	58
N+ (n = 196)	13 (7)	54 (30)	74 (41)	38 (21)	3 (2)	0.43[a]	172 (95)	10 (5)		14
Missing (n = 121)	3	17	56	21	3		95	5		121
Size										
≤20 mm (n = 481)	19 (5)	96 (23)	199 (48)	91 (22)	7 (2)	0.13	387 (94)	25 (6)	0.61	69
>20 mm (n = 181)	11 (7)	53 (31)	76 (45)	26 (15)	4 (2)	0.027[a]	157 (92)	13 (8)		11
Missing (n = 13)	1	2	10	0	0		13	0		13
ER status										
<10% stained (n = 105)	8 (8)	30 (30)	28 (28)	26 (26)	7 (7)	<0.0001	77 (78)	22 (22)	<0.0001	6
≥10% stained (n = 524)	21 (4)	120 (24)	256 (52)	91 (19)	4 (<1)	0.47[a]	476 (97)	16 (3)		32
Missing (n = 59)	2	1	1	0	0		4	0		55
PR status										
<10% stained (n = 212)	13 (7)	49 (25)	90 (45)	39 (20)	9 (5)	0.0097	175 (88)	25 (12)	<0.0001	12
≥10% stained (n = 412)	16 (4)	99 (26)	192 (50)	78 (20)	2 (<1)	0.62[a]	375 (97)	12 (3)		25
Missing (n = 8)	2	3	3	0	0		7	1		56
HER2 status										
Negative (n = 552)	29 (5)	139 (25)	268 (49)	105 (19)	11 (2)	0.24	517 (94)	35 (6)	0.93	32
Positive (n = 37)	0 (0)	11 (30)	15 (40)	11 (30)	0 (0)	0.37[a]	34 (92)	3 (8)		0
Missing (n = 67)	2	1	2	1	0		6	0		67
Ki67 staining										
<20% stained (n = 349)	18 (6)	73 (23)	153 (48)	69 (22)	6 (2)	0.40	311 (98)	8 (3)	<0.0001	30
≥20% stained (n = 266)	10 (4)	76 (29)	126 (48)	47 (18)	5 (2)	0.39[a]	234 (89)	30 (11)		2
Missing (n = 73)	3	2	6	1	0		12	0		61
Radiotherapy BC1										
No (n = 257)	9 (4)	52 (23)	119 (52)	43 (19)	5 (2)	0.41	218 (96)	10 (4)	0.15	29
Yes (n = 425)	22 (6)	97 (27)	163 (45)	74 (20)	6 (2)	0.28[a]	334 (92)	28 (8)		63
Missing (n = 5)	0	2	3	0	0		5	0		1
Chemotherapy for BC1										
No (n = 615)	27 (5)	135 (25)	253 (48)	105 (20)	10 (2)	0.98	496 (94)	34 (6)	1.0	85
Yes (n = 66)	4 (7)	14 (24)	29 (49)	11 (18)	1 (2)	0.79[a]	55 (93)	4 (7)		7
Missing (n = 7)	0	2	3	1	0		6	0		1
Tamoxifen for BC1										
All patients										
No tamoxifen (n = 467)	25 (5)	115 (25)	226 (48)	92 (20)	9 (2)	0.96	435 (93)	32 (7)	0.57	73

(*Continued*)

Table 1. (Continued)

Tamoxifen (n = 122)	6 (5)	34 (28)	56 (46)	24 (20)	2 (2)	0.73[a]	116 (95)	6 (5)		19
Missing (n = 7)	0	2	3	1	0		6	0		1
Tamoxifen treated for BC1										
BC2 diagnosis during treatment (n = 60)	1 (2)	18 (35)	19 (37)	12 (23)	2 (4)	0.089	46 (89)	6 (11)	0.013	11
BC2 diagnosis after treatment (n = 81)	5 (7)	16 (23)	37 (53)	12 (17)	0 (0)		70 (100)	0 (0)		8
Not tamoxifen treated for BC1										
BC2<5 years after BC1 (n = 222)	10 (5)	45 (24)	92 (49)	39 (21)	2 (1)	0.83	177 (94)	11 (6)	0.61	34
BC2>5 years after BC1 (n = 318)	15 (5)	70 (25)	134 (48)	53 (19)	7 (3)	0.99[a]	258 (93)	21 (7)		39
PM GPR30 status										
Negative (n = 557)	31 (6)	149 (27)	270 (48)	103 (19)	4 (<1)	<0.0001				
Positive (n = 38)	0 (0)	2 (5)	15 (40)	14 (37)	7 (18)	<0.0001[a]				

Abbreviations: BC: breast cancer; BC1: the first primary BC; BC2: the second primary BC; CBC: contralateral breast cancer; GPR30: G protein-coupled receptor 30; PM: plasma membrane; HER2: human epidermal growth factor receptor-2; N+/N0: presence or absence of lymph node metastases; ER: estrogen receptor α; PR: progesterone receptor.

Values for p are calculated using Pearson's χ^2-test without continuity correction if otherwise is not stated.

[a] Calculated using Mantel-Haenszel χ^2-test test (χ^2-test for trend).

https://doi.org/10.1371/journal.pone.0231786.t001

among patients with ER-positive tumors, but not ER-negative tumors (S2 Fig and S2 Table). However, statistical test for interaction did not show a significant difference in the prognostic value of GPR30 between ER-positive and ER-negative tumors ($GPR30_{TOT}$ $p_{interaction}$ = 0.7; $GPR30_{PM}$+ $p_{interaction}$ = 0.1). To address the combined prognostic information of GPR30 status in both BC1 and BC2, we created combination variables with information from paired BC1 and BC2 for $GPR30_{TOT}$ and $GPR30_{PM}$ respectively. This analysis showed that, although BC2 carried the higher prognostic value, BC1 also added prognostic information (S3 Fig and S3 Table).

GPR30 expression and tamoxifen treatment

To address the GPR30 expression in individual CBC cases, we matched the GPR30 variables of BC1 and BC2 within each patient individually. We observed that $GPR30_{TOT}$ was equally likely to have increased, decreased, or remained the same in BC2 compared to BC1 (Fig 4). Interestingly, the pattern was similar regardless if tamoxifen treatment had been given for BC1 or not (Fig 4). In the whole cohort, there was no association having received tamoxifen treatment for BC1, and score of $GPR30_{TOT}$ or $GPR30_{PM}$+ in BC2. However, in a subset of patients diagnosed with BC2 during adjuvant tamoxifen treatment for BC1, BC2 were more likely to be $GPR30_{PM}$+ than in BC2 diagnosed after completed tamoxifen treatment (11% vs 0%, p = 0.01; Table 1).

When stratified for tamoxifen treatment of ER-positive BC2, $GPR30_{PM}$+ exhibited higher prognostic potential in patients that did not receive tamoxifen for BC2 as compared to patients that did receive tamoxifen. The prognostic potential remained significant in both univariate analysis and multivariate analysis adjusting for attributes of BC1 and BC2 (S2 Table; univariate HR = 2.8, 95% CI = 1.3–6.0, p = 0.01; multivariate HR = 3.8, 95% CI = 1,4–11, p = 0.01). Additionally, when studying the effect of tamoxifen on ER-positive BC2, there was a trend that patients with strong $GPR30_{TOT}$ or $GPR30_{PM}$+ staining had a greater benefit from tamoxifen treatment than those with lower $GPR30_{TOT}$ or without $GPR30_{PM}$ staining (S4 Fig). However, interaction between GPR30 and tamoxifen could not be confirmed statistically (S2 Table;

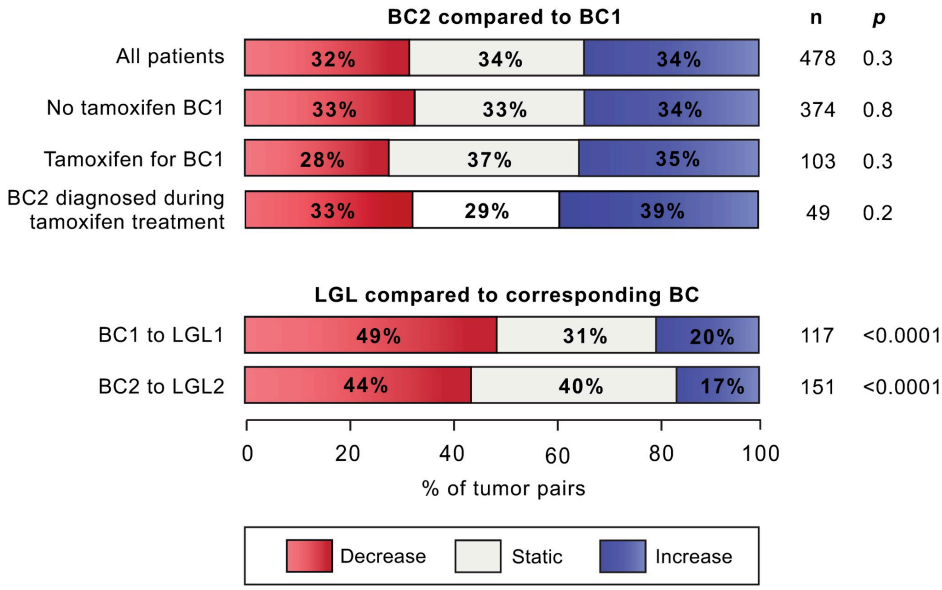

Fig 4. GPR30 staining in paired tumors. The change in GPR30 intensity (level 0–4) between paired BC and LGL. In relation to the tumor assumed to have developed earlier, the intensity shift in the second tumor is characterized as decreasing, stable or increasing for each tumor pair respectively. The intensity shift was assessed statistically using Wilcoxon matched pairs signed rank test.

https://doi.org/10.1371/journal.pone.0231786.g004

$GPR30_{TOT}$ $p_{interaction}$ = 0.4; $GPR30_{PM}$+ $p_{interaction}$ = 0.3). Finally, the prognostic effect of GPR30 in BC2 did not seem to be affected by whether tamoxifen had been given for BC1 or not ($GPR30_{TOT}$ $p_{interaction}$ = 0.2; $GPR30_{PM}$+ $p_{interaction}$ = 0.4).

Discussion

GPR30 is a G protein-coupled receptor reported to mediate non-genomic estrogenic signaling and contribute to BC progression and tamoxifen resistance. However, the literature is

Table 2. Prognostic effect of total GPR30 staining ($GPR30_{TOT}$) and PM-specific GPR30 ($GPR30_{PM}$) staining of BC2 and LGL2 calculated by Cox proportional hazards model with Wald test.

		Unadjusted					Adjusted for BC1[a]					Adjusted for BC1 and BC2[b]				
	Tumor	HR	n	Events	95% CI	*p*	HR	n	Events	95% CI	*p*	HR	n	Events	95% CI	*p*
$GPR30_{TOT}$	BC2	1.3	595	237	0.99–1.8	0.06	1.2	428	171	0.85–1.8	0.3	1.4	349	145	0.93–2.1	0.11
	LGL2	1.5	151	83	0.82–2.7	0.2	1.6	119	70	0.74–3.3	0.2	2.2	110	67	1.0–4.7	0.05
$GPR30_{PM}$+	BC2	1.7	595	237	1.1–2.7	0.03	1.5	428	171	0.87–2.7	0.1	1.6	349	145	0.89–3.0	0.1
	LGL2	2.0	151	83	1.1–3.4	0.02	1.4	119	70	0.67–2.8	0.4	3.0	110	67	1.43–6.1	0.004

[a] Adjusted for the following variables in BC1: GPR30 intensity, tumor size, node status, ER status, HER2 status and ki67 staining.

[b] Adjusted for factors in [a] and for the following factors in BC2: size, node status, ER status, HER2 status and Ki67 staining, plus age and calendar interval at BC2 diagnosis and interval between BC1 and BC2.

https://doi.org/10.1371/journal.pone.0231786.t002

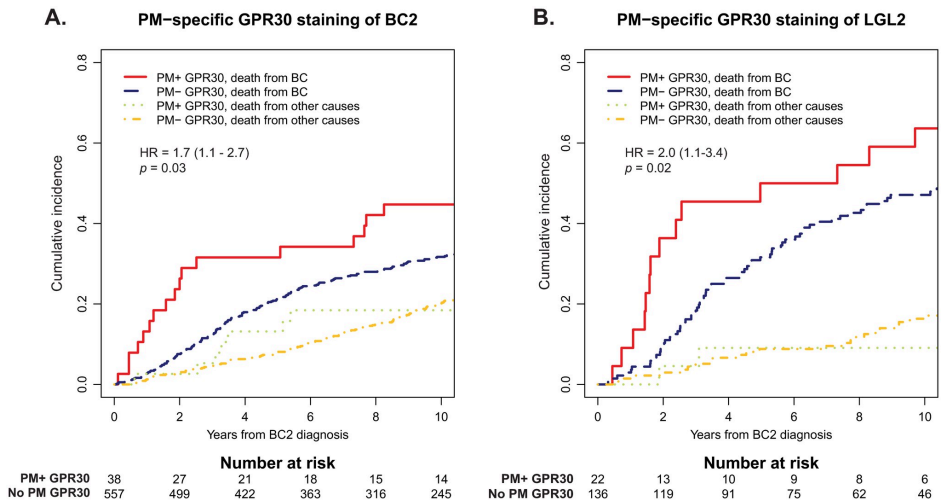

Fig 5. Cumulative incidence of BCD in relation to PM-specific GPR30 staining ($GPR30_{PM}$). *A*, cumulative incidence of BCD in relation to $GPR30_{PM}$ staining of BC2. *B*, cumulative incidence of BCD in relation to $GPR30_{PM}$ staining of LGL2. In *A* and *B*, cumulative incidences of competing event (death from other cause than BC) are shown for comparison.

https://doi.org/10.1371/journal.pone.0231786.g005

inconsistent regarding the pathophysiological profile of GPR30 in BC, and the receptor function is still poorly understood. In this study, we sought to clarify the role of GPR30 during BC development and progression with or without tamoxifen exposure. To this end, we used a unique retrospective cohort of CBC, serving as a model of tamoxifen resistance. We show in this material that GPR30 staining is a strong prognostic factor for increased risk of BCD, particularly when expressed in the PM. We also show that the total GPR30 staining generally decreases during tumor progression. Interestingly, we find that total GPR30 staining was unrelated to tamoxifen treatment during tumor development, and we found no clear relationship between the prognostic value of GPR30 and tamoxifen treatment.

Studies have indicated that GPR30 is influenced by the ER modulator tamoxifen, and this has been suggested to contribute to tamoxifen resistance [21–24]. Upregulation of GPR30 expression was observed following tamoxifen treatment in a small BC cohort [21], and GPR30 expression was associated with worse prognosis for BC patients treated with tamoxifen as-compared to tamoxifen-naïve patients [24]. In the present study, we assessed the expression of GPR30 in 688 women with metachronous CBC. In 60 of these patients, BC2 tumors developed during ongoing tamoxifen treatment for the first BC, strongly arguing for acquired tamoxifen resistance in these tumors. We hypothesized that if GPR30 contributes to tamoxifen resistance, tumors developed under exposure of tamoxifen would exhibit higher GPR30 expression as a result of selection pressure. In the whole cohort, no difference in total GPR30 staining was observed between the tamoxifen-naïve BC2 and the presumably tamoxifen-resistant BC2. As recent studies suggest that GPR30 may have unique functions when expressed specifically in the PM [12, 20, 34, 35], we also assessed if PM-localization of GPR30 may be involved in resistance mechanisms. In a subgroup analysis, we found that BC2 diagnosed during tamoxifen treatment for BC1 was more likely to express PM-specific GPR30 than BC2 diagnosed after

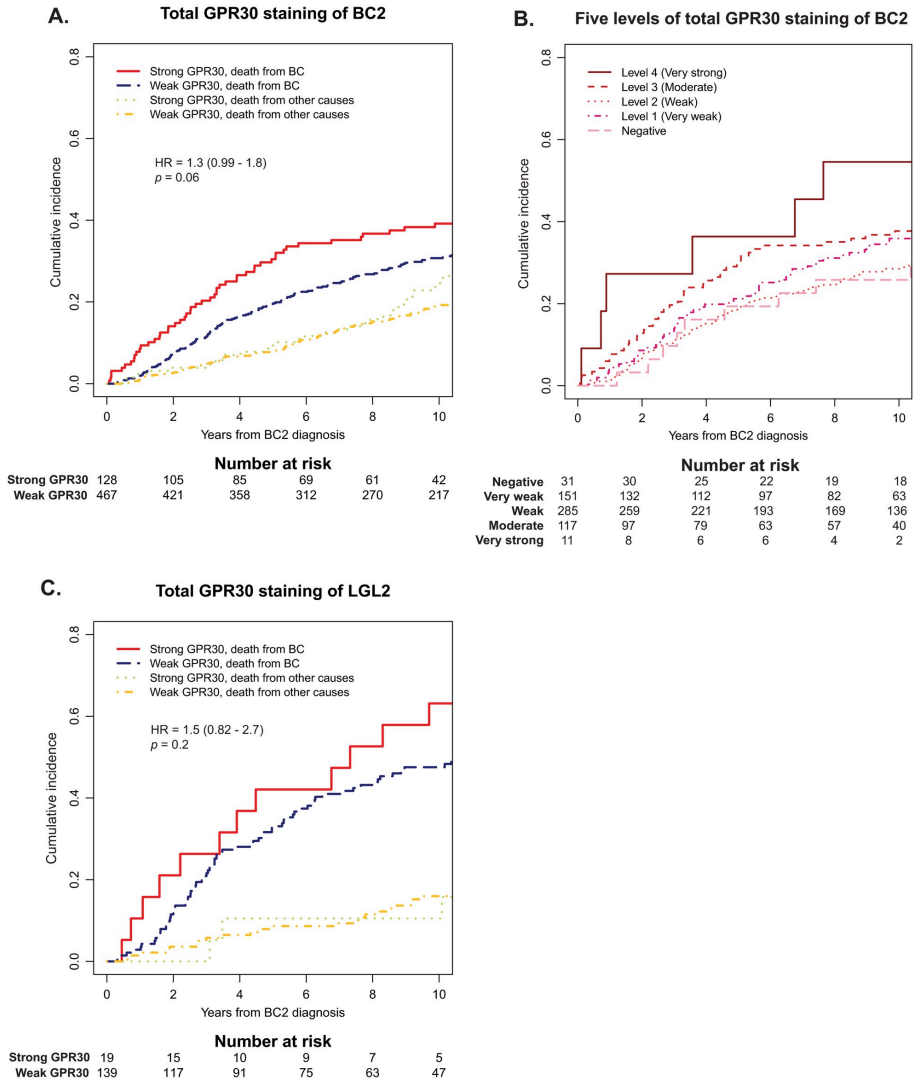

Fig 6. Cumulative incidence of BCD in relation to total GPR30 staining ($GPR30_{TOT}$). *A*, cumulative incidence of BCD in relation to $GPR30_{TOT}$ of BC2 in the whole cohort. *B*, cumulative incidence of BCD in relation to the five GPR30 staining intensity levels of BC2. *C*, cumulative incidence of BCD in relation to $GPR30_{TOT}$ of LGL2. In *A-C*, cumulative incidences of competing event (death from other cause than BC) are shown for comparison.

https://doi.org/10.1371/journal.pone.0231786.g006

completed treatment. This trend was seen both in ER-positive and ER-negative cases, and could hence not only be explained by a selection of ER-negative BC2 during tamoxifen exposure (ER-negativity associated to $GPR30_{PM}$+) [17].

To address if GPR30 expression decreases the benefit of tamoxifen, we performed a survival analysis of patients treated with tamoxifen after the diagnosis of an ER-positive BC2, stratified by GPR30 expression. In this material, GPR30 did not associate with worse prognosis. Instead, a trend was noted that among patients not treated with tamoxifen for their ER-positive BC2, PM-localized GPR30 has a higher hazard. Additionally, there was a trend that patients with PM-localized GPR30 staining in an ER-positive BC2 have a greater benefit from tamoxifen treatment. In summary, our data provides no clear evidence that tamoxifen exposure affects the prognostic value of GPR30 in BC2, or that the benefit of tamoxifen depends on GPR30 expression. However, results are not unanimous and the relationship between PM-localized GPR30 and tamoxifen needs to be further addressed in future studies.

We also explored GPR30 through disease progression. The relationship between GPR30 staining in paired BC1 and BC2 appeared to be stochastic, in line with CBC being most often considered an independent primary tumor [36]. On the other hand, LGL-metastases are seeded from, and hence clonally related to, the primary BC. GPR30 staining in the LGL was significantly lower than that observed in the corresponding BC, a pattern observed previously and suggested to reflect a successive downregulation of the receptor during cancer progression [17, 37]. However, a study on samples of normal breast tissue, invasive BC and LGL reported the mean GPR30 expression in normal breast and BC to be equal, but that the expression decreased in the LGL [37]. Unexpectedly given this background, we also show that PM-specific staining in the LGL associates with aggressive tumor characteristics and significantly higher risk of BCD, which would suggest that high GPR30 expression in the LGL is beneficial for tumor cells. Whether lower GPR30 expression is beneficial for tumor cell dissemination to the lymph nodes, or a result of environmental factors in the lymph nodes, is an interesting question for future studies.

A limited amount of data exists regarding the expression of GPR30 in healthy breast tissue. However, one study assessed GPR30 in breast tissue from 12 healthy donors in which all were defined as GPR30 positive, with strong cytoplasmic GPR30 expression in ductal and lobular epithelium, myoepithelium, and stromal fibroblasts, but no expression in smooth muscle or vascular endothelium [16]. In addition, The Human Protein Atlas database reports the level of GPR30 mRNA in normal breast tissue to be at medium level, and protein expression of GPR30 at strong levels in breast myoepithelial cells, but not detected in adipocytes or glandular cells (Data available from v19.3; www.proteinatlas.org [38]). Based on this, it seems unlikely that the mere overexpression of GPR30 could explain the pathological turn the receptor seems to undergo during BC progression. This raises the question if a transforming event changes the localization and function of GPR30, in turn yielding tumor-promoting activity in a minority of BCs. Several GPCR mutations that affect their function have been identified in cancer [39]. However, very little is still known about cancer-related mutations in GPR30. Nevertheless, it has been reported that promoter methylation suppresses GPR30 expression in both BC cell lines and primary BC tissue, and that methylation pattern of *GPER1* differ between BC tissue and healthy controls [40, 41]. Among 996 BC samples available in The Cancer Genome Atlas/PanCancer Atlas, genetic alterations in the *GPER1* gene are present in less than 2% [42–45]. Hence, it is unlikely that *GPER1* mutation causes PM-GPR30 expression, which according to data from this study and earlier is present in around 7–23% of BCs [17]. However, altered methylation may partly explain any BC-specific alterations in GPR30 expression level.

As seen here and previously [17], strong total and PM-specific GPR30 staining associate with ER-negative status. As ER-negativity is a strong marker of poor prognosis, we sought to

evaluate if GPR30 adds any prognostic information beyond ER-status. The collinearity between GPR30 and ER is reflected in Cox regression adjusted for only ER (S1 Table), where the effects of both total and PM-specific GPR30 staining are reduced. However, when evaluating the association between GPR30 staining on BC outcome with the cohort stratified for ER status (S3 Fig), we found a trend that both strong total GPR30 and PM-specific GPR30 staining associate with worse prognosis in ER-positive CBC (S2 Fig), suggesting that GPR30 adds prognostic information beyond ER, at least in ER-positive tumors. Even though no prognostic effect of total or PM-specific GPR30 was seen in ER-negative CBC, tests of statistical interaction showed no significant difference in the prognostic effect of GPR30 in the ER-positive and ER-negative groups. Thus, our data suggest that although GPR30 and ER are strongly associated, GPR30 status adds prognostic information beyond ER.

Although associated with the same ligand, ER and GPR30 manifest considerable differences in terms of cellular function. ER is a nuclear receptor; a ligand-activated transcription factor that upon binding estrogen dimerizes and translocates to the nucleus, where it alters expression of target genes [46]. On the other hand, GPR30 is a G protein-coupled receptor (GPCR), and as such an integral membrane protein. In contrast to ER, an active GPCR orchestrates rapid downstream signaling by modifying the activity of several effectors and second messengers [47]. The versatile nature of a GPCR allows it to communicate with a broad signaling network, the profile of which is dependent on the expression profile of the cell. Studies have coupled GPR30 to several signaling events through both G protein-dependent and -independent mechanisms and both in response to estrogen and constitutively. Estrogen was reported to receptor-dependently stimulate increases in intracellular Ca^{2+} [13, 19], cAMP production [12], and ERK1/2 activity [12, 48–50], the latter through EGFR transactivation [12, 48], and cFos expression [49]. Furthermore, constitutively the receptor was reported to inhibit cAMP production [34] and the Ca^{2+}-pump plasma membrane Ca^{2+}-ATPase 4b [35], and stimulate ERK1/2 activity, the latter through PI3K [20]. Interestingly, many of these effects, including modulation of cAMP production and stimulation of ERK1/2 activity via PI3K and EGFR transactivation, have been found to depend on PM localization of the receptor. In this study, we confirm our previous results that the prognostic potential of GPR30 is more pronounced when the receptor is expressed in the PM [17]. The subcellular distribution of GPR30 is complex, with *in vitro* studies showing that receptor activity occurs both in the PM [12, 20, 34, 35], endoplasmic reticulum [13], and nucleus [51]. Today, GPR30 function is best described in the PM, which is typical for a GPCR [47], whereas few if any functions have been described in the endoplasmatic reticulum or nucleus.

Recent *in vitro* data have demonstrated that GPR30-mediated ERK1/2 signaling depends on an amino acid sequence at the receptor intracellular C-terminal end, through which the receptor interacts with scaffold and adaptor proteins localized at the PM [20], and this favors receptor PM localization [20, 34, 35, 52]. Together, these results present a model where intracellular scaffold and adaptor proteins contribute to cell proliferation by retaining GPR30 in the PM, thus spatially positioning the receptor to communicate with the ERK1/2 and EGFR pathways. As both ERK1/2 and EGFR activities are hallmarks of cell proliferation, an intriguing theory is that these interactions contribute to the association of PM-localized GPR30 with high Ki67 and poor BC outcome observed in this CBC material. Therefore, it is well motivated to further study the contribution of scaffold protein interactions to the function of GPR30 in BC pathology, and the potential of PM-localized GPR30 in targeted treatment strategies should be investigated.

In conclusion, this study evaluated the estrogen-responsive receptor GPR30 in a unique and large cohort of CBC with long-term follow-up, serving as a model for tamoxifen exposure and resistance. We conclude that GPR30 has prognostic value in CBC. On the other hand, we

find no clear evidence that GPR30 is involved in tamoxifen resistance. GPR30 staining correlates with BC subtype, with the highest total and PM-specific GPR30 observed in triple-negative BC. Additionally, GPR30 is most active in CBC when located in the PM. Thus, PM-localized GPR30 is an interesting candidate for future therapeutic exploitation.

Supporting information

S1 Raw images.
(PDF)

S1 Fig. GPR30 antibody specificity. *A*, MCF7 cell lysates were immunoblotted with goat GPR30 antibody as previously described [20, 29, 34]. *B*, HeLa TET-On/Off cells were incubated without (-TET) or with 100 ng/ml tetracycline (+TET) for 12 h and then lysed and immunoblotted with GPR30 antibody. *C*, MCF7 cells were stained live with GPR30 antibody for 30 min and then fixed and stained with Alexa488-labeled anti-goat antibodies (Life Technologies) as previously described [20, 29, 34]. *D*, MCF7 cells were transiently transfected with a plasmid containing the cDNA of human GPR30 tagged in the N-terminus with the FLAG tag (FLAG-hGPR30), stained live with mouse M1 FLAG antibodies (Sigma-Aldrich) for 30 min, and then fixed and stained with Alexa488-labeled mouse IgG2b antibodies (Life Technologies) as previously described [29, 34]. In *C* and *D*, 4',6-Diamidino-2-phenylindole (DAPI) was used for nuclear staining, and fluorescence images were collected using a Nikon Eclipse confocal microscope. The results are representative of experiments performed at least three times. *Bar*, 10 μm.
(EPS)

S2 Fig. Cumulative incidence of BCD in CBC patients in relation to GPR30 staining of BC2, stratified by ER status of BC2. Cumulative incidence of competing event (death from other cause than BC) is shown for comparison. HR values were estimated using a cause-specific Cox proportional hazards model, and values of *p* were calculated using Wald test. *A-B*, cumulative incidence of BCD in relation to $GPR30_{TOT}$ in CBC patients with ER-positive BC2 (*A*) or ER-negative BC2 (*B*). *C-D*, cumulative incidence of BCD in relation to $GPR30_{PM}$ in CBC patients with ER-positive BC2 (*C*) or ER-negative BC2 (*D*).
(PDF)

S3 Fig. Cumulative incidence of BCD in relation to GPR30 staining of the tumor pair (BC1/BC2). Presented HR values were estimated using Cox proportional hazards model and p values were calculated using Wald test, where the groups with weak/weak $GPR30_{TOT}$ and PM-/PM- $GPR30_{PM}$ status were used as reference groups. *A*, cumulative incidence of BCD in relation to $GPR30_{TOT}$ in the tumor pair. *B*, cumulative incidence of BCD in relation to $GPR30_{PM}$ in the tumor pair.
(PDF)

S4 Fig. Cumulative incidence of BCD in CBC patients with ER+ BC2 in relation to tamoxifen treatment of BC2, stratified by GPR30 expression of BC2. Cumulative incidence of competing event (death from other cause than BC) is shown for comparison. HR values were estimated using a cause-specific Cox proportional hazards model, and values of *p* were calculated using Wald test. *A-D*, cumulative incidence of BCD in relation to tamoxifen treatment of BC2 in CBC patients with weak GPR30 staining (*A*) or strong GPR30 staining (*B*), and in patients without PM-specific GPR30 staining (*C*) and in patients with PM-specific staining ($GPR30_{PM}$+) (*D*).
(PDF)

S1 Table. Forest plots presenting estimates of the prognostic impact of GPR30 in multivariate analyses adjusted for only one variable per row. *A*, multivariate analyses of strong total GPR30 ($GPR30_{TOT}$) adjusted for each variable separately. *B*, multivariate analyses of plasma membrane-specific GPR30 ($GPR30_{PM}$+) adjusted for each variable separately.
(PDF)

S2 Table. Relationship between total GPR30 staining ($GPR30_{TOT}$) and PM-specific GPR30 ($GPR30_{PM}$) staining of BC2 and risk of death from BC after CBC diagnosis in patients stratified by ER status and tamoxifen treatment, and interactions between GPR30 and ER or tamoxifen. Prognostic effect was calculated by cox proportional hazards model with Wald test. Interaction between GPR30 and the stratifying variable (ER or tamoxifen) was assessed using an interaction test. Relationship between GPR30 and risk of death from BC were assessed by Cox regressions.
(PDF)

S3 Table. Relationship between GPR30 staining of the tumor pair (BC1/BC2) and risk of death from BC after CBC diagnosis. Prognostic effect was calculated by cox proportional hazards model with Wald test. The groups with weak/weak $GPR30_{TOT}$ and PM-/PM-$GPR30_{PM}$ status were used as reference groups for survival analyses. Relationship between GPR30 and risk of death from BC were assessed by Cox regressions.
(PDF)

Acknowledgments

We thank Kristina Lövgren (K.L.) for excellent technical assistance and BioCare strategic research school for providing an excellent research environment. Results shown in the Discussion section are in part based upon data generated by the TCGA Research Network: https://www.cancer.gov/tcga.

Author Contributions

Conceptualization: Julia Tutzauer, Martin Sjöström, Mårten Fernö, L. M. Fredrik Leeb-Lundberg, Sara Alkner.

Data curation: Julia Tutzauer, Martin Sjöström.

Formal analysis: Julia Tutzauer, Martin Sjöström, Pär-Ola Bendahl.

Funding acquisition: Mårten Fernö, L. M. Fredrik Leeb-Lundberg, Sara Alkner.

Investigation: Julia Tutzauer, Martin Sjöström.

Methodology: Lisa Rydén, Mårten Fernö, Sara Alkner.

Project administration: L. M. Fredrik Leeb-Lundberg, Sara Alkner.

Supervision: L. M. Fredrik Leeb-Lundberg, Sara Alkner.

Validation: Julia Tutzauer, Martin Sjöström.

Writing – original draft: Julia Tutzauer, Martin Sjöström.

Writing – review & editing: Julia Tutzauer, Martin Sjöström, Pär-Ola Bendahl, Lisa Rydén, Mårten Fernö, L. M. Fredrik Leeb-Lundberg, Sara Alkner.

References

1. Adami HO, Bergstrom R, Hansen J. Age at first primary as a determinant of the incidence of bilateral breast cancer. Cumulative and relative risks in a population-based case-control study. Cancer. 1985; 55:643–7. https://doi.org/10.1002/1097-0142(19850201)55:3<643::aid-cncr2820550328>3.0.co;2-l PMID: 3965112
2. Chen Y, Thompson W, Semenciw R, Mao Y. Epidemiology of contralateral breast cancer. Cancer Epidemiol Biomarkers Prev. 1999; 8:855–61. PMID: 10548312
3. Malone KE, Begg CB, Haile RW, Borg A, Concannon P, Tellhed L, et al. Population-based study of the risk of second primary contralateral breast cancer associated with carrying a mutation in BRCA1 or BRCA2. J Clin Oncol. 2010; 28:2404–10. https://doi.org/10.1200/JCO.2009.24.2495 PMID: 20368571
4. Carter CL, Allen C, Henson DE. Relation of tumor size, lymph node status, and survival in 24,740 breast cancer cases. Cancer. 1989; 63:181–7. https://doi.org/10.1002/1097-0142(19890101)63:1<181::aid-cncr2820630129>3.0.co;2-h PMID: 2910416
5. Duffy MJ, Harbeck N, Nap M, Molina R, Nicolini A, Senkus E, et al. Clinical use of biomarkers in breast cancer: Updated guidelines from the European Group on Tumor Markers (EGTM). Eur J Cancer. 2017; 75:284–98. https://doi.org/10.1016/j.ejca.2017.01.017 PMID: 28259011
6. Ring A, Dowsett M. Mechanisms of tamoxifen resistance. Endocr Relat Cancer. 2004; 11:643–58. https://doi.org/10.1677/erc.1.00776 PMID: 15613444
7. Early Breast Cancer Trialists' Collaborative Group (EBCTCG), Davies C, Godwin J, Gray R, Clarke M, Cutter D, et al. Relevance of breast cancer hormone receptors and other factors to the efficacy of adjuvant tamoxifen: patient-level meta-analysis of randomised trials. Lancet. 2011; 378:771–84. https://doi.org/10.1016/S0140-6736(11)60993-8 PMID: 21802721
8. Early Breast Cancer Trialists' Collaborative Group (EBCTCG). Effects of chemotherapy and hormonal therapy for early breast cancer on recurrence and 15-year survival: an overview of the randomised trials. Lancet. 2005; 365:1687–717. https://doi.org/10.1016/S0140-6736(05)66544-0 PMID: 15894097
9. Martin LA, Ribas R, Simigdala N, Schuster E, Pancholi S, Tenev T, et al. Discovery of naturally occurring ESR1 mutations in breast cancer cell lines modelling endocrine resistance. Nat Commun. 2017; 8:1865. https://doi.org/10.1038/s41467-017-01864-y PMID: 29192207
10. Fribbens C, O'Leary B, Kilburn L, Hrebien S, Garcia-Murillas I, Beaney M, et al. Plasma ESR1 Mutations and the Treatment of Estrogen Receptor-Positive Advanced Breast Cancer. J Clin Oncol. 2016; 34:2961–8. https://doi.org/10.1200/JCO.2016.67.3061 PMID: 27269946
11. Filardo E. J. Epidermal growth factor receptor (EGFR) transactivation by estrogen via the G-protein-coupled receptor, GPR30: a novel signaling pathway with potential significance for breast cancer. J Steroid Biochem Mol Biol. 2002; 80:231–8. https://doi.org/10.1016/s0960-0760(01)00190-x PMID: 11897506
12. Thomas P, Pang Y, Filardo EJ, Dong J. Identity of an estrogen membrane receptor coupled to a G protein in human breast cancer cells. Endocrinology. 2005; 146:624–32. https://doi.org/10.1210/en.2004-1064 PMID: 15539556
13. Revankar CM, Cimino DF, Sklar LA, Arterburn JB, Prossnitz ER. A transmembrane intracellular estrogen receptor mediates rapid cell signaling. Science. 2005; 307:1625–30. https://doi.org/10.1126/science.1106943 PMID: 15705806
14. Martin SG, Lebot MN, Sukkarn B, Ball G, Green AR, Rakha EA, et al. Low expression of G protein-coupled oestrogen receptor 1 (GPER) is associated with adverse survival of breast cancer patients. Oncotarget. 2018; 9:25946–56. https://doi.org/10.18632/oncotarget.25408 PMID: 29899833
15. Broselid S, Cheng B, Sjöström M, Lövgren K, Klug-De Santiago HL, Belting M, et al. G protein-coupled estrogen receptor is apoptotic and correlates with increased distant disease-free survival of estrogen receptor-positive breast cancer patients. Clin Cancer Res. 2013; 19:1681–92. https://doi.org/10.1158/1078-0432.CCR-12-2376 PMID: 23554355
16. Filardo EJ, Graeber CT, Quinn JA, Resnick MB, Giri D, DeLellis RA, et al. Distribution of GPR30, a seven membrane-spanning estrogen receptor, in primary breast cancer and its association with clinicopathologic determinants of tumor progression. Clin Cancer Res. 2006; 12:6359–66. https://doi.org/10.1158/1078-0432.CCR-06-0860 PMID: 17085646
17. Sjöström M, Hartman L, Grabau D, Fornander T, Malmström P, Nordenskjöld B, et al. Lack of G protein-coupled estrogen receptor (GPER) in the plasma membrane is associated with excellent long-term prognosis in breast cancer. Breast Cancer Res Treat. 2014; 145:61–71. https://doi.org/10.1007/s10549-014-2936-4 PMID: 24715381
18. Kuo WH, Chang LY, Liu DL, Hwa HL, Lin JJ, Lee PH, et al. The interactions between GPR30 and the major biomarkers in infiltrating ductal carcinoma of the breast in an Asian population. Taiwan J Obstet Gynecol. 2007; 46:135–45. https://doi.org/10.1016/S1028-4559(07)60007-2 PMID: 17638621

19. Ariazi EA, Brailoiu E, Yerrum S, Shupp HA, Slifker MJ, Cunliffe HE, et al. The G protein-coupled receptor GPR30 inhibits proliferation of estrogen receptor-positive breast cancer cells. Cancer Res. 2010; 70:1184–94. https://doi.org/10.1158/0008-5472.CAN-09-3068 PMID: 20086172

20. Gonzalez de Valdivia E, Broselid S, Kahn R, Olde B, Leeb-Lundberg LMF. G protein-coupled estrogen receptor 1 (GPER1)/GPR30 increases ERK1/2 activity through PDZ motif-dependent and -independent mechanisms. J Biol Chem. 2017; 292:9932–43. https://doi.org/10.1074/jbc.M116.765875 PMID: 28450397

21. Ignatov A, Ignatov T, Weissenborn C, Eggemann H, Bischoff J, Semczuk A, et al. G-protein-coupled estrogen receptor GPR30 and tamoxifen resistance in breast cancer. Breast Cancer Res Treat. 2011; 128:457–66. https://doi.org/10.1007/s10549-011-1584-1 PMID: 21607586

22. Ignatov A, Ignatov T, Roessner A, Costa SD, Kalinski T. Role of GPR30 in the mechanisms of tamoxifen resistance in breast cancer MCF-7 cells. Breast Cancer Res Treat. 2010; 123:87–96. https://doi.org/10.1007/s10549-009-0624-6 PMID: 19911269

23. Mo Z, Liu M, Yang F, Luo H, Li Z, Tu G, et al. GPR30 as an initiator of tamoxifen resistance in hormone-dependent breast cancer. Breast Cancer Res. 2013; 15:R114. https://doi.org/10.1186/bcr3581 PMID: 24289103

24. Ignatov T, Claus M, Nass N, Haybaeck J, Seifert B, Kalinski T, et al. G-protein-coupled estrogen receptor GPER-1 expression in hormone receptor-positive breast cancer is associated with poor benefit of tamoxifen. Breast Cancer Res Treat. 2019; 174:121–7. https://doi.org/10.1007/s10549-018-5064-8 PMID: 30478785

25. Alkner S, Bendahl PO, Fernö M, Manjer J, Rydén L. Prediction of outcome after diagnosis of metachronous contralateral breast cancer. BMC Cancer. 2011; 11:114. https://doi.org/10.1186/1471-2407-11-114 PMID: 21450091

26. Alkner S, Bendahl PO, Ehinger A, Lövgren K, Rydén L, Fernö M. Prior adjuvant tamoxifen treatment in breast cancer is linked to increased AIB1 and HER2 expression in metachronous contralateral breast cancer. PLoS One. 2016; 11:e0150977. https://doi.org/10.1371/journal.pone.0150977 PMID: 26959415

27. Alkner S, Ehinger A, Bendahl PO, Rydén L, Fernö M. Prognosis, stage and oestrogen receptor status of contralateral breast cancer in relation to characteristics of the first tumour, prior endocrine treatment and radiotherapy. Eur J Cancer 2015; 51:2304–13. https://doi.org/10.1016/j.ejca.2015.07.016 PMID: 26243193

28. Kotarsky K, Owman C, Olde B. A chimeric reporter gene allowing for clone selection and high-throughput screening of reporter cell lines expressing G-protein-coupled receptors. Anal Biochem. 2001; 288:209–15. https://doi.org/10.1006/abio.2000.4898 PMID: 11152592

29. Sandén C, Broselid S, Cornmark L, Andersson K, Daszkiewicz-Nilsson J, Mårtensson UE, et al. G protein-coupled estrogen receptor 1/G protein-coupled receptor 30 localizes in the plasma membrane and traffics intracellularly on cytokeratin intermediate filaments. Mol Pharmacol. 2011; 79:400–10. https://doi.org/10.1124/mol.110.069500 PMID: 21149639

30. R: A language and environment for statistical computing. (2018). R Foundation for Statistical Computing, Vienna, Austria., http://www.R-project.org/.

31. Gray B (2009) cmprsk: Subdistribution Analysis of Competing Risks. R package version 2.2–7.

32. Therneau, T. M. (2015) _A Package for Survival Analysis in S_. version 2.38.

33. Alkner S, Ehinger A, Bendahl PO, Rydén L, Fernö M. Prognosis, stage and oestrogen receptor status of contralateral breast cancer in relation to characteristics of the first tumour, prior endocrine treatment and radiotherapy. Eur J Cancer. 2015; 51:2304–13. https://doi.org/10.1016/j.ejca.2015.07.016 PMID: 26243193

34. Broselid S, Berg KA, Chavera TA, Kahn R, Clarke WP, Olde B, et al. G protein-coupled receptor 30 (GPR30) forms a plasma membrane complex with membrane-associated guanylate kinases (MAGUKs) and protein kinase A-anchoring protein 5 (AKAP5) that constitutively inhibits cAMP production. J Biol Chem. 2014; 289:22117–27. https://doi.org/10.1074/jbc.M114.566893 PMID: 24962572

35. Tran QK, VerMeer M, Burgard MA, Hassan AB, Giles J. Hetero-oligomeric Complex between the G Protein-coupled Estrogen Receptor 1 and the Plasma Membrane Ca2+-ATPase 4b. J Biol Chem. 2015; 290:13293–307. https://doi.org/10.1074/jbc.M114.628743 PMID: 25847233

36. Alkner S, Tang MH, Brueffer C, Dahlgren M, Chen Y, Olsson E, et al. Contralateral breast cancer can represent a metastatic spread of the first primary tumor: determination of clonal relationship between contralateral breast cancers using next-generation whole genome sequencing. Breast Cancer Res. 2015; 17:102. https://doi.org/10.1186/s13058-015-0608-x PMID: 26242876

37. Ignatov T, Weißenborn C, Poehlmann A, Lemke A, Semczuk A, Roessner A, et al. GPER-1 expression decreases during breast cancer tumorigenesis. Cancer Invest. 2013; 31:309–15. https://doi.org/10.3109/07357907.2013.789901 PMID: 23688258

38. Uhlén M, Fagerberg L, Hallström BM, Lindskog C, Oksvold P, Mardinoglu A, et al. Proteomics. Tissue-based map of the human proteome. Science. 2015; 347:1260419. www.proteinatlas.org/ENSG00000164850-GPER1/tissue/breast.

39. O'Hayre M, Vázquez-Prado J, Kufareva I, Stawiski EW, Handel TM, Seshagiri S, et al. The emerging mutational landscape of G proteins and G-protein-coupled receptors in cancer. Nat Rev Cancer. 2013; 13:412–24 https://doi.org/10.1038/nrc3521 PMID: 23640210

40. Weissenborn C, Ignatov T, Nass N, Kalinski T, Dan Costa S, Zenclussen AC, et al. GPER Promoter Methylation Controls GPER Expression in Breast Cancer Patients. Cancer Invest. 2017; 35:100–7. https://doi.org/10.1080/07357907.2016.1271886 PMID: 28118074

41. Weißenborn C, Ignatov T, Ochel HJ, Costa SD, Zenclussen AC, Ignatova Z, et al. GPER functions as a tumor suppressor in triple-negative breast cancer cells. J Cancer Res Clin Oncol. 2014; 140:713–23. https://doi.org/10.1007/s00432-014-1620-8 PMID: 24553912

42. Cerami E, Gao J, Dogrusoz U, Gross BE, Sumer SO, Aksoy BA, et al. The cBio cancer genomics portal: an open platform for exploring multidimensional cancer genomics data. Cancer Discov. 2012; 2:401–4. https://doi.org/10.1158/2159-8290.CD-12-0095 PMID: 22588877

43. Gao J, Aksoy BA, Dogrusoz U, Dresdner G, Gross B, Sumer SO, et al. Integrative analysis of complex cancer genomics and clinical profiles using the cBioPortal. Sci Signal. 2013; 6:pl1. https://doi.org/10.1126/scisignal.2004088 PMID: 23550210

44. Cancer Genome Atlas Network. Comprehensive molecular portraits of human breast tumours. Nature. 2012; 490:61–70. https://doi.org/10.1038/nature11412 PMID: 23000897

45. Ciriello G, Gatza ML, Beck AH, Wilkerson MD, Rhie SK, Pastore A, et al. Comprehensive Molecular Portraits of Invasive Lobular Breast Cancer. Cell. 2015; 163:506–19. https://doi.org/10.1016/j.cell.2015.09.033 PMID: 26451490

46. Métivier R, Penot G, Hübner MR, Reid G, Brand H, Kos M, et al. Estrogen receptor-alpha directs ordered, cyclical, and combinatorial recruitment of cofactors on a natural target promoter. Cell. 2003; 115:751–63. https://doi.org/10.1016/s0092-8674(03)00934-6 PMID: 14675539

47. Pierce KL, Premont RT, Lefkowitz RJ. Seven-transmembrane receptors. Nat Rev Mol Cell Biol. 2002; 3:639–50. https://doi.org/10.1038/nrm908 PMID: 12209124

48. Filardo EJ, Quinn JA, Bland KI, Frackelton AR. Estrogen-induced activation of Erk-1 and Erk-2 requires the G protein-coupled receptor homolog, GPR30, and occurs via trans-activation of the epidermal growth factor receptor through release of HB-EGF. Mol Endocrinol. 2000; 14:1649–60. https://doi.org/10.1210/mend.14.10.0532 PMID: 11043579

49. Maggiolini M, Vivacqua A, Fasanella G, Recchia AG, Sisci D, Pezzi V, et al. The G protein-coupled receptor GPR30 mediates c-fos up-regulation by 17beta-estradiol and phytoestrogens in breast cancer cells. J Biol Chem. 2004; 279:27008–16. https://doi.org/10.1074/jbc.M403588200 PMID: 15090535

50. Ding Q, Gros R, Limbird LE, Chorazyczewski J, Feldman RD. Estradiol-mediated ERK phosphorylation and apoptosis in vascular smooth muscle cells requires GPR30. Am J Physiol Cell Physiol. 2009; 297:C1178–87. https://doi.org/10.1152/ajpcell.00185.2009 PMID: 19741198

51. Pupo M, Bodmer A, Berto M, Maggiolini M, Dietrich PY, Picard D. A genetic polymorphism repurposes the G-protein coupled and membrane-associated estrogen receptor GPER to a transcription factor-like molecule promoting paracrine signaling between stroma and breast carcinoma cells. Oncotarget. 2017; 8:46728–44. https://doi.org/10.18632/oncotarget.18156 PMID: 28596490

52. Akama KT, Thompson LI, Milner TA, McEwen BS. Post-synaptic density-95 (PSD-95) binding capacity of G-protein-coupled receptor 30 (GPR30), an estrogen receptor that can be identified in hippocampal dendritic spines. J Biol Chem 2013; 288:6438–50. https://doi.org/10.1074/jbc.M112.412478 PMID: 23300088

Paper II

Supplemental material to this article can be found at:
http://molpharm.aspetjournals.org/content/suppl/2021/07/29/molpharm.121.000259.DC1
1521-0111/100/3/271–282$35.00 https://doi.org/10.1124/molpharm.121.000259
MOLECULAR PHARMACOLOGY Mol Pharmacol 100:271–282, September 2021

Ligand-Independent G Protein–Coupled Estrogen Receptor/G Protein–Coupled Receptor 30 Activity: Lack of Receptor-Dependent Effects of G-1 and 17β-Estradiol[S]

Julia Tutzauer, Ernesto Gonzalez de Valdivia, Karl Swärd, Ioannis Alexandrakis Eilard, Stefan Broselid, Robin Kahn, Björn Olde,[1] and L. M. Fredrik Leeb-Lundberg[1]

Department of Experimental Medical Science (J.T., E.G.d.V., K.S., I.A.E., S.B., L.M.F.L.-L.) and Department of Clinical Sciences Lund, Division of Pediatrics and Wallenberg Centre of Molecular Medicine (R.K.) and Division of Cardiology (B.O.), Lund University, Lund, Sweden

Received February 22, 2021; accepted June 6, 2021

ABSTRACT

G protein–coupled receptor 30 (GPR30) is a membrane receptor reported to bind 17β-estradiol (E2) and mediate rapid nongenomic estrogen responses, hence also named G protein–coupled estrogen receptor. G-1 is a proposed GPR30-specific agonist that has been used to implicate the receptor in several pathophysiological events. However, controversy surrounds the role of GPR30 in G-1 and E2 responses. We investigated GPR30 activity in the absence and presence of G-1 and E2 in several eukaryotic systems ex vivo and in vitro in the absence and presence of the receptor. Ex vivo activity was addressed using the caudal artery from wild-type (WT) and GPR30 knockout (KO) mice, and in vitro activity was addressed using a HeLa cell line stably expressing a synthetic multifunctional promoter (nuclear factor κB, signal transducer and activator of transcription, activator protein 1)–luciferase construct (HFF11 cells) and a human GPR30-inducible T-REx system (T-REx HFF11 cells), HFF11 and human embryonic kidney 293 cells transiently expressing WT GPR30 and GPR30 lacking the C-terminal PDZ (postsynaptic density-95/discs-large /zonula occludens-1 homology) motif SSAV, and yeast *Saccharomyces cerevisiae* transformed to express GPR30. WT and KO arteries exhibited similar contractile responses to 60 mM KCl and 0.3 μM cirazoline, and G-1 relaxed both arteries with the same potency and efficacy. Furthermore, expression of GPR30 did not introduce any responses to 1 μM G-1 and 0.1 μM E2 in vitro. On the other hand, receptor expression caused considerable ligand-independent activity in vitro, which was receptor PDZ motif-dependent in mammalian cells. We conclude from these results that GPR30 exhibits ligand-independent activity in vitro but no G-1– or E2-stimulated activity in any of the systems used.

SIGNIFICANCE STATEMENT

Much controversy surrounds 17β-estradiol (E2) and G-1 as G protein–coupled receptor 30 (GPR30) agonists. We used several recombinant eukaryotic systems ex vivo and in vitro with and without GPR30 expression to address the role of this receptor in responses to these proposed agonists. Our results show that GPR30 exhibits considerable ligand-independent activity in vitro but no G-1– or E2-stimulated activity in any of the systems used. Thus, classifying GPR30 as an estrogen receptor and G-1 as a specific GPR30 agonist is unfounded.

Introduction

In 2005, two groups reported that 17β-estradiol (E2) binds to and stimulates cAMP production and extracellular-regulated protein kinase (ERK) 1/2 activity through G protein–coupled receptor 30 (GPR30) in recombinant cells ectopically expressing the receptor (Thomas et al., 2005; Revankar et al., 2005), which led the International Union of Pharmacology to rename the receptor G protein–coupled estrogen receptor (GPER) (Alexander et al., 2011). Subsequently, G-1 [(±)-1-[(3aR*,4S*,9bS*)-4-(6-bromo-1,3-benzodioxol-5-yl)-3a,4,5,9b-tetrahydro-3H-cyclopenta[c]quinolin-8-yl]-ethenone], a substance structurally related to E2, was identified using similar systems and classified as a specific GPR30 agonist (Bologa et al., 2006). Since then, G-1 has been used extensively as a standard of GPR30 agonism to implicate the receptor in a number of pathophysiological systems (Prossnitz and Barton, 2014;

[1]B.O. and L.M.F.L-L. contributed equally to this work as last authors.

This work was supported by the Swedish Cancer Foundation (CAN 2016/423, 19 0479 Pj) and the Swedish Research Council (2016-02427) (to L.M.F.L.-L.).
https://doi.org/10.1124/molpharm.121.000259.

[S] This article has supplemental material available at mol.aspetjournals.org.

ABBREVIATIONS: AP-1, activator protein 1; DMEM, Dulbecco's modified Eagle's medium; E2, 17β-estradiol; ERK, extracellular-regulated protein kinase; G-1, (±)-1-[(3aR*,4S*,9bS*)-4-(6-bromo-1,3-benzodioxol-5-yl)-3a,4,5,9b-tetrahydro-3H-cyclopenta[c]quinolin-8-yl]-ethenone; GPCR, G protein–coupled receptor; GPR30, G protein–coupled receptor 30; GPR30ΔSSAV, GPR30 lacking the C-terminal PDZ motif SSAV; HEK293, human embryonic kidney 293; KO, knockout; $MAPK_{AR}$, mitogen-activated protein kinase activity reporter; NF-κB, nuclear factor κB; NFAT, nuclear factor of activated T cells; OD_{600}, optical density at 600 nm; PCR, polymerase chain reaction; PDZ, PSD-95/discs-large/zonula occludens-1 homology; pERK, phosphorylated ERK1/2; PM, plasma membrane; PMA, phorbol myristate acetate; PSD-95, postsynaptic density-95; SAP97, synapse-associated protein 97; SC, synthetic complete; STAT, signal transducer and activator of transcription; TET, tetracycline; WT, wild type.

Prossnitz and Arterburn, 2015). However, inconsistent results have emerged regarding G-1 and E2 as GPR30 agonists (Levin, 2009; Olde and Leeb-Lundberg, 2009; Langer et al., 2010; Romano and Gorelick, 2018). Indeed, several independent studies done to confirm the original observations in classic recombinant G protein–coupled receptor (GPCR) systems have failed to do so (Pedram et al., 2006; Otto et al., 2008; Kang et al., 2010; Southern et al., 2013; Broselid et al., 2014; Sousa et al., 2017; Gonzalez de Valdivia et al., 2017). Some G-1 and E2 responses are apparently sensitive to knockdown of native GPR30 expression (Prossnitz and Barton, 2014; Prossnitz and Arterburn, 2015), suggesting that these responses depend on receptor expression. However, whether these responses are consequences of a direct interaction with GPR30 or mediated by a distinct target(s) that depends on receptor expression is far from clear. Crosstalk between GPR30 and various ERα isoforms has been reported (Romano and Gorelick, 2018).

Despite conflicting observations, current GPR30 research continues to rely heavily on G-1 responses. The use of pharmacological agents to study receptors requires utmost confidence in receptor specificity. The study of ligand-independent constitutive receptor activity is less common but avoids nonspecific pharmacological effects. All GPCR exhibit ligand-independent activity owing to their nature of existing in an equilibrium between inactive and activated states (Rosenbaum et al., 2009). Assay of such activity often requires well defined recombinant systems where cells expressing the receptor can be compared with those devoid of receptor in the absence of any ligand stimulus. Although this activity is often too low to be detected with many GPCRs, being primarily in the inactive state in the absence of agonist, a number of receptors exhibit considerable constitutive activity, which can be pathophysiologically relevant (Seifert and Wenzel-Seifert, 2002). Evidence for ligand-independent GPR30 activity has been presented in both recombinant (Broselid et al., 2014; Gonzalez de Valdivia et al., 2017) and native systems (Ahola et al., 2002; Ariazi et al., 2010; Broselid et al., 2013; Broselid et al., 2014; Weißenborn et al., 2014).

Considering that G-1 and E2 continue to be used as GPR30 agonists, we felt compelled to further address the involvement of human GPR30 in responses to these agents. Here, we used a number of novel receptor assay systems to monitor several cellular signals in the absence and presence of G-1 and E2, with and without GPR30 expression in several recombinant eukaryotic systems, both ex vivo in transgenic mouse arteries and in vitro in several cell systems including yeast. We report that GPR30 does not show any activity in response G-1 or E2 in any of the investigated systems but exhibits ligand-independent constitutive GPR30 activity in all the in vitro systems used.

Materials and Methods

Mammalian Cell Culturing for Transient Transfection. Human embryonic kidney 293 (HEK293) cells (American Type Culture Collection, Manassas, VA), HeLa cells (American Type Culture Collection), and HFF11 cells were grown in phenol red–free Dulbecco's modified Eagle's medium (DMEM) supplemented with 10% FBS in 5% CO_2 at 37°C. HFF11 cells were generated from HeLa cells as previously described (Kotarsky et al., 2003).

cDNA Constructs and Transient Transfection. N-terminally FLAG-tagged human cDNAs of wild-type (WT) GPR30 and GPR30 lacking the C-terminal PSD-95/discs-large/zonula occludens-1 homology (PDZ) motif SSAV (GPR30ΔSSAV) in the pcDNA3.1 plasmid were made as previously described (Broselid et al., 2014). The Rac1-Cluc sensor was constructed by replacing the ERK1/2 sensor region of the split click beetle luciferase-based ERK1/2 sensor mitogen-activated protein kinase activity reporter ($MAPK_{AR}$) plasmid (Gonzalez-Garcia et al., 2014) with the Rac1 sensor region of Rac1 (EV) from RaichuEV-Rac1 (Komatsu et al., 2011). Briefly, the Rac1 sensor region was amplified using the primers TGGCGAATTCGAGAAAGAGAAAGAGC and TTTAGACTCGAGGCGGACTGCTCGGATC, introducing EcoRI and XhoI sites in the process. The product was then ligated into the EcoRI and XhoI sites of the $MAPK_{AR}$ plasmid. To improve membrane attachment, a CAAX motif was subsequently introduced at the C terminus of the split click beetle luciferase. The $MAPK_{AR}$ plasmid was a kind gift from Dr. Karl Swann (University of Cardiff, UK), the RaichuEV-Rac1(Raichu-2248X) Förster resonance energy transfer plasmid was a kind gift from Dr. Michiyuki Matsuda (Kyoto University, Japan), pGL3–nuclear factor of activated T cells (NFAT) luciferase was a gift from Jerry Crabtree (Addgene plasmid # 17870; http://n2t.net/addgene:17870; Research Resource Identifier: Addgene_17870), and postsynaptic density-95 (PSD-95) FLAG was a gift from Wei-dong Yao (Addgene plasmid # 15463; http://n2t.net/addgene:15463; Research Resource Identifier: Addgene_15463). TransIT-LT1 (Mirus Bio LLC, Madison, WI) was used to transfect plasmid DNA. Cells transiently transfected with plasmid containing receptor constructs were always compared with cells transfected with empty plasmid alone (mock).

Construction and Culturing of Stable T-REx HFF11 Cells. HFF11 cells were transfected with the pcDNA6/TR plasmid (Invitrogen, Carlsbad, CA) using TransIT-LT1 to create an HFF11 cell line expressing the tetracycline (TET) repressor, and stable clones were selected based on blasticidin resistance. FLAG-tagged GPR30 was ligated into the HindIII/XbaI sites of the pcDNA 4T/O plasmid (Invitrogen), the resulting plasmid transfected into HFF11 cells expressing the TET repressor to create T-REx HFF11 cells, and stable clones selected based on blasticidin and zeocin resistance. The cells were then grown in phenol red–free DMEM supplemented with 10% normal or charcoal-treated FBS (growth medium) in 5% CO_2 at 37°C.

T-REx HFF11 Promoter-Reporter Assay. T-REx HFF11 and HFF11 cells seeded in white-bottom 96-well plates (20,000 cells/well) in growth medium were incubated without and with TET (Sigma-Aldrich, St. Louis, MO) for 12 or 24 hours. Drug, vehicle (DMSO), or medium was added during the last 12 hours of TET treatment. The promoter-reporter construct was assayed as previously described (Kotarsky et al., 2003). In short, cells were lysed with 20 μl/well reporter lysis buffer (Promega, Madison, WI). After addition of 35 μl/well Luciferin reagent (Biothema, Handen, Sweden) and ATP, promoter-reporter activity was measured as luminescence in a Clariostar luminometer.

ERK Activity. ERK1/2 activity was assayed by immunoblotting as previously described (Gonzalez de Valdivia et al., 2017) using phosphorylated ERK1/2 (pERK) antibody (Santa Cruz Biotechnology, Santa Cruz, CA; 1:1000) for ERK1/2 phosphorylation and ERK1/2 (ERK) antibody (Santa Cruz Biotechnology; 1:1000) for total ERK1/2. Briefly, cells were grown to confluency in 60-mm dishes in phenol red–free DMEM with 10% FBS, washed, incubated without serum for 1 hour, and then incubated without or with vehicle (DMSO) or drug for different times. The cells were then washed, lysed, and subjected to immunoblotting, and immunoreactive bands were visualized as described below. The combined band densities of ERK1 and ERK2 were quantified using ImageJ software, and ERK1/2 activity was expressed as the ratio between the combined pERK band densities and the combined ERK band densities for each condition.

NFAT Activity. NFAT promoter activity was measured in cells transfected with pGL3-NFAT luciferase plasmid. Transfected cells in

white-bottom 96-well plates (20,000 cells/well) were grown in phenol red–free DMEM with 10% FBS overnight and then incubated with vehicle (DMSO) or drug for 12 hours. Cells were then lysed with 20 μl/well reporter lysis buffer (Promega, Madison, WI). After addition of 35 μl/well Luciferin reagent (Biothema, Handen, Sweden) and ATP, NFAT promoter activity was measured as luminescence in a Clariostar luminometer.

Rac1 Activity. Rac1 activity was measured in cells transfected with Rac1Cluc sensor plasmid. Transfected cells were grown in six-well plates for 12 hours and then transferred to white-bottom 96-well plates (20,000 cells/well) and grown in phenol red–free DMEM with 10% FBS for an additional 12 hours. The cells were then incubated with 90 μl/well HEPES-buffered DMEM containing 3% (w/v) Na-luciferin (Promega) for 2–3 hours in the dark at room temperature. Luminescence was then measured with drug for various times in a Clariostar luminometer. The Rac1Cluc sensor was activated by 1 μM bradykinin in HEK293 cells transfected with the B2 bradykinin receptor (Supplemental Fig. 1), as previously described (Wojciak-Stothard and Ridley, 2002).

Flow Cytometry. Cells were incubated with primary mouse M1 FLAG antibody (1:200) or mouse IgG (DAKO, Glostrup, Denmark) for 20 minutes with or without 0.1% saponin/PBS (Sigma-Aldrich) at room temperature, to detect intracellular and cell surface receptors, respectively. Cells were then washed with PBS with Ca^{2+}/Mg^{2+} and resuspended in PBS with phycoerythrin-labeled goat anti-mouse antibody (DAKO; 1:2000) or Alexa488-labeled donkey anti-goat antibody (ThermoFisher Scientific; 1:1000) as secondary antibody, with or without 0.1% saponin/PBS for 20 minutes at room temperature in the dark. The cells were then washed with PBS, centrifuged at 2000*g* for 5 minutes and the pellet resuspended in PBS and directly analyzed by flow cytometry. The specificity of the secondary antibody was tested by omitting the primary antibody. The cells were analyzed using a BD FACSCanto Cytometer and FACSDiva Software (Beckton Dickinson Immunocytometry Systems, San Jose, CA). Forward and side scatter measurements were attained with gain settings in linear mode. In all experiments, binding was calculated after subtracting background fluorescence of the control antibody.

Construction and Transformation of CY2797 and EY-1 Yeast Cells. The CY2797 yeast strain was a kind gift from Dr. James Broach (CADUS Corp.) (Manfredi et al., 1996). The EY-1 strain was made from the CY2797 strain by replacing the four C-terminal amino acid residues (KIGII) of with the corresponding residues (DCGLF) of human $G\alpha_{i2}$. The targeting was done using the pUG6/pSH47 system, kindly donated by Dr. Johannes Hegemann (University of Düsseldorf, Germany), essentially as described (Güldener et al., 1996). Briefly, the targeting construct was made by polymerase chain reaction (PCR) using pUG6, containing a loxP-flanked neomycin resistance gene, and the specific primers GPA1 -(AGTG CAGTCACCGATCTAATCATCCAGCAAAACCTTAAAGATTGTGGT CTATTCTGAGCCAGCTGAAGCTTCGTACG) and GPA1 - (ATTTAC GTATCTAAACACTACTTTAATTATACAGTTCCTCATAGGCCACTA GTGGATCTG). The product was purified on agarose electrophoresis, electroporated into CY2797 and then selected on G418/ plates. G418-resistant colonies were analyzed for correct construct insertion by colony PCR. The neomycin resistance cassette was removed by loxP recombinase expression using the pSH47 vector. G418-sensitive colonies were selected by replica plating, and correct removal was confirmed using colony PCR. WT GPR30 was cloned into the p426GPD plasmid (Mumberg et al., 1995), containing a *URA3* selection marker, and PSD-95 into the p415GPD plasmid, containing a *LEU2* selection marker. CY2797 and EY-1 strains were transformed by electroporation with each plasmid individually or together.

Yeast Culturing. Yeast strains were grown and maintained on synthetic complete (SC) agar plates supplemented with 200 mg/l histidine and tryptophan. SC medium was prepared by mixing 1.7 g yeast nitrogen base without amino acids and ammonium sulfate (Sigma-Aldrich), 5 g ammonium sulfate (Prolabo, Paris, France), 1.3 g yeast synthetic dropout medium without histidine, leucine, tryptophan, and uracil (Sigma-Aldrich), 200 mg L-tryptophan (Sigma-Aldrich), and 200 mg L-histidine (Sigma-Aldrich) in 900 ml water. When SC agar plates were prepared, 20 g American bacteriological agar (Pronadisa-Hispanlab, Madrid, Spain) was added. The medium was then autoclaved for 20 minutes at 121°C. After autoclaving, the medium was allowed to cool down to ∼45–50°C before 100 ml sterile-filtered 20% (w/v) D-(+)-glucose (BDH AnalaR, Poole, UK or Sigma-Aldrich) was added.

Precultures were prepared in 250 ml E-flasks (VWR, Randor, PA) the day before the main experiment by inoculating 25 ml SC medium with colonies from SC agar plates, and the cultures were then incubated overnight at 30°C under constant agitation (230 rpm). The following day, precultures were transferred to 50 ml disposable polypropylene tubes (Sarstedt, Nümbrecht, Germany) and harvested by centrifugation (5 minutes at 800*g*). Supernatants were discarded, and cell pellets were washed twice in 20 ml SC medium before final resuspension in 25 ml. Depending on the application, washed precultures were used to inoculate working cultures in SC medium at different initial values of optical density at 600 nm (OD_{600}). All absorbance measurements were performed with the Eppendorf-BioPhotometer (Eppendorf, Hamburg, Germany).

Assay of Yeast Growth. Working cultures were prepared in 50 ml disposable polypropylene tubes by inoculating 8 ml SC medium supplemented with 0.2 mM 3-amino-1,2,4-triazol with CY2797 and EY-1 precultures to an initial OD_{600} of ∼0.05. Cultures were incubated at 230 rpm for 48 hours at 30°C without or with vehicle (DMSO) or drug, and OD_{600} measurements were made at 24, 30, and 48 hours.

Cell Lysis. HEK293 cells and HeLa cells were lysed as previously described (Sandén et al., 2011), and yeast cells lysed essentially as described previously (Hoffman et al., 2002). In short, yeast cells corresponding to an OD_{600}=10.0 were centrifuged at 2000*g* for 10 minutes at 4°C. The supernatant was discarded and the cell pellet resuspended in 1 ml ice-cold H_2O, transferred to a 1.5 ml microcentrifuge tube, and centrifuged for 1 minute at 16,000*g* at room temperature. The supernatant was discarded and the cell pellet resuspended in 200 μl 1× NuPAGE LDS sample buffer (Invitrogen) supplemented with 1× cOmplete protease inhibitor (Sigma-Aldrich). The tube was then incubated at 100°C for 10 minutes, cooled at room temperature for 7 minutes, and supplemented with 200 μl glass beads (Ø=425–600 μm; Sigma-Aldrich). The tube was vortexed for 2 minutes at maximum speed and then inverted two or three times for 1 minute. The glass beads were separated from the cell lysate by introducing a hole at the bottom of each tube. The perforated tube was placed in a fresh tube and centrifuged shortly, separating the cell lysate from the glass beads. The tube was then centrifuged for 2 minutes at 16,000*g*, and the supernatant was transferred to a fresh 1.5 ml microcentrifuge tube and stored at −20°C.

Immunoprecipitation and Immunoblotting. Immunoprecipitation and immunoblotting were done as described previously (Sandén et al., 2011). Staining was done with goat GPR30 antibody (R&D Systems, Minneapolis, MN; 1:200), mouse FLAG M2 antibody (Sigma-Aldrich; 1:1000), or pan–membrane-associated guanylate kinase antibody (Merck Millipore, Billerica, MA; 1:2000). Immunoreactive bands were visualized with a chemiluminescence immunodetection kit using peroxidase-labeled secondary antibody (Invitrogen) according to the procedure described by the supplier (PerkinElmer Life and Analytical Sciences, Waltham, MA).

Animals. GPR30 knockout (KO) mice were generated as previously described (Mårtensson et al., 2009) and backcrossed 14 generations onto the C57BL/6 background. WT C57BL/6 and GPR30 KO mice were housed in a standard animal facility under controlled temperature (22°C) and photoperiod (12 hours of light, 12 hours of dark), and the mice were fed a standard phytoestrogen-free pellet diet ad libitum. Animal care was in accordance with institutional guidelines. All animal experiments had been approved by the local Ethical Committees for Animal Research (M-416).

Wire Myography. Three-month-old female GPR30 KO mice and age-matched female WT C57BL/6 mice were euthanized using CO_2. The tail was marked on the abdominal side, cut off at its base, and then placed in cold HEPES-buffered Krebs solution (135.5 mM NaCl, 11.6 mM HEPES, 11.5 mM glucose, 5.9 mM KCl, 1.2 mM $MgCl_2$, pH 7.4). The caudal artery was exposed by a midline incision (4 cm) through the skin and covering fascia. Two-millimeter segments (1.8–2.1 mm) were cut and mounted in wire myographs (610 M and 620 M, Danish Myotechnology A/S, Aarhus, Denmark) as described (Rippe et al., 2017). All segments were stretched to 5 mN under relaxed conditions. After equilibration for 25 minutes in HEPES-buffered Krebs solution containing 2.5 mM Ca^{2+}, viability was ascertained by depolarization using 60 mM KCl (obtained by exchange of NaCl for KCl). α_1-Adrenergic receptors were activated using cirazoline (0.3 μM). G-1 or forskolin was added at increasing concentrations using vehicle (DMSO) as control. At the end of the experiment, 1 μM carbachol was added to cause endothelial- and nitric oxide–dependent dilatation. For the forskolin experiment, the exact length of each preparation was recorded at the end of experiments using a dissection microscope with an ocular scale. This length was then used for normalization of some of the force data. Having established that no differences existed between WT and KO arteries, we instead normalized force to the precontraction level (100%).

Statistical Analysis. In figures, data are presented as means ± S.D. except in Fig. 1I, where data are presented as means with whiskers of min-max. In the Results section, effects are presented as fold change ± 95% confidence interval. Data distribution was assessed using Shapiro-Wilk test for normality. To evaluate statistical significance, Student's two-tailed *t* test for unpaired or paired data was used for single comparisons of parametrical data, and the Whitney-Mann *U* test was used for single comparisons of nonparametric data. For multiple comparisons of parametrical data, one-way ANOVA with Kruskal-Wallis test for multiple comparisons, or two-way ANOVA with Tukey's test of multiple comparisons was used. To test for trends in data, one-way ANOVA with test for trend was used. *P* values less than 0.05 were regarded as statistically significant. Data analysis was performed using the Prism program version 9.1.0 (GraphPad).

Results

GPR30 Activity in Mouse Caudal Artery Ex Vivo. GPR30 is expressed in mouse peripheral arteries (Isensee et al., 2009), and several studies have used G-1 to conclude that GPR30 mediates relaxation of such arteries from a number of different species (Haas et al., 2009; Broughton et al., 2010, Meyer et al., 2010, Lindsey et al., 2011; Jang et al., 2013; Lindsey et al., 2014; Arefin et al., 2014; Debortoli et al., 2017; Peixoto et al., 2017; Yu et al., 2018). To address the involvement of GPR30 in this response, we used the caudal artery from our GPR30 KO mouse strain (Mårtensson et al., 2009) and compared it with age-matched C57BL/6 WT mice. Fig. 1 shows that 60 mM KCl (Fig. 1A) and 0.1 μM of the α_1-adrenergic receptor agonist cirazoline (Fig. 1B) each constricted WT and KO arteries to the same maximal degree. Furthermore, no difference was observed in the dose-response curves of forskolin-promoted relaxation between cirazoline-preconstricted WT and KO arteries (Fig. 1C). G-1 relaxed cirazoline-preconstricted WT arteries dose-dependently and to a maximal degree very similar to that previously reported by other investigators (Fig. 1D and E). An essentially overlapping G-1 dose-response curve was observed with KO arteries (Fig. 1F, G, and H), and the maximal response was not different between the WT and KO arteries (Fig. 1I). We conclude from these results that GPR30 does not influence the contractility of the mouse caudal artery to any statistically significant degree, and that the receptor does not contribute to G-1–promoted relaxation of the artery.

Human WT GPR30 Activity in Mammalian Cells In Vitro. Next, we investigated human GPR30 activity in well defined mammalian recombinant systems in vitro. To capture a broad repertoire of receptor signals, we used HFF11 cells (Kotarsky et al., 2003), a HeLa cell line stably expressing a luciferase-based promoter-reporter construct containing a synthetic multifunctional promoter with several different response motifs [nuclear factor κB (NF -κB), signal transducer and activator of transcription (STAT), and activator protein 1 (AP-1)] upstream from the luciferase gene. In these cells, we also stably expressed a T-REx system, in which the expression of N-terminally FLAG-tagged human WT GPR30 (GPR30) is dependent on TET treatment (T-REx HFF11 cells). Treatment with 1000 ng/ml TET for 12 hours resulted in the appearance of at least three immunoreactive species, at about 35–40 kDa, 70 kDa and 130 kDa, as determined with a polyclonal goat antibody against the human GPR30 N-terminal domain (Fig. 2A). The same species were identified with a monoclonal M2 FLAG antibody, which specifically reacts with the GPR30 FLAG epitope, confirming that the GPR30 antibody recognizes the expressed receptor (Fig. 2A). As expected, removal of TET led to the disappearance of the species (Fig. 2B). Flow cytometry showed that 22% of the induced receptors were localized in the plasma membrane (PM) (Fig. 2C).

Treating T-REx HFF11 cells with increasing doses of TET (0–1000 ng/ml) for 12 hours, to dose-dependently increase GPR30 expression, yielded a trend of an increase in basal ERK1/2 activity (trend: slope=0.14 ± 0.076, $P = 0.0014$) with increased receptor expression (Fig. 2D), as previously reported in transiently transfected HEK293 cells (Gonzalez de Valdivia et al., 2017). To assay ligand-independent constitutive GPR30 activity using the luciferase-based promoter-reporter, luciferase activity was monitored after treatment of cells with 1000 ng/ml TET for 12 and 24 hours and compared with that without TET treatment (Fig. 3A). The reason for the 24-hour time point is that in contrast to receptor stimulation of ERK1/2 activity, which is rapid, the downstream stimulation of luciferase activity is slow, requiring gene transcription to occur. No change in basal reporter activity was observed after 12 hours of TET treatment, whereas a statistically significant increase was observed after 24 hours of treatment both as determined in absolute numbers (Fig. 3B; fold change for vehicle-treated cells: 1.5 ± 0.3) and as a fraction of the response to 0.1 μM phorbol myristate acetate (PMA), a potent stimulator of the promoter-reporter through protein kinase C and used here as a positive control (Fig. 3B and C; fold change for vehicle-treated cells: 2.3 ± 0.4). On the other hand, no increase in reporter activity was observed after TET treatment of HFF11 cells lacking the T-REx system (data not shown). The GPR30-promoted increase in basal reporter activity in T-REx HFF11 cells was similar to that observed in response to 1 mM ATP through native purinergic receptors (fold change 2.7 ± 0.15) (Fig. 3D). Neither 0.1 μM E2 nor 1 μM G-1 had any clear effect on the reporter activity either at low (1 ng/ml TET) or high (1000 ng/ml TET) levels of receptor expression regardless of whether the cells had been grown in normal or charcoal-treated FBS (to remove FBS-derived estrogens) (Fig. 3E). Thus, human GPR30

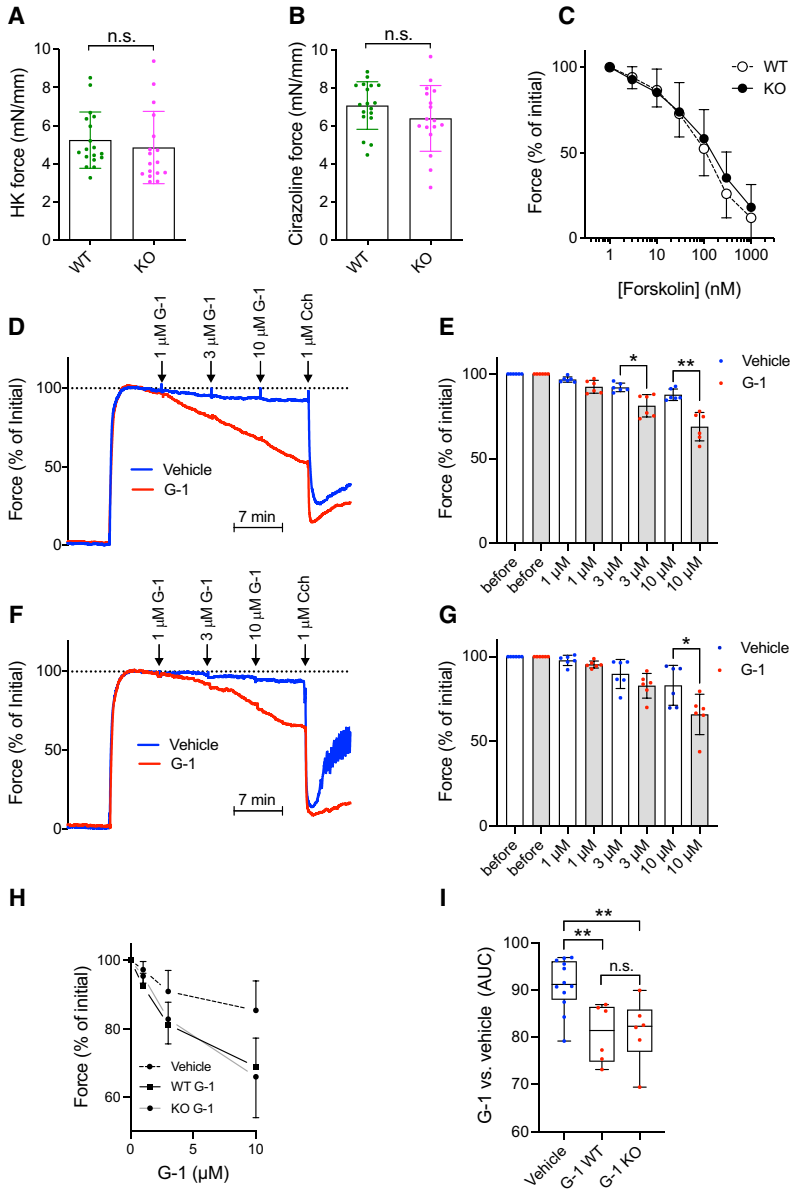

Fig. 1. Contractility and forskolin- and G-1–driven relaxation in caudal arteries from WT and GPR30 KO mice. Caudal artery tubes were prepared by microdissection and mounted in wire myograph chambers to measure active force development (at a passive force of 5 mN). The length of the arterial tube was measured at the end of the experiment and used for normalization of the force integral over the stimulation periods shown. (A, B) Force in response to depolarization (60 mM K^+, n = 17–18 preparations from a minimum of six mice of each genotype) and stimulation with the α_1-adrenergic agonist cirazoline (0.3 μM), respectively, statistically analyzed using Mann-Whitney U test. (C) Concentration-dependent relaxation by forskolin in WT and KO arteries (n = 17–18 preparations) after precontraction with cirazoline. Here and in the following panels, force was normalized to the precontraction, but results were the same using absolute force. (D) Original force records from WT arteries stimulated with 0.3 μM cirazoline followed by cumulative addition of G-1 (red trace) or vehicle (DMSO) (blue trace). The muscarinic agonist carbachol (Cch) was given at the end to ascertain endothelium-dependent dilatation. (E) Summarized data for the effect of different concentrations

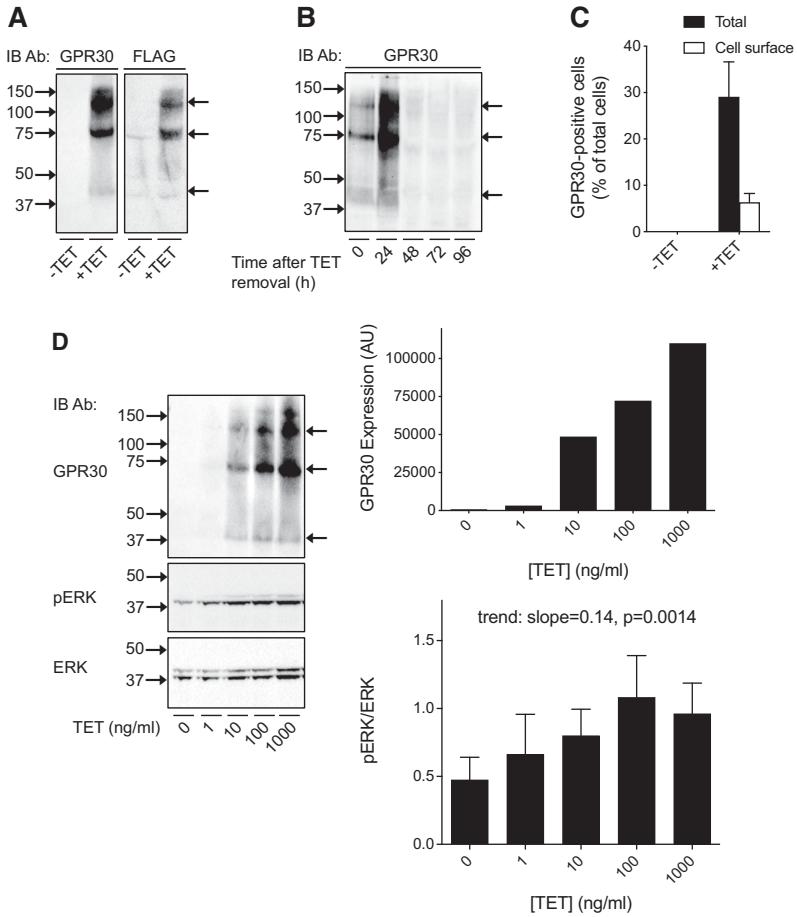

Fig. 2. Expression and ligand-independent activity of human GPR30 in T-REx HFF11 cells. (A, B) T-REx HFF11 cells were treated without (−TET) or with 1000 ng/ml TET (+TET) for 12 hours (A), washed free of TET and incubated in medium for different lengths of time as indicated (B), and then immunoblotted with GPR30 or M2 FLAG antibody. (C) T-REx HFF11 cells were treated without (−TET) or with 1000 ng/ml TET (+TET) for 12 hours, stained live (*Cell surface*) or after permeabilization (*Total*) with M1 FLAG , and then subjected to flow cytometry. The data were plotted as GPR30-positive cells as % of total cells. (D) T-REx HFF11 cells were treated without or with increasing concentrations of TET for 12 hours as indicated and then immunoblotted with GPR30 , pERK , and ERK . The combined pERK band intensities were normalized to the combined ERK band intensities for each condition and the ratio graphed and statistically analyzed using a repeated measures one-way ANOVA with test for trend. The intensity of the GPR30 band at approximately 70-kDa was graphed as arbitrary units (AU). The results are either representative or the means ± S.D. of at least three independent experiments. In (A), (B), and (D), molecular mass standards (left side) and receptor species (right side) are indicated.

exhibits ligand-independent effects on reporter activity, whereas no effect is observed after treatment with either 0.1 μM E2 or 1 μM G-1.

Activity of Human GPR30 With and Without the PSD-95/Discs-Large/Zonula Occludens-1 Homology Motif in Mammalian Cells In Vitro. Next, we evaluated human GPR30 activity in HEK293 cells and HFF11 cells transiently transfected with WT GPR30 or GPR30ΔSSAV, which has increased receptor endocytosis and attenuated ligand-independent receptor activities due to disrupted receptor interaction with the membrane scaffold proteins synapse-associated protein 97 (SAP97) and PSD-95 (Akama et al., 2013; Broselid et al., 2014; Tran et al., 2015; Gonzalez de Valdivia et al., 2017). Both constructs were expressed to approximately the same degree in HEK293 cells (Fig. 4A). Neither 0.1 μM E2 nor 1 μM G-1 had any statistically significant effect on ERK1/2 activity was similar in mock-, GPR30-, or GPR30ΔSSAV-transfected HEK293 cells (Fig. 4B). To

of G-1 in WT (n = 6 preparations receiving G-1, and n = 6 preparations receiving vehicle). (F, G) Effect of G-1 in KO arteries run in parallel with the WT arteries in (D) and (E) [n = 6 preparations receiving G-1, and n = 6 preparations receiving vehicle; six WT and six KO mice were used altogether for the experiments in (D)–(G)]. The data in (E) and (G) were statistically analyzed by paired t test. (H) Concentration-response curves for G-1 in WT and KO arteries are plotted alongside each other. Vehicle (DMSO) controls are pooled for clarity. G-1 relaxation was not different in WT compared with KO arteries but was greater than seen in vehicle-treated arteries in both cases. (I) Area under the curve (AUC) of the responses shown in (H), statistically tested using one-way ANOVA with Tukey's multiple comparisons test. The results are either representative [(D) and (F)] or means ± S.D. of n = 17–18 measurements from a minimum of 6 mice of each genotype [(A)–(C), (E), (G), (H)], or means with whiskers of min-max (I). $^*P < 0.05$; $^{**}P < 0.01$; n.s., not significant.

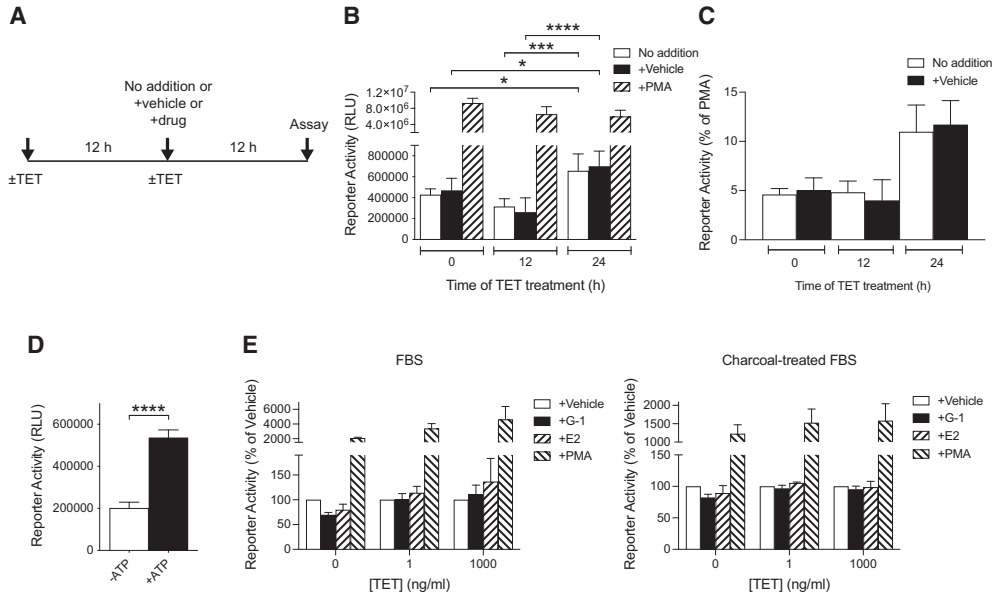

Fig. 3. Ligand-dependent and -independent activities of human GPR30 in T-REx HFF11 cells. (A) The treatment protocol of T-REx HFF11 cells for assaying GPR30 activity in (B), (C), and (E) is described. (B, C) T-REx HFF11 cells were treated without or with 1000 ng/ml TET for 12 or 24 hours. During the treatment without TET (−TET) or with TET (+TET), the cells were also treated without (no addition) or with vehicle or 0.1 μM PMA for 12 hours prior to assay for luminescence. The results are expressed as relative light units (RLU) and analyzed statistically using two-way ANOVA with Tukey's multiple comparisons test (B), or as % of PMA values (C). (D) T-REx HFF11 cells were treated without (-ATP) and with 1 mM ATP (+ATP) for 12 hours prior to assay for luminescence. The results were expressed as RLU and analyzed statistically using an unpaired *t* test. (E) T-REx HFF11 cells grown in normal FBS (left graph) or in charcoal-treated FBS (right graph) for at least 2 days were treated without or with different concentrations of TET for 24 hours as indicated. During the treatment without or with TET, the cells were also treated with vehicle, 1 μM G-1 (G-1), 0.1 μM E2 (E2), or 0.1 μM PMA for 12 hours prior to assay for luminescence. The results are graphed as % of vehicle. The data are presented as means ± S.D. of at least three independent experiments. $^{*}P < 0.05$; $^{***}P < 0.001$; $^{****}P < 0.0001$.

address if GPR30 mediates any effect of G-1 or E2 on intracellular free Ca^{2+}, HEK293 cells were transfected with the luciferase promoter-reporter plasmid pGL3-NFAT, which monitors NFAT, a specific transcription factor target for calcineurin, thus showing high sensitivity to Ca^{2+} (Clipstone and Crabtree, 1992). Although 0.1 μM E2 had a small stimulatory effect on NFAT activity in mock-transfected cells, neither E2 nor 1 μM G-1 had any statistically significant effect on NFAT activity in either GPR30- or GPR30ΔSSAV-transfected cells (Fig. 4C). On the other hand, as previously reported (Gonzalez de Valdivia et al., 2017), GPR30 expression drastically inhibited basal NFAT activity in a PDZ motif–dependent manner, with a fold change compared with mock of 0.29 ± 0.046 for WT GPR30, and 1.1 ± 0.176 for GPR30ΔSSAV (Fig. 4C). To address if GPR30 mediates any effect on Rac1 activity, a downstream effector of phosphoinositide 3-kinase, we constructed a split click beetle luciferase-based Rac1 sensor plasmid (Rac1Cluc). Again, neither 0.1 μM E2 nor 1 μM G-1 had any statistically significant effect on Rac1 activity in either mock-, GPR30-, or GPR30ΔSSAV-transfected cells (Fig. 4E). GPR30 expression inhibited basal Rac1 activity in a PDZ-dependent manner, with fold changes compared with mock-transfected cells of 0.04 ± 0.0049 for WT GPR30, and 1.2 ± 0.81 for GPR30ΔSSAV (Fig. 4D). We also addressed if GPR30 mediates any G-1 or E2 effect on the multifunctional promoter-reporter when GPR30 and GPR30ΔSSAV were transiently transfected in HFF11 cells (Fig. 4F). G-1 (1 μM) stimulated the reporter in mock-transfected cells (fold change of vehicle of 1.5 ± 0.08), whereas 0.1 μM E2 did not (fold change of vehicle of 1.0 ± 0.06). On the other hand, neither GPR30 nor GPR30ΔSSAV expression amplified the response to either G-1 (fold change of vehicle at plasmid concentration 1 $\mu g/1 \times 10^6$ cells of 1.4 ± 0.10 for GPR30 and 1.3 ± 0.15 for GPR30ΔSSAV) or E2 (fold change of vehicle at plasmid concentration 1 $\mu g/1 \times 10^6$ cells of 1.0 ± 0.05 for GPR30 and 1.1 ± 0.10 for GPR30ΔSSAV (Fig. 4G).

Human WT GPR30 Activity in Yeast. We also addressed GPR30 activity in the yeast *Saccharomyces cerevisiae*, a system previously used to study GPCR activity and pharmacology by monitoring G protein–mediated coupling to the pheromone response pathway (Liu et al., 2016). To this end, we used the *S. cerevisiae* strain CY2797, in which the endogenous α-factor GPCR gene *STE2* is disrupted and expresses the native yeast G protein Gpa1. Furthermore, the strain is auxotrophic for histidine unless activated by the pheromone pathway, and activation of the pathway leads to increased growth (Manfredi et al., 1996). From CY2797, we made EY-1, in which we expressed a chimeric Gα protein where the five C-terminal residues of Gpa1 (KIGII) were replaced with those of human $G\alpha_{i2}$ (DCGLF).

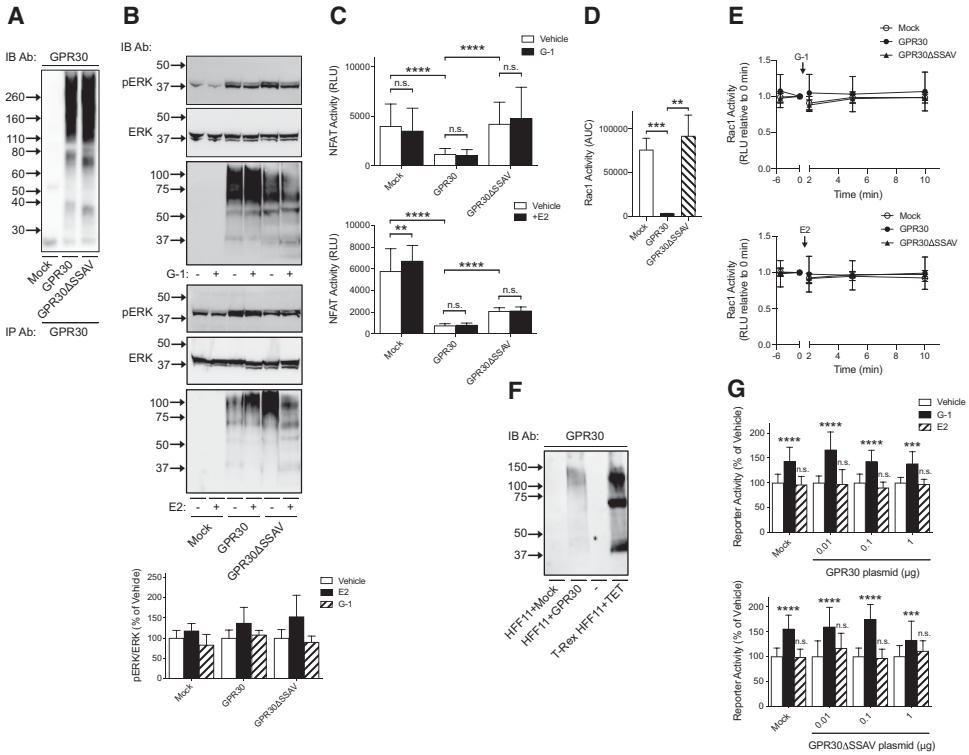

Fig. 4. Ligand -dependent and -independent activities of human GPR30 and GPR30ΔSSAV in HEK293 cells and HFF11 cells. (A) HEK293 cells transiently transfected with empty pcDNA3 plasmid (*Mock*) or plasmid containing GPR30 or GPR30ΔSSAV were immunoprecipitated with GPR30 and then immunoblotted with GPR30 Ab. (B) HEK293 cells transiently transfected with empty pcDNA3 plasmid (*Mock*) or plasmid containing GPR30 or GPR30ΔSSAV were treated with vehicle (−) or 1 μM G-1 or 0.1 μM E2 (+) for 5 minutes and then immunoblotted with pERK Ab, ERK Ab, or GPR30 Ab. The combined pERK band intensities were normalized to the combined ERK band intensities for each condition and graphed as % of vehicle. (C) HEK293 cells transiently transfected with pGL3-NFAT luciferase plasmid together with either empty pcDNA3 plasmid (*Mock*) or plasmid containing GPR30 or GPR30ΔSSAV were treated with vehicle, 1 μM G-1, or 0.1 μM E2. NFAT activity was then assayed as luminescence and the results graphed as relative light units (RLU). The data were evaluated statistically using a two-way ANOVA with Tukey's test for multiple comparisons. (D, E) HEK293 cells transiently transfected with Rac1Cluc plasmid together with either empty pcDNA3 plasmid (*Mock*) or plasmid containing GPR30 or GPR30ΔSSAV were treated with 1 μM G-1 or 0.1 μM E2 for different times. Rac1 activity was then assayed for luminescence as RLU. In (D), the RLU area under the curve (AUC) in the absence of stimulus was analyzed using an unpaired Student's *t* test, and in (E), RLU at different times after addition of stimulus was graphed normalized to time=0. (F) Cells transfected with empty pcDNA3 plasmid (*Mock*) or 1 μg GPR30 plasmid, or T-REx HFF11 cells treated with 1000 ng/ml TET for 12 hours were with GPR30 Ab. (G) HFF11 cells transiently transfected with either empty pcDNA3 plasmid (*Mock*) or different amounts of plasmid containing GPR30 or GPR30ΔSSAV were treated with vehicle, 1 μM G-1, or 0.1 μM E2 for 12 hours and luminescence was measured as RLU. Data were analyzed statistically using one-way ANOVA with Kruskal-Wallis test for multiple comparisons. Data are either representative (A), (F) or presented as means ± S.D. of at least three independent experiments. In (A), (B), and (F), molecular mass standards are indicated (left side). $^{**}P < 0.01$; $^{***}P < 0.001$; $^{****}P < 0.0001$; n.s., not significant.

GPR30 was readily expressed in both CY2797 and EY-1, migrating as a single species at about 35–40 kDa in both strains as determined using the GPR30 antibody (Fig. 5A). GPR30 expression led to a clear increase in the basal growth of both strains, with a fold change at 48 hours compared with 0 hours of 2.3 ± 0.25 and 2.0 ± 0.32 for GPR30-expressing CY2797 and EY-1, respectively, and a fold change of 1.7 ± 0.38 and 1.5 ± 0.34 for CY2797 and EY-1, respectively, without GPR30 expression (Fig. 5B and C). On the other hand, incubation with 1 μM G-1 for 30 hours had no effect on CY2797 growth either with or without GPR30 expression (Fig. 5D). Thus, GPR30 constitutively couples to the pheromone response pathway but does not respond to G-1 in this system.

We also evaluated the effect of PSD-95, a GPR30 PDZ domain partner (Broselid et al., 2014), on the ligand-independent GPR30 activity. Figure 5A shows that human FLAG-tagged PSD-95 (Zhang et al., 2007) was readily expressed in both CY2797 and EY-1 cells. PSD-95 expression had no effect on the GPR30 response in CY2797 cells (Fig. 5B). On the other hand, PSD-95 inhibited the GPR30 response when the chimeric $Gpa_1/G\alpha_{i2}$ protein was expressed in EY-1 cells, with fold change in growth at 48 hours of 1.4 ± 0.77 in yeast expressing both GPR30 and PSD-95, as compared with 1.5 ±

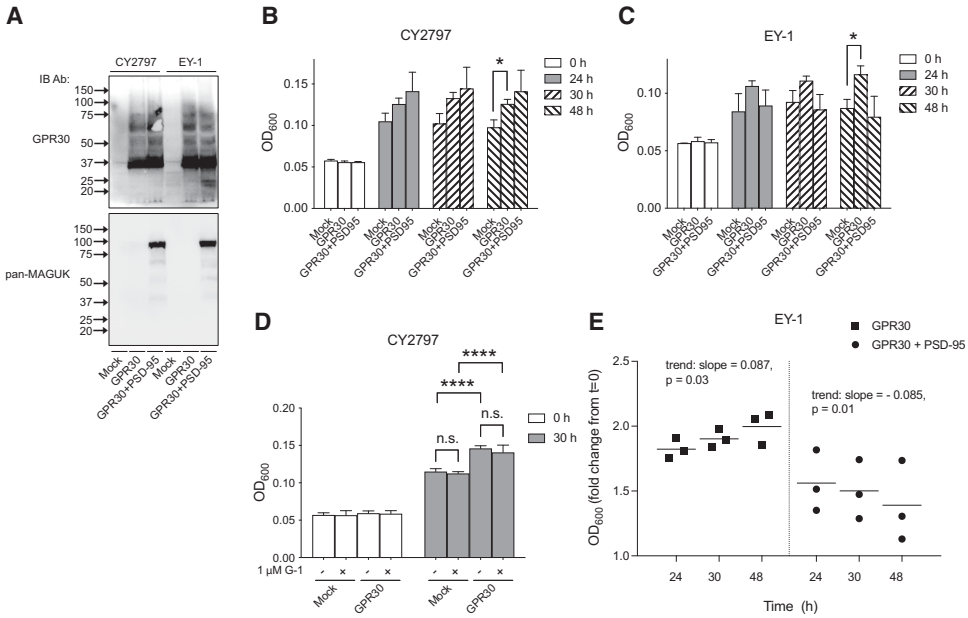

Fig. 5. Expression and ligand-independent activity human GPR30 activity with and without PSD-95 in yeast *S. cerevisiae*. (A) CY2797 and EY-1 yeast strains transformed with empty plasmid (*Mock*), plasmid containing GPR30, or plasmids containing GPR30 and PSD-95 were immunoblotted with GPR30 and pan–membrane-associated guanylate kinase (MAGUK) Ab. (B, C) Cell growth was followed for various times and graphed as OD_{600}. Two-way ANOVA with Tukey's multiple comparisons test was used to statistically analyze the relationship between all groups. (D) Cells were treated with vehicle (−) or 1 μM G-1 (+), and OD_{600} was determined and graphed for time 0 hours and 30 hours of treatment. Statistical analysis was performed using two-way ANOVA with Tukey's multiple comparisons test. (E) Data from (C) were normalized to the OD_{600} at t=0 and analyzed using repeated measures one-way ANOVA with test for trend to assess time-dependent linear relationships for each condition. The results are either representative (A) or the means ± S.D. (C)–(E) of at least three independent experiments. In (A), molecular mass standards are indicated (left side). $^*P < 0.05$; $^{****}P < 0.0001$; n.s., not significant.

0.34 in mock, and 2.0 ± 0.32 when GPR30 was expressed without PSD-95 (Fig. 5C). Indeed, although there was a positive linear relationship between time and growth in EY-1 expressing only GPR30 (trend: slope = 0.087 ± 0.07, P = 0.03), growth of EY-1 expressing both GPR30 and PSD-95 had a negative linear relationship with time (trend: slope = −0.085 ± 0.056, P = 0.01) (Fig. 5E).

Discussion

Here, we used several recombinant eukaryotic systems with and without GPR30 expression to rigorously address the ability of G-1 and E2 to influence GPR30 activity and the ligand-independent GPR30 activity ex vivo and in vitro. No receptor-dependent activity was observed in response to 1 μM G-1 ex vivo and in vitro or 0.1 μM E2 in vitro. On the other hand, ligand-independent receptor activity was observed in all the in vitro mammalian cell systems and in yeast. Thus, classifying GPR30 as an estrogen receptor sensitive to G-1 and E2 is unfounded.

Transgenic KO mouse models with and without receptor expression offer an excellent opportunity to address in a physiologic setting if the effect of a pharmacological agent is receptor-dependent. GPR30 is expressed in several peripheral arteries in mouse (Isensee et al., 2009), and numerous studies have used G-1 to conclude that GPR30 mediates relaxation of WT arteries from a number of species (Haas et al., 2009; Broughton et al., 2010, Meyer et al., 2010, Lindsey et al., 2011; Jang et al., 2013; Lindsey et al., 2014; Arefin et al., 2014; Debortoli et al., 2017; Peixoto et al., 2017; Yu et al., 2018). Considering that this conclusion is based only on one GPR30 KO mouse strain (Haas et al., 2009), and that phenotypic variations exist between different GPR30-deficient strains (Olde and Leeb-Lundberg, 2009; Langer et al., 2010), we were compelled to readdress the specificity of this response in a unique mouse KO strain (Mårtensson et al., 2009). G-1 relaxed the mouse caudal artery with a potency and to a maximal degree virtually identical to that previously reported by other investigators using other peripheral arteries. An essentially overlapping G-1 dose-response curve was obtained with the KO mouse caudal artery. Thus, GPR30 apparently does not contribute to G-1–promoted vasorelaxation, at least not of the mouse caudal artery.

At the cellular level, G-1 was previously reported to cause an antiproliferative effect through GPR30 in human vascular smooth muscle cells (Haas et al., 2009). We subsequently showed that G-1 is antiproliferative in mouse aortic endothelial and smooth muscle cells, which correlates with microtubule disruption (Holm et al., 2012). This response was identical in cells isolated from WT and GPR30 KO mice,

again showing in a physiologically relevant system that G-1 elicits effects independently of native GPR30.

Native systems are complex, rendering them difficult to use to more specifically determine if an agonist response is a consequence of a direct interaction with a receptor or mediated by a distinct target(s) that depends on receptor expression. To attempt to reduce the complexity of the system, we used T-REx HFF11 cells, which were designed to capture a multitude of receptor signals, including mitogen-activated protein kinase activity and Ca^{2+}, through a synthetic multifunctional promoter (NF-κB, STAT, AP-1) at different receptor levels. Receptor species were identified at about 35–40 kDa, about 70 kDa, and about 130 kDa, consistent with that observed by a number of investigators in several native systems (Maiti et al., 2011; Jala et al., 2012; Akama et al., 2013; Scaling et al., 2014; Waters et al., 2015). The species at 35–40 kDa, the theoretical mass of the receptor, most likely represents an immature, unglycosylated form of the receptor. On the other hand, the 70 kDa species represents a mature plasma membrane–localized receptor form (Cheng et al., 2011; Gonzalez de Valdivia et al., 2019), a form that has been reported to be functionally active (Filardo et al., 2007; Broselid et al., 2014; Gonzalez de Valdivia et al., 2017), capable of coupling to G proteins (Filardo et al., 2007; Gonzalez de Valdivia et al., 2017), and undergo receptor-mediated endocytosis (Cheng et al., 2011; Sandén et al., 2011). At least 22% of the expressed receptor resided at the plasma membrane in the T-REx HFF11 cells. Nevertheless, no GPR30-dependent reporter activity was observed in response to either G-1 or E2 at any receptor level in these cells, or in HFF11 cells transiently expressing the receptor, regardless of whether the cells had been grown in normal or charcoal-treated FBS, to remove serum-derived estrogens. Transient expression of GPR30 in HEK293 cells also did not reveal any receptor-dependent G-1 or E2 effects on intracellular free Ca^{2+}, as determined with an NFAT luciferase reporter, Rac1, as determined with a Rac1Cluc reporter, or ERK1/2 activity, as determined with pERK immunoblotting.

To further reduce system complexity, and to exclude cell- or medium-derived estrogens as a reason for the lack of ligand-stimulated GPR30 activity, we also addressed receptor activity in response G-1 in the yeast *S. cerevisiae*, a system previously used to study GPCR activity and pharmacology by monitoring G protein–mediated coupling to the pheromone response pathway (Liu et al., 2016). Even in this system did G-1 lack the ability to trigger GPR30 activity. Together, these results are in line with those of several earlier studies (Pedram et al., 2006; Otto et al., 2008; Kang et al., 2010; Southern et al., 2013; Broselid et al., 2014; Sousa et al., 2017; Gonzalez de Valdivia et al., 2017) failing to reproduce the initial observations that G-1 and E2 act as agonists at GPR30 (Thomas et al., 2005 ; Revankar et al., 2005; Bologa et al., 2006). We conclude from these results that G-1 and E2 either do not interact directly with GPR30, or that some critical information is missing in our understanding of this interaction. Unfortunately, only limited attention has been paid to resolve this disagreement, which likely has discouraged independent efforts in both academia and industry to further unravel the molecular details of this pathophysiologically interesting receptor, and to develop high-throughput screening systems to identify specific pharmacological tools.

Ligand-independent constitutive GPR30 activity is less investigated but has the advantage of being independent of any off-target pharmacological effects. Such activity can normally be observed only in well defined recombinant systems, where receptor expression can be compared with a receptor-negative control. We showed previously that GPR30 constitutively decreases cAMP production and NFAT activity and increases ERK1/2 activity in transiently transfected HEK293 or CHO cells (Broselid et al., 2014; Gonzalez de Valdivia et al., 2017). Here, we show that GPR30 also constitutively decreases Rac1 activity in HEK293 cells and increases the activity of a multifunctional promoter (NF-κB, STAT, AP-1) reporter in stable T-REx HFF11 cells. An argument can be made that ligand-independent activity is only apparent, instead being the consequence of a cell- or medium-derived ligand. However, the fact that GPR30 expression also increased yeast growth, an entirely heterologous system without any human growth factors or steroids produced by the cells or in the medium, argues against this explanation.

Evidence that native GPR30 exhibits ligand-independent activity was suggested already in 2002, when progestin treatment of estrogen receptor–positive MCF7 cells was shown to yield both increased GPR30 expression and growth inhibition in the absence of E2, and GPR30 knockdown increased growth whereas GPR30 over-expression decreased growth (Ahola et al., 2002). That receptor knockdown increased growth of MDA-MB-231, MDA-MB-468 cells (Weißenborn et al., 2014), and MCF7 cells (Ariazi et al., 2010; Broselid et al., 2013), and receptor overexpression decreased growth of HEK293 cells (Broselid et al., 2013) provided further evidence for such activity.

All ligand-independent GPR30 activities so far identified in recombinant mammalian systems depend on the receptor C-terminal PDZ motif (Broselid et al., 2014; Gonzalez de Valdivia et al., 2017, Tran et al., 2015). Removing the PDZ motif also increases GPR30 endocytosis, suggesting that these activities require PM localization (Broselid et al., 2014). Interestingly, we report here that ectopic GPR30 couples to the pheromone pathway–mediated yeast growth, which is also a PM-dependent event (Alvaro and Thorner, 2016). Furthermore, PM-localized GPR30 staining of breast cancer patient biopsies has a stronger prognostic significance than total cellular staining (Sjöström et al., 2014 ; Tutzauer et al., 2020). Thus, PM localization appears to be critical for GPR30 function and rely on the PDZ motif.

PDZ-dependent GPR30 anchoring in the PM has in some systems been found to involve a direct interaction between the receptor C-terminal PDZ motif and the PDZ domain membrane scaffold proteins PSD-95 (Akama et al., 2013; Broselid et al., 2014; Tran et al., 2015) or SAP97 (Broselid et al., 2014; Waters et al., 2015). Contributing to receptor PM anchoring may also be the direct interaction of the receptor with the PDZ domain protein , which was reported to increase GPR30 stability (Meng et al., 2016). GPR30 also interacts with and favors PM localization of the chaperone protein receptor activity–modifying protein 3 (Lenhart et al., 2013), which contains a PDZ motif capable of interacting with the PDZ domain of NHERF-1 (Bomberger et al., 2005). Through PSD-95 and/or SAP97, GPR30 in turn interacts with A-kinase anchoring protein 5 (Broselid et al., 2014). Thus, GPR30 appears to be part of a larger PM complex with

several partner proteins that may allosterically enable the receptor to elicit ligand-independent activity.

GPR30-promoted ERK1/2 activity is dependent on both pertussis toxin and PDZ (Gonzalez de Valdivia et al., 2017), suggesting that a $G_{i/o}$ protein is also part of the PM GPR30 complex. Interestingly, PSD-95 expression inhibited the growth-stimulatory effect of GPR30 when expressed in a yeast strain harboring a humanized chimeric yeast Gα protein with the five C-terminal residues from human $G\alpha_{i2}$ (DCGLF). These residues directly interact with critical functional residues in GPCR (Oldham and Hamm, 2008; Hilger et al., 2018), with the cysteine in this sequence ADP-ribosylated by pertussis toxin (West et al., 1985). Although yeast expresses very few PDZ domain proteins only distantly related to the mammalian proteins (Harris and Lim, 2001), and does not provide any direct information about complex mammalian protein networks, it has been very useful in identifying physiologically relevant binary protein-protein interactions, including PDZ-dependent interactions with GPCR (Bockaert et al., 2003). Thus, it is tempting to speculate that the binding epitopes for a PDZ domain scaffold protein and $G\alpha_i$ in GPR30 partly overlap.

How then may G-1 and E2 depend on GPR30 in some systems? Several modes of crosstalk between GPR30 and various ERα isoforms have been proposed in recent years (Romano and Gorelick, 2018). GPR30 was reported to interact with the 66-kDa main isoform of ERα (ERα66) (Vivacqua et al., 2009). GPR30 also upregulates and interacts with the 36-kDa ERα isoform (ERα36), mediating effects overlapping with those of GPR30 (Kang et al., 2010; Pelekanou et al., 2016), and both G-1 and E2 activate ERα36 (Kang et al., 2010). Furthermore, the gene promoters of receptor activity–modifying protein 3 and NHERF-1 contain ERE elements through which E2, via ERα66, upregulates these proteins (Ediger et al., 1999; Watanabe et al., 2006). In addition, G-1 increases PSD-95 expression in mouse brain (Waters et al., 2015), a membrane scaffold protein that interacts with the GPR30 PDZ motif, a motif necessary to retain the receptor in the plasma membrane (Akama et al., 2013; Broselid et al., 2013). Given this background, it is tempting to propose that E2 and G-1 influence the ligand-independent activity of GPR30 by interacting with and/or regulating the expression of one or more partners in a GPR30 PM complex.

In this study, we provide ample evidence both ex vivo and in vitro that G-1 and E2 do not act as agonists directly at GPR30. Instead, we propose that this receptor forms a PM complex with partner proteins through which it harbors ligand-independent activity. Considering that the expression or signaling of some components of this complex is sensitive to G-1 and/or E2 stimulation, this could be the reason why some responses to these agents are GPR30-dependent.

Acknowledgments

The authors thank Joanna Daszkiewicz-Nilsson for expert technical.

Authorship Contributions

Participated in research design: Olde, Leeb-Lundberg.

Conducted experiments: Tutzauer, Gonzalez de Valdivia, Swärd, Alexandrakis Eilard, Broselid, Kahn, Olde.

Contributed new reagents or analytic tools: Gonzalez de Valdivia, Olde.

Performed data analysis: Tutzauer, Gonzalez de Valdivia, Swärd, Alexandrakis Eilard, Broselid, Kahn, Leeb-Lundberg, Olde.

Wrote or contributed to the writing of the manuscript: Tutzauer, Olde, Leeb-Lundberg.

References

Ahola TM, Manninen T, Alkio N, and Ylikomi T (2002) G protein-coupled receptor 30 is critical for a progestin-induced growth inhibition in MCF-7 breast cancer cells. *Endocrinology* **143**:3376–3384.

Akama KT, Thompson LI, Milner TA, and McEwen BS (2013) Post-synaptic density-95 (PSD-95) binding capacity of G-protein-coupled receptor 30 (GPR30), an estrogen receptor that can be identified in hippocampal dendritic spines. *J Biol Chem* **288**:6438–6450.

Alexander SP, Mathie A, and Peters JA (2011) Guide to Receptors and Channels (GRAC), 5th edition. *Br J Pharmacol* **164**:S1–S324

Alvaro CG and Thorner J (2016) Heterotrimeric G protein-coupled receptor signaling in yeast mating pheromone response. *J Biol Chem* **291**:7788–7795.

Arefin S, Simoncini T, Wieland R, Hammarqvist F, Spina S, Goglia L, and Kublickiene K (2014) Vasodilatory effects of the selective GPER agonist G-1 is maximal in arteries of postmenopausal women. *Maturitas* **78**:123–130.

Ariazi EA, Brailoiu E, Yerrum S, Shupp HA, Slifker MJ, Cunliffe HE, Black MA, Donato AL, Arterburn JB, Oprea TI et al. (2010) The G protein-coupled receptor GPR30 inhibits proliferation of estrogen receptor-positive breast cancer cells. *Cancer Res* **70**:1184–1194.

Bockaert J, Marin P, Dumuis A, and Fagni L (2003) The 'magic tail' of G protein-coupled receptors: an anchorage for functional protein networks. *FEBS Lett* **546**:65–72.

Bologa CG, Revankar CM, Young SM, Edwards BS, Arterburn JB, Kiselyov AS, Parker MA, Tkachenko SE, Savchuck NP, Sklar LA et al. (2006) Virtual and biomolecular screening converge on a selective agonist for GPR30. *Nat Chem Biol* **2**:207–212.

Bomberger JM, Spielman WS, Hall CS, Weinman EJ, and Parameswaran N (2005) Receptor activity-modifying protein (RAMP) isoform-specific regulation of adrenomedullin receptor trafficking by NHERF-1. *J Biol Chem* **280**:23926–23935.

Broselid S, Cheng B, Sjöström M, Lövgren K, Klug-De Santiago HL, Belting M, Jirström K, Malmström P, Olde B, Bendahl PO et al. (2013) G protein-coupled estrogen receptor is apoptotic and correlates with increased distant disease-free survival of estrogen receptor-positive breast cancer patients. *Clin Cancer Res* **19**:1681–1692.

Broselid S, Berg KA, Chavera TA, Kahn R, Clarke WP, Olde B, and Leeb-Lundberg LMF (2014) G protein-coupled receptor 30 (GPR30) forms a plasma membrane complex with membrane-associated guanylate kinases (MAGUKs) and protein kinase A-anchoring protein 5 (AKAP5) that constitutively inhibits cAMP production. *J Biol Chem* **289**:22117–22127.

Broughton BR, Miller AA, and Sobey CG (2010) Endothelium-dependent relaxation by G protein-coupled receptor 30 agonists in rat carotid arteries. *Am J Physiol Heart Circ Physiol* **298**:H1055–H1061.

Cheng SB, Quinn JA, Graeber CT, and Filardo EJ (2011) Down-modulation of the G-protein-coupled estrogen receptor, GPER, from the cell surface occurs via a trans-Golgi-proteasome pathway. *J Biol Chem* **286**:22441–22455.

Clipstone NA and Crabtree GR (1992) Identification of calcineurin as a key signalling enzyme in T-lymphocyte activation. *Nature* **357**:695–697.

Debortoli AR, Rouver WDN, Delgado NTB, Mengal V, Claudio ERG, Pernomian L, Bendhack LM, Moysés MR, and Santos RLD (2017) GPER modulates tone and coronary vascular reactivity in male and female rats. *J Mol Endocrinol* **59**:171–180.

Ediger TR, Kraus WL, Weinman EJ, and Katzenellenbogen BS (1999) Estrogen receptor regulation of the Na+/H+ exchange regulatory factor. *Endocrinology* **140**:2976–2982.

Filardo E, Quinn J, Pang Y, Graeber C, Shaw S, Dong J, and Thomas P (2007) Activation of the novel estrogen receptor G protein-coupled receptor 30 (GPR30) at the plasma membrane. *Endocrinology* **148**:3236–3245.

Gonzalez de Valdivia E, Broselid S, Kahn R, Olde B, and Leeb-Lundberg LMF (2017) G protein-coupled estrogen receptor 1 (GPER1)/GPR30 increases ERK1/2 activity through PDZ motif-dependent and -independent mechanisms. *J Biol Chem* **292**:9932–9943.

Gonzalez de Valdivia E, Sandén C, Kahn R, Olde B, and Leeb-Lundberg LMF (2019) Human G protein-coupled receptor 30 is *N*-glycosylated and N-terminal domain asparagine 44 is required for receptor structure and activity. *Biosci Rep* **39**:BSR20182436.

Gonzalez-Garcia JR, Bradley J, Nomikos M, Paul L, Machaty Z, Lai FA, and Swann K (2014) The dynamics of MAPK inactivation at fertilization in mouse eggs. *J Cell Sci* **127**:2749–2760.

Güldener U, Heck S, Fielder T, Beinhauer J, and Hegemann JH (1996) A new efficient gene disruption cassette for repeated use in budding yeast. *Nucleic Acids Res* **24**:2519–2524.

Haas E, Bhattacharya I, Brailoiu E, Damjanović M, Brailoiu GC, Gao X, Mueller-Guerre L, Marjon NA, Gut A, Minotti R et al. (2009) Regulatory role of G protein-coupled estrogen receptor for vascular function and obesity. *Circ Res* **104**:288–291.

Harris BZ and Lim WA (2001) Mechanism and role of PDZ domains in signaling complex assembly. *J Cell Sci* **114**:3219–3231.

Hilger D, Masureel M, and Kobilka BK (2018) Structure and dynamics of GPCR signaling complexes. *Nat Struct Mol Biol* **25**:4–12.

Hoffman GA, Garrison TR, and Dohlman HG (2002) Analysis of RGS proteins in *Saccharomyces cerevisiae*. *Methods Enzymol* **344**:617–631.

Holm A, Grände PO, Ludueña RF, Olde B, Prasad V, Leeb-Lundberg LMF, and Nilsson BO (2012) The G protein-coupled oestrogen receptor 1 agonist G-1 disrupts endothelial cell microtubule structure in a receptor-independent manner. *Mol Cell Biochem* **366**:239–249.

Isensee J, Meoli L, Zazzu V, Nabzdyk C, Witt H, Soewarto D, Effertz K, Fuchs H, Gailus-Durner V, Busch D et al. (2009) Expression pattern of G protein-coupled receptor 30 in LacZ reporter mice. *Endocrinology* **150**:1722–1730.

Jala VR, Radde BN, Haribabu B, and Klinge CM (2012) Enhanced expression of G-protein coupled estrogen receptor (GPER/GPR30) in lung cancer. *BMC Cancer* **12**:624.

Jang EJ, Seok YM, Arterburn JB, Olatunji LA, and Kim IK (2013) GPER-1 agonist G1 induces vasorelaxation through activation of epidermal growth factor receptor-dependent signalling pathway. *J Pharm Pharmacol* **65**:1488–1499.

Kang L, Zhang X, Xie Y, Tu Y, Wang D, Liu Z, and Wang ZY (2010) Involvement of estrogen receptor variant ER-alpha36, not GPR30, in nongenomic estrogen signaling. *Mol Endocrinol* **24**:709–721.

Komatsu N, Aoki K, Yamada M, Yukinaga H, Fujita Y, Kamioka Y, and Matsuda M (2011) Development of an optimized backbone of FRET biosensors for kinases and GTPases. *Mol Biol Cell* **22**:4647–4656.

Kotarsky K, Antonsson L, Owman C, and Olde B (2003) Optimized reporter gene assays based on a synthetic multifunctional promoter and a secreted luciferase. *Anal Biochem* **316**:208–215.

Langer G, Bader B, Meoli L, Isensee J, Delbeck M, Noppinger PR, and Otto C (2010) A critical review of fundamental controversies in the field of GPR30 research. *Steroids* **75**:603–610.

Lenhart PM, Broselid S, Barrick CJ, Leeb-Lundberg LMF, and Caron KM (2013) G-protein-coupled receptor 30 interacts with receptor activity-modifying protein 3 and confers sex-dependent cardioprotection. *J Mol Endocrinol* **51**:191–202.

Levin ER (2009) G protein-coupled receptor 30: estrogen receptor or collaborator? *Endocrinology* **150**:1563–1565.

Lindsey SH, Carver KA, Prossnitz ER, and Chappell MC (2011) Vasodilation in response to the GPR30 agonist G-1 is not different from estradiol in the mRen2.Lewis female rat. *J Cardiovasc Pharmacol* **57**:598–603.

Lindsey SH, Liu L, and Chappell MC (2014) Vasodilation by GPER in mesenteric arteries involves both endothelial nitric oxide and smooth muscle cAMP signaling. *Steroids* **81**:99–102.

Liu R, Wong W, and IJzerman AP (2016) Human G protein-coupled receptor studies in *Saccharomyces cerevisiae*. *Biochem Pharmacol* **114**:103–115.

Maiti K, Paul JW, Read M, Chan EC, Riley SC, Nahar P, and Smith R (2011) G-1-activated membrane estrogen receptors mediate increased contractility of the human myometrium. *Endocrinology* **152**:2448–2455.

Manfredi JP, Klein C, Herrero JJ, Byrd DR, Trueheart J, Wiesler WT, Fowlkes DM, and Broach JR (1996) Yeast alpha mating factor structure-activity relationship derived from genetically selected peptide agonists and antagonists of Ste2p. *Mol Cell Biol* **16**:4700–4709.

Mårtensson UEA, Salehi SA, Windahl S, Gomez MF, Swärd K, Daszkiewicz-Nilsson J, Wendt A, Andersson N, Hellstrand P, Grände PO et al. (2009) Deletion of the G protein-coupled receptor 30 impairs glucose tolerance, reduces bone growth, increases blood pressure, and eliminates estradiol-stimulated insulin release in female mice. *Endocrinology* **150**:687–698.

Meng R, Qin Q, Xiong Y, Wang Y, Zheng J, Zhao Y, Tao T, Wang Q, Liu H, Wang S et al. (2016) NHERF1, a novel GPER associated protein, increases stability and activation of GPER in ER-positive breast cancer. *Oncotarget* **7**:54983–54997.

Meyer MR, Baretella O, Prossnitz ER, and Barton M (2010) Dilation of epicardial coronary arteries by the G protein-coupled estrogen receptor agonists G-1 and ICI 182,780. *Pharmacology* **86**:58–64.

Mumberg D, Müller R, and Funk M (1995) Yeast vectors for the controlled expression of heterologous proteins in different genetic backgrounds. *Gene* **156**:119–122.

Olde B and Leeb-Lundberg LMF (2009) GPR30/GPER1: searching for a role in estrogen physiology. *Trends Endocrinol Metab* **20**:409–416.

Oldham WM and Hamm HE (2008) Heterotrimeric G protein activation by G-protein-coupled receptors. *Nat Rev Mol Cell Biol* **9**:60–71.

Otto C, Rohde-Schulz B, Schwarz G, Fuchs I, Klewer M, Brittain D, Langer G, Bader B, Prelle K, Nubbemeyer R et al. (2008) G protein-coupled receptor 30 localizes to the endoplasmic reticulum and is not activated by estradiol. *Endocrinology* **149**:4846–4856.

Pedram A, Razandi M, and Levin ER (2006) Nature of functional estrogen receptors at the plasma membrane. *Mol Endocrinol* **20**:1996–2009.

Peixoto P, Aires RD, Lemos VS, Bissoli NS, and Santos RLD (2017) GPER agonist dilates mesenteric arteries via PI3K-Akt-eNOS and potassium channels in both sexes. *Life Sci* **183**:21–27.

Pelekanou V, Kampa M, Kiagiadaki F, Deli A, Theodoropoulos P, Agrogiannis G, Patsouris E, Tsapis A, Castanas E, and Notas G (2016) Estrogen anti-inflammatory activity on human monocytes is mediated through cross-talk between estrogen receptor ERα36 and GPR30/GPER1. *J Leukoc Biol* **99**:333–347.

Prossnitz ER and Arterburn JB (2015) International Union of Basic and Clinical Pharmacology. XCVII. G protein-coupled estrogen receptor and its pharmacologic modulators. *Pharmacol Rev* **67**:505–540.

Prossnitz ER and Barton M (2014) Estrogen biology: new insights into GPER function and clinical opportunities. *Mol Cell Endocrinol* **389**:71–83.

Revankar CM, Cimino DF, Sklar LA, Arterburn JB, and Prossnitz ER (2005) A transmembrane intracellular estrogen receptor mediates rapid cell signaling. *Science* **307**:1625–1630.

Rippe C, Zhu B, Krawczyk KK, Bavel EV, Albinsson S, Sjölund J, Bakker ENTP, and Swärd K (2017) Hypertension reduces soluble guanylyl cyclase expression in the mouse aorta via the Notch signaling pathway. *Sci Rep* **7**:1334.

Romano SN and Gorelick DA (2018) Crosstalk between nuclear and G protein-coupled estrogen receptors. *Gen Comp Endocrinol* **261**:190–197.

Rosenbaum DM, Rasmussen SG, and Kobilka BK (2009) The structure and function of G-protein-coupled receptors. *Nature* **459**:356–363.

Sandén C, Broselid S, Cornmark L, Andersson K, Daszkiewicz-Nilsson J, Mårtensson UE, Olde B, and Leeb-Lundberg LMF (2011) G protein-coupled estrogen receptor 1/G protein-coupled receptor 30 localizes in the plasma membrane and traffics intracellularly on cytokeratin intermediate filaments. *Mol Pharmacol* **79**:400–410.

Scaling AL, Prossnitz ER, and Hathaway HJ (2014) GPER mediates estrogen-induced signaling and proliferation in human breast epithelial cells and normal and malignant breast. *Horm Cancer* **5**:146–160.

Seifert R and Wenzel-Seifert K (2002) Constitutive activity of G-protein-coupled receptors: cause of disease and common property of wild-type receptors. *Naunyn Schmiedebergs Arch Pharmacol* **366**:381–416.

Sjöström M, Hartman L, Grabau D, Fornander T, Malmström P, Nordenskjöld B, Sgroi DC, Skoog L, Stål O, Leeb-Lundberg LMF, et al. (2014) Lack of G protein-coupled estrogen receptor (GPER) in the plasma membrane is associated with excellent long-term prognosis in breast cancer. Breast Cancer Res Treat **145**:61–71.

Sousa C, Ribeiro M, Rufino AT, Leitão AJ, and Mendes AF (2017) Assessment of cell line competence for studies of pharmacological GPR30 modulation. *J Recept Signal Transduct Res* **37**:181–188.

Southern C, Cook JM, Neetoo-Isseljee Z, Taylor DL, Kettleborough CA, Merritt A, Bassoni DL, Raab WJ, Quinn E, Wehrman TS et al. (2013) Screening β-arrestin recruitment for the identification of natural ligands for orphan G-protein-coupled receptors. *J Biomol Screen* **18**:599–609.

Thomas P, Pang Y, Filardo EJ, and Dong J (2005) Identity of an estrogen membrane receptor coupled to a G protein in human breast cancer cells. *Endocrinology* **146**:624–632.

Tran QK, VerMeer M, Burgard MA, Hassan AB, and Giles J (2015) Hetero-oligomeric complex between the G protein-coupled estrogen receptor 1 and the plasma membrane Ca2+-ATPase 4b. *J Biol Chem* **290**:13293–13307.

Tutzauer J, Sjöström M, Bendahl P-O, Rydén L, Fernö M, Leeb-Lundberg LMF, and Alkner S (2020) Plasma membrane expression of G protein-coupled estrogen receptor (GPER)/G protein-coupled receptor 30 (GPR30) is associated with worse outcome in metachronous contralateral breast cancer. PLoS ONE **15**:e0231786

Vivacqua A, Lappano R, De Marco P, Sisci D, Aquila S, De Amicis F, Fuqua SA, Andò S, and Maggiolini M (2009) G protein-coupled receptor 30 expression is up-regulated by EGF and TGF alpha in estrogen receptor alpha-positive cancer cells. *Mol Endocrinol* **23**:1815–1826.

Watanabe H, Takahashi E, Kobayashi M, Goto M, Krust A, Chambon P, and Iguchi T (2006) The estrogen-responsive adrenomedullin and receptor-modifying protein 3 gene identified by DNA microarray analysis are directly regulated by estrogen receptor. *J Mol Endocrinol* **36**:81–89.

Waters EM, Thompson LI, Patel P, Gonzales AD, Ye HZ, Filardo EJ, Clegg DJ, Gorecka J, Akama KT, McEwen BS et al. (2015) G-protein-coupled estrogen receptor 1 is anatomically positioned to modulate synaptic plasticity in the mouse hippocampus. *J Neurosci* **35**:2384–2397.

Weißenborn C, Ignatov T, Ochel HJ, Costa SD, Zenclussen AC, Ignatova Z, and Ignatov A (2014) GPER functions as a tumor suppressor in triple-negative breast cancer cells. *J Cancer Res Clin Oncol* **140**:713–723.

West Jr RE, Moss J, Vaughan M, Liu T, and Liu TY (1985) Pertussis toxin-catalyzed ADP-ribosylation of transducin. Cysteine 347 is the ADP-ribose acceptor site. *J Biol Chem* **260**:14428–14430.

Wojciak-Stothard B and Ridley AJ (2002) Rho GTPases and the regulation of endothelial permeability. *Vascul Pharmacol* **39**:187–199.

Yu X, Stallone JN, Heaps CL, and Han G (2018) The activation of G protein-coupled estrogen receptor induces relaxation via cAMP as well as potentiates contraction via EGFR transactivation in porcine coronary arteries. *PLoS One* **13**:e0191418.

Zhang J, Vinuela A, Neely MH, Hallett PJ, Grant SG, Miller GM, Isacson O, Caron MG, and Yao WD (2007) Inhibition of the dopamine D1 receptor signaling by PSD-95. *J Biol Chem* **282**:15778–15789.

Address correspondence to: L. M. Fredrik Leeb-Lundberg, Department of Experimental Medical Science, BMC D12, Sölvegatan 19, 22184 Lund, Sweden. E-mail: fredrik.leeb-lundberg@med.lu.se

SUPPLEMENTAL MATERIAL

Ligand-independent G protein-coupled Estrogen Receptor (GPER)/GPR30 Activity: Lack of receptor-dependent effects of G-1 and 17β-estradiol

Julia Tutzauer, Ernesto Gonzalez de Valdivia, Karl Swärd, Ioannis Alexandrakis Eilard, Stefan Broselid, Robin Kahn, Björn Olde[1], and L.M. Fredrik Leeb-Lundberg[1]

Department of Experimental Medical Science (J.T., E.G.deV., K.S., I.A.E., S.B., L.M.F.L.-L.) and Department of Clinical Sciences Lund, Division of Pediatrics and Wallenberg Centre of Molecular Medicine (R.K.) and Division of Cardiology (B.O.), Lund University, 22184 Lund, Sweden

[1]These authors contributed equally as last authors

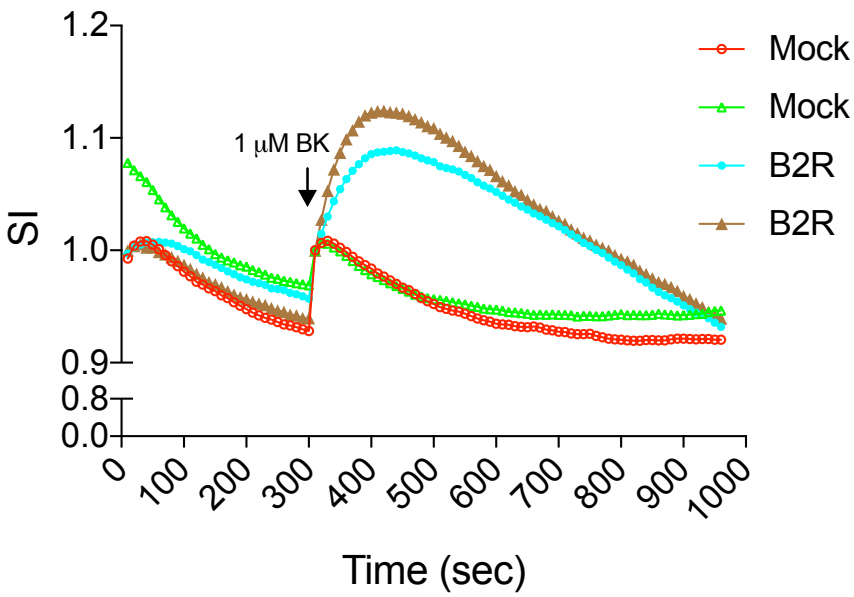

Supplemental Fig. 1. Bradykinin-stimulated Rac1 activity in HEK293 cells transiently transfected with the bradykinin B2 receptor and Rac1Cluc. HEK293 cells were transfected with bradykinin (BK) B2 receptor cDNA in pcDNA3.1 (1.25 ug) and pRac1Cluc (1.25 ug) in a 35-mm dish using Lipofectamine 3000. After 24 h, the medium was replaced with serum-free medium, and after 48 h, the medium was replaced with 1 ml of HEPES-buffered phenol red-free DMEM containing 2 mM Na-luciferin (Promega) and incubated for 2-3 h in the dark at room temperature. Luminescence was then measured as signal intensity (SI) with and without 1 μM BK for various times in a Glomax 20/20 luminometer (ThermoFisher Scientific, Waltham, MA).

Paper III

British Journal of Cancer www.nature.com/bjc

ARTICLE OPEN

Clinical Studies

Breast cancer hypoxia in relation to prognosis and benefit from radiotherapy after breast-conserving surgery in a large, randomised trial with long-term follow-up

Julia Tutzauer[1], Martin Sjöström[2], Erik Holmberg[3], Per Karlsson[3], Fredrika Killander[2,4], L. M. Fredrik Leeb-Lundberg[1], Per Malmström[2,4], Emma Niméus[2,5,6], Mårten Fernö[2] and Annika Jögi[7,8]✉

BACKGROUND: Breast-conserving surgery followed by radiotherapy is part of standard treatment for early-stage breast cancer. Hypoxia is common in cancer and may affect the benefit of radiotherapy. Cells adapt to hypoxic stress largely via the transcriptional activity of hypoxia-inducible factor (HIF)-1α. Here, we aim to determine whether tumour HIF-1α-positivity and hypoxic gene-expression signatures associated with the benefit of radiotherapy, and outcome.
METHODS: Tumour HIF-1α-status and expression of hypoxic gene signatures were retrospectively analysed in a clinical trial where 1178 women with primary T1-2N0M0 breast cancer were randomised to receive postoperative radiotherapy or not and followed 15 years for recurrence and 20 years for breast cancer death.
RESULTS: The benefit from radiotherapy was similar in patients with HIF-1α-positive and -negative primary tumours. Both ipsilateral and any breast cancer recurrence were more frequent in women with HIF-1α-positive primary tumours (hazard ratio, $HR_{0-5\ yrs}$1.9 [1.3–2.9], $p = 0.003$ and $HR_{0-5\ yrs} = 2.0$ [1.5–2.8], $p < 0.0001$). Tumour HIF-1α-positivity is also associated with increased breast cancer death ($HR_{0-10\ years}$ 1.9 [1.2–2.9], $p = 0.004$). Ten of the 11 investigated hypoxic gene signatures correlated positively to HIF-1α-positivity, and 5 to increased rate/risk of recurrence.
CONCLUSIONS: The benefit of postoperative radiotherapy persisted in patients with hypoxic primary tumours. Patients with hypoxic primary breast tumours had an increased risk of recurrence and breast cancer death.

British Journal of Cancer (2022) 126:1145–1156; https://doi.org/10.1038/s41416-021-01630-4

BACKGROUND

Breast cancer is the most common malignancy affecting women. Today, breast-conserving surgery followed by radiotherapy (RT) to the affected breast is part of the standard treatment for early-stage breast cancer. Systemic adjuvant therapy is selected based on patient and tumour characteristics and aims to target micrometastatic disease. About 80% of primary breast tumours express oestrogen receptor (ER) and are eligible for endocrine treatment [1].

RT after breast-conserving surgery considerably decreases the risk for ipsilateral breast tumour recurrence (IBTR), and to a minor extent also distant recurrence, and breast cancer death (BCD) [2, 3]. However, RT also confers side-effects [4–6], underscoring the importance of identifying potential patient-groups that do or do not benefit from RT. A number of factors that influence the therapeutic effect of RT have been identified in experimental systems, as well as in clinical materials [7]. The availability or shortage of oxygen was early identified as a major influencer of the outcome of RT [8, 9].

Oxygen levels are lower than those required to maintain normal metabolism and function in tissue, i.e., hypoxia, frequently occur in tumours, including breast cancer. Hypoxic adaptation at the cellular level is primarily controlled by the hypoxia-inducible transcription factors, HIF-1α and HIF-2α. Both are mainly regulated at the protein level and in response to hypoxia, the HIF alpha-subunits accumulate and become activated [10–13]. Tumour hypoxia contributes to tumour progression and therapy resistance, including RT-resistance [14], in direct as well as indirect ways [9]. Oxygen is required to make radiation-induced DNA-damage permanent, i.e. the oxygen enhancement effect. The hypoxic response, conveyed by HIF-induced gene expression, leads to altered metabolism, increased expression of growth factors, proliferation, and expression of cytokines [15]. In breast cancer, HIF-1α protein is a marker of poor prognosis and disease

[1]Department of Experimental Medical Science, Lund University, Lund, Sweden. [2]Division of Oncology, Department of Clinical Sciences Lund, Lund University, Lund, Sweden. [3]Department of Oncology, Institute of Clinical Sciences, Sahlgrenska Academy, University of Gothenburg, Gothenburg, Sweden. [4]Department of Haematology, Oncology and Radiation Physics, Skåne University Hospital, Lund, Sweden. [5]Division of Surgery, Department of Clinical Sciences Lund, Lund University, Lund, Sweden. [6]Department of Surgery Malmö, Skåne University Hospital, Malmö, Sweden. [7]Translational Cancer Research, Department of Laboratory Medicine, Lund University Cancer Center at Medicon Village, Lund University, Lund, Sweden. [8]Skåne University Hospital, Malmö, Sweden. ✉email: Annika.jogi@med.lu.se

Received: 4 July 2021 Revised: 17 October 2021 Accepted: 3 November 2021
Published online: 9 February 2022

Published on Behalf of CRUK

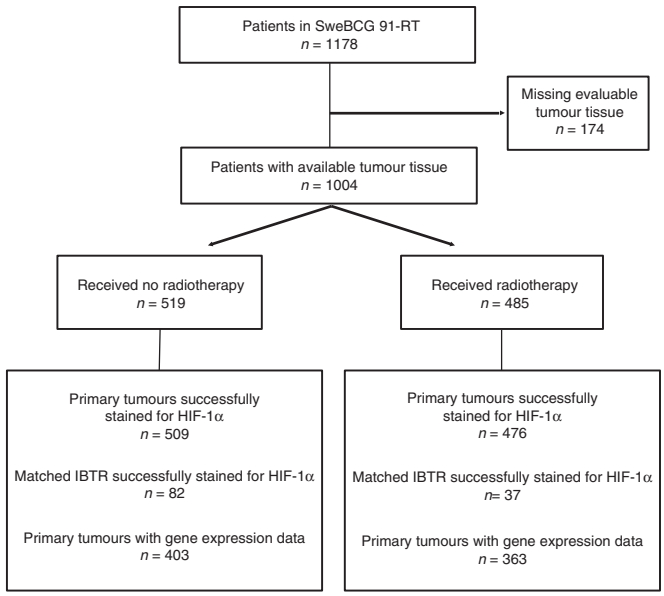

Fig. 1 Study design. Diagram of inclusion and exclusion to the study according to Remark criteria.

progression [16–18]. Upon reoxygenation the half-life of HIF-1α is in the minute range, creating a need for surrogate markers of hypoxia, such as more robust proteins induced by hypoxia, e.g. CAIX or hypoxic gene-expression signatures [19–21].

Here, we primarily aimed to test whether the hypoxia-marker HIF-1α affects the patient benefit of RT in a large population-based cohort with long follow-up of patients randomised to receive post-surgery RT or not after breast-conserving surgery. A second aim was to investigate whether tumour hypoxia and HIF-1α accumulation are associated with IBTR. Finally, we aimed to study whether hypoxic gene-expression signatures could complement or even replace HIF-1α protein detection as a prognostic or predictive marker.

METHODS

Patients and study design

Patients were from the Swedish breast cancer group trial, SweBCG91-RT, and study details are found in the previous publications [4, 5, 22–24]. Briefly, breast cancer patients with lymph node-negative (N0), stage I and IIA tumours were randomised to whole-breast RT (tangential opposed fields of 4–6 MV photons, 48–54 Gy in 24–27 fractions to the remaining breast parenchyma) or no RT after breast-conserving surgery from 1991 to 1997. Administration of systemic adjuvant treatment was according to regional guidelines of the time; 6% of patients had endocrine treatment only, 1% chemotherapy only, and 1% combined endocrine treatment and chemotherapy. The median follow-up times for event-free patients were 15.2 years (IBTR), 15.2 years (any breast cancer recurrence), 20.1 years (BCD) for the indicated endpoint. A flow diagram of the SweBCG91-RT trial is shown in Fig. 1.

TMA construction

Tumour tissue was collected from formalin-fixed, paraffin-embedded blocks of the primary tumours from 1004 of the original 1178 randomised patients. The material includes 140 surgically treated IBTRs from patients with a primary tumour available in the TMA for matching. TMA construction was in a semi-automated TMA arrayer (Pathology Devices, Westminster, MD) by extraction of two 1.0-mm cylinders from representative tissue from each tumour block.

Immunohistochemistry (IHC) and evaluation of markers

IHC staining, evaluation and assessment for ER, progesterone receptor (PgR), human epidermal growth factor receptor 2 (HER2) and Ki-67 were previously performed [24]. Tumours with 1% or more positive nuclei were considered ER- and PgR-positive, respectively. For dividing tumours between luminal A and B subtypes, a 20% cut-off for PgR was used. HER2 was scored with IHC as 0, 1+, 2+ or 3+ and with silver in situ hybridisation and considered positive if 3+ and/or amplified. Ki-67 scoring was according to guidelines [25], the cut-off was 10% positive cells resulting in 27% of tumours being Ki-67 high [24]. Histologic grade was previously evaluated as described by Elston and Ellis [26]. HIF-1α IHC was performed as previously described [17]. Briefly, IHC was performed on 4 µm sections of formalin-fixed paraffin-embedded sections (Autostainer Plus, Dako) according to the manufacturer's protocol. A monoclonal antibody recognising HIF-1α (BD610959, Becton Dickinson) diluted 1:50 was employed. Two experienced evaluators blinded to patient treatment, outcome, and tumour characteristics (Kristina Lövgren and Annika Jögi) independently assessed IHC staining for HIF-1α. Each TMA-core was semi-quantitatively scored for IHC-staining intensity, 0 (negative), 1 (weak), 2 (moderate) and 3 (intense) and quantitatively scored for proportion positive cancer cells. Proportion score 0 represented less than 1% positive cells, 1: 1–10%, 2: 11–50%, and 3: 51–100%. Based on IHC intensity and proportion of positive cells each tumour sample was grouped as negative (less than 1% positive cells or 1–9% cells with intensity ≤1, Supplemental Fig. 1 A), low (1–9% of cells with intensity ≥2 or ≥10% of cells with intensity 1, Supplemental Fig. 1B) or high (≥10% of cells with intensity ≥2, Supplemental Fig. 1C). In case of discrepant staining between the two cores from the same tumour, the highest score was used. Cases (13%) with differing results between the viewers were re-evaluated in consensus. Only 60 tumours (6%) fell into the low-category whereas 227 (23%) fell into the high-category (Table 1). Due to this skew distribution, the samples of the two positive categories were merged into one HIF-1α positive group, as previously described [17]. Although not postulated in the evaluation criteria, all positive cancer cells had nuclear HIF-1α IHC-signal and very few,

Table 1. Patient and tumour characteristics in 985 T1-2N0M0 breast cancer patients randomised to postoperative RT or no RT after breast-conserving surgery, stained for HIF-1α.

	Total	HIF-1α immunoreactivity			*p*
		Negative (%)	Low (%)	High (%)	
	985	698 (70.9)	60 (6.1)	227 (23.0)	
Age (median = 60)					
≤49	192	137 (71.4)	15 (7.8)	40 (20.8)	0.80[a]
50–59	300	210 (70.0)	18 (6.0)	72 (24.0)	
60–69	375	267 (71.2)	22 (5.9)	86 (22.9)	
≥70	118	84 (71.2)	5 (4.2)	29 (24.6)	
Premenopausal	196	137 (69.9)	17 (8.7)	42 (21.4)	0.26[b]
Postmenopausal	765	541 (70.7)	43 (5.6)	181 (23.7)	
Missing	24	20	0	4	
Tumour size (median = 12 mm)					
Tumour >20 mm	841	604 (71.8)	49 (5.8)	188 (22.4)	0.37[b]
Tumour ≤20 mm	138	91 (65.9)	10 (7.3)	37 (26.8)	
Missing	6	3	1	2	
ER-negative	100	40 (40.0)	8 (8.0)	52 (52.0)	<0.0001[b]
ER-positive	858	642 (74.8)	49 (5.7)	167 (19.5)	
Missing	27	16	3	8	
PgR-negative	253	154 (60.9)	16 (6.3)	83 (32.8)	<0.0001[b]
PgR-positive	705	528 (74.9)	41 (5.8)	136 (19.3)	
Missing	27	16	3	8	
HER2-negative	889	645 (72.6)	52 (5.8)	192 (21.6)	0.001[c]
HER2-positive	64	33 (51.6)	5 (7.8)	26 (40.6)	
Missing	32	20	3	9	
Ki-67 low	714	550 (77.0)	46 (6.5)	118 (16.5)	<0.0001[2]
Ki-67 high	244	132 (54.1)	11 (4.5)	101 (41.4)	
Missing	27	16	3	8	
Histological grade 1	146	118 (80.8)	9 (6.2)	19 (13.0)	<0.0001[a]
Histological grade 2	567	420 (74.1)	34 (6.0)	113 (19.9)	
Histological grade 3	235	136 (57.9)	15 (6.4)	84 (35.7)	
Missing	37	24	2	11	
St Gallen subgroup					<0.0001[b]
Luminal A	552	431 (78.1)	34 (6.1)	87 (15.8)	
Luminal B (HER2−)	257	181 (70.4)	13 (5.1)	63 (24.5)	
HER2+	64	33 (51.6)	5 (7.8)	26 (40.6)	
Triple negative	80	33 (41.3)	5 (6.3)	42 (52.5)	
Missing	32	20	3	9	
No RT	509	349 (68.6)	34 (6.7)	126 (24.7)	0.26[b]
RT	476	349 (73.3)	26 (5.5)	101 (21.2)	
Other treatments					0.11[b]
Chemotherapy	9	7 (77.8)	0 (0)	2 (22.2)	
Endocrine	63	43 (68.3)	6 (9.5)	14 (22.2)	
Chemo + endocrine	8	2 (25.0)	1 (12.5)	5 (62.5)	
No other treatment	905	646 (71.4)	53 (5.8)	206 (22.8)	

[a]Calculated using linear regression.
[b]Calculated using chi-squared test.
[c]Calculated using Fisher's exact test.

in addition, had cytoplasmic staining, as previously demonstrated [17]. We recently published positive and negative controls for HIF-1α immunostaining on cell lines and a similar breast cancer TMA-material of patients with contralateral tumours [17].

Tumour subtyping

The tumours were, as previously reported [24], subtyped according to the St Gallen International Breast Cancer Conference (2013) Expert Panel [27] as luminal A-like (ER-positive, PgR-high, HER2-negative, and Ki-67 low),

luminal B-like (ER-positive, PgR-low and/or Ki-67 high, and HER2-negative), HER2-positive (HER2-positive, any ER or PgR status, any Ki-67 expression), and triple negative (ER-negative, PgR-negative, HER2-negative, any Ki-67). The HER2-positive group thus included both luminal and non-luminal tumours due to group size.

Gene-expression analysis

Gene-expression analysis of this trial material was previously described [28]. In brief, RNA was extracted from the 922 available paraffin-fixed patient tumour samples. Patient and tumour characteristics were similar in the excluded and analysed tumours. RNA was extracted and hybridised (GeneChip Human Exon 1.0 ST microarray, Thermo Fisher) in a Clinical Laboratory Improvement Amendments certified laboratory (Decipher Biosciences). Samples from 766 primary tumours passed the quality control of RNA, cDNA, and microarray analysis (Gene-expression Omnibus GSE119295). Single Channel Array Normalisation was used for gene-expression data normalisation [29].

Scoring of hypoxia-related expression signatures from the literature

Eleven previously published hypoxia-related gene-expression signatures, here referred to as the name of the first author of the publication, were identified from the literature. The signatures Buffa*, Buffa reduced* [30], Denko [31], Elvidge [32], Hu [33], Mense [34], Sorensen [35], and Winter* [36] were selected from a review by Harris et al [20]. Signatures marked by * are related and derived from "Winter", where in brief, genes co-expressed with classical hypoxia-driven genes were chosen and tested in clinical tumour samples, including breast cancer [36]. The signatures from Denko, Elvidge, Mense, and Sorensen were extracted from in vitro hypoxia (1% oxygen) treated human cells. The Hu signature comprises 13 genes

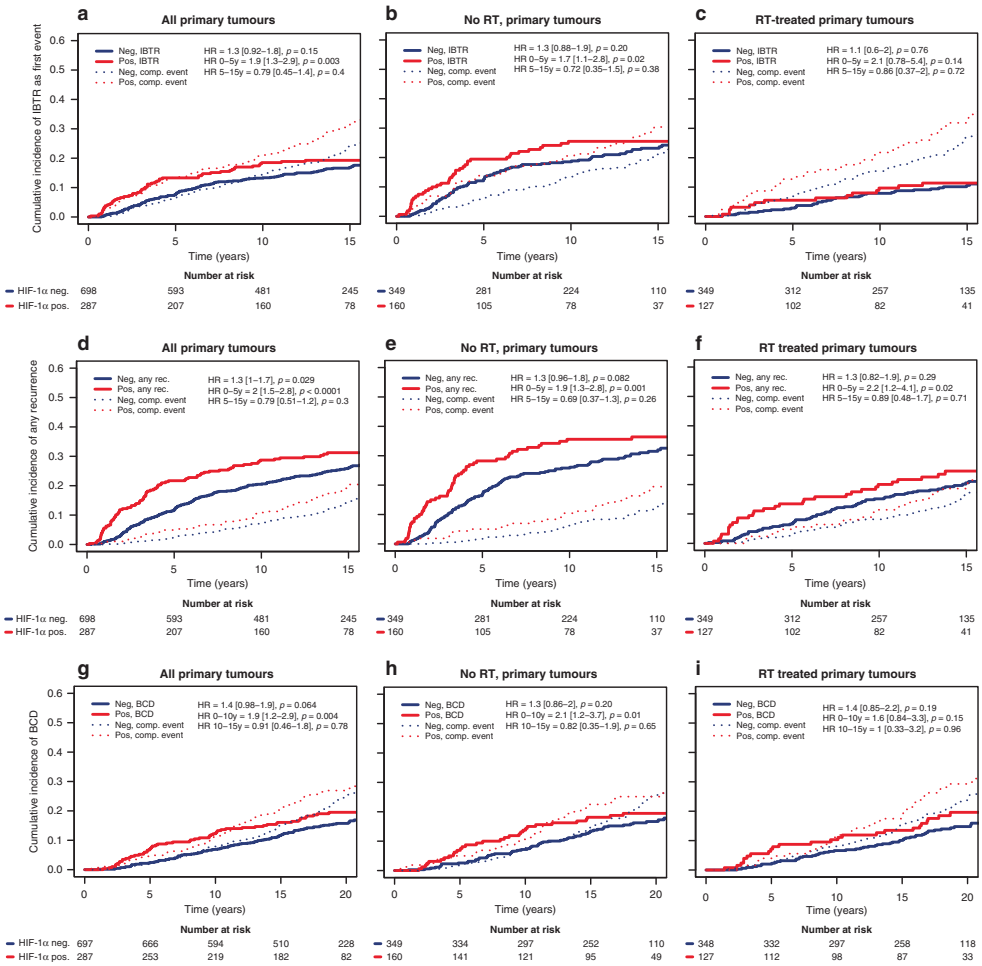

Fig. 2 Higher risk of recurrence and BCD in patients with a HIF-1α positive primary tumour. Cumulative incidence of IBTR after surgery of the primary tumour (**a**–**c**), any recurrences (**d**–**f**), and BCD (**g**–**i**) in 985 T1-2N0M0 breast cancer patients randomised to RT (**c**, **f**, **g**) or no RT (**b**, **e**, **h**) after breast-conserving surgery in patients with HIF-1α negative (blue line) and HIF-1α positive (red line) primary tumour.

referred to as a VEGF-profile, 8 of the genes having a hypoxia-responsive element that can bind HIF in their promoters. The Farmer signature was based on GSEA hypoxia genes in breast cancer cells with apocrine phenotype, i.e. not based on actual hypoxic exposure [37]. The signature referred to as "Yang" was the most recently published, and based on in vitro hypoxic treatment of prostate cancer cell lines and validated in several publicly available prostate and bladder cancer materials [38]. The Hallmark of Cancer hypoxia gene signature was included since it has been widely used in literature. It is based on several sources including the Winter, Elvidge, Mense gene-expression signatures mentioned above, and includes genes regulated by the von Hippel–Lindau factor and several metabolic pathways such as the glycolysis.

Individual hypoxia scores for primary tumours in SweBCG91-RT were calculated using the singscore package in R [39], or as described by the authors. Scores were considered as continuous variables or combined into a binary variable of high or low, with the 4th quartile being defined as high, and quartiles 1–3 as low, thus giving a similar proportion of hypoxic tumours as detected by HIF-1α IHC (29%). Interaction tests were performed with scores as a continuous variable to avoid introduction of bias from cut-off. If any gene ID was not matched in our expression set, synonym gene names were retrieved using the R package HGNChelper [40]. If one signature gene ID corresponded to multiple synonym IDs, a search was conducted on GeneCards database of human genes [41] to select the matching synonym. Genes were excluded if an ID match was not identified.

Statistical methods

All statistical analyses were performed with R (3.5.2). The primary endpoint was IBTR in any quadrant of the ipsilateral breast, though 90% were located in the same quadrant as the primary tumour, as first event within 5 years [22]. Other recurrences and death by any cause were competing events. Secondary endpoints were any breast cancer recurrence within 5 years, (including IBTR, regional and distant recurrence, but not contralateral breast cancer), with death by any cause without recurrence as competing event, and BCD, with death by other cause as competing event. For the descriptive, exploratory analysis of the relationship between HIF-1α in IBTR and BCD, the start point was the date of surgery for the IBTR, and the endpoint was BCD. Cumulative incidence with competing events was displayed graphically using the R package cmprisk [42] and presented with hazard ratio (HR) and 95% confidence interval calculated using cause-specific Cox proportional hazards model. The interactions between the benefit of RT and markers of hypoxia were evaluated using cause-specific Cox proportional hazards model with an interaction term. The proportional hazards assumption was checked graphically and tested with Schoenfeld residuals [43]. As seen before in this cohort [24], HRs over the full follow-up were generally non-proportional, thus we present estimations of HR in intervals (0–5 years, 5–15 years, and >15 years for IBTR and any recurrence as first event, or 0–10 years, 10–15 years, and >15 years for BCD as first event) along with the HR for the full follow-up. All HR estimations should be interpreted as an average over the studied time interval. Associations between HIF-1α and other patient and tumour characteristics were assessed using the chi-squared test or Fisher's exact test or tested for trend using linear regression. Statistical significance was defined as $p < 0.05$, but due to the multiple hypothesis testing performed in this study, the interpretation of p as level of evidence for or against the null hypothesis should be careful.

RESULTS

HIF-1α in primary breast tumours

Of the 1004 tumours available in the TMA, 985 were successfully stained and evaluated for HIF-1α (Fig. 1), where 698 (71%) were HIF-1α negative. Primary tumours with IHC-staining positive for HIF-1α were similarly distributed in the RT and non-RT groups (27% and 31%, respectively). Patient and tumour characteristics are described in Table 1. Tumour HIF-1α status correlated to histological grade, with a higher frequency of HIF-1α positivity among high-grade tumours ($p < 0.0001$). Furthermore, HIF-1α positivity was associated with cell proliferation in that it correlated to high Ki-67 ($p < 0.0001$). A considerably higher proportion of ER-negative tumours, compared to ER-positive tumours, were HIF-1α positive (60% vs 25%, $p < 0.0001$). Luminal A-like tumours were the largest subgroup with 552 tumours and 22% of these were HIF-1α positive, while luminal B tumours had a 30% frequency of HIF-1α positivity (76 of 257, Table 1).

Higher risk of recurrence and BCD in patients with HIF-1α positive primary tumours

Patients with a HIF-1α positive primary tumour had an increased incidence of IBTR as a first event within 5 years compared to patients with a HIF-1α negative primary tumour both in the total patient population ($HR_{0–5\ yrs} = 1.9$ [1.3–2.9], $p = 0.003$, Fig. 2a and Table 2) and among patients that did not receive RT ($HR_{0-5\ yrs} = 1.7$ [1.1–2.8], $p = 0.02$, Fig. 2b and Table 2). The higher occurrence of IBTR in patients that had HIF-1α positive primary tumours was apparent in both ER-positive and -negative disease (Supplemental Fig. 2). Patients that received RT suffered less IBTR, with no difference between HIF-1α positive and negative groups (Fig. 2c). In multivariable analysis adjusted for patient age, tumour size, tumour subtype (St Gallen), and systemic adjuvant therapy, the increased risk for IBTR in the HIF-1α positive group remained an independent risk factor in the total patient population ($HR_{adjusted} = 1.8$ [1.1–2.8], $p = 0.01$, Table 2).

In analyses of any recurrences in the whole patient material as well as in the non-irradiated group, HIF-1α primary tumour

Table 2. Uni- and multivariable analysis of the hazard of HIF-1α (positive vs negative) in relationship to IBTR during the first 5 years after the primary tumour, any recurrences during the first 5 years after the primary tumour, and BCD during the first 10 years after the primary tumour in breast cancer patients randomised to receive RT or no RT after breast-conserving surgery.

All patients	Univariable analysis			Multivariable analysis		
	HR (95% CI)	p	n (event)	HR (95% CI)	p	n (event)
IBTR (0–5 years)						
All patients	1.9 (1.3–2.9)	0.003	985 (92)	1.8 (1.1–2.8)	0.01	948 (85)
No RT	1.7 (1.1–2.8)	0.02	509 (75)	1.6 (0.97–2.7)	0.065	492 (68)
RT	2.1 (0.78–5.4)	0.14	476 (17)	2.1 (0.78–5.8)	0.14	456 (17)
Any recurrence (0–5 years)						
All patients	2.0 (1.5–2.8)	<0.0001	985 (144)	1.7 (1.2–2.4)	0.003	948 (137)
No RT	1.9 (1.3–2.8)	0.001	509 (104)	1.6 (1–2.5)	0.03	492 (97)
RT	2.2 (1.2–4.1)	0.02	476 (40)	1.7 (0.89–3.2)	0.11	456 (40)
BCD (0–10 years)						
All patients	1.9 (1.2–2.9)	0.004	985 (83)	1.5 (0.93–2.3)	0.097	948 (82)
No RT	2.1 (1.2–3.7)	0.01	509 (47)	1.5 (0.82–2.9)	0.18	492 (46)
RT	1.6 (0.84–3.3)	0.15	476 (36)	1.3 (0.64–2.6)	0.48	456 (36)

positivity was associated with an increase in early recurrences ($HR_{0-5\ years}$ 2, [1.5–2.8], $p = 0.0001$ and $HR_{0-5\ years}$ 1.9, [1.3–2.8], $p = 0.001$, Fig. 2d, e and Table 2), with a similar pattern in patients with ER-positive and -negative tumours (Supplemental Fig. 2). Postoperative RT led to an overall decrease in any recurrence, however, there were still a higher number of recurrences in patients with a HIF-1α positive primary tumour (Fig. 2f and Table 2).

There was a higher occurrence of BCD within 10 years of surgery in patients with HIF-1α positive primary tumour in the entire study population and in patients that did not receive RT ($HR_{0-10\ years}$ 1.9 [1.2–2.9], $p = 0.004$, and $HR_{0-10\ years}$ 2.1 [1.2–3.7], $p = 0.01$ Fig. 2g, h and Table 2), while this difference diminished after RT (Fig. 2l). In patients with ER-negative tumours, with a high frequency of HIF-1α positive primary tumours (60%), BCD within 10 years was higher compared to ER-positive tumours irrespective of primary tumour HIF-1α status (Supplemental Fig. 2e, f).

Preserved benefit of RT in patients with HIF-1α positive primary tumours

Taking all primary tumours into account, patients receiving RT had a distinct reduction of IBTR within 5 years ($HR_{0-5years}$ 0.23, [0.13–0.39], $p < 0.0001$; Fig. 3a and Table 3), and the full follow-up ($HR_{full\ FU}$ 0.42, [0.3–0.58], $p < 0.0001$; Fig. 3a). Dividing the patients into those with HIF-1α negative and positive primary tumours, there was a similar reduction in IBTR with RT in the two groups (test for

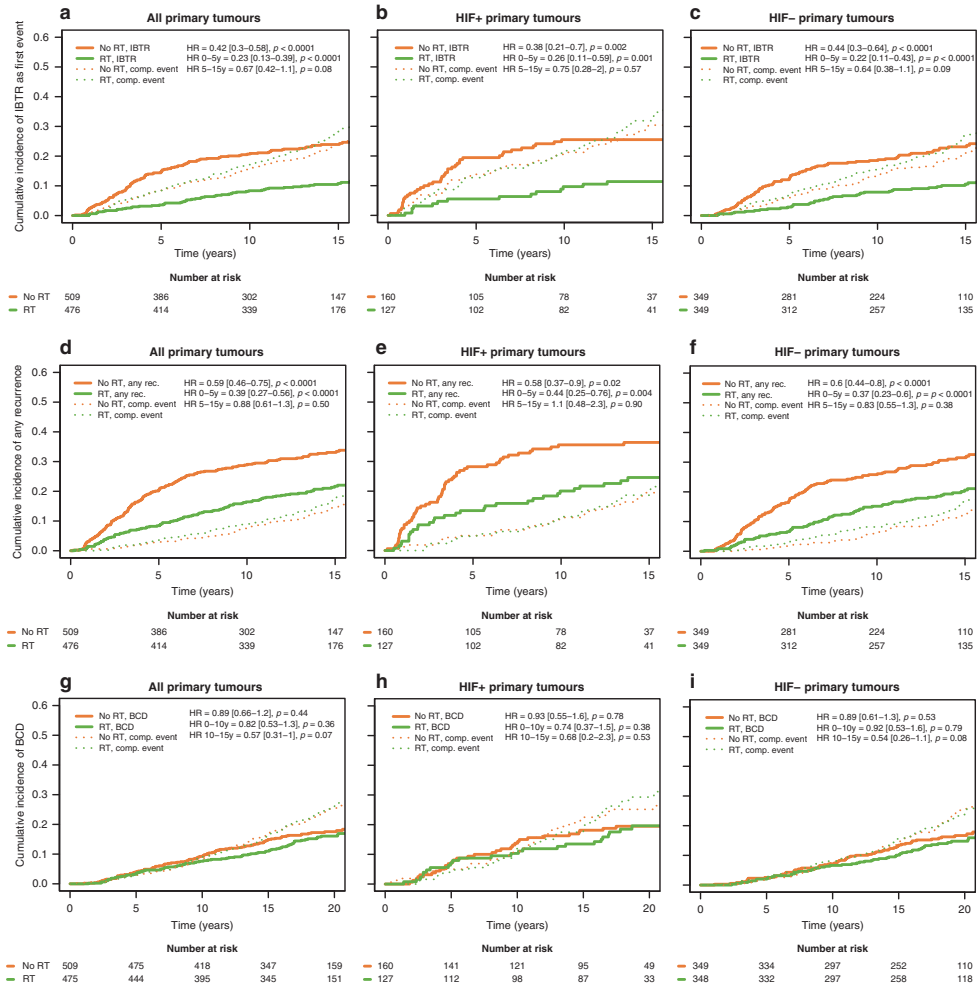

Fig. 3 Reduction in recurrence with RT was independent of primary tumour HIF-α status. Cumulative incidence of IBTR after surgery of the primary tumour (**a**–**c**), any recurrences (**d**–**f**) as first event, and BCD (**g**–**i**) in 985 T1-2N0M0 breast cancer patients randomised to RT (green line) or no RT (orange line) after breast-conserving surgery for all primary tumours (**a**, **d**, **g**), HIF-1α positive primary tumours (**b**, **e**, **h**), and HIF-1α negative primary tumours (**c**, **f**, **i**).

Table 3. Uni- and multivariable analysis of the benefit of RT in relationship to IBTR during the first 5 years after the primary tumour, any recurrences during the first 5 years after the primary tumour, and BCD during the first 10 years after the primary tumour in breast cancer patients randomised to receive RT or no RT after breast-conserving surgery.

	Univariable analysis			Multivariable analysis		
	HR (95% CI)	***p***	***n* (event)**	**HR (95% CI)**	***p***	***n* (event)**
IBTR (0–5 years)						
All patients	0.23 (0.13–0.39)	<0.0001	985 (92)	0.25 (0.14–0.42)	<0.0001	948 (85)
HIF-1α+	0.26 (0.12–0.59)	0.001	287 (38)	0.30 (0.12–0.69)	0.005	272 (35)
HIF-1α−	0.21 (0.11–0.43)	<0.0001	698 (54)	0.22 (0.11–0.46)	<0.0001	676 (50)
Any recurrence (0–5 years)						
All patients	0.39 (0.27–0.56)	<0.0001	985 (144)	0.42 (0.29–0.61)	<0.0001	948 (137)
HIF-1α+	0.44 (0.25–0.76)	0.003	287 (62)	0.48 (0.27–0.86)	0.01	272 (59)
HIF-1α−	0.37 (0.23–0.6)	<0.0001	698 (82)	0.37 (0.23–0.62)	<0.0001	676 (78)
BCD (0–10 years)						
All patients	0.82 (0.53–1.3)	0.36	985 (83)	0.87 (0.56–1.4)	0.54	948 (82)
HIF-1α+	0.74 (0.37–1.5)	0.38	287 (35)	0.84 (0.42–1.7)	0.62	272 (35)
HIF-1α−	0.92 (0.53–1.6)	0.79	698 (48)	0.97 (0.54–1.7)	0.91	676 (47)

interaction$_{0–5\ years}$ $p = 0.90$, test for interaction$_{full\ FU}$ $p = 0.66$, Fig. 3b, c and Table 3). The incidence for any recurrences within 5 years, and full follow-up, was also reduced in patients that had received RT (HR$_{0–5years}$ 0.39, [0.27–0.56], $p < 0.0001$, and HR$_{full\ FU}$ 0.59, [0.46–0.75], $p < 0.0001$; Fig. 3d and Table 3), and this effect of RT on recurrence was independent of HIF-1α status (test for interaction$_{0–5\ years}$ $p = 0.70$, test for interaction$_{full\ FU}$ $p = 0.79$, Fig. 3e, f and Table 3). In the present study, there was no statistically significant effect of RT on the incidence of BCD (HR$_{0–10\ years}$ 0.82 [0.53–1.3], $p = 0.36$, Table 3), and this was unaffected by HIF-1α status (test for interaction$_{0–10\ years}$ $p = 0.54$, test for interaction$_{full\ FU}$ $p = 0.80$, Fig. 3g–i, Table 3).

HIF-1α in IBTR and relation to outcome

For a fraction of the cohort, IHC staining of HIF-1α in matched primary and IBTR tumour material was available ($n = 119$). HIF-1α positive IBTR was more prevalent among patients that had a HIF-1α positive, compared to negative, primary tumour (61% vs 27%, $p < 0.001$: Fig. 4a). In line with this, when considering HIF-1α IHC on three levels (negative, low and high), the IBTRs most often had the same HIF-1α staining intensity as their corresponding primary tumour (65%, $n = 75$), while 21% ($n = 24$) of the IBTRs had increased intensity, and 14% ($n = 16$) had decreased HIF-1α intensity. Addressing the prognostic relevance of HIF-1α expression in IBTR, we found that HIF-1α positivity in IBTR was associated with an increased risk of BCD (HR$_{fullFU}$2.6 [1.3–5.0], $p = 0.007$; Fig. 4b).

Hypoxic gene-expression signatures and relation to outcome and benefit of RT treatment

There was a concordance between HIF-1α IHC signal and *HIF-1α* mRNA-expression levels (rho = 0.40, $p < 0.0001$, Fig. 4c). However, there was no association between high *HIF-1α* mRNA expression (highest quartile) and breast cancer recurrence or survival (data not shown). In general, the hypoxic signature scores exhibited a high positive correlation with HIF-1α positive IHC status, with the Mense hypoxia score being the only exception (Fig. 5a). The strongest correlations to HIF-1α positive IHC were observed for "Buffa" (rho = 0.26, $p < 0.0001$), "Farmer" (rho = 0.27, $p < 0.0001$), and "Hu" (rho = 0.26, $p < 0.0001$, Fig. 5a). The calculated hypoxia scores of most gene signatures correlated strongly (Fig. 5b). The Mense hypoxia score did not correlate with the majority of other hypoxia scores, whereas the Yang signature had a clear negative correlation to several other hypoxia scores. Although most hypoxia scores correlated strongly, the gene overlaps were modest with a relatively low number of shared genes (Fig. 5c). Nine genes were present in ≥5 signatures: *ADM*, *NDRG1*, *SLC2A1*, *VEGFA*, *ALDOA*, *IGFBP3*, *LDHA*, *P4HA1* and *TPI1*.

To address the hypothesis that benefit of RT is affected by a hypoxic tumour microenvironment, we evaluated the benefit of RT in relation to gene expression of the hypoxic gene-expression signatures. The cohort was stratified based on the scores of each hypoxia signature and tested for statistical interaction between benefit of RT and hypoxia scores with respect to outcome (Fig. 5d). Patients had benefit from RT in prevention of early IBTR, regardless of hypoxia scores (Fig. 5d).

Several signature scores associated with an increased incidence of IBTR as a primary event, with the Buffa signatures ("Buffa" HR$_{5yrs}$ 1.5 [1.2–1.9], $p < 0.001$), and "Buffa reduced" (HR$_{5yrs}$ 1.4 [1.1–1.8], $p = 0.002$) and Hu signature (HR$_{5yrs}$ 1.4 [1.1–1.7], $p = 0.005$) being most prognostic for IBTR (Fig. 6a, b and Supplemental Fig. 3). Additionally, some signatures were associated with any recurrence, with the "Buffa reduced" (HR$_{0–5yrs}$ 1.5 [1.3–1.8], $p < 0.001$), "Hu" (HR$_{0–5yrs}$ 1.5 [1.2–1.7], $p < 0.001$), and "Winter" (HR$_{0–5yrs}$ 1.4 [1.2–1.7], $p < 0.001$) being most pronounced (Fig. 6b and Supplemental Fig. 4). Lastly, some signature scores were associated to an increased incidence of BCD (Fig. 6b and Supplemental Fig. 5), where the "Buffa reduced" (HR$_{0–10yrs}$ 1.6 [1.3–2.1], $p < 0.001$), "Yang" (HR$_{0–10yrs}$ 1.4 [1.1–1.7], $p = 0.004$) and "Hu" (HR$_{0–10yrs}$ 1.5 [1.2–1.9], $p < 0.001$) were most prominent.

DISCUSSION

In this study, we address the role of tumour hypoxia, detected by HIF-1α IHC or hypoxic gene-expression signatures, in relation to outcome and benefit of RT in a large, randomised trial of postoperative RT in early breast cancer.

In contrast to our initial hypothesis, we show that breast cancer patients benefit from postoperative RT regarding IBTR, and any recurrence, also when the primary tumour was HIF-1α IHC positive or had high expression of hypoxic gene signatures. We found no effect of postoperative RT on BCD, irrespective of primary tumour HIF-1α status. However, a benefit of postoperative RT in the prevention of BCD has been demonstrated in meta-analyses [3]. Thus, RT directed to the remaining breast tissue was similarly

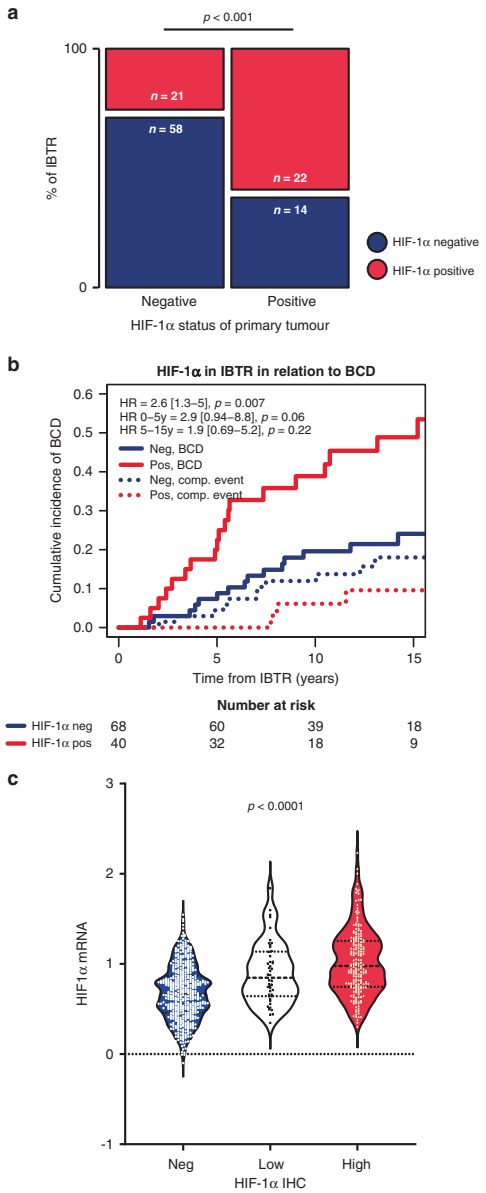

Fig. 4 HIF-1α and IBTR. Distribution of HIF-1α positive (red boxes) and negative (blue boxes) IBTRs in relation to primary tumour status, statistically tested using the chi-squared test (**a**). Cumulative incidence of BCD in relation to HIF-1α status of the resected IBTR, with the date of surgery for the IBTR as starting point (**b**), patients with HIF-1α positive IBTR (red line) compared to those with HIF-1α negative IBTR (blue line). Time from IBTR resection. Concordance between HIF-1α IHC and *HIF-1α* mRNA levels in tumour samples, tested using Spearman's rank test (**c**), showing HIF-1α IHC signal in three levels; negative (blue), low (white), and high (red).

effective on disseminated cancer cells whether these were schooled in a hypoxic or non-hypoxic primary tumour.

For breast cancer, RT is most often given after tumour resection. In cancers that are primarily treated with radiation (e.g. some head and neck cancers and bladder cancers) the hypoxic microenvironment remains and may even be enhanced due to radiation-induced tissue damage. The cells residing in the hypoxic microenvironment may then continue communicating with the microenvironment through the release of growth factors and other signalling molecules in a hypoxia-adapted state, potentially affecting the outcome. This could explain why hypoxia has been associated with RT resistance [44–46], but not in this postoperative study.

Tumour HIF-1α positivity correlated to unfavourable tumour characteristics. Analyses of the non-irradiated patient group, as well as the total study population, showed that patients with HIF-1α positive primary tumours were more prone to develop IBTR during the first five years after surgery. Multivariable analysis showed that primary tumour HIF-1α positivity was an independent risk factor for IBTR in the total patient population. In addition, primary tumour HIF-1α positivity correlated to an increase in any recurrence in the whole study population and remained an independent risk factor after adjustment for patient age, tumour subtype, size, and systemic treatment. Primary tumour HIF-1α positivity was also associated with an increase in BCD, but not when adjusted for patient age, tumour subtype, size and systemic treatment. The association between primary tumour HIF-1α positivity and IBTR is, to our knowledge, a novel finding, and in line with previous reports that hypoxia and HIF-1α are associated with distant metastasis and poor prognosis in breast cancer [16–18]. Breast tumour hypoxia and HIF-1α-regulated gene expression contribute to aggressive tumour behaviour and seeding of cancer cells with a metastatic capacity [47, 48].

We found that most tumour samples from surgically removed IBTRs had the same HIF-1α status as their corresponding primary tumour, indicating that hypoxia and HIF-1α positivity is an inherent tumour trait. Additionally, of 11 hypoxia-related gene-expression signatures from the literature, 10 correlated with HIF-1α protein level, and 5 with an increased risk of IBTR within 5 years after resection of the primary tumour. The presence of a HIF-1α-positive IBTR correlated to an increased risk for BCD compared to having a HIF-1α negative IBTR, analysed in relation to time after IBTR-surgery (Fig. 4b).

To specifically address whether ER affects the role of tumour hypoxia, we investigated the hazard of the investigated hypoxia markers in ER-positive and -negative groups separately. We found that primary tumour HIF-1α positivity was a risk factor for IBTR and any recurrence within 5 years after surgery in the ER-positive subgroup as well as in the entire study population. The study included too few patients with ER-negative primary tumour to allow for meaningful multivariable analyses in this subgroup. In this large breast cancer material, we establish that HIF-1α positivity is associated with the tumour subtype. Luminal A tumours have the lowest frequency of HIF-1α positivity, and the frequency of HIF-1α-positivity is then increasing step by step in luminal B, HER2-positive and triple-negative tumours. HIF-1α positivity, thus, has a negative correlation to the distribution of ER expression in the breast cancer subtypes. The ER-negative breast tumours generally have a worse prognosis and a high frequency of HIF-1α-positivity. However, as stated above, within the ER-positive group HIF-1α-positivity remains associated with a

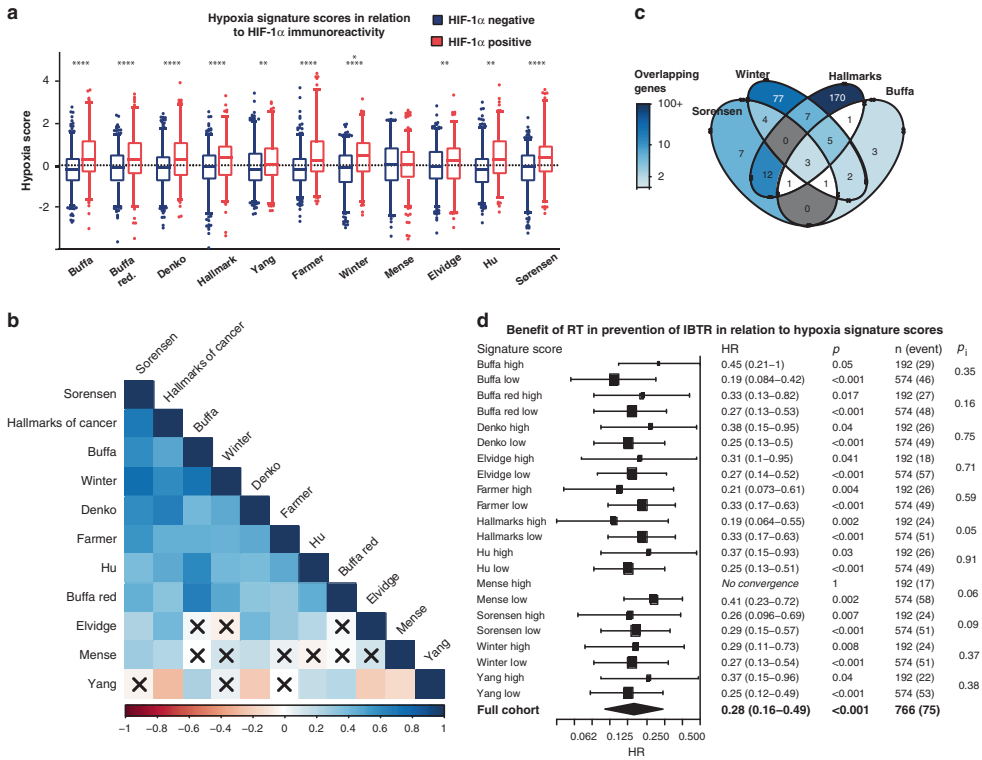

Fig. 5 Hypoxic gene-expression signatures. Hypoxia signature scores in relation to HIF-1α IHC status, negative (blue) and positive (red), presented as boxes of the 25th–75th percentiles with whiskers at percentile 2.5–97.5 $*p < 0.05$, $**p < 0.01$, $***p < 0.001$, $****p < 0.0001$ (**a**). Correlations were tested using Spearman's correlation. Correlation plot of hypoxia signature scores, ordered according to the first principal component order (**b**). Positive correlations in increasing intensity of blue and negative in red. Crossed squares mark correlations where $p < 0.0001$. Venn diagram of gene overlaps in four of the hypoxia signatures between which the scores exhibited the highest correlation (**c**), darker colour representing higher percentage of overlapping genes. Forest plot presenting the benefit of RT in prevention of IBTR the first 5 years after the primary tumour in relation to hypoxia signature scores (**d**). The tumours were stratified based on hypoxia scores, where the 4th quartile was defined as high, and quartile 1–3 as low.

worse prognosis. We have previously shown, on the molecular level, that in hypoxic breast cancer cells ER-expression diminishes as HIF-1α accumulate [17, 49]. It is plausible that, in the generally less proliferative ER-positive tumours, the additive effect of growth factors, cytokines and other effectors induced by HIF-regulated transcription have a relatively greater impact than in ER-negative tumours.

Regulation of HIF-1α is mainly post-translational as described above, but we found that HIF-1α IHC signal correlated to *HIF-1α* mRNA-expression levels. Albeit, with a great degree of variability, and *HIF-1α* mRNA-expression did not correlate to tumour characteristics or patient outcome (data not shown). Thus, the need for a hypoxic gene-expression signature remains. To further study the role of tumour hypoxia in relation to patient outcome, we calculated a series of hypoxic scores according to hypoxia-related gene-expression signatures from the literature for each tumour in the cohort. Eleven literature-derived hypoxia gene-expression signatures [30–38] were analysed in relation to patient outcome. There was a high degree of correlation between several of the signatures, which was anticipated as some were published by associated research groups. The signatures were enriched in genes known to be regulated by HIF. Furthermore, we found that their expression correlated with HIF-1α IHC positivity, indicating that IHC detected transcriptionally active HIF-1α. High expression of most of the analysed hypoxia signatures correlated to a higher incidence of IBTR, any recurrence, and BCD, similarly to the pattern seen for HIF-1α IHC positivity. Notably, the Elvidge, Mense and Yang signatures did not correlate to increased occurrence of IBTR and were also among those with the least gene overlap and score correlation with the other signatures (Fig. 5b, c). However, the hallmarks of cancer signature, which had a large overlap with other hypoxic signatures, also did not correlate to increased IBTRs (Fig. 6). None of the hypoxic signatures, similar to HIF-1α IHC, correlated to RT-resistance.

In conclusion, patients with HIF-1α positive primary tumours had a worse outcome with increased recurrences, but these patients still had equal benefit from postoperative RT as patients with a non-hypoxic primary tumour.

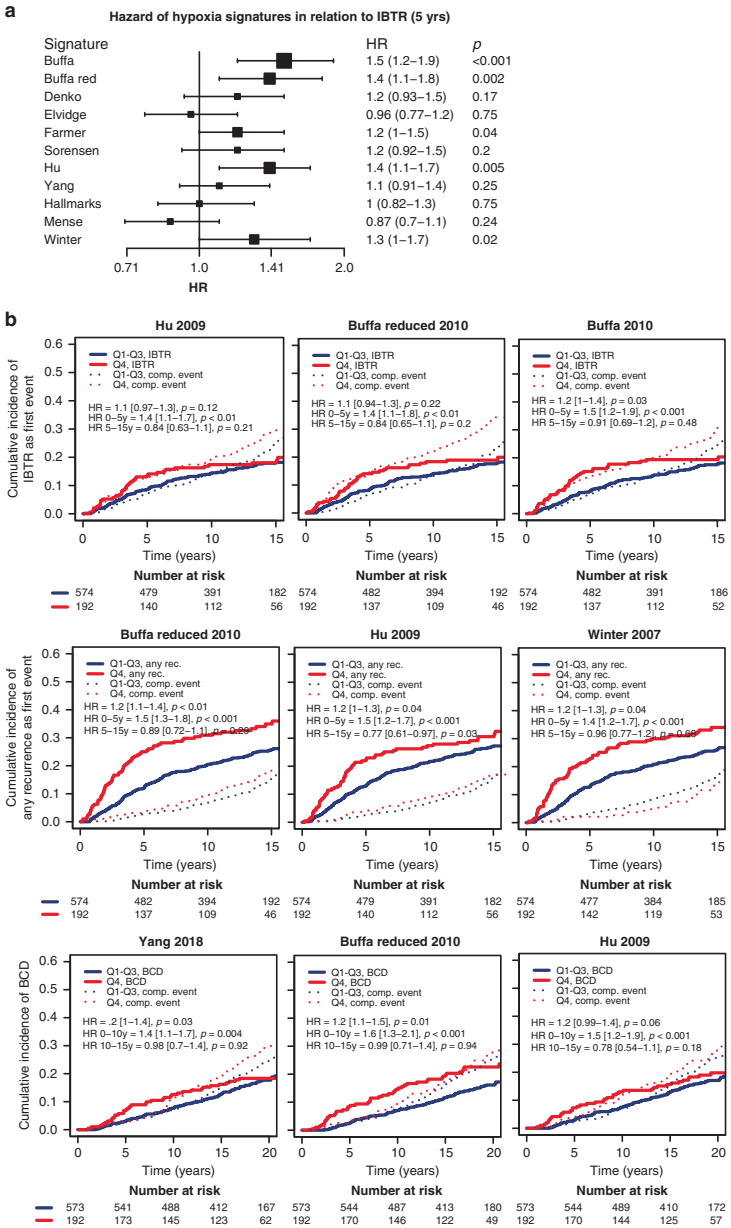

Fig. 6 Hypoxic gene-expression signatures in relation to recurrence and BCD. Forest plot presenting HR of hypoxic signature scores as continuous variables in relation to IBTR during the first 5 years after the primary tumour (**a**). For all rows, *n* and events were 766 and 75, respectively. Competing risk curves presenting the relationship between risk of IBTR, any recurrence, or BCD as first event. For each endpoint, the three hypoxia signatures with the strongest association to outcome are shown (**b**). The scores were plotted as a dichotomous variable of high vs. low, where low included quartile 1–3 (Q1–3, blue line), and high included quartile 4 (Q4, red line). Survival data presented as text in the plot area were obtained from Cox proportional hazards model with the score as a continuous variable.

DATA AVAILABILITY

The gene-expression datasets analysed during this study are available at Gene Expression Omnibus with accession number GSE119295. The IHC datasets generated and analysed during the current study are available from the corresponding author on reasonable request.

REFERENCES

1. Harvey JM, Clark GM, Osborne CK, Allred DC. Estrogen receptor status by immunohistochemistry is superior to the ligand-binding assay for predicting response to adjuvant endocrine therapy in breast cancer. J Clin Oncol. 1999; 17:1474–81.
2. Clarke M, Collins R, Darby S, Davies C, Elphinstone P, Evans V, et al. Effects of radiotherapy and of differences in the extent of surgery for early breast cancer on local recurrence and 15-year survival: an overview of the randomised trials. Lancet. 2005;366:2087–106.
3. Early Breast Cancer Trialists' Collaborative Group, Darby S, McGale P, Correa C, Taylor C, Arriagada R, et al. Effect of radiotherapy after breast-conserving surgery on 10-year recurrence and 15-year breast cancer death: meta-analysis of individual patient data for 10,801 women in 17 randomised trials. Lancet. 2011;378: 1707–16.
4. Lundstedt D, Gustafsson M, Malmström P, Johansson KA, Alsadius D, Sundberg A, et al. Symptoms 10-17 years after breast cancer radiotherapy data from the randomised SWEBCG91-RT trial. Radiother Oncol. 2010;97:281–7.
5. Lundstedt D, Gustafsson M, Steineck G, Malmström P, Alsadius D, Sundberg A, et al. Risk factors of developing long-lasting breast pain after breast cancer radiotherapy. Int J Radiat Oncol Biol Phys. 2012;83:71–8.
6. Taylor C, Correa C, Duane FK, Aznar MC, Anderson SJ, Bergh J, et al. Estimating the risks of breast cancer radiotherapy: evidence from modern radiation doses to the lungs and heart and from previous randomized trials. J Clin Oncol. 2017;35: 1641–9.
7. Cohen-Jonathan-Moyal E, Vendrely V, Motte L, Balosso J, Thariat J. Radioresistant tumours: From identification to targeting. Cancer Radiother. 2020;24:699–705.
8. Gray LH, Conger AD, Ebert M, Hornsey S, Scott OC. The concentration of oxygen dissolved in tissues at the time of irradiation as a factor in radiotherapy. Br J Radiol. 1953;26:638–48.
9. Vaupel P. Prognostic potential of the pre-therapeutic tumor oxygenation status. Adv Exp Med Biol. 2009;645:241–6.
10. Wang GL, Jiang BH, Rue EA, Semenza GL. Hypoxia-inducible factor 1 is a basic-helix-loop-helix-PAS heterodimer regulated by cellular O2 tension. Proc Natl Acad Sci USA. 1995;92:5510–4.
11. Tian H, Hammer RE, Matsumoto AM, Russell DW, McKnight SL. The hypoxia-responsive transcription factor EPAS1 is essential for catecholamine homeostasis and protection against heart failure during embryonic development. Genes Dev. 1998;12:3320–4.
12. Jaakkola P, Mole DR, Tian YM, Wilson MI, Gielbert J, Gaskell SJ, et al. Targeting of HIF-a to the von Hippel-Lindau ubiquitylation complex by o2-regulated prolyl hydroxylation. Science. 2001;292:468–72.
13. Jiang BH, Rue E, Wang GL, Roe R, Semenza GL. Dimerization, DNA binding, and transactivation properties of hypoxia-inducible factor 1. J Biol Chem. 1996;271: 17771–8.
14. Vaupel P, Mayer A. Hypoxia in cancer: significance and impact on clinical outcome. Cancer Metastasis Rev. 2007;26:225–39.
15. Jögi A Tumour hypoxia and the hypoxia-inducible transcription factors: key players in cancer progression and metastasis. In: Mazurek S, Shoshan MC, editors. Tumor cell metabolism. Wien: Springer-Verlag; 2014.
16. Bos R, van der Groep P, Greijer AE, Shvarts A, Meijer S, Pinedo HM, et al. Levels of hypoxia-inducible factor-1alpha independently predict prognosis in patients with lymph node negative breast carcinoma. Cancer. 2003;97:1573–81.
17. Jögi A, Ehinger A, Hartman L, Alkner S. Expression of HIF-1alpha is related to a poor prognosis and tamoxifen resistance in contralateral breast cancer. PLoS ONE. 2019;14:e0226150.
18. Generali D, Berruti A, Brizzi MP, Campo L, Bonardi S, Wigfield S, et al. Hypoxia-inducible factor-1alpha expression predicts a poor response to primary chemoendocrine therapy and disease-free survival in primary human breast cancer. Clin Cancer Res. 2006;12:4562–8.
19. Loncaster JA, Harris AL, Davidson SE, Logue JP, Hunter RD, Wycoff CC, et al. Carbonic anhydrase (CA IX) expression, a potential new intrinsic marker of hypoxia: correlations with tumor oxygen measurements and prognosis in locally advanced carcinoma of the cervix. Cancer Res. 2001;61:6394–9.
20. Harris BH, Barberis A, West CM, Buffa FM. Gene expression signatures as biomarkers of tumour hypoxia. Clin Oncol. 2015;27:547–60.
21. Ye IC, Fertig EJ, DiGiacomo JW, Considine M, Godet I, Gilkes DM. Molecular portrait of hypoxia in breast cancer: a prognostic signature and novel HIF-regulated genes. Mol Cancer Res. 2018;16:1889–901.
22. Malmström P, Holmberg L, Anderson H, Mattsson J, Jonsson PE, Tennvall-Nittby L, et al. Breast conservation surgery, with and without radiotherapy, in women with lymph node-negative breast cancer: a randomised clinical trial in a population with access to public mammography screening. Eur J Cancer. 2003;39:1690–7.
23. Killander F, Karlsson P, Anderson H, Mattsson J, Holmberg E, Lundstedt D, et al. No breast cancer subgroup can be spared postoperative radiotherapy after breast-conserving surgery. Fifteen-year results from the Swedish Breast Cancer Group randomised trial, SweBCG 91 RT. Eur J Cancer. 2016;67:57–65.
24. Sjöström M, Lundstedt D, Hartman L, Holmberg E, Killander F, Kovacs A, et al. Response to radiotherapy after breast-conserving surgery in different breast cancer subtypes in the Swedish Breast Cancer Group 91 Radiotherapy Randomized Clinical Trial. J Clin Oncol. 2017;35:3222–9.
25. Leung SCY, Nielsen TO, Zabaglo L, Arun I, Badve SS, Bane AL, et al. Analytical validation of a standardized scoring protocol for Ki67: phase 3 of an international multicenter collaboration. NPJ Breast Cancer. 2016;2:16014.
26. Elston CW, Ellis IO. Pathological prognostic factors in breast cancer. I. The value of histological grade in breast cancer: experience from a large study with long-term follow-up. Histopathology. 1991;19:403–10.
27. Goldhirsch A, Winer EP, Coates AS, Gelber RD, Piccart-Gebhart M, Thurlimann B, et al. Personalizing the treatment of women with early breast cancer: highlights of the St Gallen International Expert Consensus on the Primary Therapy of Early Breast Cancer 2013. Ann Oncol. 2013;24:2206–23.
28. Sjöström M, Chang SL, Fishbane N, Davicioni E, Hartman L, Holmberg E, et al. Comprehensive transcriptomic profiling identifies breast cancer patients who may be spared adjuvant systemic therapy. Clin Cancer Res. 2020;26:171–82.
29. Piccolo SR, Sun Y, Campbell JD, Lenburg ME, Bild AH, Johnson WE. A single-sample microarray normalization method to facilitate personalized-medicine workflows. Genomics. 2012;100:337–44.
30. Buffa FM, Harris AL, West CM, Miller CJ. Large meta-analysis of multiple cancers reveals a common, compact and highly prognostic hypoxia metagene. Br J Cancer. 2010;102:428–35.
31. Koong AC, Denko NC, Hudson KM, Schindler C, Swiersz L, Koch C, et al. Candidate genes for the hypoxic tumor phenotype. Cancer Res. 2000;60:883–7.
32. Elvidge GP, Glenny L, Appelhoff RJ, Ratcliffe PJ, Ragoussis J, Gleadle JM. Concordant regulation of gene expression by hypoxia and 2-oxoglutarate-dependent dioxygenase inhibition: the role of HIF-1alpha, HIF-2alpha, and other pathways. J Biol Chem. 2006;281:15215–26.
33. Hu Z, Fan C, Livasy C, He X, Oh DS, Ewend MG, et al. A compact VEGF signature associated with distant metastases and poor outcomes. BMC Med. 2009;7:9.
34. Mense SM, Sengupta A, Zhou M, Lan C, Bentsman G, Volsky DJ, et al. Gene expression profiling reveals the profound upregulation of hypoxia-responsive genes in primary human astrocytes. Physiol Genomics. 2006;25:435–49.
35. Sorensen BS, Toustrup K, Horsman MR, Overgaard J, Alsner J. Identifying pH independent hypoxia induced genes in human squamous cell carcinomas in vitro. Acta Oncol. 2010;49:895–905.
36. Winter SC, Buffa FM, Silva P, Miller C, Valentine HR, Turley H, et al. Relation of a hypoxia metagene derived from head and neck cancer to prognosis of multiple cancers. Cancer Res. 2007;67:3441–9.
37. Farmer P, Bonnefoi H, Becette V, Tubiana-Hulin M, Fumoleau P, Larsimont D, et al. Identification of molecular apocrine breast tumours by microarray analysis. Oncogene. 2005;24:4660–71.
38. Yang L, Roberts D, Takhar M, Erho N, Bibby BAS, Thiruthaneeswaran N, et al. Development and validation of a 28-gene hypoxia-related prognostic signature for localized prostate cancer. EBioMedicine. 2018;31:182–9.
39. Foroutan M, Bhuva DD, Lyu R, Horan K, Cursons J, Davis MJ. Single sample scoring of molecular phenotypes. BMC Bioinformatics. 2018;19:404.
40. Waldron L, Riester M. HGNChelper: identify and correct invalid HGNC human gene symbols and MGI mouse gene symbols. R package version 0.8.1. 2019. https://CRAN.R-project.org/package=HGNChelper.
41. Stelzer G, Rosen R, Zimmerman S, Twik M, Fishilevich S, Iny Stein T, et al. The GeneCards Suite: From Gene Data Mining to Disease Genome Sequence Analysis. Current Protocols in Bioinformatics 2016;54:1.30.1–33.
42. Gray B. cmprsk: Subdistribution analysis of competing risks. R package version 2. 2-7.
43. Schoenfeld D. Partial residuals for the proportional hazard regression model. Biometrika 1982;69:239–41.
44. Nordsmark M, Bentzen SM, Rudat V, Brizel D, Lartigau E, Stadler P, et al. Prognostic value of tumor oxygenation in 397 head and neck tumors after primary radiation therapy. An international multi-center study. Radiother Oncol. 2005;77: 18–24.
45. Overgaard J, Eriksen JG, Nordsmark M, Alsner J, Horsman MR, Danish H, et al. Plasma osteopontin, hypoxia, and response to the hypoxia sensitiser nimorazole in radiotherapy of head and neck cancer: results from the DAHANCA 5 randomised double-blind placebo-controlled trial. Lancet Oncol. 2005;6:757–64.

46. Brizel DM, Scully SP, Harrelson JM, Layfield LJ, Bean JM, Prosnitz LR, et al. Tumor oxygenation predicts for the likelihood of distant metastases in human soft tissue sarcoma. Cancer Res. 1996;56:941–3.
47. Harris AL. Hypoxia-a key regulatory factor in tumour growth. Nat Rev Cancer. 2002;2:38–47.
48. Rankin EB, Giaccia AJ. Hypoxic control of metastasis. Science. 2016;352:175–80.
49. Helczynska K, Kronblad A, Jögi A, Nilsson E, Beckman S, Landberg G, et al. Hypoxia promotes a dedifferentiated phenotype in ductal breast carcinoma in situ. Cancer Res. 2003;63:1441–4.

ACKNOWLEDGEMENTS

We wish to acknowledge the skilful technical assistance of Kristina Lövgren, and Sara Baker and Carina Forsare for database management and support. We gratefully acknowledge the South Swedish and West Swedish Breast Cancer Groups and all participating departments of Surgery, Pathology and Oncology. We thankfully acknowledge S. Laura Chang (Exact Sciences), Felix Feng (University of California, San Francisco), Corey Speers (University of Michigan) and Lori Pierce (University of Michigan) for mRNA retrieval and generation of gene-expression data.

AUTHOR CONTRIBUTIONS

Conception and design: AJ, EH, JT, MF, MS, PK and PM. Data acquisition, analysis and interpretation: AJ, EH, EN, FK, LMFL-L, JT, MF, MS, PK and PM. Writing, review and/or revision of the manuscript: AJ, EH, EN, FK, LMFL-L, JT, MF, MS, PK and PM. Administrative, technical or material support: AJ, EH, LMFL-L, JT, MF, MS, PK and PM. Study supervision: AJ, EH, EN, FK, LMFL-L, JT, MF, MS, PK and PM.

FUNDING

This work was supported by Allmänna Sjukhusets i Malmö stiftelse för bekämpande av cancer (cancerforskningmalmo.se, AJ), The Anna and Edwin Berger Foundation (MF and EN), Governmental Funding of Research within the National Health Services (ALF) (MF and EN), the Gunnar Nilsson Cancer Society (MF and EN), the Hans von Kantzows Foundation (AJ), Marianne and Marcus Wallenberg Foundation (EN), the Mrs Berta Kamprad Research Foundation (MF, PM), the O.E. and Edla Johansson's foundation (oervetstiftelse.se, AJ), the Percy Falk Foundation (c/o Thomas Kramar, Sweden, AJ), the Swedish Breast Cancer Association (BRO)(FK, MF, PM, and EN), the Swedish Cancer and Allergy Foundation (MF), the Swedish Cancer Society (MF, PM, and EN), and the Swedish Cancer Foundation (190479 Pi; LMFL-L). The funders had no role in study design, data collection, decision to publish, or preparation of the manuscript.

ETHICS APPROVAL AND CONSENT TO PARTICIPATE

The trial and follow-up including tissue microarrays (TMAs) were conducted in accordance with the declaration of Helsinki and approved by the local ethics committees. Gene-expression analyses were approved by the Lund University Ethical Review Board (2010/127, 2015/548). Oral informed consent was obtained from all patients, which was approved by the Ethical Review Board for the original trial and for the gene-expression study.

CONSENT FOR PUBLICATION

No individual person's data is presented.

COMPETING INTERESTS

The authors AJ, FK, EN, JT, LMFL-L and MS declare no competing interests. PK, EH, PM and MF research contract with PFS Genomics.

ADDITIONAL INFORMATION

Supplementary information The online version contains supplementary material available at https://doi.org/10.1038/s41416-021-01630-4.

Correspondence and requests for materials should be addressed to Annika Jögi.

Reprints and permission information is available at http://www.nature.com/reprints

Publisher's note Springer Nature remains neutral with regard to jurisdictional claims in published maps and institutional affiliations.

Paper IV